Satellite Image Atlas of Glaciers of the World

SOUTH AMERICA

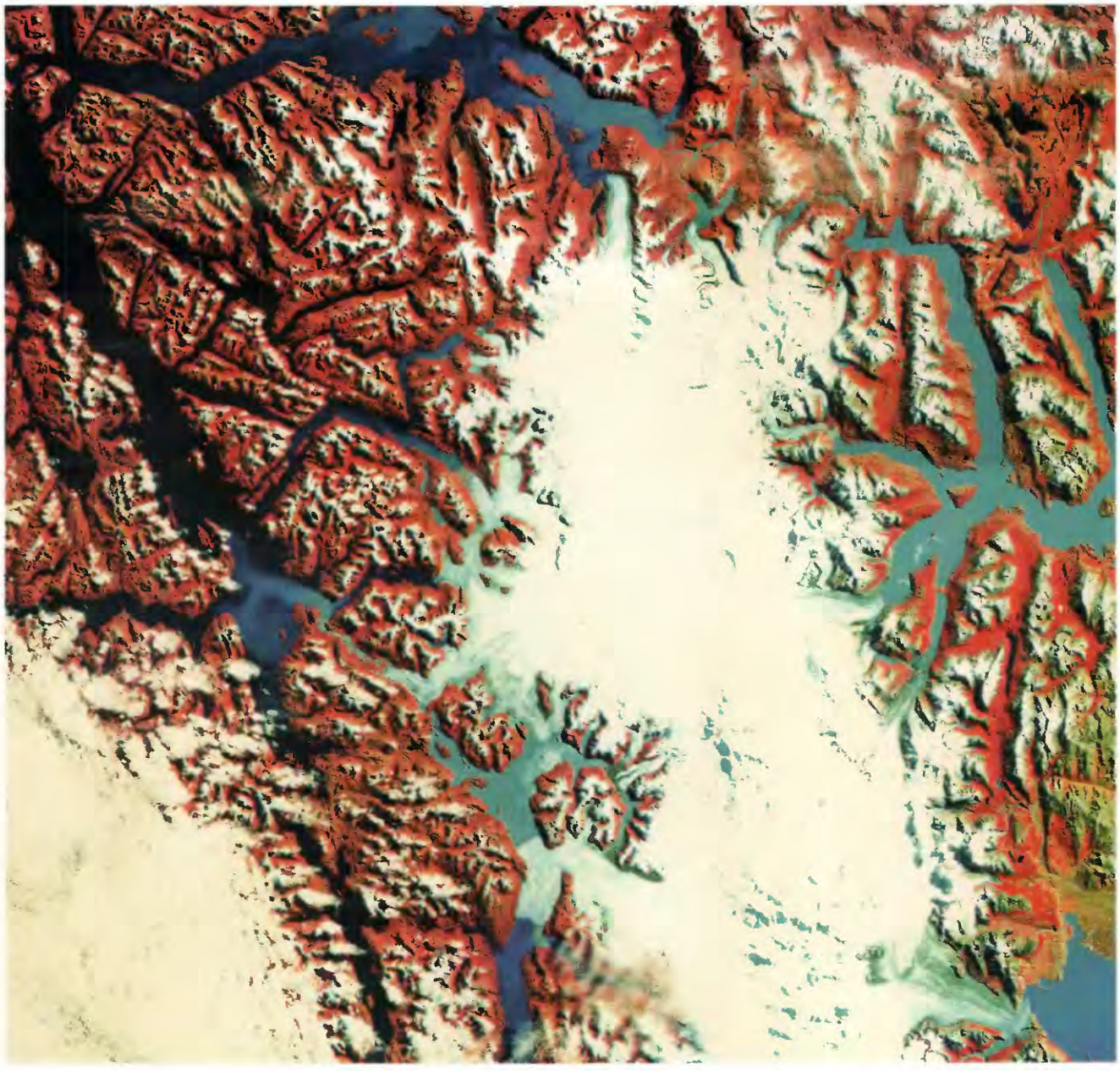

United States Geological Survey
Professional Paper 1386–I

Cover: *Landsat false-color image of the Southern Patagonian Ice Field, a heavily glacierized segment of the Andes Mountains that extends from about latitude 48° 15'S. to about latitude 51°30'S. along the border between Chile and Argentina. (Landsat image 2399–13410; 25 February 1976; Path 248, Row 94 from the EROS Data Center, Sioux Falls, S. Dak.)*

GLACIERS OF SOUTH AMERICA–

SATELLITE IMAGE ATLAS OF GLACIERS OF THE WORLD

Edited by RICHARD S. WILLIAMS, Jr., *and* JANE G. FERRIGNO

U.S. GEOLOGICAL SURVEY PROFESSIONAL PAPER 1386-I

Landsat images, together with aerial photographs and maps where available, have been used to produce glacier inventories, define glacier locations, support on-going field studies of glacier dynamics, and monitor the extensive glacier recession that has taken place and is continuing in many parts of South America

UNITED STATES GOVERNMENT PRINTING OFFICE, WASHINGTON: 1998

U.S. DEPARTMENT OF THE INTERIOR

BRUCE BABBITT, *Secretary*

U.S. GEOLOGICAL SURVEY

Charles G. Groat, *Director*

Technical editing by Susan Tufts-Moore

Design, layout, and illustrations by Kirsten E. Cooke

Text review and typesetting by Janice G. Goodell

Text review by Josephine S. Hatton

Layout review by Carolyn H. McQuaig

Library of Congress Cataloging in Publication Data

(Revised for vol. I)
Satellite image atlas of glaciers of the world.
(U.S. Geological Survey professional paper; 1386)
Includes bibliography.
Contents: — Ch. B. Antarctica, by Charles Swithinbank; with sections on The "dry valleys" of Victoria Land, by Trevor J. Chinn, [and] Landsat images of Antarctica, by Richard S. Williams, Jr., and Jane G. Ferrigno — Ch. C. Greenland, by Anker Weidick — Ch. E. Glaciers of Europe — Ch. G. Glaciers of the Middle East and Africa — Ch. H. Glaciers of Irian Jaya, Indonesia, and New Zealand — Ch. I. Glaciers of South America.
Supt. of Docs. no.: I 19.16:1386–I
1. Glaciers—Remote sensing. I. Williams, Richard S., Jr. II. Ferrigno, Jane G. III. Series.
GB2401.72.R42S28 1988 551.3'12 87-600497

For sale by the U.S. Geological Survey, Information Services
Box 25286, Federal Center,
Denver, CO 80225

Foreword

On 23 July 1972, the first Earth Resources Technology Satellite (ERTS 1 or Landsat 1) was successfully placed in orbit. The success of Landsat inaugurated a new era in satisfying mankind's desire to better understand the dynamic world upon which we live. Space-based observations have now become an essential means for monitoring global change.

The short- and long-term cumulative effects of processes that cause significant changes on the Earth's surface can be documented and studied by repetitive Landsat images. Such images provide a permanent historical record of the surface of our planet; they also make possible comparative two-dimensional measurements of change over time. This Professional Paper demonstrates the importance of the application of Landsat images to global studies by using them to determine the current distribution of glaciers on our planet. As images become available from future satellites, the new data will be used to document global changes in glacier extent by reference to the image record of the 1970's.

Although many geological processes take centuries or even millennia to produce obvious changes on the Earth's surface, other geological phenomena, such as glaciers and volcanoes, cause noticeable changes over shorter periods. Some of these phenomena can have a worldwide impact and often are interrelated. Explosive volcanic eruptions can produce dramatic effects on the global climate. Natural or culturally induced processes can cause global climatic cooling or warming. Glaciers respond to such warming or cooling periods by decreasing or increasing in size, which in turn causes sea level to rise or fall.

As our understanding of the interrelationship of global processes improves and our ability to assess changes caused by these processes develops further, we will learn how to use indicators of global change, such as glacier variation, to manage more wisely the use of our finite land and water resources. This Professional Paper is an excellent example of the way in which we can use technology to provide needed earth-science information about our planet. The international collaboration represented by this report is also an excellent model for the kind of cooperation that scientists will increasingly find necessary in the future in order to solve important earth-science problems on a global basis.

Charles G. Groat,
Director,
U.S. Geological Survey

Preface

This chapter is the sixth to be released in U.S. Geological Survey Professional Paper 1386, Satellite Image Atlas of Glaciers of the World, a series of 11 chapters. In each chapter, remotely sensed images, primarily from the Landsat 1, 2, and 3 series of spacecraft, are used to study the glacierized regions of our planet and to monitor glacier changes. Landsat images, acquired primarily during the middle to late 1970's, were used by an international team of glaciologists and other scientists to study various geographic regions or to discuss glaciological topics. In each geographic region, the present areal distribution of glaciers is compared, wherever possible, with historical information about their past extent. The atlas provides an accurate regional inventory of the areal extent of glacier ice on our planet during the 1970's as part of a growing international scientific effort to measure global environmental change on the Earth's surface.

The Andes Mountains of South America, from the Sierra Nevada de Mérida, Venezuela, to Tierra del Fuego, Chile and Argentina, are glacierized to a lesser or greater extent depending on latitude, altitude, and annual precipitation. The largest area and volume of glacier ice, including two large ice fields, each with numerous outlet glaciers, occurs in the Patagonian Andes, southern South America. Landsat images are particularly valuable for monitoring fluctuations of large glaciers, especially outlet glaciers from ice fields and for delineating the areal distribution of large glaciers.

Venezuela has five cirque glaciers with a total area of 2 km^2. A rapid loss of glacier ice has taken place during the last century, a process that has accelerated since 1972.

Colombia has many small glaciers with a total area of 104 km^2 on six peaks. Its largest glacier (<20 km^2) is an ice cap on the active Nevado del Ruiz volcano; in November 1985, an explosive eruption melted part of the summit ice cap, which, when combined with heavy precipitation, generated lahars that killed more than 23,000 people, more than 20,000 in the town of Armero. A consistent and progressive loss of glacier ice and snowpack has been noted since the late 1800's, and many glaciers have completely disappeared during the 20th century.

Ecuador has more than 100 small ice caps, outlet glaciers, ice fields, and mountain glaciers with a total area of about 97 km^2. Since the 1800's, the glacier area has undergone a significant continuing reduction.

Perú has a total glacier-covered area of 2,600 km^2 on 20 distinct cordilleras. The glacierized cordilleras are important sources of water and as locations of glacier-related avalanches and floods that have destroyed towns and killed tens of thousands of inhabitants.

Bolivia has a total glacier-covered area of more than 560 km^2. A few small summit ice caps, outlet and crater glaciers (~10 km^2) are located on extinct volcanoes of the Cordillera Occidental in northern Bolivia. Ice caps, valley glaciers, and mountain glaciers (550 km^2) are located on the highest peaks of the Cordillera Oriental.

Numerous glaciers in Chile and Argentina occur along the more than 4,000-km length of the Andes Mountains, from very small snow patches and glacierets of the *Desert Andes* and the 2,200 km^2 of glaciers in the Central Andes to the large ice fields and outlet glaciers of Patagonia. The Southern Patagonian Ice Field (~13,000 km^2) is the largest glacier outside Antarctica in the Southern Hemisphere. The Northern Patagonian Ice Field (~4,200 km^2) and the glacierized Cordillera Darwin in Tierra del Fuego (~2,300 km^2) also contain a substantial volume of glacier ice.

Richard S. Williams, Jr.
Jane G. Ferrigno
Editors

About this Volume

U.S. Geological Survey Professional Paper 1386, Satellite Image Atlas of Glaciers of the World, contains 11 chapters designated by the letters A through K. Chapter A is a general chapter containing introductory material and a discussion of the physical characteristics, classification, and global distribution of glaciers. The next nine chapters, B through J, are arranged geographically and present glaciological information from Landsat and other sources of data on each of the geographic areas. Chapter B covers Antarctica; Chapter C, Greenland; Chapter D, Iceland; Chapter E, Continental Europe (except for the European part of the former Soviet Union), including the Alps, the Pyrenees, Norway, Sweden, Svalbard (Norway), and Jan Mayen (Norway); Chapter F, Asia, including the European part of the former Soviet Union, China (P.R.C.), India, Nepal, Afghanistan, and Pakistan; Chapter G, Turkey, Iran, and Africa; Chapter H, Irian Jaya (Indonesia) and New Zealand; Chapter I, South America; and Chapter J, North America. The final chapter, K, is a topically oriented chapter that presents related glaciological topics.

The realization that one element of the Earth's cryosphere, its glaciers, was amenable to global inventorying and monitoring with Landsat images led to the decision, in late 1979, to prepare this Professional Paper, in which Landsat 1, 2, and 3 multispectral scanner (MSS) and Landsat 2 and 3 return beam vidicon (RBV) images would be used to inventory the areal occurrence of glacier ice on our planet within the boundaries of the spacecraft's coverage (between about 81° north and south latitudes). Through identification and analysis of optimum Landsat images of the glacierized areas of the Earth during the first decade of the Landsat era, a global benchmark could be established for determining the areal extent of glaciers during a relatively narrow time interval (1972 to 1982). This global "snapshot" of glacier extent could then be used for comparative analysis with previously published maps and aerial photographs and with new maps, satellite images, and aerial photographs in order to determine the areal fluctuation of glaciers in response to natural or culturally induced changes in the Earth's climate.

To accomplish this objective, the editors selected optimum Landsat images of each of the glacierized regions of our planet from the Landsat image data base at the EROS Data Center in Sioux Falls, S. Dak., although some images were also obtained from the Landsat image archives maintained by the Canada Centre for Remote Sensing, Ottawa, Ontario, Canada, and by the European Space Agency in Kiruna, Sweden, and Fucino, Italy. Between 1979 and 1981, these optimum images were distributed to an international team of more than 50 scientists who agreed to write a section of the Professional Paper concerning either a geographic area or a glaciological topic. In addition to analyzing images of a specific geographic area, each author was also asked to summarize up-to-date information about the glaciers within the area and to compare their present areal distribution with historical information (for example, from published maps, reports, and photographs) about their past extent. Completion of this atlas will provide an accurate regional inventory of the areal extent of glaciers on our planet during the 1970's.

Richard S. Williams, Jr.
Jane G. Ferrigno
Editors

CONTENTS

Glaciers of South America–

GLACIERS OF VENEZUELA

By CARLOS SCHUBERT

SATELLITE IMAGE ATLAS OF GLACIERS OF THE WORLD

Edited by RICHARD S. WILLIAMS, Jr., *and* JANE G. FERRIGNO

U.S. GEOLOGICAL SURVEY PROFESSIONAL PAPER 1386–I–1

Venezuela has five cirque glaciers that have a total area of 2 square kilometers and are situated on three separate mountain peaks in the Sierra Nevada de Mérida. A rapid loss of glacier ice has taken place during the last century, a process that has accelerated since 1972

CONTENTS

GLACIERS OF SOUTH AMERICA–

GLACIERS OF VENEZUELA

By CARLOS SCHUBERT[1 2]

Abstract

The glaciers of Venezuela consist of five cirque glaciers situated on three peaks (Pico Bolívar, 5,002 meters; Pico Humboldt, 4,942 meters; and Pico Bonpland, 4,893 meters) in the Sierra Nevada de Mérida and encompass an area of 2 square kilometers. The present-day glacier area covers only about 1 percent of the 200-square-kilometer area covered in the Sierra Nevada during the late Pleistocene Mérida Glaciation. The total glacier-covered area in the Cordillera de Mérida during this glaciation was approximately 600 square kilometers. Rapid deglaciation has taken place in the Sierra Nevada in the last century, a process that has accelerated since 1972.

Introduction

The Sierra Nevada de Mérida[3] is part of the largest massif in Venezuela, the Cordillera de Mérida, which is part of the northern extent of the Cordillera de los Andes (Andes Mountains) (figs. 1 and 2). The Sierra Nevada includes the highest peak in Venezuela, Pico Bolívar, which has an elevation of 5,002 m.

Similar to other high mountain systems in temperate and tropical regions, this area was affected by Quaternary glaciation. The last ice advance in this area, which was at its maximum about 20,000 years before present (B.P.) and ended about 13,000 years B.P., was called the Mérida Glaciation. The glacierized area in the Cordillera de Mérida was approximately 600 km^2; this included the following high areas from southwest to northeast: Páramo de Tamá, Páramo Batallón, Páramo Los Conejos, Páramo Piedras Blancas, and Teta de Niquitao. Approximately 200 km^2 of the total glacierized area was in the Sierra Nevada de Mérida, and of that amount, the largest concentration, 50 km^2, was in the areas of Picos Bolívar, Humboldt (4,942 m), and Bonpland (4,893 m). Moraines from the Mérida Glaciation are found between 2,600 and 3,500 m above sea level (asl). Since that time, deglaciation has been widespread. Probable "Little Ice Age" moraines have been found at 4,200 m asl, but at present, the snowline is above 4,700 m asl. As a result, the only glaciers currently in existence in Venezuela are five cirque glaciers of approximately 2 km^2 in total area on Picos Bolívar, Humboldt, and Bonpland, tiny remnants of the former extent of Pleistocene ice (Schubert 1974, 1975, 1987; Schubert and Clapperton, 1990) (fig. 3).

Manuscript approved for publication 18 March 1998.

[1] Instituto Venezolano de Investigaciones Científicas, Apartado 21827, Caracas 1020A, Venezuela.

[2] Deceased on 22 July 1994.

[3] The names used in this section are approved by the U.S. Board on Geographic Names (Defense Mapping Agency, 1993) with the exception of Sierra Nevada de Mérida, a name in common use that is used here to identify that part of the Cordillera de Mérida that has snow or ice cover.

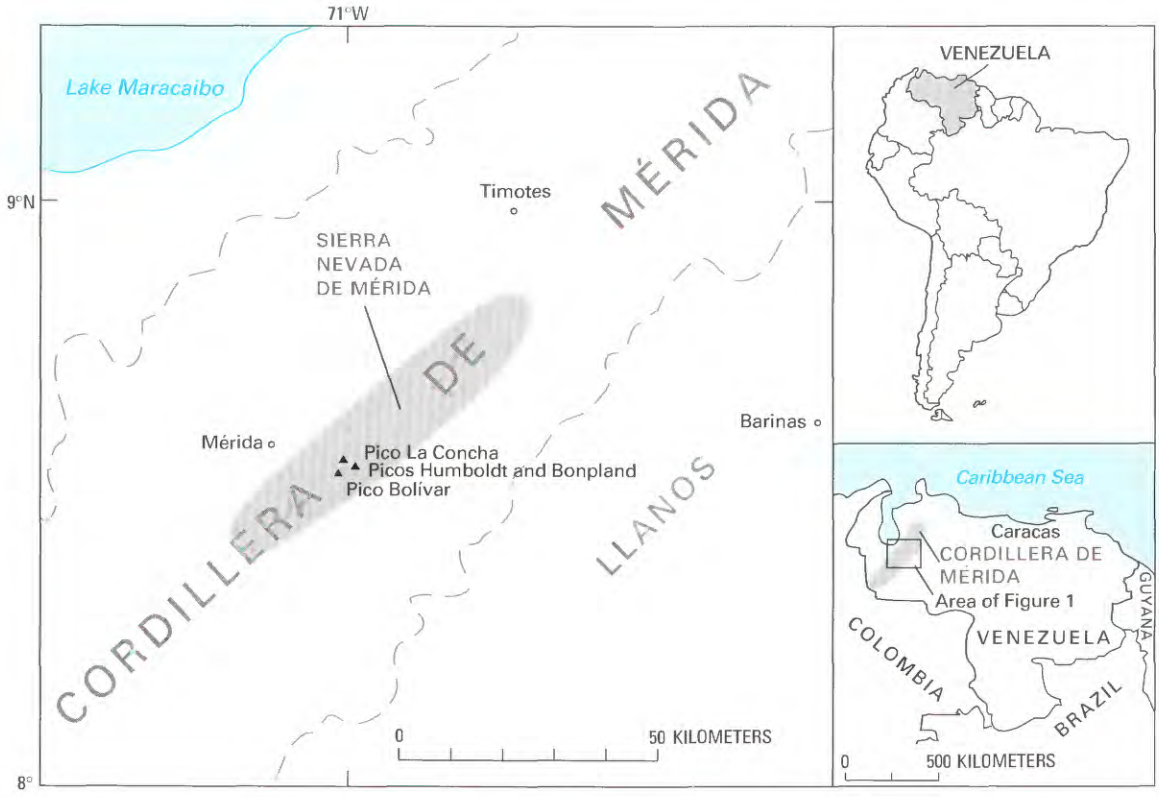

Figure 1. *— The Sierra Nevada de Mérida in northwestern Venezuela. Broken lines show general area of Cordillera de Mérida.*

The most important early references to the Venezuelan glaciers are those by Sievers (1886, 1908, 1911) and Jahn (1912a, b, 1925, 1931). These reports (reviewed by Schubert, 1980, 1984) include maps, data, and photographs that can be compared with present-day glacier conditions. More recent reports are those of Schubert (1972, 1980, 1984, 1992) and Giegengack and Grauch (1975). The reports by Schubert present comparative data on glacier retreat between the mid-19th century and 1991, data that strongly suggest a reduction of more than 95 percent of the glacier-covered area during that interval of time. The American Geographical Society also compiled information on the glaciers of the northern Andes in three publications (Fuchs, 1958; Field and associates, 1958; Lehr, 1975).

Mapping of Glaciers

Earliest Maps

The earliest published map of the Sierra Nevada de Mérida was based on field work by Jahn in 1910 (Jahn, 1925). The Jahn map was the only map showing the distribution of glaciers in the Sierra Nevada de Mérida until maps were published by Schubert (1972, 1980, 1984). The Schubert maps are based on vertical aerial photographs acquired in 1952, the only ones available so far for this region. The glacierized area was mapped by the author of this paper on 1:100,000-scale maps by reconstructing the extent of the 1952 glacier from the aerial photographs (approximate scale 1:40,000) and field observations; area measurements were made by the use of a Maho No. 80 planimeter.

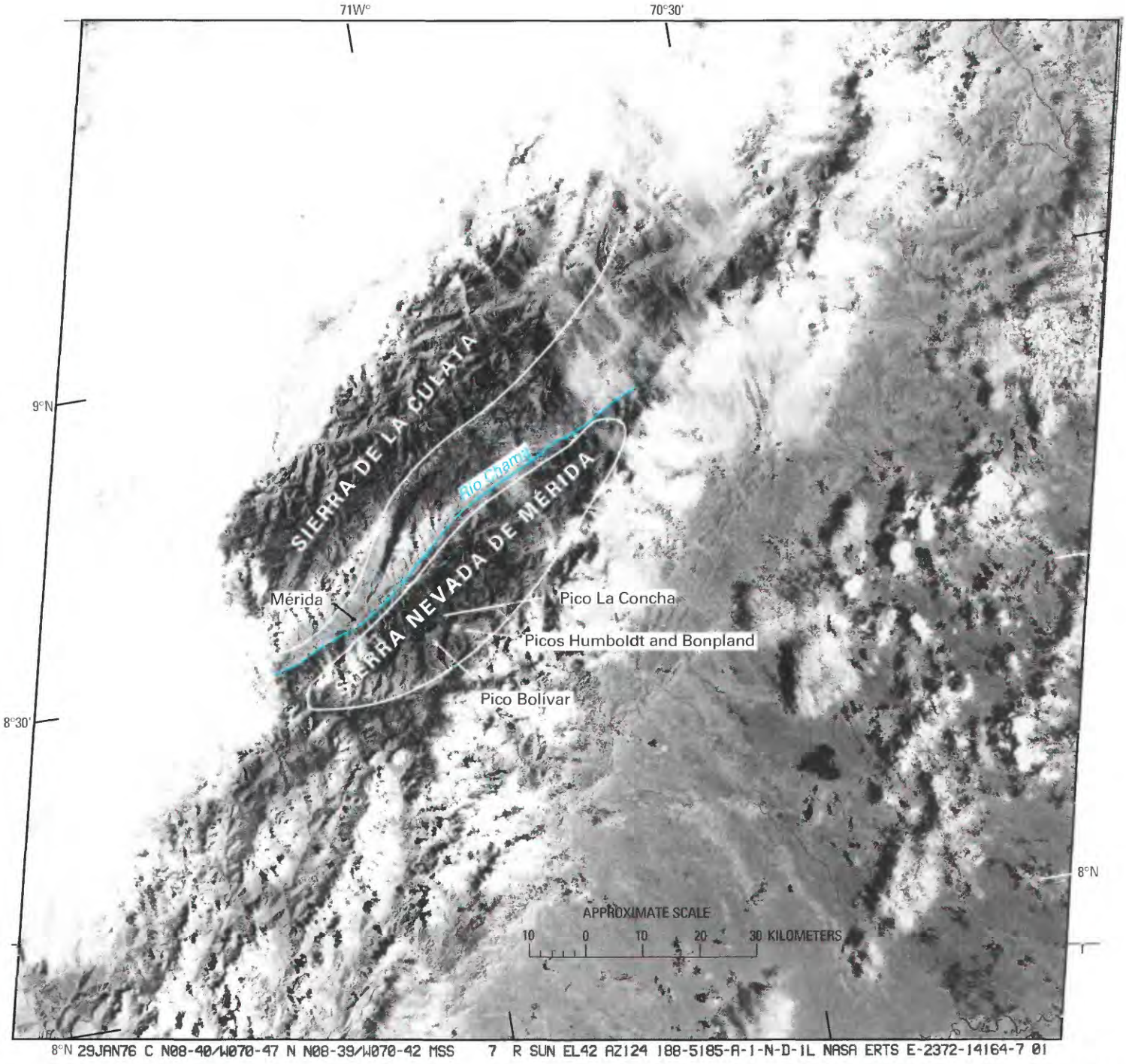

Figure 2.—*Annotated Landsat 2 MSS image showing the location of glaciers in the Sierra Nevada de Mérida. Landsat 2 image (2372-14164, band 7; 29 January 1976; Path 6, Row 54) from EROS Data Center, Sioux Falls, S. Dak.*

Figure 3.—*Small cirque glaciers on Pico Bolívar photographed in December 1988. A considerable recession has been noted since 1952.*
A, *Remnants of Espejo Glacier on the southwestern face of Pico Bolívar. The glacier has melted and consists of two small firn patches.*
B, *Remnants of El Encierro Glacier on the north face. Photographs by B.A. Eiswerth, U.S. Geological Survey.*

A comparison of the glacierized area in 1910 mapped by Jahn and in 1952 mapped by Schubert is shown in figure 4 (no effort was made to compare them quantitatively because Jahn did not specify how he mapped the glaciers; this author's estimate, based on planimetric measurements, is that they covered more than 10 km^2 in 1910). The map by Jahn shows two broad areas covered by glaciers (Picos Bolívar-Espejo-La Concha and Picos Humboldt-Bonpland) and also a small glacier on the northwest flank of Pico El Toro, about 4.5 km west of Pico Espejo. The topographic accuracy of Jahn's map (originally at a scale of 1:100,000) is estimated on the basis of a comparison with the Cartografía Nacional (1977) map no. 5941 at the same scale of ±0.5 km.

Modern Maps of Glaciers

Figure 5 shows the latest map of the Sierra Nevada de Mérida glaciers (modified after Schubert, 1980) based on the 1952 vertical aerial photographs. Table 1 gives the areas of the glaciers measured by the author.

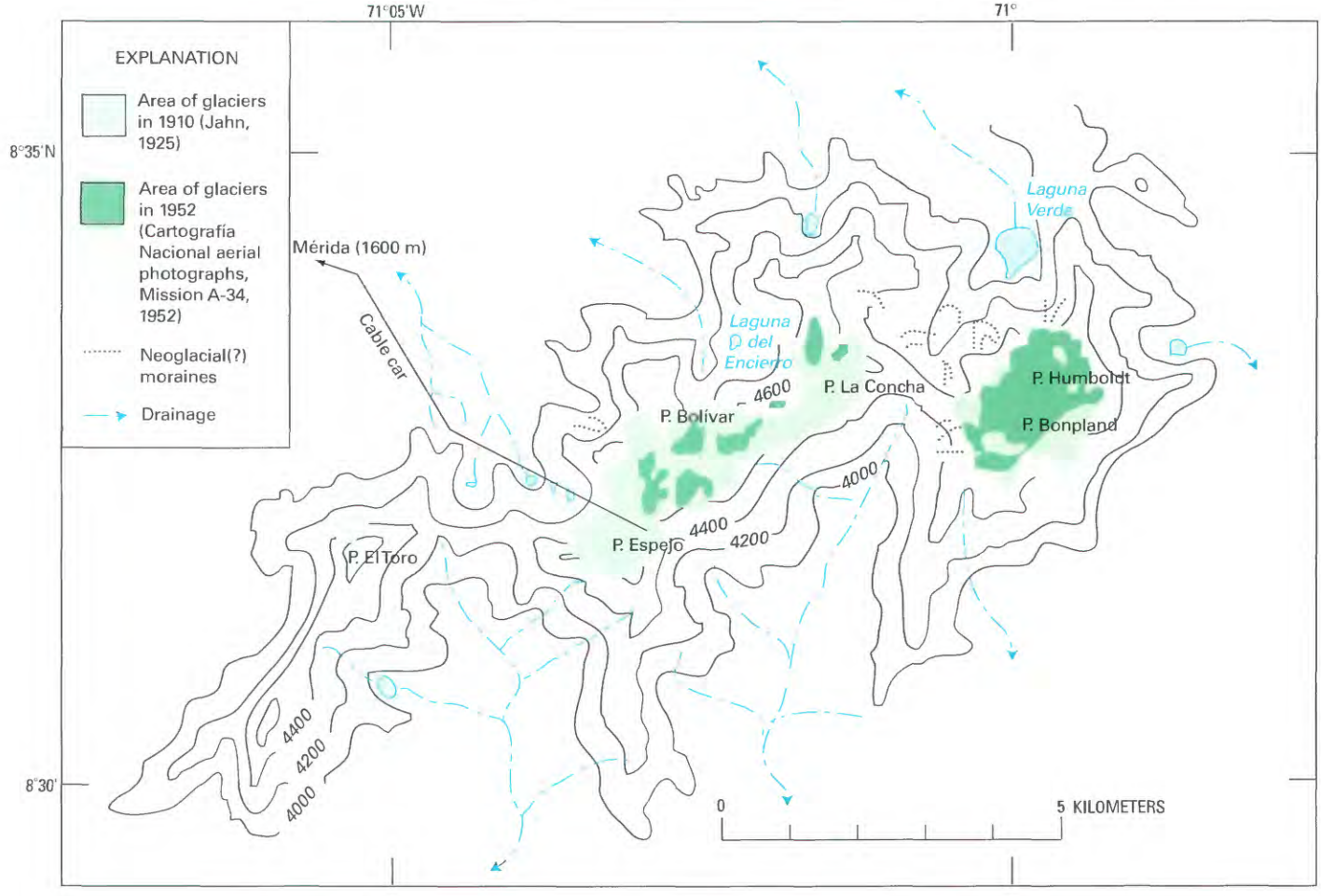

Figure 4.—*Comparison of areas covered by glaciers in the Sierra Nevada de Mérida in 1910 and 1952. Elevations of peaks are given in figure 5, except for Pico Espejo (4,765 m) and Pico El Toro (4,727 m). Elevations are in meters above mean sea level; contour interval, 200 m. Base maps: Cartografía Nacional, Caracas, nos. 5941 and 6041, scale 1:100,000. Arrows show direction of drainage.*

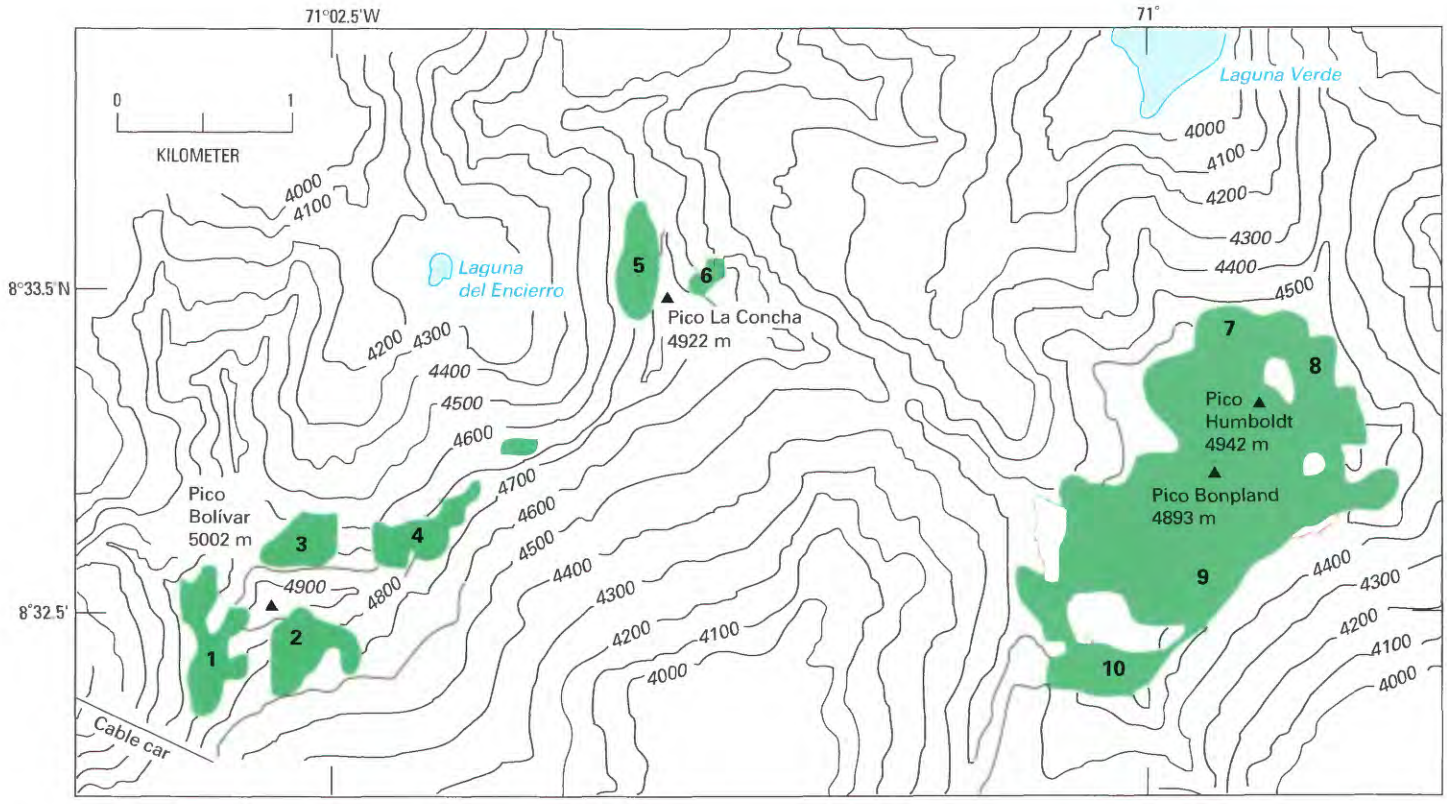

Figure 5.—*Distribution of glaciers (green areas) in the Sierra Nevada de Mérida in 1952. The numbers identify glaciers listed in table 1. Data derived from Cartografía Nacional aerial photographs, Mission A–34, 1952. Base maps: Cartografía Nacional, Caracas, nos. 5941–I–SE and 6041–IV–SO, scale 1:100,000. Elevations are in meters above mean sea level; the contour interval is 100 m.*

TABLE 1.– *Names of the glaciers in the Sierra Nevada de Mérida, measurements based on 1952 aerial photography, and recent changes*

Massif	Glacier[1]	Area in 1952[2] (square kilometers)	Appearance in 1991[3]
Pico Bolívar (8°32.5'N., 71°02.5'W.)	Espejo (1)	.27	Melted into 2 small firn patches
	Timoncito (2)	.17	Almost completely disappeared
	El Encierro (3)	.17	Lost at least 50 percent of its area
	El Encierro (4)	.10	Retreated
Pico La Concha (8°33.5'N., 71°01.5'W.)	Ño Leon (5)	.10	Completely disappeared
	Coromoto west remnant (6)	.07	Completely disappeared
Picos Humboldt/Bonpland (8°32'N., 71°00'W.)	Coromoto east remnant (7, 8)	2.03	Retreated[4]
	Sinigüis (9)		Retreated
	Nuestra Señora (10)		Completely disappeared
	Total	2.91	Approx. 2.00 km^2

[1] Number in parentheses refers to number on figure 5.

[2] Measured by author by use of a planimeter on maps modified with data from 1952 vertical aerial photographs; approximate scale, 1:40,000.

[3] Based on field work and ground photographs from 1991 (Schubert, 1992).

[4] Based on the Landsat image shown in figure 6*A* (2372–14164; 29 January 1976).

Imaging of Glaciers

Aerial Photography

The only aerial photographs available for the Sierra Nevada de Mérida are those that were taken for the Dirección de Cartografía Nacional (Caracas), Mission A–34 (nos. 972 to 982), in 1952 at an approximate scale of 1:40,000. These photographs are the primary source of data used to compile the latest glacier map (fig. 5).

Satellite Imagery

Not many Landsat images have been acquired of the Sierra Nevada de Mérida area. Only 18 Landsats 1, 2, and 3 multispectral scanner (MSS) images are archived at the EROS Data Center, Sioux Falls, S. Dak., and many of these are covered by clouds. The best early Landsat image obtained of the Sierra Nevada de Mérida glaciers is a Landsat 2 image (2372–14164) that was acquired on 29 January 1976. Figure 6*A* shows an annotated enlargement of MSS band 7 of that image. Two other early Landsat images of the area (listed in table 2) are cloud free but have slightly more snow cover. The most useful Landsat 4 and 5 MSS scenes were acquired in February 1985 and March 1991 (see table 2). Both show substantially less snow-and-ice cover than the 1976 image. The March 1991 image, which coincides closely with the author's 1991 visit to the area, confirms the major retreat described in table 1 and by Schubert (1992). A 1:250,000-scale enlargement of the 1991 scene is shown in figure 6*B* for comparison.

In the enlarged 1976 Landsat MSS image (fig. 6*A*), the outline of the Picos Humboldt and Bonpland glaciers can be discerned. All other glaciers show as white spots, principally because of the relatively small area of glacierization (about 3 km^2). In the enlarged 1991 MSS image (fig. 6*B*), it is clear that the glaciers on Pico La Concha have disappeared. The glaciers on Pico Bolívar are so small that seeing them is almost impossible. The glaciers on Picos Humbolt-Bonpland are visible but greatly reduced in size. Figure 7 is an index map showing the location and coverage of the optimum Landsat imagery.

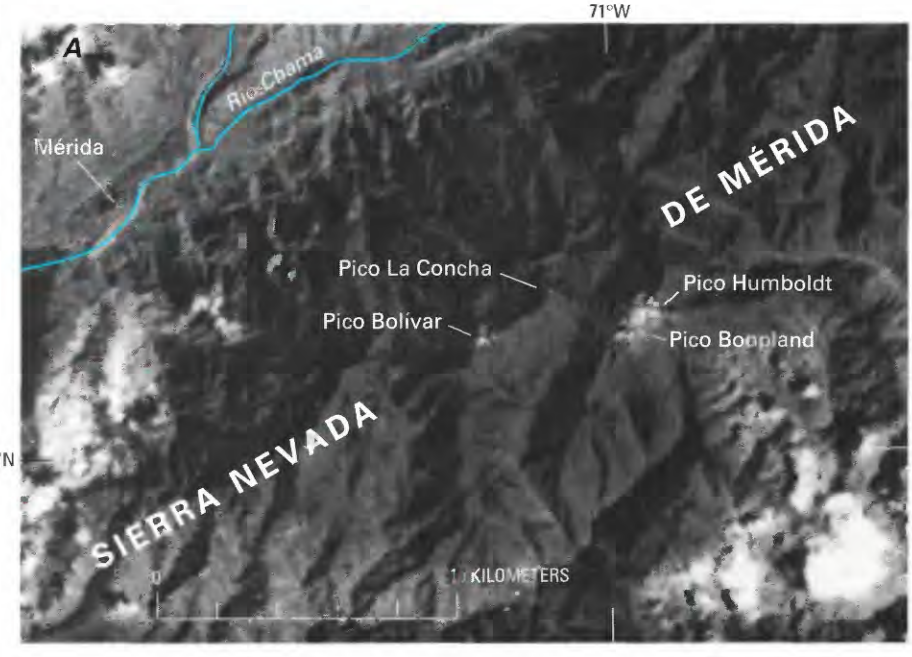

***Figure 6.**—Enlarged 1:250,000-scale Landsat images showing the Sierra Nevada de Mérida glaciers.*
A, *Annotated Landsat 2 MSS image. Compare with figures 5 and 6*B. *The town of Mérida is indicated. Landsat 2 image (2372–14164, band 7; 29 January 1976; Path 6, Row 54) from EROS Data Center, Sioux Falls, S. Dak.*
B, *See following page.*

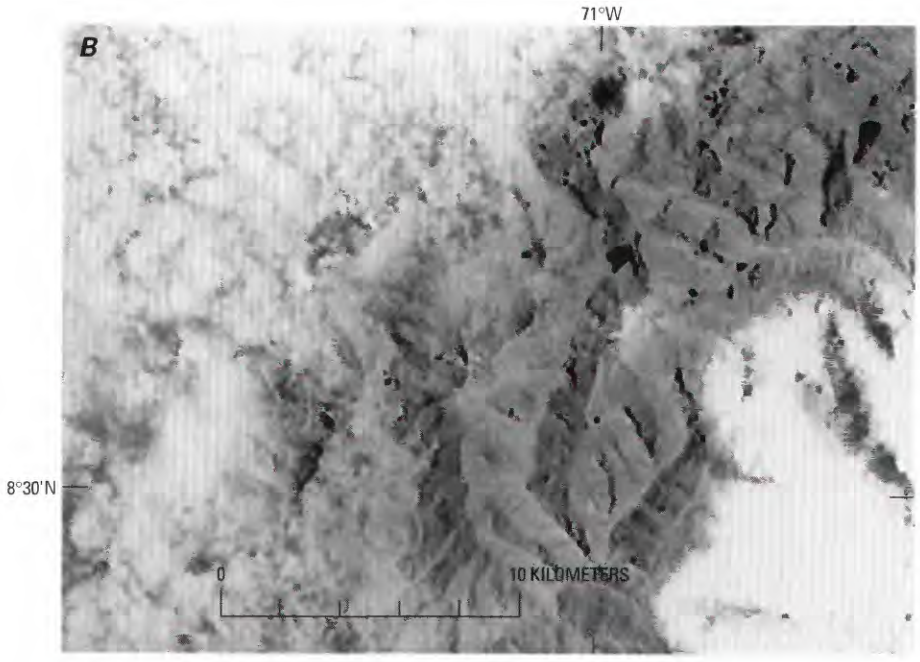

***Figure 6B**.—Landsat 5 MSS image. In spite of some clouds, it is possible to see that the glaciers have substantially retreated. Landsat 5 MSS image (52580–14204, band 4; 25 March 1991; Path 6, Row 54) from EROS Data Center, Sioux Falls, S. Dak.*

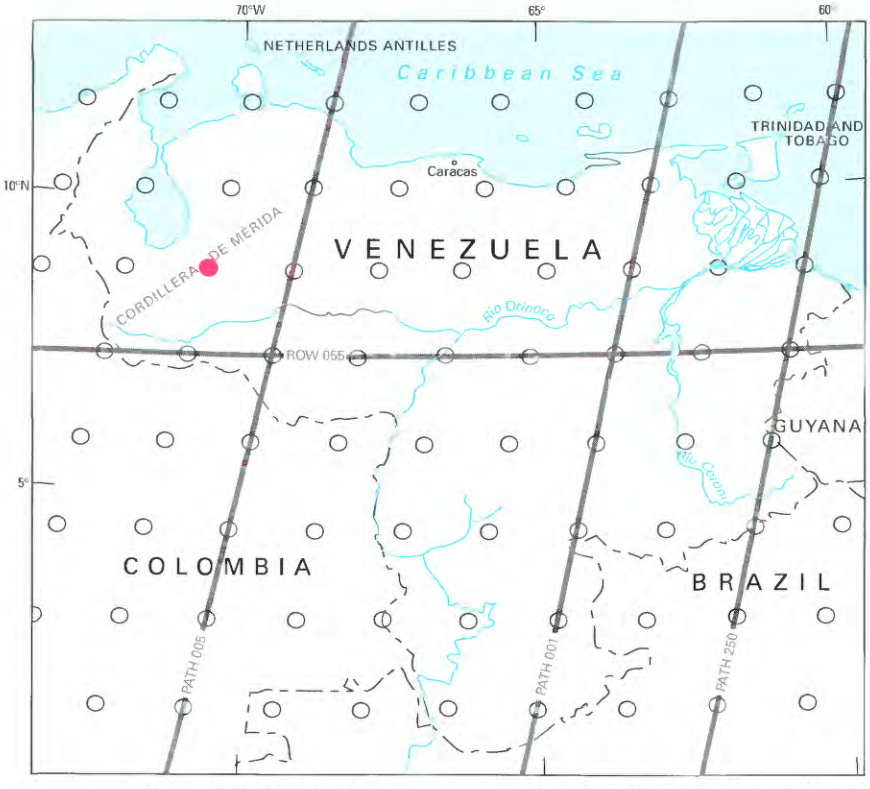

***Figure 7**.—Optimum Landsat 1, 2, and 3 images of the glaciers of Venezuela.*

TABLE 2.—*Optimum Landsat 1, 2, and 3 images of the glaciers of Venezuela*
[See fig.7 for explanation of symbols used in "Code" column]

Path-Row	Nominal scene center (lat-long)	Landsat identification number	Date	Solar elevation angle (degrees)	Code	Cloud cover (percent)	Remarks
6–54	08°40'N. 70°38'W.	2372–14164	29 Jan 76	42	●	0	Pico Bolívar, Pico La Concha, Pico Humboldt, and Pico Bonpland glaciers; image used for figures 2, 6
6–54	08°40'N. 70°38'W.	21434–14055	26 Dec 78	40	●	0	Pico Bolívar, Pico La Concha, Pico Humboldt, and Pico Bonpland glaciers
6–54	08°40'N. 70°38'W.	31385–14195	19 Dec 81	40	●	0	
			Selected Landsat 4 and 5 images				
6–54	08°41'N. 70°29'W.	50356–14293	20 Feb 85	48	●	0	Pico Bolívar, Pico La Concha, Pico Humboldt, and Pico Bonpland glaciers
6–54	08°41'N. 70°29'W.	52580–14204	25 Mar 91	52	◕	10	Pico Bolivar, Pico La Concha, Pico Humboldt, and Pico Bonpland glaciers; image used for figure 6

Recent Glacier Recession

Early reports and paintings can be used to determine the approximate location and extent of the glaciers in the Sierra Nevada de Mérida in the mid- to late-1800's. A comparison of these sources with present-day conditions indicates that a rapid retreat has taken place during the last 100 years (Schubert, 1980, 1984, 1987). The amount of retreat can be estimated by comparing the mapping of the glaciers by Jahn in 1910 (fig. 4) with the mapping and analysis by this author using 1952 data (figs. 4 and 5). The glaciers in the Sierra Nevada de Mérida, estimated to cover 200 km^2 during the Pleistocene (Schubert, 1972, 1984), were approximately 10 km^2 in 1910 and about 3 km^2 in 1952 (Schubert, 1972, 1980). However, the 1952 area was probably somewhat larger than indicated by these figures because the high slope angle of the glacier surfaces was not taken into account when the measurements were made. In addition, the accuracy of the measurements also is affected by the distortion within the aerial photographs caused by the rugged topography.

Since 1952, ground photographs and fieldwork have documented a significant retreat of the glaciers; the recession is particularly evident since 1972 (Schubert, 1992). Of the 10 glaciers mapped in 1952, 4 have completely or almost completely disappeared, 1 has disintegrated into firn patches, and the remaining 5 are substantially smaller (see table 1). Although it is not possible to quantify the difference exactly, the remaining glacier area is now probably less than 2 km^2. This type of rapid retreat is also found in other parts of South America; such as Colombia, Ecuador, and Perú.

References Cited

Cartografía Nacional, 1977, Map sheets 5941 and 6041: Caracas, República de Venezuela Ministerio de Obras Públicas, Dirección de Cartografía Nacional, scale 1:100,000.

Defense Mapping Agency, 1993, Gazetteer of Venezuela, names approved by the U.S. Board on Geographic Names: Washington, D.C., Defense Mapping Agency, v. 1 and 2, 701 p.

Field, W.O., and associates, 1958, Glaciers of Middle America, map no. 4, *in* Atlas of mountain glaciers in the Northern Hemisphere: Natick, Mass., U.S. Army, Quartermaster Research and Engineering Command Headquarters, Quartermaster Research and Engineering Center, Environmental Protection Research Division, Technical Report EP–92, scale 1:20,000,000.

Fuchs, I.M., 1958, Glaciers of the northern Andes, *in* Geographic study of mountain glaciation in the Northern Hemisphere: New York, American Geographical Society, pt. 3, chap. 4, 14 p.

Giegengack, Robert, and Grauch, R.I., 1975, Quaternary geology of the central Andes, Venezuela: A preliminary assessment: Boletín de Geología (Venezuela), Publicación Especial 7, v. 1, p. 241–283.

Jahn, A., 1912a, La cordillera Venezolana de los Andes [The Andean Cordillera of Venezuela]: Caracas, Revista Técnica del Ministerio de Obras Públicas, p. 1–40.

———1912b, Mis ascensiones a la Sierra Nevada de Mérida [My ascents to the Sierra Nevada de Mérida]: Caracas, El Cojo Illustrado, no. 497, p. 466–474.

———1925, Observaciones glaciológicas en los Andes venezolanos [Glaciological observations in the Venezuelan Andes]: Caracas, Cultura Venezolana, no. 64, p. 265–280.

———1931, El deshielo de la Sierra Nevada de Mérida y sus causas [The deglaciation of the Sierra Nevada de Mérida and its causes]: Caracas, Cultura Venezolana, no. 110, p. 5–15.

Lehr, Paula, 1975, Glaciers of the northern Andes, *in* Field, W.O., ed., Mountain glaciers of the Northern Hemisphere: Hanover, N.H., U.S. Army Corps of Engineers, Cold Region Research and Engineering Laboratory, v. 1, p. 479–490.

Schubert, Carlos, 1972, Geomorphology and glacier retreat in the Pico Bolívar area, Sierra Nevada de Mérida, Venezuela: Zeitschrift für Gletscherkunde und Glazialgeologie, v. 8, no. 1–2, p. 189–202.

———1974, Late Pleistocene Mérida Glaciation, Venezuelan Andes: Boreas, v. 3, no. 4, p. 147–151.

———1975, Glaciation and periglacial morphology in the northwestern Venezuelan Andes: Eiszeitalter und Gegenwart, v. 26, p. 196–211.

———1980, Contribución de Venezuela al inventario mundial de glaciares [Venezuelan contribution to the World Glacier Inventory]: Caracas, Boletín de la Sociedad Venezolana de Ciencias Naturales, v. 34, no. 137, p. 267–279.

———1984, The Pleistocene and recent extent of the glaciers of the Sierra Nevada de Mérida, Venezuela: Stuttgart, Erdwissenschaftliche Forschung, v. 18, p. 269–278.

———1987, La extensión de los glaciares pleistocenos en la Sierra Nevada de Mérida [The extent of Pleistocene glaciers in the Sierra Nevada de Mérida]: Caracas, Boletín de la Sociedad Venezolana de Ciencias Naturales, v. 41, no. 144, p. 299–308.

———1992, The glaciers of the Sierra Nevada de Mérida (Venezuela), a photographic comparison of recent deglaciation: Erdkunde, v. 46, p. 58–64.

Schubert, Carlos, and Clapperton, C.M., 1990, Quaternary glaciation in the northern Andes (Venezuela, Colombia and Ecuador): Quaternary Science Reviews, v. 9, p. 123–125.

Sievers, W., 1886, Über Schneeverhältnisse in der Cordillere Venezuelas [On snow conditions in the Venezuelan Cordillera]: Jahresbericht der Geographischen Gesellschaft in München, 1885, p. 54–57.

———1908, Zur Vergletscherung der Cordilleren des tropischen Südamerikas [Glaciation of the Cordillera of tropical South America]: Zeitschrift für Gletscherkunde, v. 2, no. 4, p. 271–284.

———1911, Die heutige und die frühere Vergletscherung Südamerikas [Present-day and past glaciation in South America]: Leipzig, Vogel Verlag, Sammlung Wissenschaftlicher Vorträge, Heft 5, p. 1–24.

Glaciers of South America–

GLACIERS OF COLOMBIA

By FABIAN HOYOS-PATIÑO

SATELLITE IMAGE ATLAS OF GLACIERS OF THE WORLD

Edited by RICHARD S. WILLIAMS, Jr., *and* JANE G. FERRIGNO

U.S. GEOLOGICAL SURVEY PROFESSIONAL PAPER 1386–I–2

Colombia has many small glaciers that have a total area of approximately 104 square kilometers on six nevados in four areas within the Sierra Nevada de Santa Marta, Cordillera Oriental, and Cordillera Central. The largest glacier (less than 20 square kilometers) is an ice cap on the active Nevado del Ruiz volcano. A consistent and progressive loss of glacier and snowpack area has been noted since the late 1800's in the Colombian Andes, and many glaciers have disappeared altogether during the 20th century

CONTENTS

GLACIERS OF SOUTH AMERICA–

GLACIERS OF COLOMBIA

By FABIAN HOYOS-PATIÑO[1]

Abstract

Snowfields and glaciers in Colombia are limited to the highest peaks and ranges in the Cordillera Central and Cordillera Oriental and above the 4,700–meter elevation on the Sierra Nevada de Santa Marta. The total area of snowfields and glaciers was estimated to be about 104 square kilometers in the early 1970's.

Historical, geographical, and pictorial records point toward a consistent and progressive depletion of ice-and-snow masses in the Colombian Andes since the end of the "Little Ice Age" in the late 1800's. Many glaciers have disappeared during the 20th century, and others are expected to disappear in the coming decades.

Introduction

Geographic Setting

The northernmost extent of the Andes Mountains consists of three branches in southern Colombia (fig. 1). The branches are known from west to east as the Cordillera Occidental[2], Cordillera Central, and Cordillera Oriental. The Cordillera Oriental continues into Venezuela, where it is called the Cordillera de Mérida (Mérida Andes) (see subchapter I–1, "Glaciers of Venezuela"). The Sierra Nevada de Santa Marta, a huge tetrahedral-shaped massif that is detached from the Cordillera Central, rises as an isolated mountain near the Caribbean coast. Two relatively small coastal ranges, the Serranía de Baudó, bordering the northern Pacific coast, and the Serranía de San Jacinto, rising from the Caribbean lowlands, do not belong to the Andes Mountains either geologically or geographically.

Two large rivers, the Río Cauca and the Río Magdalena, divide the three cordilleras. The cordilleras are bordered by extensive coastal lowlands on the north, large plains on the east, and a complex landscape of alluvial plains and valleys, tidal flats, and the Serranía de Baudó on the west. Snowfields and glaciers are restricted to the highest peaks and ranges of the Cordillera Central, Cordillera Oriental, and Sierra Nevada de Santa Marta.

History of Glacier Observations

Glacier phenomena have not received widespread attention in Colombia in the past because of geographic, economic, and cultural reasons. The ordinary layman generally has not been aware of the importance of snow-and-ice masses, either as natural-resource assets or as potential hazards. Water is taken for granted, and geologic hazards, especially if located in remote and poorly known areas, were generally ignored before the catastrophic eruption of the glacier-clad Nevado del Ruiz in 1985, which produced several major lahars (mudflows caused by volcanic activity). However, arid and semiarid lands depend on the nearby snow-covered

Manuscript approved for publication 18 March 1998.

[1] Universidad Nacional de Colombia, Apartado Aéreo 1027, Medellín, Colombia.

[2] Geographic place-names used in this section conform to the usage recommended by the U.S. Board on Geographic Names (Defense Mapping Agency, 1988) in its Gazetteer of Colombia.

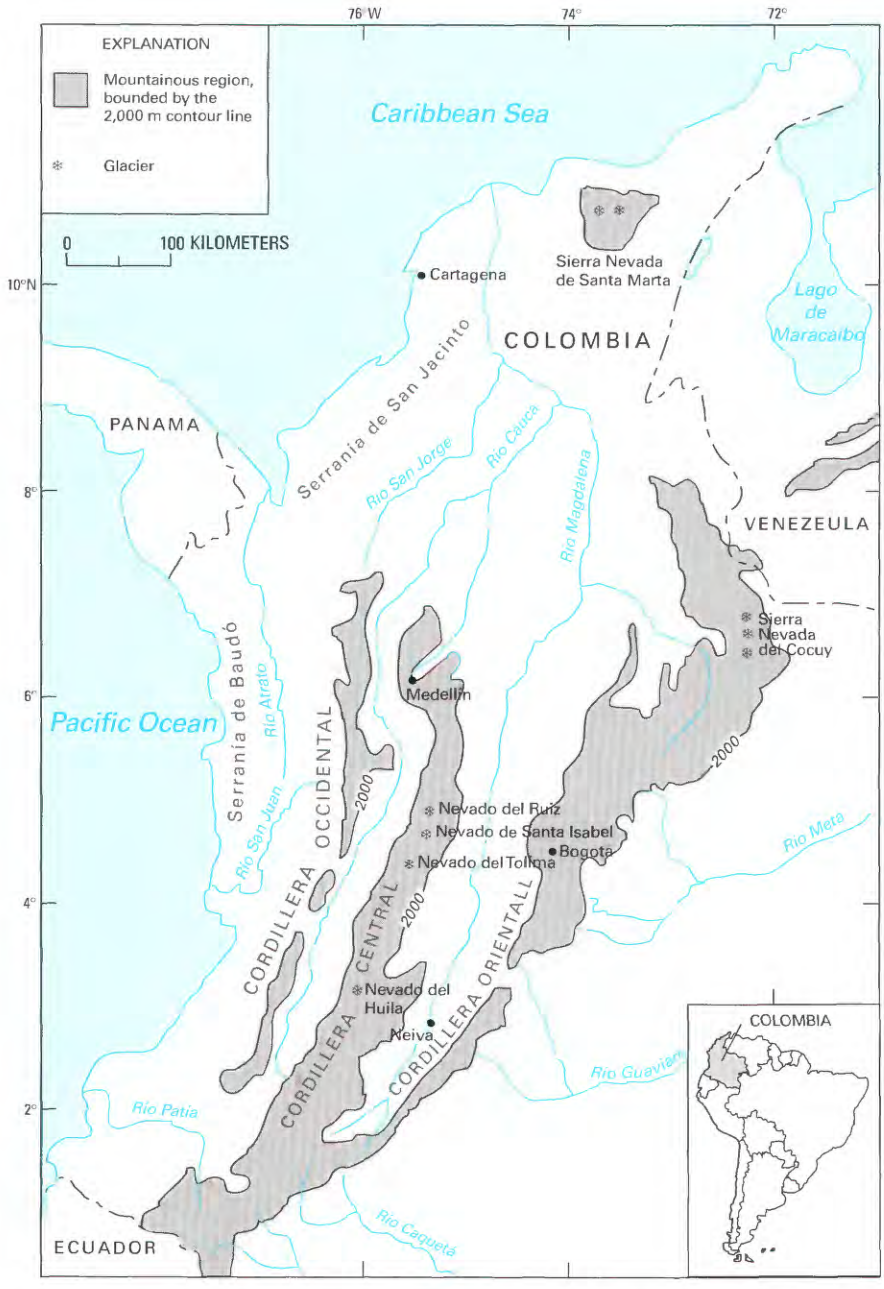

Figure 1.—*Location of glaciers in Colombia. Mountains are delineated by the 2,000-m contour line (heavy dark line).*

mountain ranges for their water supply. Even in humid regions, glaciers act as gigantic reservoirs that regulate seasonal water flow in their respective drainage basins.

The juxtaposition of glaciers and active volcanoes, as well as glaciers and earthquakes, poses a significant geologic hazard that can produce jökulhlaups (outburst floods) and (or) lahars and (or) debris avalanches. Examples are the 1985 eruption of Nevado del Ruiz and the earthquake-generated ice-and-debris avalanche from the Nevados Huascarán massif in Perú that buried the village of Yungay (see subchapter I–4, "Glaciers of Perú"). These types of events have been documented by Acosta (1846) in the 19th century, as well as more recently with respect to the devastation wrought in November 1985 by the volcanic activity of Nevado del Ruiz, a large volcano surmounted by an ice cap (Smithsonian Institution, 1985; Herd and Comité de Estudios Vulcanológicos, 1986; Jordan and Mojica, 1988; Williams, 1990 a, b; Finsterwalder, 1991; Mileti and others, 1991; and Thouret, n.d.). The lahars associated with the Nevado del Ruiz eruption were deemed to be the deadliest ever recorded, as the death toll was estimated to be as much as 23,000 (probably several thousand more if

undocumented migrant workers were included), and most of Armero, a city of about 25,000, disappeared under a huge mudflow.

In June 1994, an avalanche originating in the Nevado del Huila took a toll of at least 1,500 lives and destroyed hundreds of dwellings, tens of bridges, and kilometers of roads in the basin of the Río Páez. This avalanche was unleashed from the glacierized area of the Nevado del Huila and from the steep slopes of the upper Río Páez basin by an earthquake of Richter magnitude 6.2.

The study of snowfields, glaciers, and related features in Colombia has drawn the attention of several scientists, including geologists and geographers (Fuchs, 1958; Lehr, 1975). However, the remoteness of most of the snow-and-ice features has prevented, in the past, a systematic study of their physical characteristics and history. A compilation of available information suggests a consistent snowline retreat during the 20th century or since the end of the "Little Ice Age" in the late 1800's. A more extensive snow cover in the mountain massifs in the past is suggested by the common reference to the "sierras nevadas" (snow-covered summits) in the southern part of the country by the conquistadores and in old chronicles cited by Freire (1958). The Sierra Nevada de los Coconucos (4,300–4,850 m; lat 2°16'N., long 76°22'W.) no longer deserves the name nevada, and the Cerro Nevado at the Páramo de Sumapaz (4,300 m) in the Cordillera Oriental south of Bogotá definitely lost its mantle of snow by 1917 and later changed its name. La Piraña (4,600 m), Nevado del Cisne (5,100 m), and Nevado del Quindío (5,120 m), three formerly snowcapped summits in the Ruiz-Tolima massif (Thouret, n.d.), and the Volcán Chiles (4,750 m) and Nevado de Cumbal (4,764 m), two volcanoes near the southern border, cannot be considered nevados any longer, although they still had a snow or firn cover at the beginning of the 20th century and, in some cases, retain ephemeral snow areas. In the case of today's glacierized areas, this trend toward loss of snow cover is very apparent and will be discussed in more detail later. A similar long-term retreat of the snowline and the recession of glaciers throughout the country is corroborated by a comparison of ancient paintings (Mark, 1976) with recent ground and aerial photographs from different dates and by the evaluation of the physical geographic descriptions of the highlands from old documents and reports (Ancízar, 1853; Reiss and Stübel, 1892; Vergara y Velasco, 1892; Stübel and Wolf, 1906; and Freire, 1958).

Subzero-degree temperatures and the high precipitation necessary to produce snow are found in the high mountains near the Equator. Unlike the climate at mid- and high-latitudes, the seasonal temperature varies little; mean daily temperature is nearly constant. At high altitudes, the largest daily variations (maximum to minimum) of about 25°C take place during the diurnal cycle; however, the average daily temperature does not vary more than ±2°C throughout the year. Solar radiation also varies only slightly (Guhl, 1983). The 0°C air temperature isotherm altitude is at about 4,800 m, although local variations caused by the orographic setting and cloud cover can be found. At low latitudes, the equilibrium line altitude (ELA) roughly coincides with the 0°C air temperature isotherm altitude, although snowfalls can develop as low as 4,000 m. Local differences in snowline altitude can be explained by the orographic effect on moisture distribution and temperature. Short-term variations in snowline altitude originate within a narrow range and are caused by variations in precipitation rather than in temperature. On the other hand, long-term variations in snowline may be caused by changes in precipitation and temperature associated with changes in either local or global climate. Indicators of the level of snowline during the last glacial maximum in the Colombian Andes, such as moraines, reveal that during the Pleistocene, Colombia had a much more extensively glacierized area. Moraines are found consistently all over the Colombian

Andes at 3,800 m; where a sufficient accumulation surface existed, ice reached at least as low as the 3,300-m level during the last advance. An older snowline has been proposed close to the 3,000-m level, and the correlated glacial drift has been observed at least as low as 2,700 m (Coleman, 1935; Oppenheim, 1940, 1942; Raasveldt, 1957; Brunschweiler, 1981; Van der Hammen, 1984; and Helmens, 1990).

Present Snowfields and Glacier Distribution

Work by Thouret and others (1996) examined glacial stades in the Ruiz-Tolima massif and possibly equivalent stades in other glacierized areas (table 1). Thouret and others (1996) noted that the late neoglacial stade (approximately 1600's to 1900's), named the "Little Ice Age," is well documented on the basis of terminal moraines near present glacier termini. Evidence for earlier neoglacial stades is more problematical (Thouret and others, 1992, 1996).

TABLE 1.— *Estimate of the glaciated areas in the Colombian and Ecuadorean Andes during the last ("Fuquene") glaciation*
[Modified from Thouret and others, 1996. Abbreviations: yrs B.P., years before present; ca., circa; MIS, marine isotope stage]

Glacial stade number	Age (yrs B.P.)	Approximate extent of glacierized areas (square kilometers)							Average elevation of ice fronts Ruiz-Tolima (meters above mean sea level)	Average elevation of valley glacier fronts Ruiz-Tolima
		Massif				Total area				
		Nevado del Ruiz, Nevado del Tolima[1]	Sierra Nevada del Cocuy[1]	Sierra Nevada de Santa Marta[1]	Nevada del Huila	Colombian Andes[2]	Ecuadorean Andes[2]	Eastern Africa[2]		
	Present	34–36	28–30	14–18	25–28	100–112	220	9.5	4,750–4,700	4,500–4,400
1b....	Late neoglacial, late Holocene (?)	Inner Ruiz 100	150	107	30(?)	350–400	255	31	4,600–4,300	4,300–4,200
1a....	Early neoglacial, late Holocene (?)	Outer Ruiz	Corralitos	Bolívar						
2b....	Late Santa Isabel-early Holocene [ca. 6,200 (?)]								4,300–4,150	4,300–4,200
2a....	Early Santa Isabel (7,400–7,200)									4,200–4,100
3b....	Late Otun, late late-glacial (ca. 11,000–10,000)		Bocatoma	Naboba		2,600	460	190	4,000–3,800	3,800–3,600
3a....	Early Otun, early late-glacial (MIS 2; ca. 13,000–12,400)	800	1,000 Late Lagunilla	850	250(?)	3,500	2,050		3,800–3,600	3,400–3,300
4b....	Late Murillo-late late full-glacial (ca. 18,000–14,000)		Early Lagunilla	Mamancanaca					3,600–3,400	3,300–3,100
4a....	Early Murillo-early late full-glacial (MIS 3–2; ca. 27,000–24,000)	1,500(?)	2,000(?) Concavo	1,500(?) Aduria-meina	(?)	12,000–15,000	(?)	800	3,400–3,300	3,300–3,100
5b....	Late "Río Recio" early to middle full-glacial (MIS 3; ca. 40,000?)		Río Negro						3,300–3,200	3,100–2,900
5a....	Early "Río Recio" early full-glacial or early glacial(?) (MIS 4; >53,000?)								3,300–3,200	3,100–2,900

[1] Glacial stades in the Ruiz-Tolima massif are given along with possible equivalents in the Sierra Nevada del Cocuy (Van der Hammen and others, 1980/81) and the Sierra Nevada de Santa Marta (Raasveldt, 1957; Van der Hammen, 1984).

[2] Compare the total glacierized area in the Colombian Andes with that in the Ecuadorean Andes (Hastenrath, 1981) and eastern Africa (Hastenrath, 1984). During the full-glacial period, the glaciers of the Colombian and Ecuadorean Andes were probably the most extensive ice fields among the equatorial high-mountains.

TABLE 2.— *Glaciers of Colombia*
[Modified from Jordan and others, 1989]

Area	Flight years of plotted aerial photographs		Number of glaciers	Position (lat-long)	Size of total glacier area (square kilometers)
Sierra Nevada de Santa Marta	1957, 1974		88	10°34'N., 73°43'W.	16.26
Sierra Nevada del Cocuy	1959, 1978		88	06°27'N., 72°18'W.	39.12
Ruiz			15 (16)		21.4
El Cisne			4		.11
Santa Isabel			16		9.78
Quindio			7		.44
Tolima			11		2.22
Parque Nacional de los Nevados	1959	Subtotal	53 (54)	04°50'N., 75°20'W.	33.95
Nevado del Huila	1965		17	02°55'N., 76°05'W.	19.77
		Total	246 (247)		108.49

TABLE 3.— *Glaciers and snowfields of Colombia measured from Landsat images*

Glacierized area	Date of image	Size (square kilometers)
Sierra Nevada de Santa Marta	01 Jan 73	14.1
Sierra Nevada del Cocuy	18 Jan 73	28.0
Ruiz-Tolima massif (Parque Nacional de los Nevados)	01 Feb 76	
Ruiz		21.3
Santa Isabel		10.8
Tolima		3.8
Nevado del Huila	01 Feb 76	26.0
	Total	104.0

Herd (1973) estimated the extension of the Ruiz-Tolima glaciers to have been 100 km^2 during the "Little Ice Age," and Raasveldt (1957) calculated the extent of the last ice advance during the Bolívar stade to have covered 105 km^2 on the Sierra Nevada de Santa Marta.

Four different areas in Colombia are glacierized at the present: the Sierra Nevada de Santa Marta, the Sierra Nevada del Cocuy (Cordillera Oriental), the Ruiz-Tolima massif (Cordillera Central), and the Nevado del Huila (Cordillera Central). Glaciers in the Sierra Nevada de Santa Marta and in the Sierra Nevada del Cocuy are classified as either mountain or alpine; the Ruiz-Tolima massif and Nevado del Huila are large stratovolcanoes that have shieldlike summit ice caps and a few outlet glaciers.

Various figures have been given for the total extent of glacierized areas in recent years. The variation depends on the technique of measurement and the date of the source materials. Work by Jordan and others (1989) gave the total number of glaciers at 246 or 247 on 9 mountains, with a total area of approximately 109 km^2. His work was based on fieldwork and aerial photography dating from 1957 to 1978 (table 2). This author has measured the extent of ice-and-snow areas on Landsat 1–3 multispectral scanner (MSS) images from the early 1970's and determined a total area of 104 km^2 (see table 3). Although the Landsat imagery does not supply the spatial resolution of vertical aerial photography, it offers the opportunity to look at all the glaciers at the same time by the use of a uniform method. Thouret and others (1996) gave a range from 100 to 112 km^2 for the presently glacierized areas of Colombia.

Sierra Nevada de Santa Marta

Rapidly disappearing glaciers are found on the Sierra Nevada de Santa Marta massif along its east-trending watershed above the 4,700-m elevation; maximum elevations are reached by the 5,775-m-high twin peaks, Pico Simón Bolívar and Pico Cristóbal Colón. Rapid deglaciation in this region was reported in 1939 by Notestein (1939) and confirmed in 1969 by Wood (1970). Van der Hammen (1984) found that considerable expansion of the glaciers took place between about 1500 and 1850 but noted a continuous retreat of glacier termini during the 20th century.

At the time of the Cabot Expedition (Cabot, 1939), the glaciers of the Sierra Nevada comprised five groups, as described by Raasveldt (1957). As previously noted, Raasveldt (1957) estimated the ice extent during the

Bolívar stade to be 105 km^2; he also gave 4,700 m as the generalized elevation of glacier termini and a minimum of 4,500 m based on 1954 aerial photographs. The five groups of glaciers are as follows:

- The Nevado Parra Lleras, the northernmost glaciers of this range
- The glaciers of the Méndez and Ruiz Wilches summits
- The central and largest snow-and-ice-capped tract comprising Ruiz Erazo and Picos Simons, Simón Bolívar, Cristóbal Colón, and Americo Vespucio on an east-trending ridge
- The twin ridges complex of Picos Ojeda-Codazzi-Tulio Ospina and La Reina-Ramírez
- The southernmost glaciers of Picos Tayrona and El Guardián

Maps were compiled that documented the glacier extent at the time of the Cabot Expedition and published by Wood (1941) and Raasveldt (1957) (fig. 2). The glacier extent shown in Wood's map was measured by the use of a planimeter, and the surface area of ice-covered terrain was estimated to be approximately 17.5 km^2 (Wood, 1970). Raasveldt (1957), however, cited the glacier area as covering 39 km^2. Wood (1970), on the basis of 1969 fieldwork and aerial photographs, sketched the glacier extent (fig. 3) and made a very rough estimate that at least one-third of the glacier area had disappeared between 1939 and 1969. Using aerial photography from 1957 and 1974, Jordan and others (1989) gave a preliminary estimate of total glacier area of 16.26 km^2 (table 2). This author measured the ice- and snow-extent in a 1973 Landsat image and estimated a total area of 14.1 km^2 (fig. 4; table 3). Although the measurement techniques used by each author differed, everyone is in agreement that the deglaciation is continuing.

Kraus and Van der Hammen (1959, 1960) reported elevations of glacier termini during 1958, and Van der Hammen (1984) gave corrected elevations (–75 m for each) of 4,745 m for the glacier between Picos Tayrona and El Guardián, 4,855 m for the glacier descending from Pico La Reina, and 4,830 m for the glacier descending between Picos Ojeda and Simón Bolívar. A comparison of these elevations with the earlier maps and later reports indicates that the mass wasting of the glaciers seems to have been more severe on the south-facing slopes and below the 5,100-m elevation. The glaciers of Nevado Parra Lleras and the Méndez, Ruiz Wilches, and Tayrona peaks had disappeared, as had most of the ice-and-snow cover of the south slopes of the Ojeda-La Reina twin ridges. The equilibrium line altitude (ELA) here is estimated to be about 5,100 m. Figure 5 is an oblique aerial photograph of the Sierra Nevada de Santa Marta seen from the east.

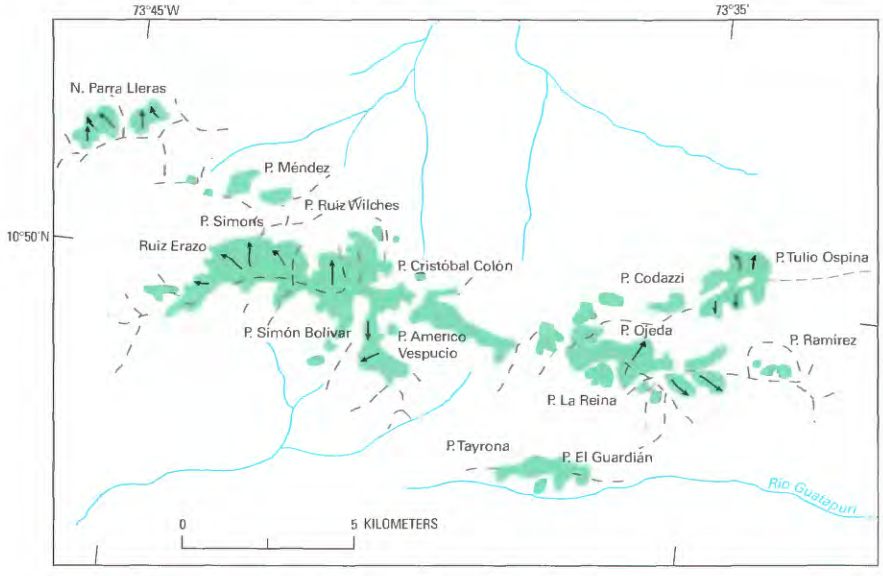

***Figure 2.**—Extent of the glacierized area (green) on the Sierra Nevada de Santa Marta in 1940 drawn from aerial photographs (modified from Raasveldt, 1957).*

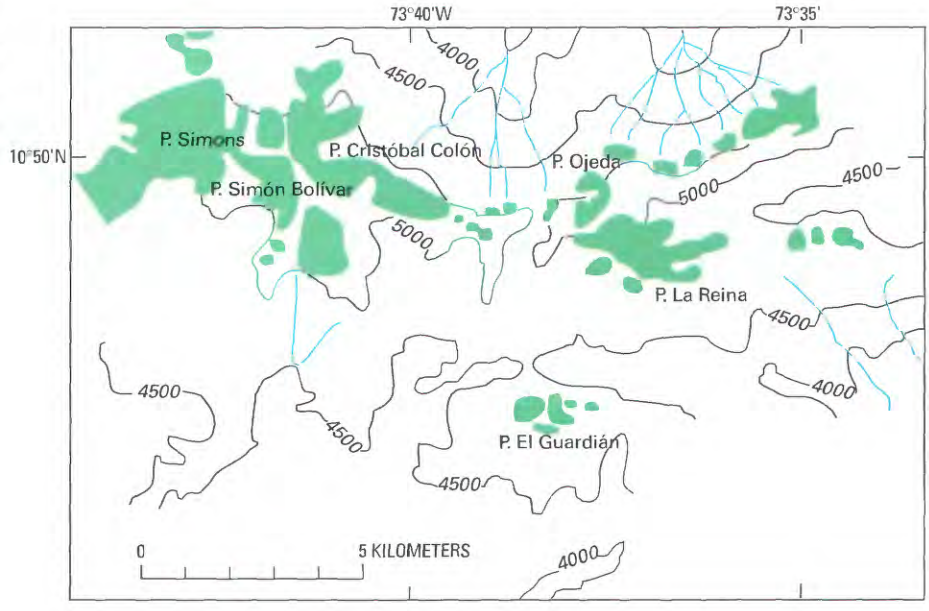

Figure 3.—*Extent of the glacierized area (green) on the Sierra Nevada de Santa Marta in 1969 drawn on the "Cabot" map (Wood, 1941) by using oblique aerial photographs (modified from Wood, 1970).*

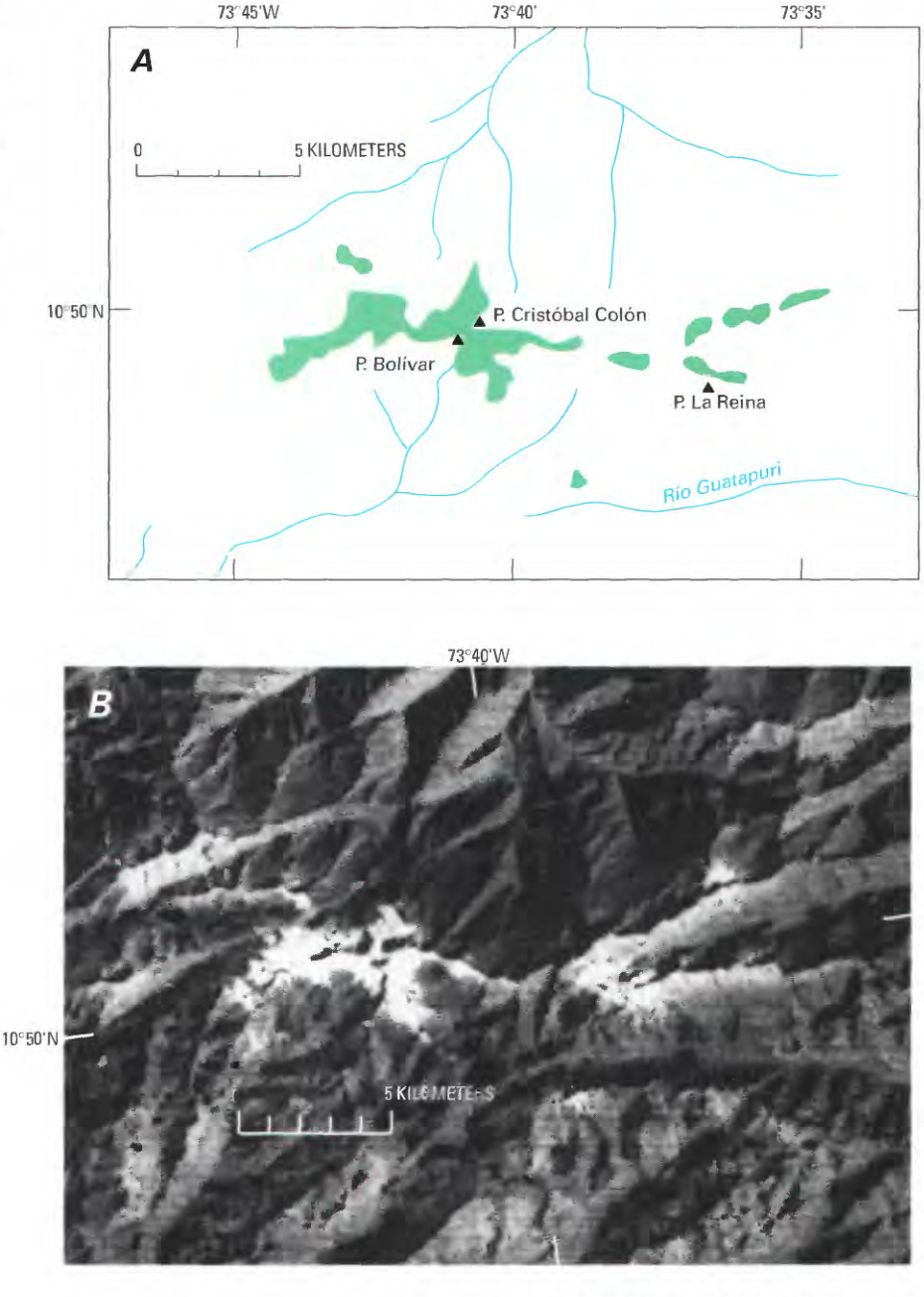

Figure 4.—*Glaciers and snowfields of the Sierra Nevada de Santa Marta.*
A, *Area of glaciers and snowfields, shown in green, calculated from a Landsat 1 MSS image acquired on 1 January 1973, band 7.*
B, *Enlargement of northwestern part of a Landsat 1 MSS image (1162–14421; 1 January 1973; Path 8, Row 53) from the EROS Data Center, Sioux Falls, S. Dak.*

Figure 5.—Oblique aerial photograph of the highest peaks of the Sierra Nevada de Santa Marta seen from the east. Photograph courtesy of Movifoto.

Sierra Nevada del Cocuy (Cordillera Oriental)

The Sierra Nevada del Cocuy trends north-south on the Cordillera Oriental. Mountain glaciers extend along an 18-km-long segment, and glaciers and snowfields measured on a 1973 Landsat image covered an area of 28 km^2 (table 3). However, Jordan and others (1989), using 1959 and 1978 aerial photographs, gave a preliminary estimate of 39.12 km^2 (table 2). In contrast, Thouret and others (1996) gave a range from 28 to 30 km^2 for the glacierized area. Glaciers flow only to the west because of the extremely steep eastern slopes of the range. The highest peak in the range rises 5,493 m above mean sea level. The lowest elevation for a glacier terminus was reported by Ancízar (1853) to be 4,150 m. One hundred years later, Kraus and Van der Hammen (1959, 1960) reported the termini elevations of four glaciers to be between 4,325 and 4,425 m, an estimated average annual retreat of about 1.6 m a^{-1}. The snowline elevation was reported to be at 4,676 m by Ancízar (1853), at 4,780 by Notestein and King (1932), and at 4,900 m by the Cambridge Expedition (Stoddart, 1959). Older long-time residents of the Sierra Nevada del Cocuy have observed a significant retreat of the snowline and glacier termini during the last 50 years.

Figure 6 shows a sketch map prepared from 1955 aerial photographs (Kraus and Van der Hammen, 1959, 1960). Van der Hammen and others (1980/81) published a revised map of the glaciers compiled at a scale of 1:40,000 from 1955 and 1959 aerial photos. Figure 7*A* illustrates the glacier extent in 1973, which was estimated to be about 22 km^2 as shown on a Landsat MSS image (1179–14373; 18 January 1973; fig. 7*B*). A small but noticeable change in area took place during the 1955–1973 period, which can be estimated as a reduction of 6 km^2.

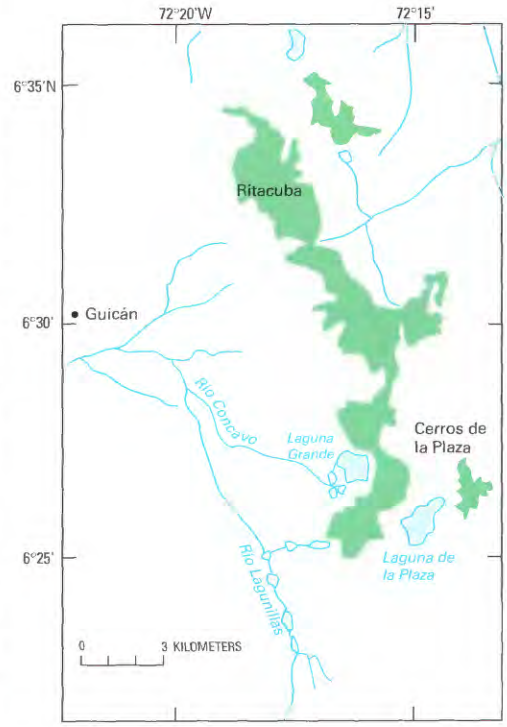

Figure 6.—Glacierized area (green) on the Sierra Nevada del Cocuy drawn from 1955 aerial photographs (modified from Kraus and Van der Hammen, 1959, 1960). Van der Hammen and others (1980/81) produced a revised map of part of the area encompassed by figure 6.

Ruiz-Tolima Volcanic Massif (Cordillera Central)

The Ruiz-Tolima volcanic massif comprises five different formerly ice-clad stratovolcanoes ("nevados"): El Ruiz, El Cisne, Santa Isabel, El Quindío, El Tolima (figs. 8, 9). El Cisne and El Quindío have nearly lost their snowfields; their ephemeral snow- and ice-covered areas are barely 1 km^2 each. The other three may be classified as mountain ice caps. Figure 8*A* is a sketch map of the glaciers and snowfields of the Ruiz-Tolima massif drawn from a 1 February 1976 Landsat 2 MSS color-composite image (shown in fig. 8*B*).

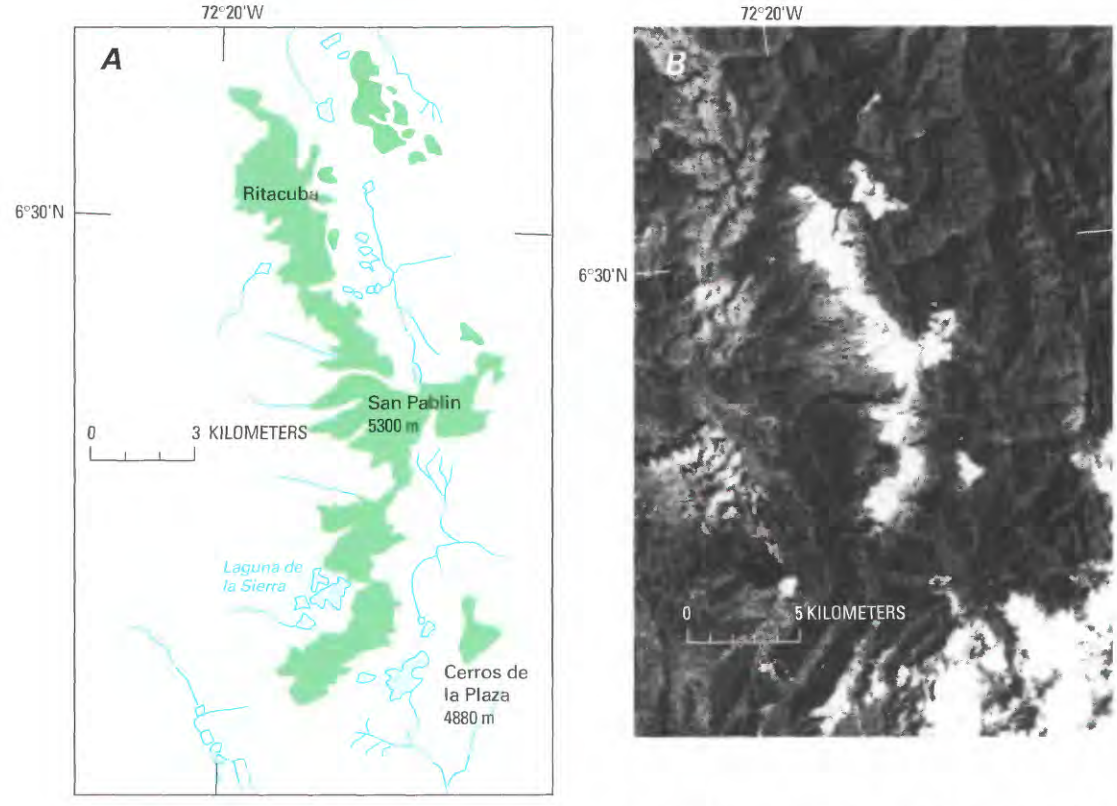

Figure 7. *—Glaciers and snowfields of the Sierra Nevada del Cocuy.* **A**, *Area of glaciers and snowfields, shown in green, calculated from a Landsat 1 MSS image acquired on 18 January 1973.* **B**, *Enlargement of northeastern part of Landsat 1 MSS image (1179–14373, band 7; 18 January 1973; Path 7, Row 56) from the EROS Data Center, Sioux Falls, S. Dak.*

Nevado del Ruiz is the highest and most extensive stratovolcano in this massif (figs. 9, 10, 11). It rises more than 5,300 m above mean sea level and supports an ice cap that had an area of 21.3 km^2 measured on a 1976 Landsat image. The snowline is at an altitude of 4,900 m on its west flank and 4,800 m on the east flank. A comparison between 19th century paintings (Mark, 1976) (figs. 10*A*, *B*) and a recent photograph (fig. 11) shows an impressive retreat of the margins of the ice cap, which Herd (1982) estimated at 150 m, equivalent to a shrinkage of 64 percent from the area of the ice cap in 1845.

In 1983, the Central Hidroelectrica de Caldas (CHEC) (1983) published a study of geothermal activity in the Nevado del Ruiz volcanic massif. However, in November 1985, Nevado del Ruiz erupted (Sigurdsson and Carey, 1986), and according to Thouret (1990), about 16 percent (4.2 km^2) of the surface area of the ice and snow of this nevado was lost, and 25 percent of the remaining ice was fractured and destabilized by earthquakes and explosive volcanic activity. The associated volume decrease was estimated to be approximately 6×10^7 m^3 or 9 percent of the total volume of ice and snow (Thouret, 1990; Williams, 1990a, b); figure 12 illustrates the extent of the ice and snow lost during the 1985 eruption. Glaciological changes have also been analyzed by Jordan and others (1987). A digital, color orthophoto map by Finsterwalder (1991) provides a precise topographic and image baseline for comparison with past and future maps of the glaciological status and extent (area and volume) of the ice cap on Nevado del Ruiz.

Between 1986 and 1995, the average retreat rate of the glacierized area of the Nevado del Ruiz has increased to 3–4 m a^{-1}, which amounts to 20–30 m in elevation, owing to the decrease in albedo associated with the tephra cover deposited during the 1985 volcanic activity. Faster retreat has been noted on individual glaciers. Ramírez and Guarnizo (1994) reported 13 m for the vertical retreat of a single, isolated glacier on the western flank

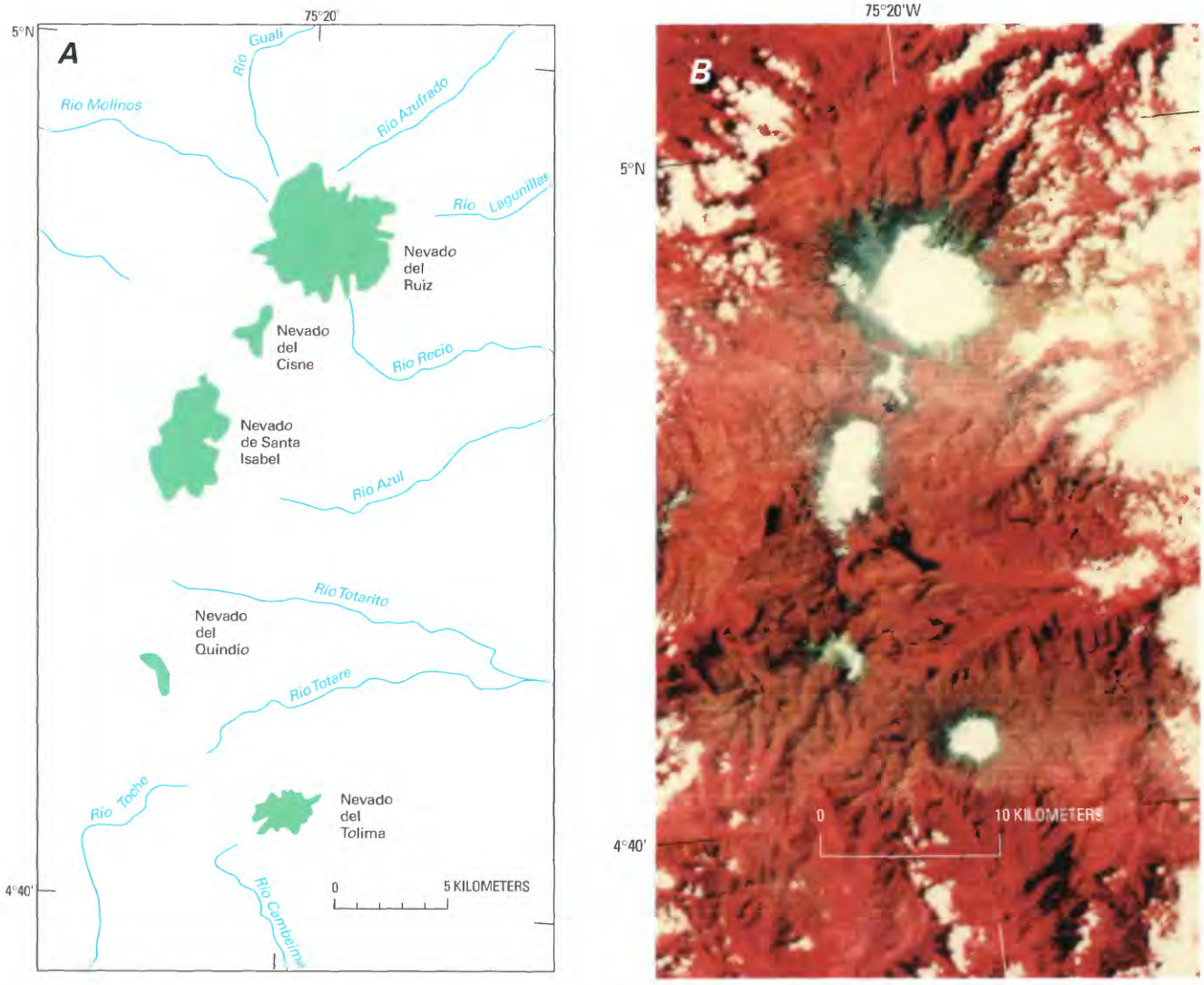

Figure 8.—*Glaciers and snowfields of the Ruiz-Tolima volcanic massif.* **A**, *Area of glaciers and snowfields, shown in green, calculated from a Landsat 2 MSS image acquired on 1 February 1976.* **B**, *Enlargement of northeastern part of Landsat 2 MSS false-color composite image (2375–14350; 1 February 1976; Path 9, Row 57) from the EROS Data Center, Sioux Falls, S. Dak.*

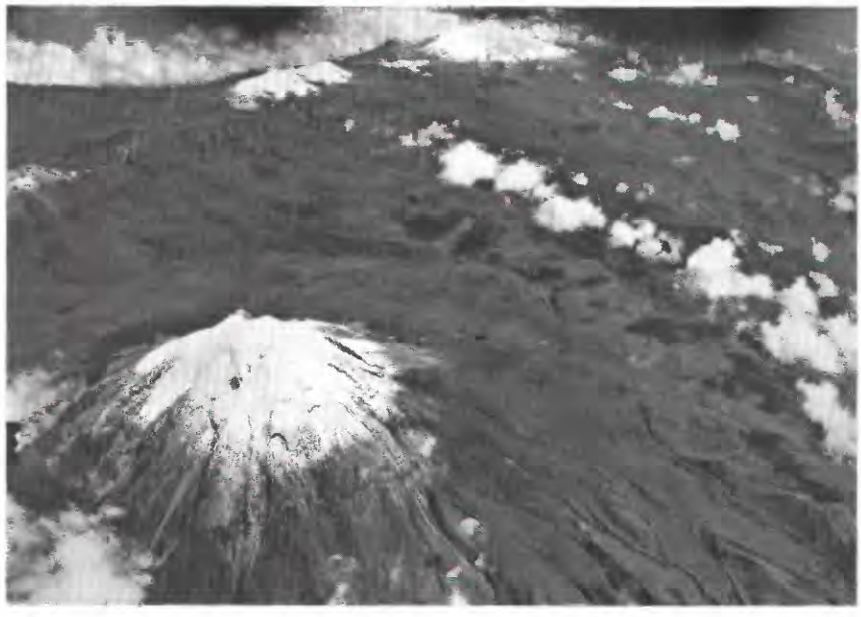

Figure 9.—*Oblique aerial photograph looking to the north-northwest across Nevado del Tolima (foreground) towards Nevado de Santa Isabel, Nevado del Ruiz, and Nevado del Cisne in the background. Part of Nevado del Quindío is on the left margin. Photograph courtesy of Instituto Geográfico Augustín Codazzi taken in 1959.*

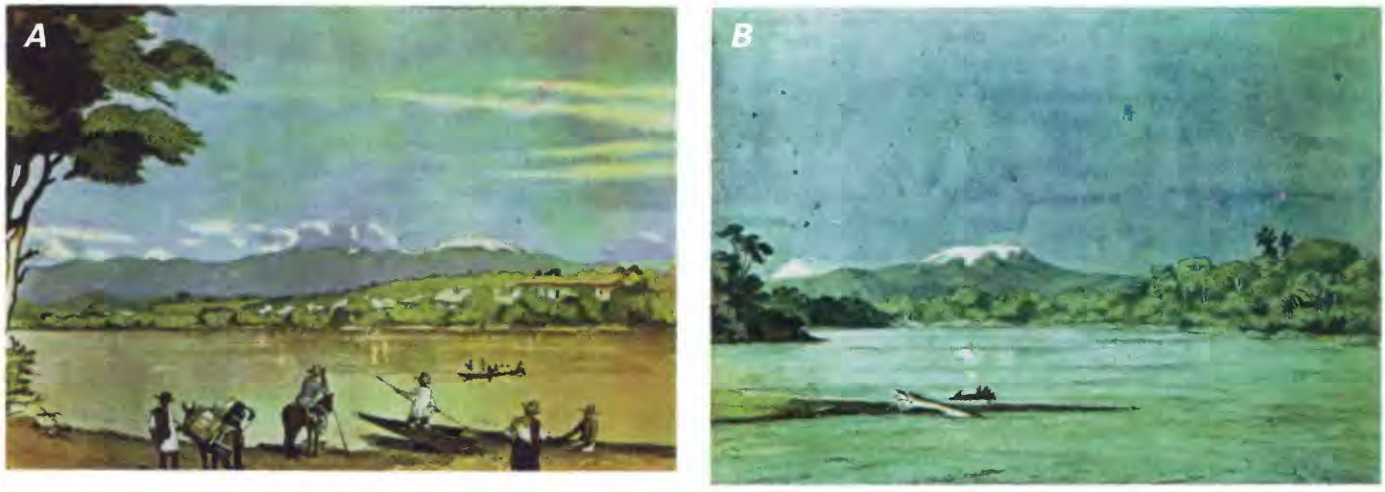

Figure 10.—*Nineteenth-century paintings of the Ruiz-Tolima volcano complex by E. Mark.* **A**, *Nevado del Ruiz (right), Nevado de Santa Isabel, and Nevado del Tolima (left) are seen from the Magdalena Valley (watercolor painted in 1846).* **B**, *Nevado del Ruiz (right) and Nevado del Tolima (left) also seen from the Magdalena Valley (watercolor painted in 1845). Reproduced with the permission of the Biblioteca Luis Angel Arango, Bogotá, Colombia.*

Figure 11.—*Ruiz-Tolima massif looking south-southwest in 1986. The active Nevado del Ruiz volcano is in the foreground, the Nevado del Tolima is in the left background and the Nevado de Santa Isabel is in the center background. Photograph courtesy of Ingeominas.*

of the glacierized area over the period 1987–1988 and 8.8 m over the period 1990–1991. Linder (1991, 1991/1993), Linder and Jordan (1991), and Linder and others (1994), using aerial photogrammetric methods and digital elevation models, calculated posteruptive loss of ice volume. The figures show that ice loss is continuing at a greater rate than the average preeruption retreat.

El Cisne has a maximum elevation of 5,100 m, and its accumulation area is now so small that it is no longer considered to be a nevado. It supports only ephemeral snowfields.

The Nevado de Santa Isabel rises to 5,110 m above mean sea level and has a snowline at 4,800 m on its west flank and 4,700 m on its east flank. The snow-and-ice cover was measured as 10.8 km^2 on a 1976 Landsat image. Since 1986, this nevado has undergone a similar but more moderate increase in loss of its glacierized area compared to the Nevado del Ruiz. In addition, the snowline has risen 10–15 m in the period 1986–1994.

The maximum elevation of El Quindío is 5,120 m above mean sea level. Although above the regional snowline, the accumulation area is so small that it can no longer be considered to be a perennial snowfield.

The highest point on Nevado del Tolima is 5,280 m above mean sea level (fig. 13). Glaciers descend to 4,740 m on the west side of the volcano and to 4,690 m on the east side (Herd, 1982). The area of its ice cap was 3.8 km^2 measured on a 1976 Landsat image (fig. 8*B*). A newly published, digital, color orthophoto map accurately shows the ice cap and outlet glaciers on the summit of Nevado del Tolima (Finsterwalder, 1992).

Nevado del Huila (Cordillera Central)

The snow-capped Nevado del Huila volcano (fig. 14), which rises to 5,750 m above mean sea level, supported a snow- and ice-covered area

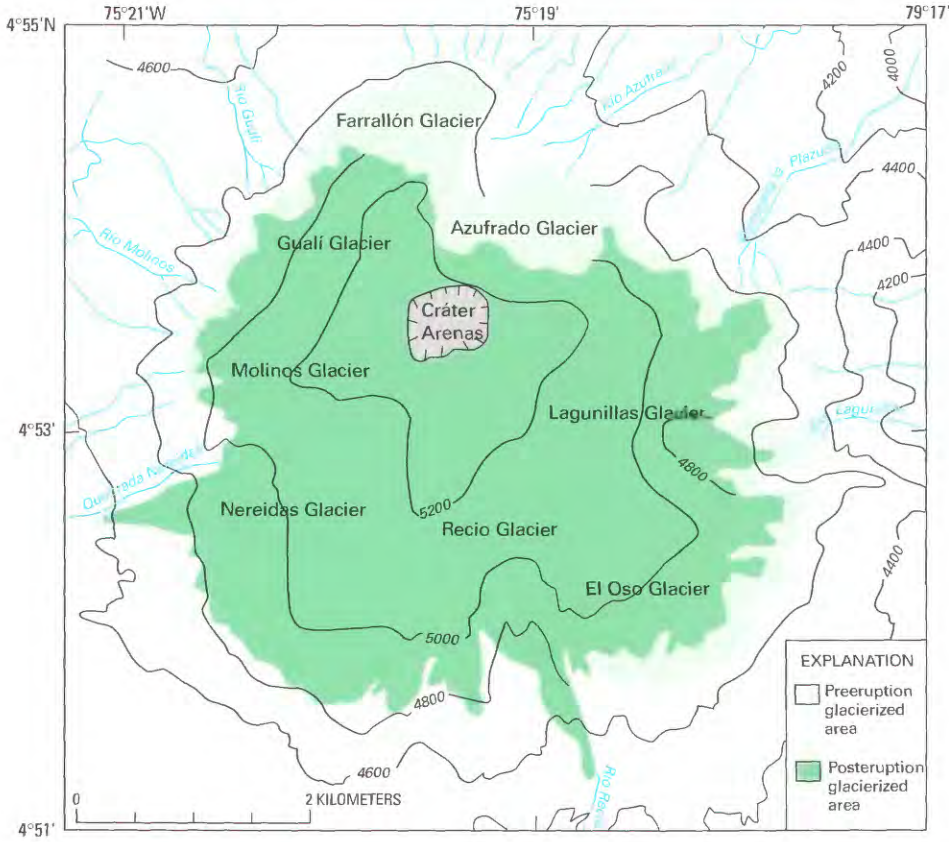

Figure 12.—*Effect of the November 1985 volcanic eruption on the Nevado del Ruiz ice cap (modified from Thouret, 1990).*

Figure 13.—*Nevado del Tolima in the foreground and Nevado de Santa Isabel in the background seen from the southeast. Photograph courtesy of Villegas (1993).*

Figure 14.—*Nevado del Huila seen from the southeast. Photograph courtesy of Villegas (1993).*

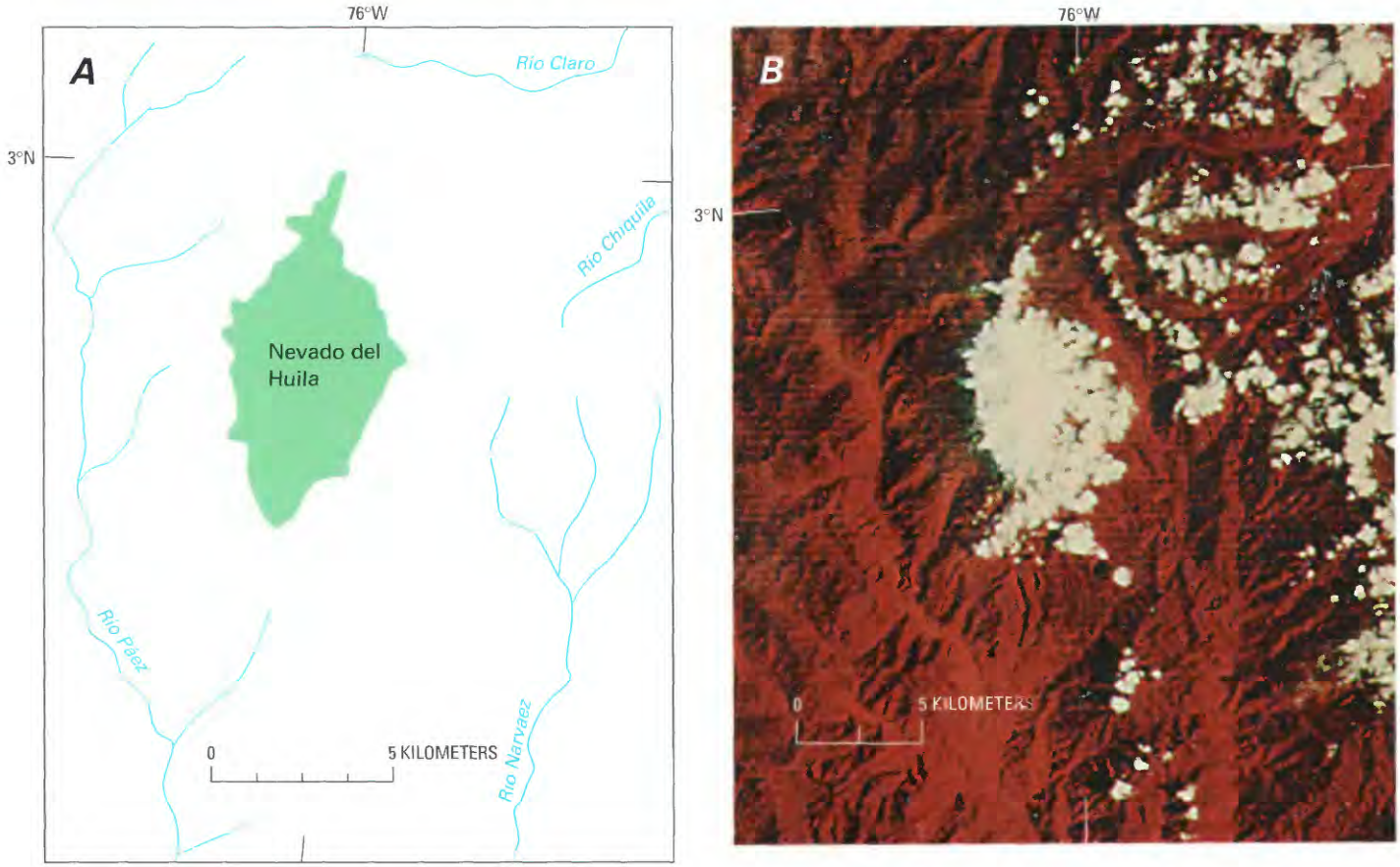

Figure 15.—*Glaciers and snowfields of the Nevado del Huila.* **A**, *Area of glaciers and snowfields, shown in green, calculated from a Landsat 2 MSS image acquired on 1 February 1976.* **B**, *Enlargement of northeastern part of a Landsat 2 MSS false-color composite image (2375–14353; 1 February 1976; Path 9, Row 58) from EROS Data Center, Sioux Falls, S. Dak.*

of 26 km^2 measured on a 1976 Landsat image (fig. 15A, B). Early maps (Vergara y Velasco, 1892) compared to the 1976 Landsat image (2375–14353; 1 February 1976) suggest little change in snow cover during the last 100 years. However, no reason exists to believe that this mountain constitutes an exception to the general trend of glacier recession in the Colombian Andes. In fact, Reiss and Stübel (1892) reported the terminus of a large glacier at 4,337 m and the snowline at 4,484 m, whereas an Ingeominas (1984) report locates the limit of the glacierized area at about 5,100 m. These figures indicate that the snowline and glacier termini have receded similarly to, although at a higher rate than, other glacierized areas in Colombia. If these figures can be reliably compared, they indicate that the rate of average glacier retreat in this area amounted to more than 8 $m\,a^{-1}$ between 1892 and 1984.

Maps and Aerial Photographs of the Glaciers of Colombia

Table 4 provides a list of maps that cover the glacierized areas of Colombia from various sources and at various scales. Maps published by the Instituto Geográfico Augustin Codazzi (IGAC) range in scale from 1:25,000 to 1:100,000. Table 5 provides a list of aerial photographs of the glacierized areas of Colombia at scales ranging from 1:10,600 to 1:60,000.

TABLE 4.— *List of maps covering the glacierized areas of Colombia*
[Abbreviation: Do., ditto]

Agency or author	Sheet number	Scale	Glacier areas covered
IGAC (Instituto Geográfico Augustin Codazzi)	19	1:100,000	Sierra Nevada de Santa Marta
IGAC	137	1:100,000	Sierra Nevada del Cocuy
IGAC	225	1:100,000	Ruiz-Tolima massif
IGAC	321	1:100,000	Nevado del Huila
IGAC	19–IV–A	1:25,000	Sierra Nevada de Santa Marta
IGAC	19–IV–B	1:25,000	Do.
IGAC	19–IV–C	1:25,000	Do.
IGAC	19–IV–D	1:25,000	Do.
IGAC	137–IV–A	1:25,000	Sierra Nevada del Cocuy
IGAC	137–IV–B	1:25,000	Do.
IGAC	137–IV–C	1:25,000	Do.
IGAC	137–IV–D	1:25,000	Do.
IGAC	225–II–A	1:25,000	Nevado del Ruiz
IGAC	225–II–C	1:25,000	Nevado de Santa Isabel
IGAC	225–IV–C	1:25,000	Nevado del Tolima
IGAC	321–IV–B	1:25,000	Nevado del Huila
Cabot, 1939[1]		1:1,000,000[2]	Sierra Nevada de Santa Marta
Raasveldt, 1957[1]		1:300,000[2]	Do.
Cambridge Colombian Expedition, Stoddart, 1959[1]	Sketch	1:100,000[2]	Sierra Nevada del Cocuy
Wood, 1970[1]	Sketch	1:100,000[2]	Sierra Nevada de Santa Marta
Kraus and Van der Hammen, 1959[1]	Sketch	1:55,000[2]	Sierra Nevada del Cocuy
Herd, 1973[1]		1:200,000[2]	Nevado del Ruiz-Nevado del Tolima
Thouret, 1990[1]		1:50,000[2]	Nevado del Ruiz

[1] As in cited references.
[2] Approximate scales.

TABLE 5.— *Aerial photographic coverage of the glacerized areas of Colombia*
[Abbreviation: Do., ditto]

Year	Flight line number	Frame	Approximate scale	Scene
1954	M226054	1876–1879	1:60,000	Sierra Nevada de Santa Marta
1954	M226054	1914–1920	1:60,000	Do.
1954	M246054	2190–2197	1:60,000	Do.
1954	M246054	2239–2245	1:60,000	Do.
1954	M266054	2312–2320	1:60,000	Do.
1954	M266054	2335–2340	1:60,000	Do.
1989	C23722389	0053–0072	1:22,500	Do.
1989	C23732489	0033–0052[1]	1:24,400	Do.
1989	C23732589	0073–0087	1:24,200	Do.
1989	C23732689	0003–0020	1:24,700	Do.
1989	C23732989	0156–0160	1:29,200	Do.
1989	C23732989	0165–0175	1:29,200	Do.
1960	M5456059	6243–6252	1:60,000	Sierra Nevada del Cocuy
1960	M5986059	8059–8073	1:60,000	Do.
1960	M8026059	8365–8375	1:60,000	Do.
1961	M10066059	10437–10444	1:60,000	Do.
1961	M10446059	12021–12030	1:60,000	Do.
1962	M11536059	20012–20028	1:60,000	Do.
1959	M5476059	6558–6562	1:60,000	Nevado del Ruiz
1959	M5476059	6578–6580	1:60,000	Nevado de Santa Isabel
1959	M5476059	6584	1:60,000	Nevado del Tolima
1959	M5486059	7031–7034	1:60,000	Nevado de Santa Isabel
1959	M5526059	7573–7576	1:60,000	Nevado del Ruiz
1959	M5526059	7581–7583	1:60,000	Do.
1959	M5526059	7603–7605	1:60,000	Nevado de Santa Isabel
1959	M5526059	7606–7609	1:60,000	Nevado del Ruiz
1986	C22692786	0145–0147	1:26,750	Nevado del Tolima
1986	C22692786	0154–0160	1:26,750	Nevado del Ruiz
1987	C23081387	0043–0071	1:12,650	Nevado del Ruiz-Nevado de Santa Isabel
1987	C23081187	0097–0116[2]	1:10,600	Nevado del Ruiz
1987	C23941287	0048–0085	1:12,300	Nevado del Ruiz-Nevado del Tolima
1990	C24181990	0101–0144	1:18,800	Nevado del Ruiz
1965	M13436061	35610–35616	1:60,000	Nevado del Huila
1995	R11942895	0029–0036	1:25,800	Do.
1995	R11942695	0163–0171	1:25,800	Do.
1995	R11942595	0230–0238	1:25,800	Do.

[1] Frame 52 partially cloud covered.

[2] Frames 0097–0101 partially cloud covered.

Landsat Imagery

Only a limited number of cloud-free Landsat 1–3 images were acquired of the glacierized areas of Colombia. The best are listed in table 6, and their area of coverage is shown in figure 16. The imagery has been used in this chapter to delineate the areal coverage of ice and snow on the Colombian nevados,

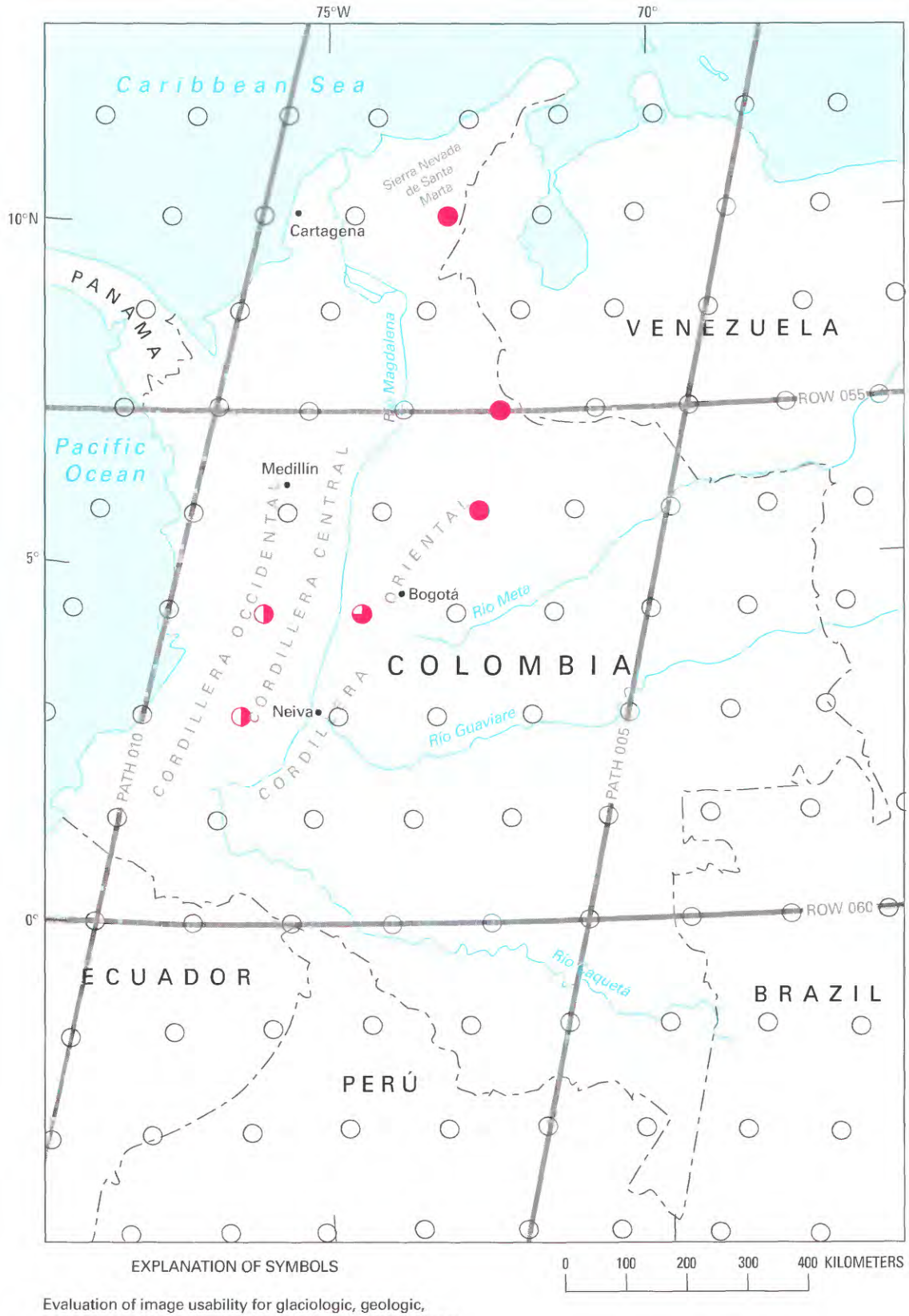

Figure 16.—*Optimum Landsat 1, 2, and 3 images of the glaciers of Colombia.*

TABLE 6. — *Optimum Landsat 1, 2, and 3 images of the glaciers of Colombia*
[See fig. 16 for explanation of symbols used in "Code" column]

Path-Row	Nominal scene center (lat-long)	Landsat identification number	Date	Solar elevation angle (degrees)	Code	Cloud cover (percent)	Remarks
7–55	07°13'N. 72°24'W.	30306–14262	05 Jan 79	43	●	0	Sierra Nevada del Cocuy
7–56	05°47'N. 72°45'W.	1179–14373	18 Jan 73	46	●	0	Sierra Nevada del Cocuy; image used for figure 7
8–53	10°06'N. 73°10'W.	1162–14421	01 Jan 73	43	●	0	Sierra Nevada de Santa Marta; image used for figure 4*B*
8–53	10°06'N. 73°10'W.	2716–14170	07 Jan 77	38	●	0	Sierra Nevada de Santa Marta
8–57	04°20'N. 74°31'W.	2716–14184	07 Jan 77	41	◕	10	Nevado del Tolima
9–57	04°20'N. 75°57'W.	2375–14350	01 Feb 76	44	◑	20	Nevado del Ruiz-Nevado del Tolima; image used for figure 8*B*
9–58	02°53'N. 76°17'W.	2375–14353	01 Feb 76	44	◑	40	Sierra Nevada del Huila; image used for figure 15*B*

but it is difficult to differentiate the snow cover from the glacier areas because of the small size of the Colombian glaciers and the limitation of resolution of the Landsat MSS sensor.

The mapping and measurements of snow-and-ice areas from Landsat images tend to be less accurate than measurements of glacierized areas made by the use of vertical aerial photography. This is because of the limitations of the Landsat sensor, particularly the difficulty in differentiating snow from ice. However, the Colombian glaciers appear to be receding fairly rapidly, and until new aerial photography is acquired and analyzed of all the glacier areas, this study offers the best comprehensive baseline comparison of the glacierized areas of Colombia. Higher resolution Système Probatoire d'Observation de la Terre (SPOT) images were used by Vandemeulebrouck and others (1993) in their study of tephra and lahar deposits in the vicinity of the ice cap on Nevado del Ruiz (fig. 12). Both the Landsat 4 and 5 Thematic Mapper (TM) images (30-m pixels) and the SPOT images (20-m and 10-m pixels) provide higher resolution images than Landsat MSS images (79-m pixels). These and higher resolution, satellite-imaging systems in the future will slowly replace the aerial photogrammetric methods of mapping ice caps and outlet glaciers.

Conclusions

A historical review of glacier fluctuation in Colombia leads to the conclusion that here, as in many places around the world, deglaciation is the rule. The Sierra Nevada de Santa Marta lost at least one-third of its snow- and ice-covered area in the 34 years between 1939 and 1973, and several former glaciers have vanished during this century. In the Sierra Nevada del Cocuy, where actual figures are available, an average retreat of 1.6 m a^{-1} has been computed from Ancízar (1853) and Kraus and Van der Hammen (1959, 1960) during a period of slightly more than 100 years. A similar figure would probably be valid for the Ruiz-Tolima massif, where the snow- and ice-covered area is now reduced to one-third of its 1845 extent. If the Reiss and Stübel (1892) and Ingeominas (1984) figures on the Nevado del Huila are correct, glacier recession there averages more than 8 m a^{-1}. Should the present trend continue, the 104 km^2 of snowfields and glaciers estimated for Colombia in the early 1970's will vanish in the not too distant future.

References Cited

Acosta, J., 1846, Relation de l'éruption boueuse sortie du volcan Ruiz et de la catastrophe de Lagunilla dans la République de la Nouvelle-Grenade [Account of the mud eruption (lahar) originating from the Nevado del Ruiz volcano and the Lagunilla catastrophe in the Republic of New Granada (Colombia)]: Paris, Académie des Sciences, Comptes Rendus, v. 22, p. 709–710.

Ancízar, Manuel, 1853, Peregrinación de Alpha (M. Ancízar) por las provincias del norte de la Nueva Granada, en 1850 i 51 [Pilgrimage of Alpha (M. Ancízar) in the northern provinces of New Granada (Colombia), in 1850 and 1851]: Bogotá, Echeverría hermanos, 524 p.

Brunschweiler, D., 1981, Glacial and periglacial form systems of the Colombian Quaternary: Bogotá, Revista CIAF [Centro Interamericano por Fotointerpretación], v. 6, p. 53–76.

Cabot, T.D., 1939, The Cabot Expedition to the Sierra Nevada de Santa Marta of Colombia: Geographical Review, v. 29, no. 4, p. 587–621.

Central Hidroelectrica de Caldos (CHEC), 1983, Investigación geotérmica en el Macizo Volcánico del Ruiz [Geothermal investigation of the volcanic massif of Ruiz], phase 2, stage A: Bogotá, Geovulcanología, v. 3, 194 p.

Coleman, A.P., 1935, Pleistocene glaciation in the Andes of Colombia: Geographical Journal, v. 86, no. 4, p. 330–334.

Finsterwalder, R., 1991, Nevado del Ruiz: 1:12,500-scale orthophoto map; prepared with the assistance of the Deutschen Forschungsgemeinschaft at the Lehrstuhl für Kartographie und Reproduktionstechnik der Technischen Universität München: Munich, Arbeitsgemeinschaft für Vergleichende Hochgebirgsforschung.

———1992, Nevado del Tolima: 1:12,500-scale orthophoto map; prepared at the Lehrstuhl für Kartographie und Reproduktionstechnik der Technischen Universität München: Munich, Arbeitsgemeinschaft für Vergleichende Hochgebirgsforschung.

Freire, J., 1958, Invasión del país de los Chibchas [Invasion of the country of the Chibchas]: Bogotá, Ediciones Tercer Mundo, 156 p.

Fuchs, I.M., 1958, Glaciers of the northern Andes, *in* Geographic study of mountain glaciation in the Northern Hemisphere: New York, American Geographical Society, pt. 3, chap. 4, 14 p.

Guhl, E., 1983, Los páramos circundantes de la Sabana de Bogotá [The paramos (high plateau) surrounding the Sabana (extended plain) of Bogotá]: Bogotá, Jardin Botánico José Celestino Mutis, 127 p.

Hastenrath, S., 1981, The glaciation of the Ecuadorian Andes: Rotterdam, A.A. Balkema Publishers, 159 p.

———1984, The glaciers of equatorial East Africa: Dordrecht, Boston, Lancaster, D. Reidel Publishing Company, 353 p.

Helmens, K., 1990, Neogene-Quaternary geology of the high plain of Bogotá, Eastern Cordillera, Colombia (stratigraphy, paleoenvironments and landscape evolution): Berlin-Stuttgart, J. Cramer Verlag, Dissertationes Botanicae, 202 p.

Herd, D.G., 1973, Quaternary glaciation and volcanism in the central Cordillera Central, Colombia [abs.]: Geological Society of America Abstracts with Programs, v. 5, no. 1, p. 53–54.

———1982, Glacial and volcanic geology of the Ruiz-Tolima volcanic complex, Cordillera Central, Colombia: Bogotá, Publicationes Geológicas Especiales del Ingeominas, no. 8, 48 p. (Publication of 1974 Ph.D. dissertation at the University of Washington, Seattle, Wash.)

Herd, D.G., and Comité de Estudios Vulcanológicos, 1986, The 1985 Ruiz volcano disaster: EOS (American Geophysical Union Transactions), v. 67, no. 19, p. 457–460.

Ingeominas, 1984, Compilación sobre glaciares en Colombia [Compilation of the glaciers of Colombia]: Bogotá, Oficina de Planeación, Instituto Nacional de Investigaciones Geológico-Mineras [Ingeominas].

Jordan, E., Brieva, J., Calvache, M., Cepeda, H., Colmerares, F., Fernandez, B., Joswig, R., Mojica, J., and Nuñez, A., 1987, Die Vulkangletscherkatastrophe am Nevado del Ruiz/Kolumbien; geowissenschaftliche Zusammenhänge, Ablauf- und kulturlandschaftliche Auswirkungen [The volcano-glacial catastrophe of Nevado del Ruiz, Colombia; geoscientific mechanisms, outlet- and cultural-landscape consequences]: Geoökodynamik, v. 8, no. 2–3, p. 223–244.

Jordan, E., Geyer, K., Linder, W., Fernandez, B., Florez, A., Mojica, J., Niño, O., Torrez, C., and Guarnizo, F., 1989, The recent glaciation of the Colombian Andes: Zentralblatt für Geologie und Paläontologie, pt. 1, no. 5–6, p. 1113–1117.

Jordan, E., and Mojica, J., 1988, Geomorphologische Aspekte der Gletscher-vulkankatastrophe am Nevado del Ruiz/Kolumbien [Geomorphological aspects of the glacio-volcanic catastrophe at Nevado del Ruiz/Colombia], *in* Tagungsbericht und wissenschaftliche Abhandlungen 46 Deutscher Geographentag, München, 1987: Stuttgart, Franz Steiner Verlag, Geomorphologische Hochgebirgsforschung, p. 426–430.

Kraus, E., and Van der Hammen, Thomas, 1959, Las expediciones de glaciología del A.G.I. a las Sierras Nevadas de Santa Marta y del Cocuy [The glaciological expeditions of the International Geophysical Year to the Sierra Nevada de Santa Marta and the Sierra Nevada del Cocuy]: unpublished manuscript, 7 p.

———1960, Las expediciones de glaciología del A.G.I. a las Sierras Nevadas de Santa Marta y del Cocuy [The glaciological expeditions of the International Geophysical Year to the Sierra Nevada de Santa Marta and the Sierra Nevada del Cocuy]: Bogotá, Comité Nacional del Año Geofísico, Instituto Geográfico "Augustín Codazzi," unpublished manuscript, 68 p.

Lehr, Paula, 1975, Glaciers of the northern Andes, *in* Field, W.O., ed., Mountain glaciers of the Northern Hemisphere: Hanover, N.H., U.S. Army Corps of Engineers, Cold Regions Research and Engineering Laboratory, v. 1, p. 479–490.

Linder, Wilfried, 1991, Klimatisch und eruptionsbedingte Eismassenverluste am Nevado del Ruiz, Kolumbien, während der letzten 50 Jahre; Eine Untersuchung auf der Basis digitaler Höhenmodelle [Climatic and eruption-related ice-cap volume reduction on Nevado del Ruiz, Colombia, during the last 50 years; an investigation based on a digital elevation model]: Hannover, Universität Hannover, Ph.D. dissertation, 125 p., 3 maps, scale 1:15,000.

———1991/1993, Perdidas en la masa de hielo en el Nevado del Ruiz causadas por procesos climaticos y eruptivos durante los ultimos 50 años; investigación basada en modelos altitudinales digitales [Loss in the ice mass on Nevado del Ruiz caused by climatic and eruptive processes during the last 50 years; investigation based on digital elevation models]: Instituto Geográfico "Augustín Codazzi," Santa Fé de Bogotá, Analisis Geograficos No. 23 (1993) (Traduccion del Aleman), 113 p.

Linder, Wilfried, and Jordan, Ekkehard, 1991, Ice-mass losses at the Nevado del Ruiz, Colombia, under the effect of the volcanic eruption of 1985; a study based on digital elevation models: Santa Fé de Bogotá, Revista Cartográfica, no. 59, p. 105–134.

Linder, Wilfried, Jordan, Ekkehard, and Christke, Kornelia, 1994, Post-eruptive ice-mass losses on the Nevado del Ruiz, Colombia: Zentralblatt für Geologie und Paläontologie, pt. 1, no. 1–2, p. 479–484.

Mark, E., 1976, Colombia: Acuarelas de Mark [Colombia: Watercolors by Mark]: Bogotá, Biblioteca Luis Angel Arango, 330 p.

Mileti, D.S., Bolton, P.A., Fernandez, G., and Updike, R.G., 1991, The eruption of Nevado del Ruiz volcano, Colombia, South America, November 13, 1985: Washington, D.C., National Academy Press, Natural Disaster Studies, v. 4, 109 p.

Notestein, F.B., 1939, Geologic and physiographic notes, appendix II, *in* Cabot, T.D., The Cabot Expedition to the Sierra Nevada de Santa Marta of Colombia: Geographical Review, v. 29, no. 4, p. 616–621.

Notestein, F.B., and King, R.E., 1932, The Sierra Nevada de Cocuy: Geographical Review, v. 22, no. 3, p. 423–430.

Oppenheim, Victor, 1940, Glaciaciones Cuaternarias en la Cordillera Oriental de la Republica de Colombia [Quaternary glaciations in the Cordillera Oriental of the Republic of Colombia]: Revista de la Academia Colombiana de Ciencias Exactas, Físicas y Naturales, v. 4, no. 13, p. 70–81.

———1942, Pleistocene glaciations in Colombia, South America: Congreso Panamericano de Ingeniería de Minas y Geología, 1st Anales, v. 2, pt. 1, p. 834–848.

Raasveldt, H.C., 1957, Las glaciaciones de la Sierra Nevada de Santa Marta [The glaciations of the Sierra Nevada de Santa Marta]: Revista de la Academia Colombiana de Ciencias Exactas, Físicas y Naturales, v. 9, no. 38, p. 469–482.

Ramírez, J., and Guarnizo, L.F., 1994, Valores de ablación de un relicto de glaciar en el volcán Nevado del Ruiz utilizando metodos topográficos [Amount of ablation on a relict glacier on the Nevado del Ruiz volcano using topographic methods]: Boletin de Vias, v. 80, p. 85–112.

Reiss, Wilhelm, and Stübel, Alfons, 1892, Reisen in Sud-America; Geologische Studien in der Republik Colombia [Expeditions in South America; geological studies in the Republic of Colombia]: Berlin, A. Asher and Co., v. 1, 204 p.

Sigurdsson, H., and Carey, S., 1986, Volcanic disasters in Latin America and the 13th eruption of Nevado del Ruiz volcano in Colombia: Disasters, v. 10, p. 205–216.

Smithsonian Institution, 1985, Volcanic events: SEAN [Scientific Event Alert Network] Bulletin: v. 10, no. 10, p. 2–4.

Stoddart, D.R., 1959, Report of the glaciological party of the Cambridge Expedition to the Sierra Nevada del Cocuy: Cambridge, England, Cambridge University, St. John's College, unpublished manuscript, 30 p.

Stübel, Alfons, and Wolf, Theodor, 1906, Die Vulkanberge von Colombia [The volcanic mountains of Colombia]: Dresden, Wilhelm Baensch, 154 p.

Thouret, J.–C., [n.d.], Le massif volcanique du Ruiz-Tolima, Cordillère Centrale, Colombie; carte géomorphologique des interrelations volcano-glaciaires [The volcanic massif of Ruiz-Tolima, Cordillera Central, Colombia; geomorphological map of the interrelation of volcanoes and glaciers]: Paris, Laboratoire IMAGEO CNRS [Centre National de la Recherche Scientifique], scale 1:50,000.

———1990, Effects of the November 13, 1985, eruption on the snow pack and ice cap of Nevado del Ruiz Volcano, Colombia: Journal of Volcanology and Geothermal Research, v. 41, no. 1–4, special issue, p. 177–201.

Thouret, J.–C., Van der Hammen, Thomas, Salomons, B., and Juvigné, E., 1992, Stratigraphy, chronology, and paleoecology of the last glaciation in the Andean Central Cordillera, Colombia—A short note: Zeitschrift für Geomorphologie, v. 84 supp., p. 13–18, 1 map.

———1996, Palaeoenvironmental changes and glacial stades of the last 50,000 years in the Cordillera Central, Colombia: Quaternary Research, v. 46, no. 1, p. 1–18.

U.S. Board on Geographic Names (3rd ed.), 1988, Defense Mapping Agency, Gazetteer of Colombia: Washington, D.C., Defense Mapping Agency, 859 p.

Van der Hammen, Thomas, 1984, Datos sobre la historía de clima, vegetación y glaciación de la Sierra Nevada de Santa Marta [Data about the history of climate, vegetation, and glaciation of the Sierra Nevada de Santa Marta], *in* Van der Hammen, Thomas, and Ruiz, P.M., eds., La Sierra Nevada de Santa Marta (Colombia): Studies on tropical Andean ecosystems: Berlin-Stuttgart, J. Cramer Verlag, v. 2, p. 561–580.

Van der Hammen, Thomas, Barolds, J., deHong, H., and de Veer, A.A., 1980/81, Glacial sequence and environmental history in the Sierra Nevada del Cocuy (Colombia): Palaeogeography, Palaeoclimatology, Palaeoecology, v. 32, no. 3–4, p. 247–340.

Vandemeulebrouck, J., Thouret, J.–C., and Dedieu, J.–P., 1993, Reconnaissance par télédétection des produits éruptifs et des lahars sur et autour de la calotte glaciaire du Nevado del Ruiz, Colombie [Remote sensing survey of the eruptive products and lahars on and around the ice cap of Nevado del Ruiz, Colombia]: Société Géologique de France Bulletin, v. 164, no. 6, p. 795–806.

Vergara y Velasco, F.J., 1892, Nueva geografía de Colombia [New geography of Colombia]: Bogotá, Imprenta de vapor de Zalamea hermanos. [Second edition published in 1901 as "Nueva Geografía de Colombia escrita por Regiones Naturales"; the 1901 edition was reprinted in 1974 in Bogotá by El Banco de la Republica in 3 v., 1,265 p.]

Villegas, B., ed., 1993, Colombia from the air: Bogotá, Villegas Editores, 192 p.

Williams, S.N., ed., 1990a, Nevado del Ruiz Volcano, Colombia, I: Journal of Volcanology and Geothermal Research, v. 41, no. 1–4, special issue, 379 p.

Williams, S.N., ed., 1990b, Nevado del Ruiz Volcano, Colombia, II: Journal of Volcanology and Geothermal Research, v. 42, no. 1–2, special issue, 224 p.

Wood, W.A., 1941, Mapping the Sierra Nevada de Santa Marta, the work of the Cabot Colombian Expedition: Geographical Review, v. 31, no. 4, p. 639–643.

———1970, Recent glacier fluctuations in the Sierra Nevada de Santa Marta, Colombia: Geographical Review, v. 60, no. 3, p. 374–392.

Glaciers of South America–

GLACIERS OF ECUADOR

By EKKEHARD JORDAN *and* STEFAN L. HASTENRATH

SATELLITE IMAGE ATLAS OF GLACIERS OF THE WORLD

Edited by RICHARD S. WILLIAMS, Jr., *and* JANE G. FERRIGNO

U.S. GEOLOGICAL SURVEY PROFESSIONAL PAPER 1386-I-3

Ecuador has more than 100 small ice caps, outlet glaciers, small ice fields, and mountain glaciers that have a total area of 97.21 square kilometers. The glaciers are located on the high summits of 4 mountains of the Cordillera Occidental (21.92 square kilometers) and 13 mountains of the Cordillera Oriental (75.29 square kilometers). Since the 1800's, the glacier area has undergone a significant and continuing reduction

CONTENTS

GLACIERS OF SOUTH AMERICA–

GLACIERS OF ECUADOR

By EKKEHARD JORDAN[1] *and* STEFAN L. HASTENRATH[2]

Abstract

Even though Ecuador sits astride the Equator, 4 mountains in the Cordillera Occidental (Western Cordillera) and 13 mountains in the Cordillera Oriental (Eastern Cordillera) have summits that extend above the regional snowline and support more than 100 small glaciers. Ecuadorean glacier types include ice caps and outlet glaciers, small ice fields, and mountain glaciers on both volcanoes and nonvolcanic mountains. The total area of glaciers on the 17 volcanoes and other mountains is 97.21 square kilometers, 21.92 square kilometers in the Cordillera Occidental and 75.29 square kilometers in the Cordillera Oriental. Field surveys, photogrammetric analysis of vertical aerial photographs and Landsat images, and modern maps were used to calculate the total glacier area. The Cotopaxi stratovolcano, one of the highest active volcanoes on Earth at 5,911 meters, has an ice cap from which 23 outlet glaciers flow (total area of 19.09 square kilometers). Climatic conditions in Ecuador vary considerably, being influenced by the availability of moisture from either the Pacific Ocean or the Amazon basin, terrain elevation, and the orientation of mountain ranges. Glacierization is generally more developed on the eastern flanks of the cordilleras. A significant reduction in glacier area has been noted in Ecuador since the 1800's and apparently still continues.

Introduction

Ecuador's glaciers are situated close to the Equator in South America and thus can be considered to be among the best examples of continental tropical glaciation. The glaciers are restricted to the highest peaks in the Andes Mountains because of the proximity to the Equator and the prevailing climatic conditions. The individual peaks, mostly of volcanic origin, do not contain large contiguous ice fields, such as those found in Perú, Bolivia, Chile, and Argentina; instead, the glaciers occur as ice caps that feed numerous outlet glaciers and are confined to the limited summit areas. Table 1 provides information on the area and elevation of the small ice caps, outlet glaciers, small ice fields, and mountain glaciers.

The glaciers in Ecuador are located on the two chains of the Andes Mountains that flank the *inter-Andean depression*, the Cordillera Occidental and the Cordillera Oriental (fig. 1). The peaks range in elevation from around 4,000 m to more than 6,000 m. In the Cordillera Occidental, the four glacierized mountains are, proceeding from north to south, Cotacachi,[3] Iliniza, Carihuairazo, and Chimborazo. In the Cordillera Oriental, the following 13 mountains are glacierized: Cayambe, Saraurcu, Antisana, Sincholagua, Cotopaxi, Quilindaña, Cerro Hermoso, Tungurahua, Altar, *Cubillín*, Sangay, Collay, and Cerro Ayapungo (*Soroche*). Contradictory information exists, however, in the literature regarding the presence of

Manuscript approved for publication 18 March 1998.

[1] Lehrstuhl für Physische Geographie, Heinrich-Heine-Universität, Universitätstrasse 1, 40225 Düsseldorf, Germany.

[2] Department of Atmospheric and Oceanic Sciences, University of Wisconsin, 1225 West Dayton Street, Madison, WI 53706, U.S.A.

[3] The names in this section conform to the usage authorized by the U.S. Board on Geographic Names in its Gazetteer of Ecuador (U.S. Board on Geographic Names, 1987). The names not listed in the gazetteer are shown in italics.

TABLE 1.—*The glacierized areas of Ecuador*

[Table 1 was compiled by Ekkehard Jordan from the following sources: field surveys in 1977 and 1980–1981; STEREOCORD interpretation of Cotopaxi (Jordan, 1983); official topographic map of Instituto Geográfico Militar, Quito, Ecuador; Hastenrath (1981); and satellite image interpretation using STEREOCORD (Jordan, 1984). Mountain type: IV, inactive volcano during the Holocene; AV, active volcano; and NVM, nonvolcanic mountain]

Mountain type	Locality	Latitude	Longitude (west)	Type of glacier(s)	Number of outlet glacier(s)	Area (square kilometers)	Highest elevation (meters)	Lowest glacier terminus (meters)
	Cordillera Occidental (Western Cordillera)							
	Cordillera Occidental	0°22'N.–1°29'S.	78°20'–78°48'	—	—	—	6,310	4,600
IV	Cotacachi	0°22'N.	78°20'	Mountain	—	0.06	4,939	4,750
IV	Iliniza	0°39'S.	78°42'	Ice cap	10	.84	5,263	4,800
IV	Carihuairazo	1°24'S.	78°45'	Ice cap	9	.78	5,020	4,600
IV	Chimborazo	1°29'S.	78°48'	Ice cap	22	20.24	6,310	4,600
					Total	21.92		
	Cordillera Oriental (Eastern Cordillera)							
	Cordillera Oriental	0°1'N.–2°20'S.	77°54'–78°33'	—	—	—	5,911	4,150
IV	Cayambe	0°1'N.	77°59'	Ice cap	20	17.73	5,790	4,200
IV	Saraurcu	0°4'S.	77°54'	—	—	.05	4,676	4,500
AV	Antisana	0°29'S.	78°08'	Ice cap	17	22.58	5,704	4,200
IV	Sincholagua	0°32'S.	78°22'	3 ice fields	—	.18	4,893	4,700
AV	Cotopaxi	0°41'S.	78°25'	Ice cap	23	19.09	5,911	4,400
IV	Quilindaña	0°47'S.	78°19'	2 mountain	—	.06	4,760	4,650
NVM	Cerro Hermoso	1°17'S.	78°17'	Mountain	—	.02	4,640	4,600
AV	Tungurahua	1°28'S.	78°26'	Ice cap	—	.78	5,016	4,800
IV	Altar	1°40'S.	78°24'	Ice cap, 3 mountain	6	14.80	5,319	4,150
IV	*Cubillín*	—	—	—	—	—	—	—
AV	Sangay	1°58'S.	78°20'	Snowpack or ice cap ?	—	3.32	5,230	—
NVM	Collay	2°14'S.	78°32'	—	—	—	4,630	—
NVM	Cerro Ayapungo (*Soroche*)	2°20'S.	78°33'	—	—	—	4,730	—
					Total	75.29		
					Grand total	97.21		

glaciers on Sangay and Cerro Ayapungo. Some references describe a partial glacier cover, and others mention only névé (perennial snow or firn) that persists for several years.

The total glacierized area in Ecuador is 97.21 km^2, 21.92 km^2 in the Cordillera Occidental and 75.29 km^2 in the Cordillera Oriental. The glacierization is more pronounced in the Cordillera Oriental because this eastern range is better exposed to the moisture supply from the Amazon basin. Also, glaciers are more abundant on the eastern, as opposed to the western, flanks of individual mountains.

Historical documentation of varying ice conditions in Ecuador is among the most numerous and continuous in all of the glacierized tropical areas (Hastenrath, 1981). The earliest reference to the glacierization of the Ecuadorean Andes dates back to the era of Spanish colonization in the 1500's. A geodetic expedition of the French Academy made observations in the middle 1700's. Von Humboldt visited the country in 1802, and geographic information from a variety of travelers remains abundant to the beginning of the 20th century. Recent surveys of ice conditions in Ecuador include those of Mercer (1967) and Hastenrath (1981). These varied sources indicate a rather extensive glacierization from the 1500's to the first part of the 1800's,

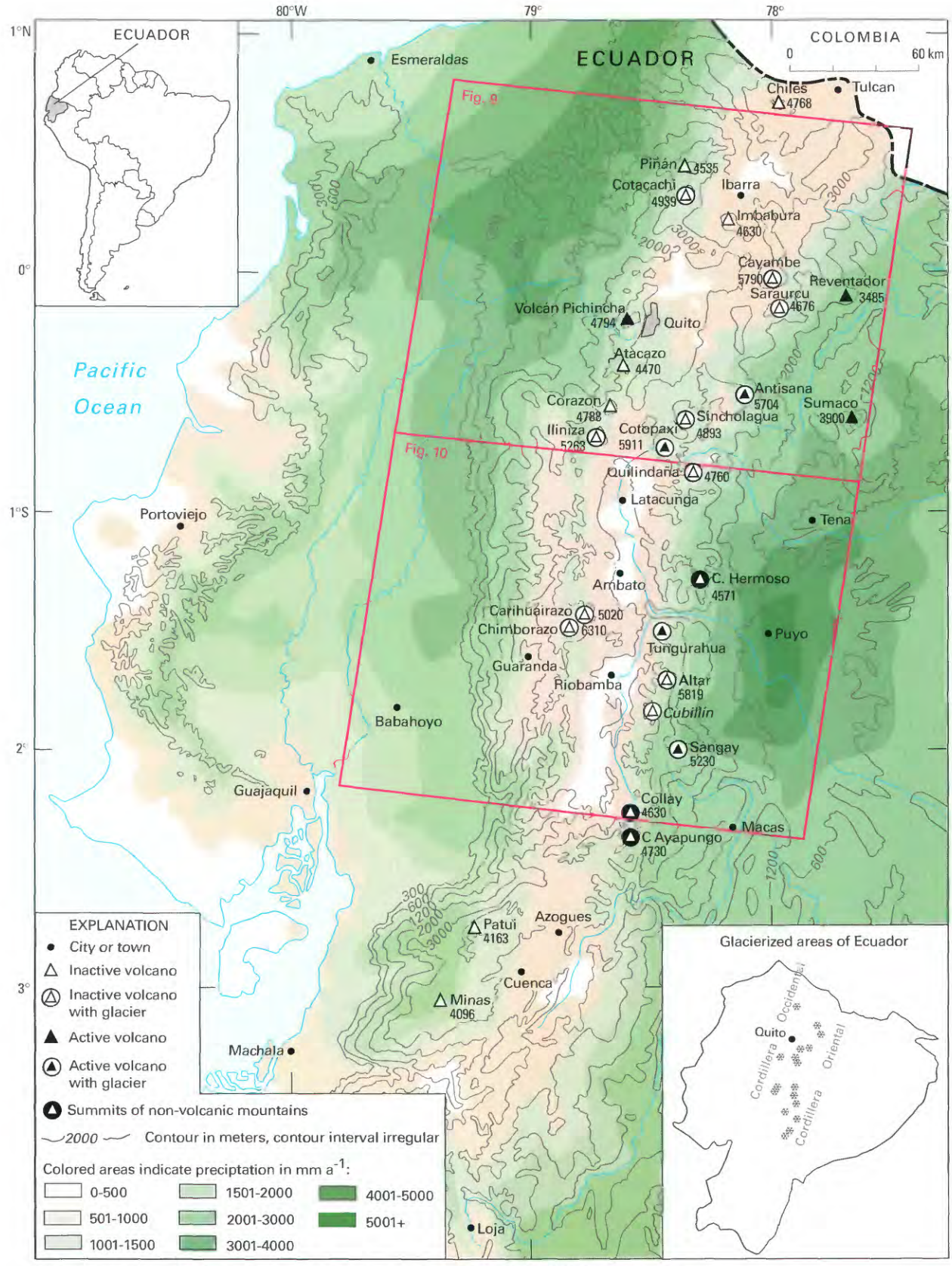

Figure 1.—*Ecuador's Andean region at a scale of 1:2,000,000 showing glacierized areas characterized by volcano type, topography, and precipitation distribution. The map is based on (1) the Atlas Geográfico de la República del Ecuador (Instituto Geográfico Militar, 1978?), (2) official maps of the Instituto Geográfico Militar, and (3) fieldwork by the author (Ekkehard Jordan) in 1977, 1980, and 1981.*

followed by a drastic ice recession starting around the middle of the past century and continuing to the present time (Hastenrath, 1981). Heine's (1995) studies of moraines in Ecuador documented the historical recession of its glaciers, a global phenomenon of mountain glaciers during the 20th century. Clapperton's (1993) studies of late Pleistocene to early Holocene moraines in the Andes Mountains indicate an advance of glaciers and a lowering of the equilibrium line altitude by 300 to 400 m in the northern and north-central part of the Andes Mountains.

Climatic Conditions of Ecuadorean Glacierization

Climatic conditions generally determine the possibility of glacier development, and different climatic patterns in different areas produce different types of glacier development. The climatic conditions in the Ecuadorean part of the Andes Mountains are highly varied, and the factors that control the weather patterns are not completely understood because of the lack of upper atmosphere observations (see also Hastenrath, 1981, p. 8).

Monthly mean temperatures follow the typical tropical pattern and have very minor fluctuations throughout the year, normally less than 2°C. In contrast, temperature differences between day and night are quite large, and the difference increases with elevation. On Cotopaxi, at an elevation of 3,560 m above sea level (asl), the absolute maximum and minimum daily temperatures are +20.4°C and –4.8°C, respectively. According to Graf (1981, p. 16), the average temperature gradient in the mountain region is about 6.5°C/1,000 m, the 0° annual isotherm being at an elevation of about 4,700 m. The average regional snowline is a little higher, about 4,800–4,900 m, and has a fluctuation of about ±200 m, depending on differing precipitation conditions and slope orientation.

Precipitation conditions in the two areas of the Ecuadorean Andes are influenced by air masses from two different regions. The western Cordillera Occidental gets its moisture from the Pacific Ocean, and the intensity decreases toward the south, as is clearly shown by the general map (fig. 1). The cordillera is characterized by rainy and dry seasons that are accentuated toward the south. Precipitation maximums coincide with the higher positions of the Sun in March and April. The Cordillera Oriental, on the other hand, gets its precipitation from the Amazon basin and has an almost uniform precipitation distribution throughout the year but an increase in amount toward the south (see fig. 2).

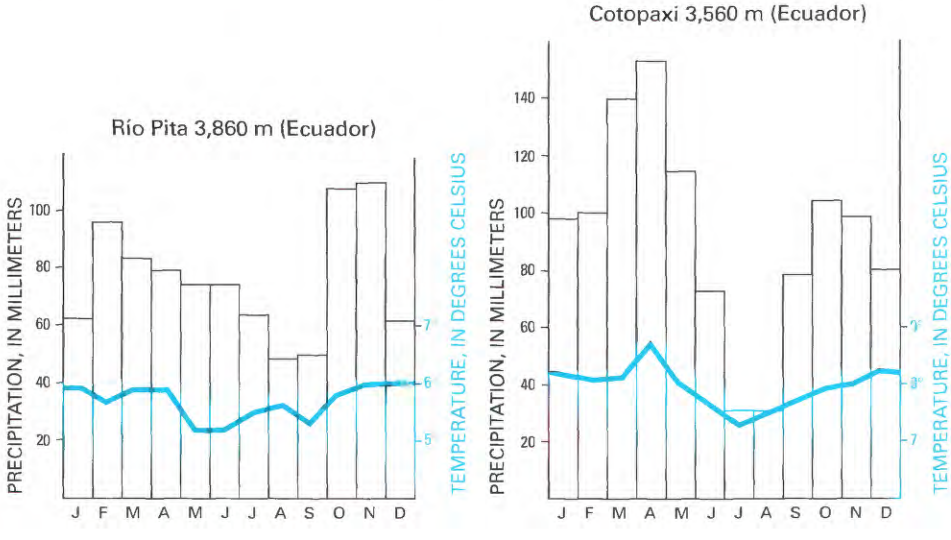

Figure 2.—*Average monthly precipitation and temperatures from two meteorological stations near Cotopaxi volcano. Both stations are located south of the Equator and reveal the double precipitation maximum and only minor fluctuations in the average monthly temperatures, which are characteristic of the Andean area. Graphs modified from Blandin Landivar (1976–77).*

These two precipitation patterns collide in the Andes Mountains and are considerably influenced by the topographic relief. Whereas the outer crests of the two cordillera ranges are heavily influenced by the adjacent precipitation regions, the inner high-valley region and the mountain slopes adjacent to it are typically characterized by a twin-peak precipitation distribution. This twin-peak distribution reaches its maximum around the times that the Sun is at its highest elevation in March and September and is at a minimum in July and August.

A vertical precipitation differential also exists in Ecuador, in which the maximum precipitation is found at the middle elevations of the western slope of the Cordillera Occidental and the eastern slope of the Cordillera Oriental below an elevation of 2,000 m asl (fig. 1). This phenomenon is known as well from tropical mountains in Colombia (Weischet, 1969) and in Bolivia (Jordan, 1979). Satellite images and weather observations confirm that a second condensation level develops in summit locations above 5,000 m, as shown on the ground photograph of Cayambe (fig. 3). Just exactly how large the total annual precipitation is cannot be documented because of the absence of meteorological measurements on the high peaks. The two highest weather stations in the middle Ecuadorean Andes near Cotopaxi are at 3,860 m and 3,560 m. A meteorological station has been installed at Antisana, but sufficient data are not yet available. The difference in elevation between the meteorological stations and the summits of the high peaks probably means a significant differential in actual precipitation at the higher elevations.

The glacierized regions of both cordillera ranges seem to be influenced most heavily by air masses from the Amazon basin to the east; this is indicated by the fact that glacierization is generally stronger on the east sides of the ranges and by the observation of daily cloud movements. The two weather stations near Cotopaxi reveal the characteristic twin-peak annual precipitation curve for the cordillera zone and document the precipitation pattern prevailing throughout the year (fig. 2). This pattern is typical of continental tropical glaciers, which have periodic fluctuations and no pronounced dry season.

This twin-peak precipitation pattern not only influences the development of the glaciers but has an effect on the investigations of glaciers that depend on aerial or satellite surveys. The frequent cloud cover, including its daily periodic (diurnal) development (fig. 4), severely restricts the scheduling of aerial photographic surveys. In addition, the frequent fresh

Figure 3.—*Cerro Cayambe (5,790 m) and its pronounced afternoon cloud layer above the second condensation level at about 5,000 m. A second, lower cloud layer can also be seen over the eastern slope leading down to the selva (jungle forest). This cloud layer is rather weakly indicated in the right background by cumulus clouds that are just barely protruding beyond the horizon. This secondary cloud level, which is a particularly well-developed phenomenon associated with the highest mountains, contributes greatly to glacier formation because of the greater annual precipitation and the protection that it affords from solar radiation. Photograph by Ekkehard Jordan taken on 3 January 1981 near* Huayllabamba, *about 40 km west-southwest of Cayambe, at an elevation of about 2,700 m.*

Figure 4.—*Oblique aerial photograph of the snow-covered ice cap on Chimborazo (6,310 m) and, in front of it, the snow-covered ice cap of Carihuairazo (5,020 m). As for the other ice-covered peaks of Ecuador's Andes Mountains, these peaks protrude from the broken nighttime cloud cover during the early morning hours and can be seen from a great distance. Shortly after sunrise, they disappear in the rising clouds and, starting in the late morning, they frequently receive precipitation in the form of snow. Photograph by Ekkehard Jordan on 31 May 1977 looking from the northeast at an altitude of about 9,000 m and a distance of about 50 km.*

snowfalls make it difficult for a photogrammetrist to plot elevation contours when mapping glaciers from aerial photographs because of the lack of discernible features and the lack of contrast. The most favorable times to look for maximum glacier exposure are in the two drier periods from December to February and from July to early September (see the section on Bolivia in this volume). In spite of the precipitation minimum in July and August, this is not the best time for field research and investigations in the glacierized areas because violent east winds sweep the higher summit regions during these months. The normal presence of maximum glacier exposure at the end of the summer, which is known in areas outside the tropics, does not apply here; instead, the optimum condition depends on accidentally having periods that have few clouds during the timespan mentioned. Therefore, it is also very difficult to find satellite images that are sufficiently free of clouds to be useful in the delineation of the glaciers.

Ice Balance on Active Volcanoes and the Problems in Determining Glacier Asymmetry

As one can see in the index map (fig. 1), four of Ecuador's active volcanoes have glacierized peaks: Antisana, Cotopaxi, Sangay, and Tungurahua. The ice-capped volcanoes of the Andes Mountains represent locations in South America where scientists can study the interplay of the exogenous climatic ice with endogenous subglacial geothermal and volcanic activity. A study on the glaciation of Cotopaxi is a good example of this type of work (Jordan, 1983a). Cotopaxi, a stratovolcano, has an elevation of 5,911 m and is one of the Earth's highest active volcanoes. Antisana is a large stratovolcano, 5,753 m high, that last erupted in 1801–02 from the north-northeast side of its summit (Simkin and Siebert, 1994). The interaction of glacial and volcanic processes is quite complex. For example, the rapid compaction of snow in the crater region is caused by a reduction in albedo resulting from very thin tephra blankets on snow. On the other hand, large volumes of ice can be melted by the lava flows and result in devastating lahars[4] (Lipman and Mullineaux, 1981; Jordan and others, 1987). Because of its history of catastrophic eruptions, the Cotopaxi stratovolcano has attained consider-

[4] Lahar, an Indonesian loanword that refers to a mudflow composed primarily of volcanic material that moves down the flank of a volcano (Bates and Jackson, 1980, p. 347).

able notoriety. Between 1532 and 1942, Cotopaxi had 59 explosive eruptions from its summit crater, including 3 nuées ardentes (a French loanword that refers to a "swiftly flowing, turbulent gaseous cloud, sometimes incandescent, erupted from a volcano and containing ash and other pyroclastics in its lower part" (Bates and Jackson, 1980, p. 479)). Lava flows also accompanied 27 of the eruptions. Fatalities resulted from 5 eruptions, destruction of property took place in 11 instances, and lahars formed in 27 cases (Simkin and Siebert, 1994). The effect of the eruptions on the ice volume becomes more noticeable following recent and (or) frequent eruptions.

Sangay is also among the Earth's most active volcanoes. Three eruptions were recorded between 1628 and 1934, and a low level of continuous eruption has been noted since then (Simkin and Siebert, 1994). One cannot be certain, however, whether Sangay supports a continuously developed ice cover or only remnants of glacier ice. Several times a year, the alternation of brilliantly shining, fresh snow blankets and earth-colored ash cover can be observed on the peak (fig. 5). The active Tungurahua volcano, which last erupted in 1944, does not possess as much ice cover as the two gigantic volcanoes (Cotopaxi and Sangay) because its summit is only a little bit above the regional snowline.

No cloud-free Landsat 1, 2 or 3 imagery has been found of Sangay, but Antisana, Cotopaxi, and Tungurahua can be seen. Evidence of active volcanism is particularly evident on a Landsat image of Cotopaxi (fig. 6). On the Landsat image taken on 4 February 1979, it appears as if the crater region has no glaciers and that the western slope is more heavily influenced by volcanism. One can also see that a narrow ice-free area extends along the western slope all the way up to the crater—a phenomenon probably caused by geothermal processes. This phenomenon can also be seen quite well on terrestrial photographs (fig. 7). Figure 8 also clearly shows the asymmetrical distribution of the ice cover on this very uniform, conical stratovolcano. The naturally occurring symmetrical shape of the ice cover that results from climatic effects does not remain constant because of the geothermal activity. Active volcanism, however, is not the only factor affecting the glacier's shape. These small, relatively thin glaciers are also strongly influenced by any type of relief anomaly.

Figure 5.—*The Sangay stratovolcano is one of our planet's most active volcanoes (three eruptions between 1628 and 1934 and in continuous eruption since then) and has a crater that constantly emits fumes. Even though Sangay has a summit elevation of 5,230 m, it protrudes only a little above the snowline. Because of contradictory reports from those who have climbed it, it is not certain even today whether it has only a névé (firn or perennial snow cover) or whether a glacier underlies the névé. Three different stages of snow cover on Sangay are shown in the following illustrations:*

A, *An oblique aerial photograph shows an almost completely smooth, fresh blanket of snow. The photograph was taken by Ekkehard Jordan from the northwest at an elevation of about 9,000 m on 31 May 1977.*

B ***and*** **C,** *See following pages.*

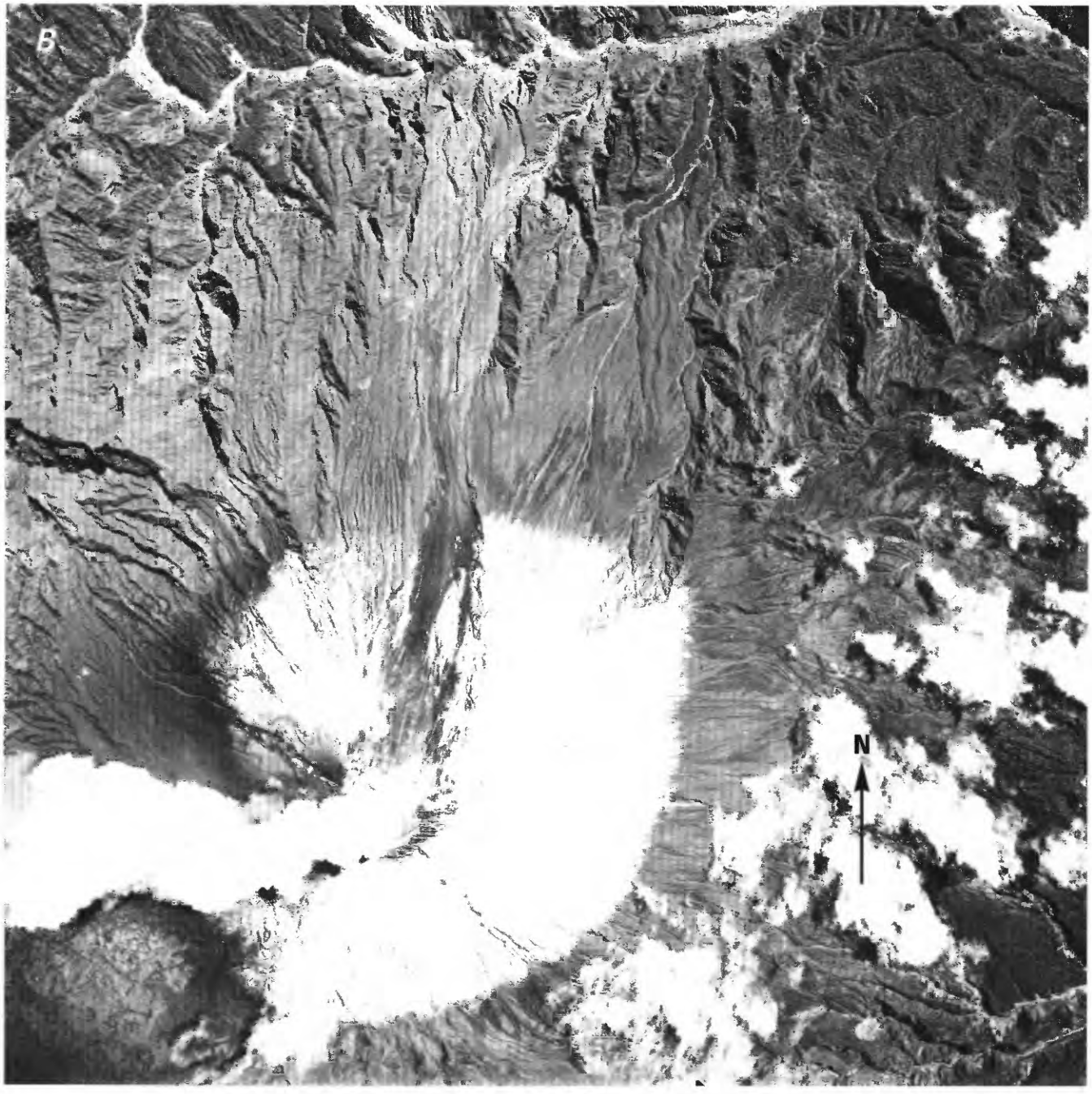

Figure 5B.—*A vertical aerial photograph shows the partially destroyed snow cover. Photograph acquired 13 June 1956 by HYCON, M–172, no. 29671, from an elevation of approximately 8,500 m. The scale is approximately 1:50,000. Photograph from the Instituto Geográfico Militar, Quito, Ecuador, and released by Order No. 326, dated 7 July 1980.*

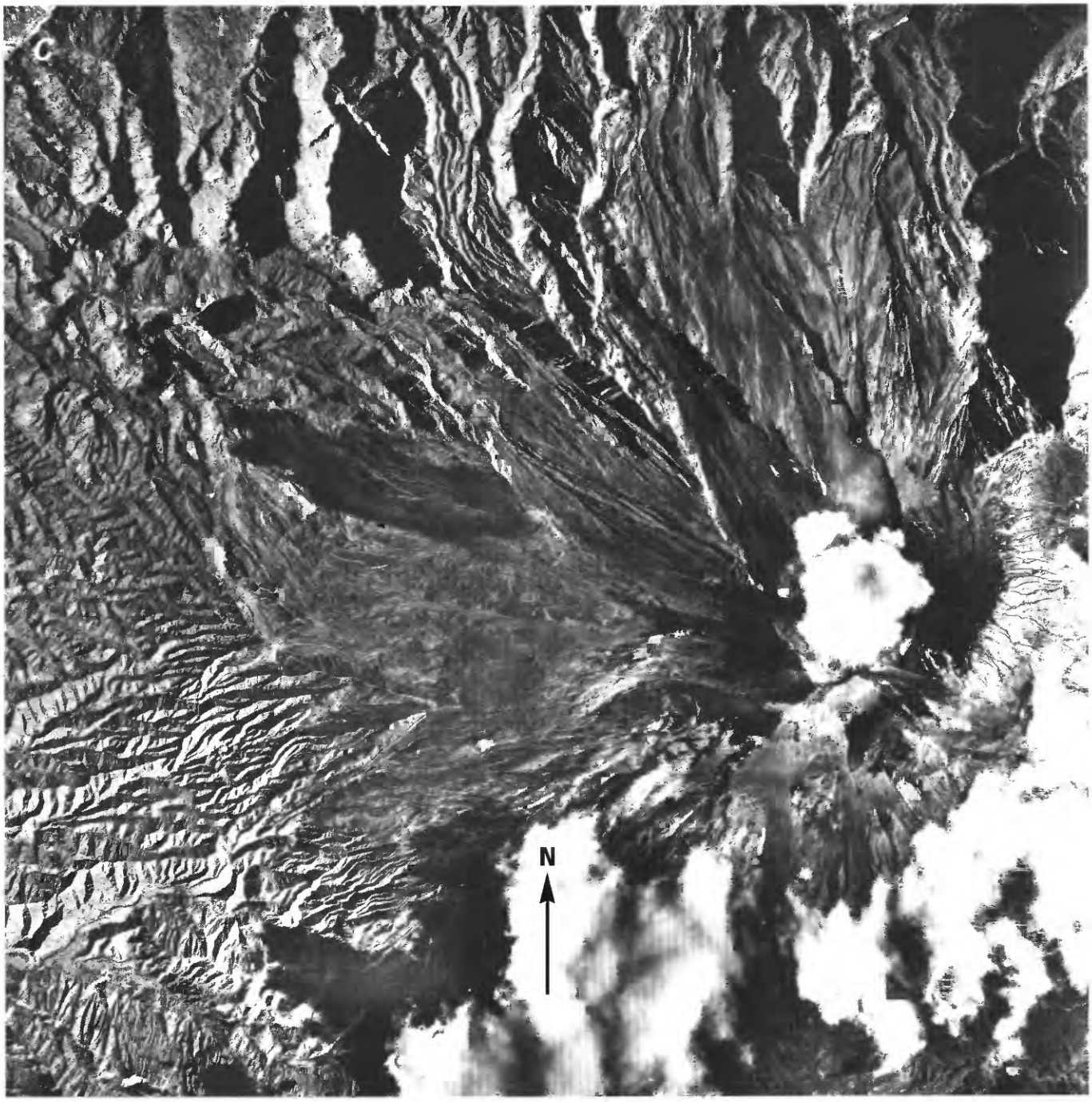

Figure 5C.—*A vertical aerial photograph shows the predominantly snow-and-ice free summit region. Photograph acquired on 8 February 1965 by the U.S. Air Force, AF 60–16, R–77, no. 6894, from an elevation of approximately 8,500 m. The scale is approximately 1:60,000. Photograph from the Instituto Geográfico Militar, Quito, Ecuador, and released by Order No. 326, dated 7 July 1980.*

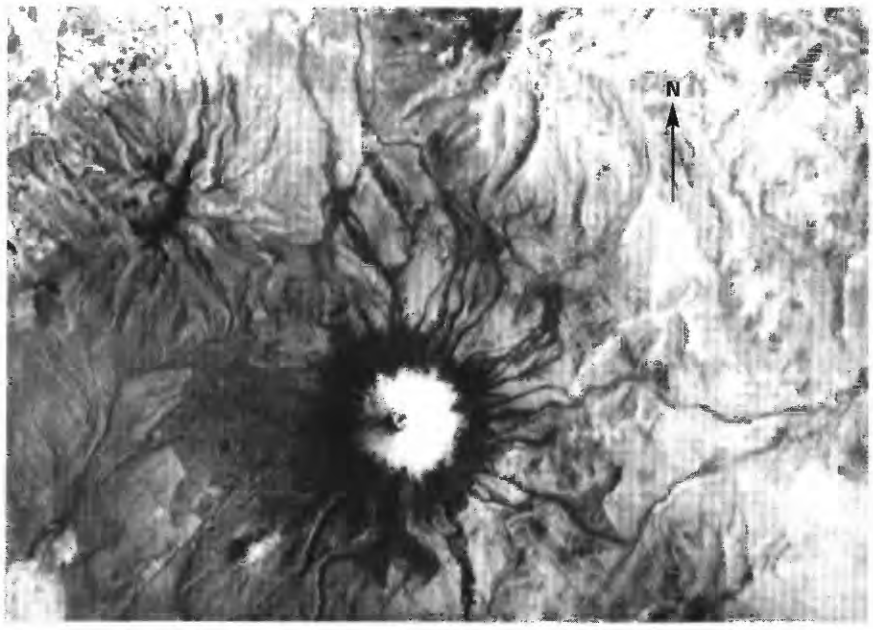

Figure 6.—*Segment of a Landsat 2 MSS image enlarged to a scale of 1:250,000 showing the active Cotopaxi stratovolcano (5,911 m) and its pronounced asymmetrical ice cap. It is possible to discern the lack of snow cover along the crater's edge. Cotopaxi is the best example of a glacierized active volcano in the tropics. The strikingly dark-looking ring below the glacier area is caused by the ash cover that is very visible because of the absence of vegetation. The bands thus represent elevation steps on Cotopaxi. The moraine area near the glacier is not identifiable in this image. Landsat MSS image (21474–14323, band 7; 4 February 1979; Path 10, Row 60) from the EROS Data Center, Sioux Falls, S. Dak.*

Figure 7.—*Glaciers on the west slope of Cotopaxi during a temporary cloud breakup during the afternoon. The highest ice-covered north peak (5,911 m) is visible. The large glacier-free area, extending from the crater's edge in the middle of the picture, is probably due to geothermal activity.*

The best example of a glacier that is affected by relief anomaly in this area is the glacier development on the inactive volcano of Altar, a peak having a steep-walled caldera that is breached toward the west. The prevailing climate conditions normally produce more extensive glaciation along the east slopes. Here, however, the situation is almost exactly the opposite because an extensive glacier snout, which is present on the west slope, is presumably caused by the strong, relief-induced horizontal shading.

A strikingly good delineation of the Ecuadorean tropical glaciers, which even many vertical aerial photographs do not reveal, is shown by two Landsat images taken on 4 and 13 February 1979 (figs. 9, 10). Where image reproduction is good, it is possible to identify the snowline on the glaciers and to determine an approximate separation between the accumulation and ablation areas, something that has not been available for Ecuadorean glaciers. (These features can be seen even better on more recent Landsat Thematic Mapper (TM) and Satellite pour l'Observation de la Terre (SPOT) images and other newer, remotely sensed data that have increased resolution.) These images also make it possible to recognize evidence of Pleis-

Figure 8.—*Vertical aerial photograph of Cotopaxi showing the crater area and most of the summit ice cap. The photograph was taken earlier than figures 6 and 7, and the ice-free areas caused by geothermal activity are not visible. A recent snowfall also masks the "ash cover" below the glacierized area. Photograph number PI0–69–22b was acquired on 22 June 1963 and is from U.S. Geological Survey photograph collection. The approximate scale is 1:30,000.*

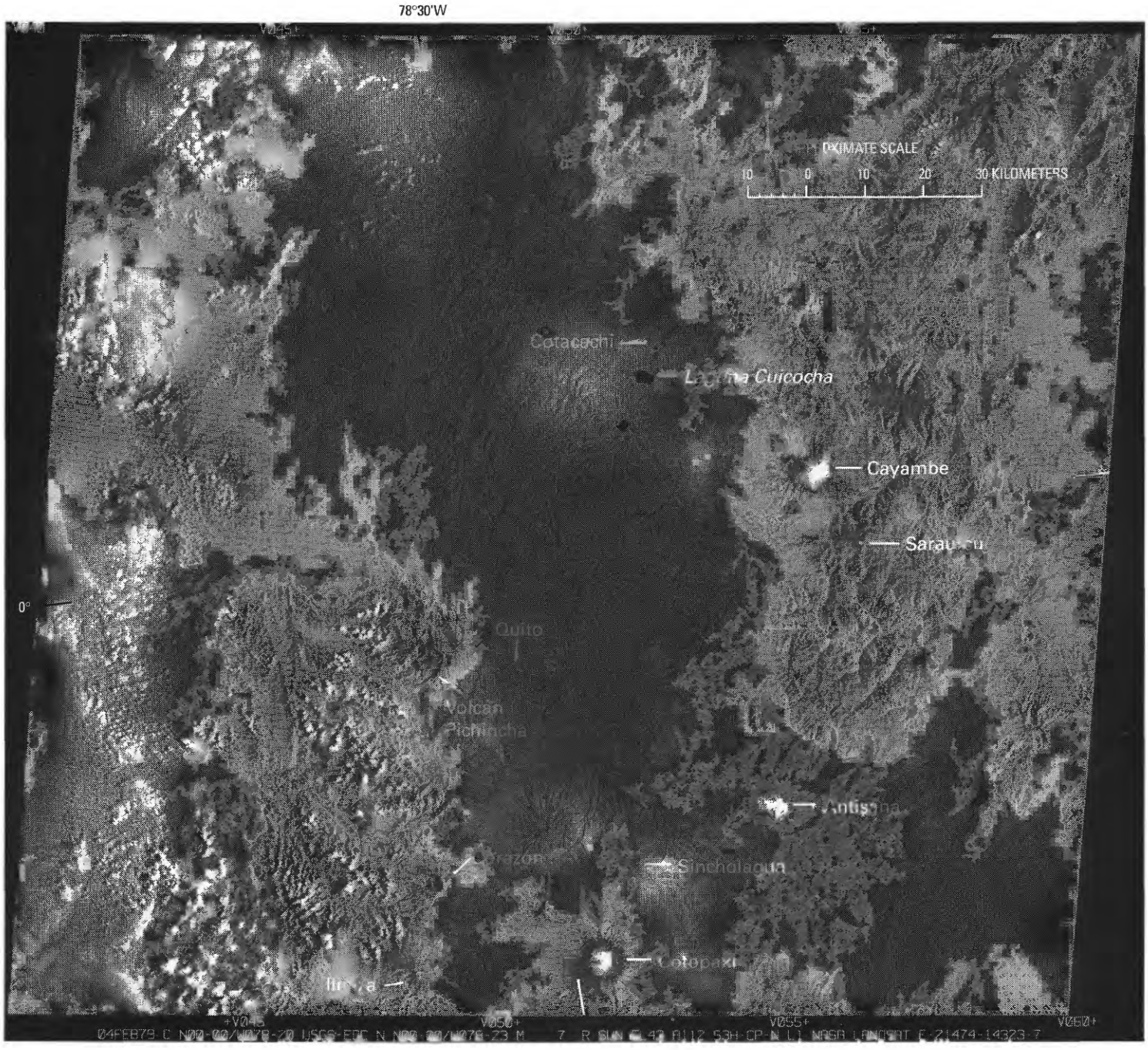

tocene glaciation that appears very clearly in many regions, including the mountains near Cotopaxi. It is not possible to see any evidence of Pleistocene glaciation on the active volcanoes Cotopaxi, Sangay, and Tungurahua, however, some former moraine morphology is seen on Antisana.

***Figure 9.**—Landsat 2 MSS image of the northern part of the Ecuadorean Andes (see location in fig. 1) showing the glacierized volcanoes discussed in the text. Some peaks are free of glaciers but show evidence of Pleistocene glaciation. Landsat image (21474–14323, band 7; 4 February 1979; Path 10, Row 60) from the EROS Data Center, Sioux Falls, S. Dak.*

Glacier Mapping

Sketch maps of the glaciers of Chimborazo, the highest mountain of the Ecuadorean Andes, are the result of work by Whymper (1892), Meyer (1907), and Sauer (1971). In recent decades, topographic maps based on aerial photogrammetry have been produced for part of the Andes Mountains at scales of 1:50,000 and 1:25,000. (Refer to Hastenrath (1981) and table 2 for a detailed listing of these maps.) In addition, systematic mapping

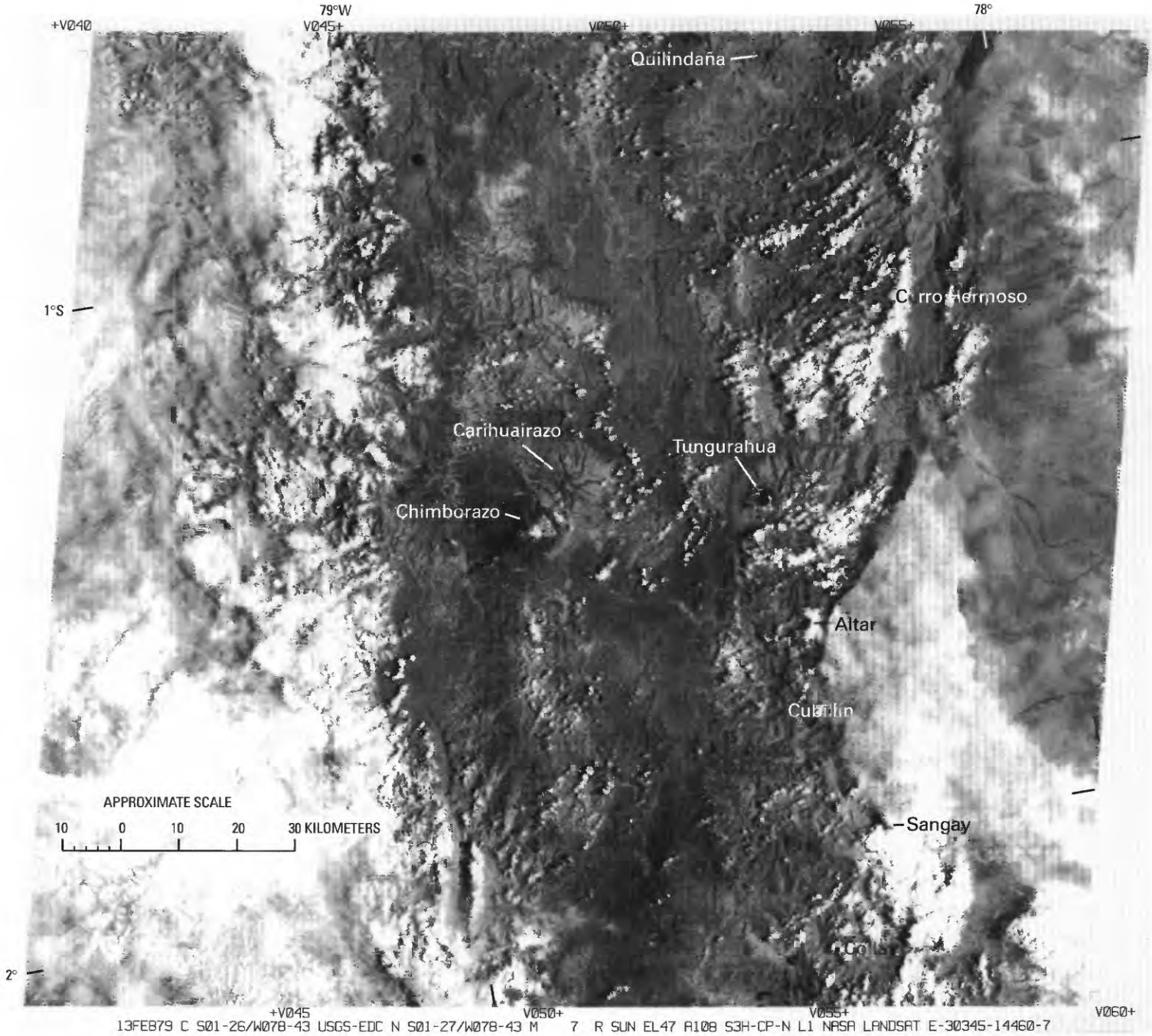

Figure 10.—*Landsat 3 MSS image of the southern part of the Ecuadorean Andes (see location in fig. 1) showing the area of the glacierized volcanoes and two nonvolcanic mountains discussed in the text; none of the other peaks support glaciers. The cloud cover extends into the Andean area and obscures glacier identification. The glacier peaks in the southeast, Altar,* Cubillín, *Sangay, and Collay are partially or completely hidden.* Cubillín *and Collay cannot be recognized at all. Cerro Ayapungo is located south of the image. Landsat image (30345–14460, band 7; 13 February 1979; Path 10, Row 61) from the EROS Data Center, Sioux Falls, S. Dak.*

of glaciers during the 1970's (Hastenrath, 1981) combined fieldwork with evaluation of aerial photographs and topographic maps.

A detailed study of Cotopaxi, a combination of fieldwork and analytical aerial photogrammetry using the STEREOCORD (an analytical photogrammetric instrument) was completed in 1983 (Jordan, 1984). Regrettably, the official maps do not distinguish between snow and glacier surfaces; instead, all 3 surface areas covered with snow are reproduced on the aerial graph by blue contour lines. As a result, a series of summits, which do not have any glaciers, appear to have glaciers on them because of the cartographic illustration method, or they show ice surface areas that are larger than the actual glacier cover. This is particularly true of the glacier areas of summits around and below 5,000 m, such as those on Cotacachi, Sincholagua, Quilindaña, Cerro Hermoso, Tungurahua, *Cubillín*, Collay, and Cerro Ayapungo.

TABLE 2.—*Maps of the glacierized mountains of Ecuador*

[The maps listed are topographic maps unless otherwise indicated. All are available from the Instituto Geográfico Militar, Quito, Ecuador. The 1:100,000-scale topographic maps are part of Series J 621. The 1:50,000-scale maps are part of Series J 721. The 1:25,000-scale maps are part of Series J 821]

Glacierized area	Scale	Map information
	Cordillera Occidental	
Cotacachi	1:50,000	CC N III–D3 (Plaza Gutiérrez) censo 40
	1:25,000	Plancheta 2 de hoja 28 (Cotacachi)
Iliniza	1:50,000	N III–C3 (San Roque) (3892–III) N III–C4 (Machachi) (3892–II) N III–E1 (Sigchos) (3891–IV) N III–E2 (Mulalo) (3891–I)
Iliniza	1:25,000	N III–C3b (Río Zarapullo) (3892–III–NE) N III–C3d (Tungosillin) (3892–III–SE) N III–C4c (Iliniza) (3892–II–SW) N III–E1b (Yalo) (3891–IV–NE) N III–E1d (Isinlivi) (3891–IV–SE) N III–E2a (Pastocalle) (3891–I–NW)
Chimborazo-Carihuairazo	1:50,000	N IV–A3 (Simiatug) (3890–III) N IV–C1 (Chimborazo) (3889–IV) N IV–C3 (Guaranda) (3889–III) N IV–A4 (Ambato) (3890–II) N IV–C2 (Quero) (3889–I)
	Cordillera Oriental	
Cayambe	1:50,000	CC N II–F4 (Cayambe) censo 65 CC O II–E3 (Laguna San Marcos) censo 66 CC N III–B2 (Cancagua) censo 79 CC O III–A1 (Saraurcu) censo 80
Saraurcu	1:50,000	CC O III–A1 (Saraurcu) censo 80
Antisana	1:50,000	N III–D2 (Papallacta) censo 114 N III–D4 (Laguna Miracocha) censo 130
	1:25,000	N III–D2c (Antisana) N III–D2d (Río Quinjua) N III–D4a (Laguna de Miracocha) N III–D4b (Río Quijos)
Sincholagua	1:50,000	N III–D1 (Pintag) (3992–IV) N III–D3 (Sincholagua) (3992–III)
	1:25,000	N III–D1d (La Cocha) (3992-IV–SE) N III–D3a (Rayoloma) (3992–III–NW) N III–D3b (Sincholagua) (3992–III–NE) N III–D3d (Lago Sinigchocha) (3992–III–SE)
Cotopaxi	1:50,000	N III–C4 (Machachi) (3892–II) N III–D3 (Sincholagua) (3992–III) N III–E2 (Mulalo) (3891–I) N III–F1 (Cotopaxi) (3991–IV)
	1:25,000	N III–D3c (Río Pita) (3992–III–SW) N III–F1a (Cotopaxi) (3991–IV–NW)
Quilindaña	1:50,000	N III–F1 (Cotopaxi) (3991–IV) N III–F3 (Laguna de Anteojos) (3991–III)
	1:25,000	N III–F4 (Chalupas) censo 152
Cerro Hermoso	1:50,000	N IV–B3 (Sucre) (3990–III)
Tungurahua	1:50,000	N IV–D1 (Banos) censo 173 N IV–D3 (El Pungal) censo 180
Altar	1:50,000	N IV–D3 (El Pungal) censo 180 N IV–F1 (Huamboya) censo 187
Cubillín	1:50,000	N IV–F1 (Huamboya) censo 187
Sangay		Not available
Collay	1:100,000	Sheet 71 (Alausi) published 1975 (Geologic map)
	1:50,000	N V–A4 (Totoras)
Cerro Ayapungo	1:100,000	Sheet 71 (Alausi) published 1975 (Geologic map)
	1:50,000	N V–A4 (Totoras) N V–C2 (Huangra)

Glacier Imagery

Aerial Photographs

Vertical aerial photographs of good quality exist for most of the glacierized mountains. (Refer to Hastenrath (1981) and table 3 for a detailed listing of these photographs.) Because the aerial photographs were taken for general survey, not glaciological purposes, and because of the frequent cloud cover in the humid-tropical Ecuadorean Andes, the aerial surveys were flown at the first favorable opportunity. Therefore, most photographs do not record the optimum glacier exposure possible during the cloud-free intervals of the minimum precipitation months (see fig. 2). This, in most cases, makes it more difficult and sometimes impossible to make a good glaciological evaluation from the aerial photographs. In addition, owing to the diurnal precipitation total and the year-round frequent snowfall events, the aerial photographs in many instances show a fresh snowfall, which reveals little in the way of relief contrast. It is, therefore, understandable that the contour lines on maps derived from these photographs can render only a very rough approximation to the actual relief. All these facts make accurate interpretation of glaciologic features from the existing aerial photography very difficult.

TABLE 3.—*Aerial photographs of the glacierized mountains of Ecuador*

[Abbreviations: HYCON, JET, Ecuadorean, aerial photographic mission designations; USAF, U.S. Air Force; VM, vertical mapping; PMW, Photo-Mapping Wing; IGM, Instituto Geográfico Militar; AMS, U.S. Army Map Service]

Glacier area	Date	Photograph identification
		Cordillera Occidental
Cotacachi	15 Feb 1956	HYCON: nos. 124256–124257, 124268–124269
	07 Mar 1963	USAF: nos. 2637–2638, 2653–2654
Iliniza	24 Jun 1962	USAF: VM AST–2, 1370 PMW, roll 26, nos. 1855–1856
	22 Jun 1963	USAF: VM CAST–9, 1370 PMW, roll 52, nos. 4451–4453
Chimborazo-Carihuairazo	24 Jun 1962	USAF: VM AST–2, 1370 PMW, roll 27, nos. 2048–2050
	24 Jun 1962	USAF: VM AST–2, 1370 PMW, roll 26, nos. 1878–1884
	26 Jun 1962	USAF: VM AST–2, 1370 PMW, roll 26, nos. 1946–1949
	12 Nov 1963	USAF: VM CAST–9, 1370 PMW, roll 71, nos. 6313A–6315A
	01 Nov 1977	Proyecto: Carta Nacional, R–28 IGM, nos. 5542–5544
	10 Nov 1977	Proyecto: Carta Nacional, R–29 IGM, nos. 5791–5794
		Cordillera Oriental
Cayambe	08 Feb 1965	USAF: linea 52A, nos. 7117–7119
	08 Feb 1965	USAF: linea 54, nos. 7177–7178
	17 Feb 1966	USAF: linea 56, nos. 7595–7598
	31 May 1978	Proyecto: Carta Nacional, R–33 IGM, nos. 6763–6765
Saraurcu	17 Nov 1966	USAF: linea 56, nos. 7601–7602
	02 Aug 1978	IGM JET: linea 30–D–R–33, nos. 6766, 6782–6783
Antisana	16 Feb 1956	HYCON: VV, HY, M, 142 AMS 153, linea 538, nos. 124156–124159; linea 539, nos. 124217–124220
	07 Feb 1965	USAF: VM 1370 PMW, R-76, linea 49, nos. 6730–6732; linea 52, nos. 6711–6714
	08 Feb 1965	USAF: VM 1370 PMW, R–78, linea 52A, nos. 7102–7104
	02 Apr 1977	Proyecto: Carta Nacional, R–20 IGM, nos. 3885–3888, 3825–3827
Sincholagua	15 Feb 1956	HYCON: VV, HY, M, 142 AMS 163, nos. 124289–124292, 124312, 124234
Cotopaxi	15 Feb 1956	HYCON: VV, HY, M, 142 AMS 163, nos. 124293–124294, 124307–124309
	25 Nov 1956	HYCON: VV, HY, M, 174 AMS 153, nos. 29767–29768
	03 Jan 1976	IGM JET: linea R6, nos. 1076–1078
Quilindaña	15 Feb 1956	HYCON: VV, HY, M, 142 AMS 153, nos. 124295–124297, 124227–124228
	01 Feb 1966	USAF: VM, 1370 PMW, AF 60–16, R83, nos. 7690–7691

TABLE 3.—*Aerial photographs of the glacierized mountains of Ecuador*—Continued

[Abbreviations: HYCON, JET, Ecuadorean, aerial photographic mission designations; USAF, U.S. Air Force; VM, vertical mapping; PMW, Photo-Mapping Wing; IGM, Instituto Geográfico Militar; AMS, U.S. Army Map Service]

Glacier area	Date	Photograph identification
		Cordillera Oriental—Continued
Cerro Hermoso	13 Jun 1956	HYCON: linea 546, nos. 29652–29653
	17 Sep 1976	IGM JET linea 1–R–12, nos. 2342–2344; linea 2–R–12, nos. 2353–2355
Tungurahua	15 Feb 1956	HYCON: linea 541, nos. 29602–29604; linea 542, nos. 29538–29540; linea 543, nos. 29787–29788
	04 Apr 1977	Proyecto: Carta Nacional, R-21 IGM, nos. 4000–4002
Altar	15 Feb 1956	HYCON: linea 541, nos. 29595–29599; linea 543, nos. 29543–29545; linea 543, nos. 29792–29793
	02 Apr 1977	IGM JET: linea 24–R–21, nos. 4004–4011
	31 May 1978	Proyecto: Carta Nacional, R–33 IGM, nos. 6848–6851
Cubillín	22 Apr 1963	USAF: linea 44, nos. 4688–4690
	04 Apr 1977	IGM JET: linea 23–R–21, nos. 4041–4042
Sangay	13 Jun 1956	HYCON: M–172, nos. 29671–29672
	08 Feb 1965	USAF: VM, 1370 PMW, AF 60–16, R–77, nos. 6893–6895
Collay	15 Feb 1956	HYCON: linea 543, nos. 29809–29812
	04 Apr 1977	IGM JET: linea 22–R–21, nos. 4107–4108; linea 23–R–21, nos. 4028–4031
Cerro Ayapungo	15 Feb 1956	HYCON: linea 543, nos. 29809–29812
	04 Apr 1977	IGM JET: linea 22–R–21, nos. 4107–4108; linea 23–R–21, nos. 4028–4031

Satellite Imagery

Optimum Landsat imagery of glacierized areas of Ecuador is listed in table 4 and located in figure 11. These images, namely Landsat multispectral scanner (MSS) images 21474–14323 and 30345–14460, acquired on 4 and 13 February 1979, respectively (figs. 9 and 10), are particularly useful because they are comparatively cloud free. They include the northern and southern parts of the Ecuadorean Andes, respectively. Proceeding from north to south, we will discuss first the Cordillera Occidental and then the Cordillera Oriental with reference to these two satellite images. For more general aspects look also at the section on Bolivia in this volume. In the northern part of the Cordillera Occidental, Cotacachi can be identified on Landsat image 21474–14323 (fig. 9) only a short distance to the north of Laguna Cuicocha. This mountain still carries perennial ice, but it cannot be seen on the satellite image because the glacier area is too small. The mountains Volcán Pichincha and Corazón can be identified in the Quito region. They are not glacierized presently, but perennial ice persisted into the last century. Southward from Corazón lie the twin peaks of Iliniza. The more southerly peak carries an ice cap from which 10 outlet glaciers descend. The mountain appears free of clouds on the satellite image, and the ice cover can be seen with difficulty. The gross morphology of an older moraine system is well depicted.

In the southern part of the Cordillera Occidental lies the highest mountain in Ecuador, Chimborazo (6,310 m), and the neighboring but much lower peak of Carihuairazo (5,020 m) (fig. 10). Both carry ice caps; the former has 22 and the latter, 9 outlet glaciers. The mountains appear nearly free of clouds on Landsat image 30345–14460. The glaciers on Carihuairazo can be seen only on the false-color composite image and not on the black-and-white Landsat image; the glacierization of Chimborazo is conspicuous in both versions. The gross morphology of older moraines on the Chimborazo-Carihuairazo massif can also be recognized on the satellite image.

In the northern part of the Cordillera Oriental, Cayambe is well depicted in figure 9. This mountain carries an ice cap that feeds 20 outlet glaciers. Saraurcu to the southeast is free of clouds on the satellite image and can be seen as a small white point. Antisana is cloud free and has an ice cap that

EXPLANATION OF SYMBOLS

Evaluation of image usability for glaciologic, geologic, and cartographic applications. Symbols defined as follows:

- Excellent image (0 to ≤5 percent cloud cover)
- Fair to poor image (>10 to ≤100 percent cloud cover)
- Unusable image (100 percent cloud cover)
- Nominal scene center for a Landsat image outside the area of glaciers

***Figure 11.**—Optimum Landsat 1, 2, and 3 images of the glaciers of Ecuador.*

TABLE 4.—*Optimum Landsat 1, 2, and 3 images of glaciers of Ecuador*
[See fig. 11 for explanation of symbols used in the "code" column]

Path-Row	Nominal scene center (lat-long)	Landsat identification number	Date	Solar elevation angle (degrees)	Code	Cloud cover (percent)	Remarks
10–60	00°00'N. 78°23'W.	21474–14323	04 Feb 79	43	●	0	Excellent of all glacierized areas
10–61	01°26'N. 78°44'W.	30345–14460	13 Feb 79	47	◑	60	Cloud-free image of glaciers of Quilindaña and Chimborazo-Carihuairazo. Other glaciers partially or completely cloud covered
10–62	02°53'S. 79°04'W.				◔		No cloud-free image available of glaciers of Cerro Ayapungo

feeds 17 outlet glaciers. The gross features of modern ice extent and older moraine morphology are shown especially well. Sincholagua also appears free of clouds on the satellite image. The mountain carries three small ice fields, but these are not apparent at all on the black-and-white version, and they are only barely visible on the false-color composite version of the satellite image. The gross features of older moraine morphology are, however, very well delineated. The volcanic cone of Cotopaxi is particularly conspicuous on the satellite image. With a summit elevation of 5,911 m, it is considered to be one of the highest active volcanoes on our planet. An ice cap that covers all but a few rock outcrops on the upper part of the mountain feeds 23 outlet glaciers.

The part of the Cordillera Oriental that lies south of Cotopaxi is covered by figure 10. Quilindaña, which is free of clouds, supports only two small glaciers, but these do not show on the black-and-white image and are only barely visible on the false-color composite version of the satellite image. The area of Cerro Hermoso is obscured by clouds on this image. The small summit ice cap of Tungurahua appears partly obscured by clouds. Altar, the most beautiful mountain of the Ecuadorean Andes, is also partly obscured by clouds. Altar has a caldera that opens toward the west. It is especially heavily glacierized on its eastern flank, where 6 separate outlet glaciers are present, although these are not discernible on the satellite imagery. An additional three ice masses present in the caldera are partially shaded in the satellite images. However, the large caldera lake that formed during the course of this century is visible. Gross features of older moraine morphology can likewise be recognized. The identification of ice and snow on *Cubillín* is marginal. A cloud sheet on the Amazon side of the cordillera extends to the region of Sangay, so this active, ice-clad volcano cannot be discerned on the satellite imagery. The ice extent on Collay appears to be too small to show on the satellite image, and Cerro Ayapungo lies just south of the image.

Because the 4 February and 13 February 1979 Landsat images provide an excellent record of many of the glaciers, it has been possible to determine the ice surfaces with a greater degree of accuracy than has been the case so far for most of the glacierized regions in Ecuador. Additional certainty has been gained through comparison with the precisely surveyed Cotopaxi glacierization pattern (Jordan, 1983). Table 1, which provides information on the glacierized areas of the Ecuadorean Andes, was based—as far as Chimborazo, Cayambe, Antisana, and Altar, are concerned—on analysis of satellite images using the STEREOCORD, which especially for Cotopaxi, reveals an excellent agreement with the area calculated by means of aerial photogrammetry (±3 percent). Further information on this method can be found in papers by Mohl (1980), Jordan and Kresse (1981), and Schwebel and Mohl (1984).

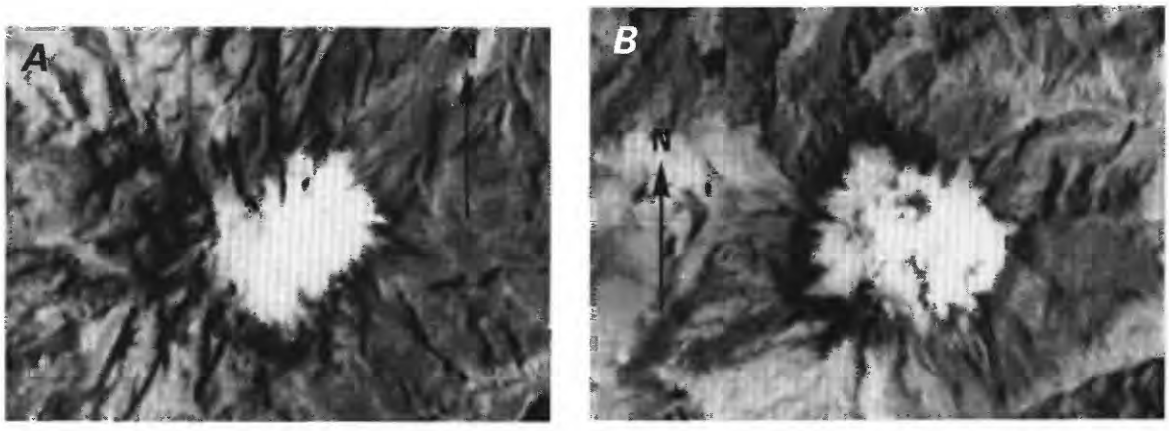

Even though small glaciers cannot be easily identified on Landsat MSS images and are even sometimes hard to identify on Landsat TM and SPOT satellite images with absolute certainty, especially where they appear obscured by clouds, the interpretation of larger ice surfaces (covering more than 0.2 km^2 (20 ha) is very accurate. It would even be possible, in case of high-quality, cloud-free imagery, such as the February 1979 data, to distinguish accumulation and ablation areas from each other on larger glaciers and thus make glaciological determinations that are not possible now. The use of high-resolution satellite imagery is especially important for glaciological studies here because no suitable aerial photography exists. Images of Chimborazo, Cayambe, Antisana, and Cotopaxi have been enlarged to scales of about 1:250,000 and 1:200,000 (see figs. 6 and 12) in an attempt to illustrate these applications. Ecuador's characteristic glacier type stands out very clearly on the Landsat images. The ice caps on the compact volcanic cones appear to be round to oval in a flat-surface projection, and the outlet glaciers, which diverge in the ice-free areas downslope, appear as frazzled edges. This special type of continental tropical glacier, an ice cap on the summit of a conical volcano, is suitable, where large enough, for interpretation from satellite imagery. These ice caps are generally less obscured by shadow-casting features, with the exception of the Altar nevado (snowfield), than are marginal tropical glaciers (see the section on the glaciers of Bolivia in this volume). The Landsat images, especially the one of 4 February 1979, would be worth processing digitally by using contrast-enhancement methods. The digitally enhanced images could be used to distinguish more clearly the glacier features and boundaries and to determine glacier areas.

***Figure 12.**—Parts of Landsat MSS images of volcanoes in Ecuador that have glacier areas greater than 0.2 km^2 (20 ha). These images are enlarged to a scale of about 1:200,000 in order to illustrate the typical continental tropical glacier on a volcanic cone. The ice caps have round to oval outlines and lobate edges (outlet glaciers). In some areas, it is possible to separate the accumulation and ablation areas on the glaciers by means of the different gray tones.*

A, *Cayambe, in the northern part of the Cordillera Oriental, carries an ice cap that feeds 20 outlet glaciers, many of which can be delineated on the image.*

B, *Antisana, also in the northern part of the Cordillera Oriental, has an ice cap that feeds 17 outlet glaciers. Many of these are visible, in addition to ablation features on the ice cap.*

C, *See facing page.*

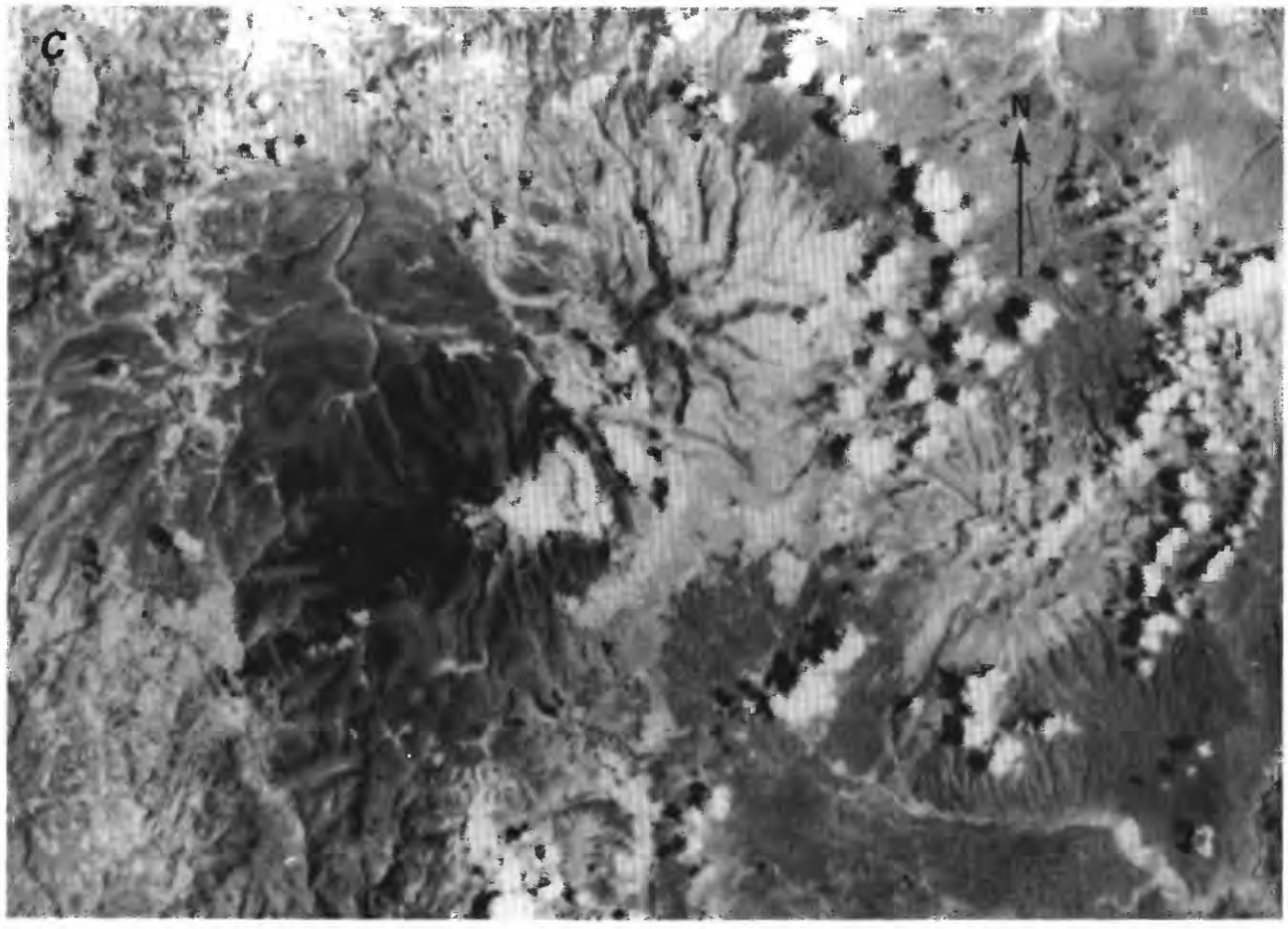

Figure 12C.—*Chimborazo, in the southern part of the Cordillera Occidental, has an ice cap that has 22 outlet glaciers. Clouds obscure some of the glaciers, but the majority are visible. Also visible on the image to the northeast of Chimborazo is Carihuairazo, although its ice cap and nine outlet glaciers cannot be delineated. Figures 12A and 12B are from Landsat image 21474–14323, band 7; 4 February 1979; Path 10, Row 60. Figure 12C is from Landsat image 30345–14460, band 7; 13 February 1979; Path 10, Row 61. Both images are from EROS Data Center, Sioux Falls, S. Dak.*

References Cited

Bates, R.L., and Jackson, J.A., eds., 1980, Glossary of geology (2d ed.): Falls Church, Va., American Geological Institute, 749 p.

Blandin Landivar, C., 1976–77, The climate and its characteristics in Ecuador: Instituto Geográfico Militar, Biblioteca Ecuador, Asamblea general del Instituto Panamericano de Geografía e Historía [General Meeting of the Pan-American Institute of Geography and History], 11th, Quito, Ecuador, 1977, 83 p.

Clapperton, C.M., 1993, Glacier readvances in the Andes at 12,500–10,000 yr B.P.: Implications for mechanism of late-glacial climatic change: Journal of Quaternary Science, v. 8, no. 3, p. 197–215.

Graf, Kurt, 1981, Zum Höhenverlauf der Subnivalstufe in den tropischen Anden, insbesondere in Bolivien und Ecuador [On the altitude pattern of the subnival step in the tropical Andes, especially in Bolivia and Ecuador]: Zeitschrift für Geomorphologie, Supplementband 37, p. 1–24.

Hastenrath, Stefan, 1981, The glaciation of the Ecuadorian Andes: Rotterdam, A.A. Balkema Publishers, 159 p.

Heine, Klaus, 1995, Bedded slope deposits with respect to the late Quaternary glacial sequence in the high Andes of Ecuador and Bolivia, *in* Slaymaker, O., ed., Steepland geomorphology: New York, John Wiley and Sons, p. 257–278.

Instituto Geográfico Militar [1978?], Atlas geográfico de la República del Ecuador [Geographic atlas of the Republic of Ecuador]: Quito, Ecuador, Instituto Geográfico Militar, 82 p.

Jordan, Ekkehard, 1979, Grundsätzliches zum Unterschied zwischen tropischem und aussertropischem Gletscherhaushalt unter besonderer Berücksichtigung der Gletscher Boliviens [Fundamental comments on the difference between tropical and extra-tropical glacier balance with special emphasis on Bolivia's glaciers]: Erdkunde, v. 33, no. 4, p. 297–309.

———1983, Die Vergletscherung des Cotopaxi-Ecuador [The glaciation of Cotopaxi, Ecuador]: Zeitschrift für Gletscherkunde und Glazialgeologie, v. 19, no. 1, p. 73–102.

———1984, Möglichkeiten und Grenzen der Herstellung und synchronen Auswertung biowissenschaftlicher Verbreitungskarten aus Luftbildern mit dem neuen Kartiersystem des STEREOCORD's am Beispiel ausgewählter Vegetationsbereiche Boliviens [Possibilities and limitations of the production and synchronous analysis of bioscience distribution maps from aerial photographs using the new STEREOCORD mapping system with the help of the example of selected vegetation regions in Bolivia]: Verhandlungen der 12. Jahrestagung der Gesellschaft für Ökologie, Bern, 1982, v. 11, Göttingen.

Jordan, Ekkehard, Brieva, Jorge, Calvache, Marta, Cepeda, Hector, Colmenares, Fabio, Fernandez, Benjamin, Joswig, Reinnar, Mojica, Jairo, and Nuñez, Alberto, 1987, Die Vulkangletscherkatastrophe am Nevado del Ruiz, Kolumbien [Volcano-glacier catastrophe at Nevado del Ruiz, Colombia]: Bensheim, Geoökodynamik v. 8, no. 2–3, p. 223–244.

Jordan, Ekkehard, and Kresse, Wolfgang, 1981, Die computergestützte quantitative Luftbildauswertung mit dem Zeiss-STEREOCORD und seinen Peripheriegeräten zur Rationalisierung der Feldforschungen in den Geowissenschaften [Computer-assisted quantitative air photo interpretation using the STEREOCORD and its peripheral instruments for rationalization of field research in the earth sciences]: Erdkunde, v. 35, no. 3, p. 222–231.

Lipman, P.W., and Mullineaux, D.R., 1981, The 1980 eruptions of Mount St. Helens, Washington: U.S. Geological Survey Professional Paper 1250, 844 p.

Mercer, J.H., 1967, Glaciers of Ecuador, *in* Southern Hemisphere glacier atlas: U.S. Army Natick Laboratories, Earth Sciences Laboratory, Series ES–33, Technical Report 67–76–ES, p. 1–22.

Meyer, Hans, 1907, In den Hoch-Anden von Ecuador [In the high Andes of Ecuador]: Berlin, Dietrich Reimer, 551 p.

Mohl, Hans, 1980, Konzeption und Genauigkeitsleistung des neuen Programmsystems zum STEREOCORD G2 [Conception and accuracy of the program system for the STEREOCORD G2]: International Society for Photogrammetry, XIV Congress, Hamburg, 1980, v. 23, part 2, p. 177–186.

Sauer, Walther, 1971, Geologie von Ecuador, *in* Beiträge zur Regionalen Geologie der Erde [Geology of Ecuador, *in* Contributions to the regional geology of the Earth]: Berlin-Stuttgart, Gebrüder Borntraeger, 316 p.

Schwebel, Reiner, and Mohl, Hans, 1984, The Zeiss-STEREOCORD for manifold measuring and interpretation applications: Karlsruhe, Germany, Bildmessung und Luftbildwesen, v. 52, issue 3a, p. 153–162.

Simkin, Tom, and Siebert, Lee, 1994, Volcanoes of the world (2d ed.): Tucson, Ariz., Geoscience Press, Inc., in association with the Smithsonian Institution, 349 p.

U.S. Board on Geographic Names, 1987, Gazetteer of Ecuador (2d ed.): Washington, D.C., Defense Mapping Agency, 375 p.

Weischet, Wolfgang, 1969, Klimatologische Regeln zur Vertikalverteilung der Niederschläge in Tropengebirgen [Climatological regime of the vertical distribution of precipitation in the mountains of the tropics]: Die Erde, 100 Jahrgang, no. 2–4, p. 287–306.

Whymper, Edward, 1892, Travels amongst the great Andes of the Equator: New York, Charles Scribner's Sons, 456 p.

Glaciers of South America–

GLACIERS OF PERÚ

By BENJAMÍN MORALES ARNAO

With sections on the CORDILLERA BLANCA ON LANDSAT IMAGERY *and QUELCCAYA ICE CAP*

By STEFAN L. HASTENRATH

SATELLITE IMAGE ATLAS OF GLACIERS OF THE WORLD

Edited by RICHARD S. WILLIAMS, Jr., *and* JANE G. FERRIGNO

U.S. GEOLOGICAL SURVEY PROFESSIONAL PAPER 1386–I–4

Perú has a total glacier-covered area of 2,600 square kilometers located on 20 distinct cordilleras. The largest ice concentrations are in the Cordillera Blanca (723.4 square kilometers) and the Cordillera de Vilcanota (539 square kilometers). The glacierized areas are important as water sources and as the sites of glacier-related avalanches and floods that have destroyed towns and killed tens of thousands of inhabitants

CONTENTS

GLACIERS OF SOUTH AMERICA–

GLACIERS OF PERÚ

By BENJAMÍN MORALES ARNAO[1]

With sections on the CORDILLERA BLANCA ON LANDSAT IMAGERY *and QUELCCAYA ICE CAP*[2]

By STEFAN L. HASTENRATH[3]

Abstract

The glacierized areas of Perú are found in 20 distinct mountain ranges (cordilleras) extending from central northern Perú to its southern border, and they include two major glacier systems. The largest system, which is in the central northern part of Perú in the Cordillera Blanca, extends along a distance of 200 kilometers; it has a total glacierized area of 723.4 square kilometers. The second largest system has a glacierized area of 539 square kilometers and is in the southeastern part of Perú in the Cordillera de Vilcanota. The estimated total ice-covered area within Perú is about 2,600 square kilometers.

The glacierized areas are very important because runoff (meltwater) from glaciers is used for agricultural, industrial, and domestic purposes. Runoff from glaciers is particularly important in the hyperarid coastal areas. On the other hand, some glacierized cordilleras have historically been the sites of catastrophes such as ice avalanches, floods, and the like. In the Río Santa valley, adjacent to the Cordillera Blanca, for example, 22 such catastrophes of glaciological origin have taken place since 1702 and have caused the destruction of towns, villages, and croplands and have killed tens of thousands of inhabitants.

In this century, studies were begun in 1927 for agricultural, industrial, and scientific purposes, and since 1941, studies and construction projects have been undertaken to prevent damage from glacier hazards. The Government of Perú has completed many successful engineering projects that drain glacier lakes in order to reduce the danger of failure and catastrophic flooding. From 1974 to 1984, the *Quelccaya ice cap* in the Cordillera de Vilcanota, southern Perú, has been intensively studied by Ohio State University, in cooperation with Peruvian institutions, in order to determine paleoclimatic conditions. In addition, a national inventory of the glaciers of Perú was finished in 1988 by the Department of Glaciology and Hydrology of Hidrandina S.A.

Occurrence of Glaciers

Perú is located on the western side of South America between lat 0° and 18°S. and long 69° and 81°W.; it is traversed by the great Andean mountain system that extends along the entire western side of South America (Peterson, 1958; Ricker, 1977). Extensive areas of this mountain system are glacierized. The Peruvian Andes comprise three major ranges or cordilleras: Cordillera Occidental on the west, Cordillera Central in the middle, and Cordillera Oriental on the east (fig. 1). The high average elevation of the

Manuscript approved for publication 18 March 1998.

[1] Consult Control S.A., Avenida Javier Prado Este 210–4to. Piso B San Isidro, Lima, Perú.

[2] The names in this section conform to the usage authorized by the U.S. Board on Geographic Names in its Gazetteer of Peru (U.S. Board on Geographic Names, 1989). The names not listed in the gazetteer are shown in italics, with the exception of Perú for which the Peruvian spelling is retained.

[3] Department of Atmospheric and Oceanic Sciences, University of Wisconsin, 1225 West Dayton Street, Madison, Wis. 53706 U.S.A.

three cordilleras, together with regional and local climatic conditions, has resulted in the extensive development of glaciers in many locations (Heim, 1947; Morales Arnao, C., 1953–1995, 1964; Morales Arnao, B., 1969c; Francou, 1984). In fact, the Peruvian Andes have the largest area of tropical glaciers on Earth (Mercer, 1967; Kinzl, 1968). The total ice-covered area is estimated to be 2,600 km^2 (Hidrandina,1988). The average minimum elevation of glaciers in Perú is 4,800 m above sea level (asl). In the discussion that follows, the glacierized areas have been grouped into 20 distinct cordilleras (Morales Arnao, C., 1964) (fig. 2, table 1). Each of these areas is briefly described, first those in the Cordillera Occidental followed by those in the Cordillera Central and then those in the Cordillera Oriental. Within each cordillera, the areas are described from north to south. The largest single glacier, the *Quelccaya ice cap*, is in the Cordillera de Vilcanota. Of the next 11 largest glaciers, 8 are located in the Cordillera Blanca (table 2).

***Figure 1.**—Principal cordilleras of the Andes Mountains in Perú.*

TABLE 1.—*Location, orientation, and area of the principal glacierized areas of Perú*

[Abbreviations: N, north; W, west; E, east]

Cordillera (see fig. 2)	Latitude south	Longitude west	Ice-covered area (square kilometers)	Extent (kilometers) and orientation		Highest elevation (meters above mean sea level)	Drainage basin	Data source
Blanca	08°08'–09°58'	77°00'–77°52'	723.40	200	NW	6,768	Pacific-Atlantic	1
Huallanca	09°52'–10°03'	76°58'–77°04'	22.41	19	NW	5,480	Pacific-Atlantic	1, 2
Huayhuash	10°11'–10°26'	76°50'–77°00'	88.11	26	NW	6,634	Pacific-Atlantic	1, 2
Raura	10°21'–10°31'	76°41'–76°50'	57.03	20	NW	5,727	Pacific-Atlantic	1, 2
La Viuda	10°33'–11°37'	76°07'–76°42'	28.5	130	NW	5,780	Pacific-Atlantic	1, 2
Central	11°37'–12°26'	75°30'–76°18'	176.3	100	N	5,817	Pacific-Atlantic	1
Chonta	12°37'–13°07'	75°00'–75°30'	42	50	N	5,305	Pacific-Atlantic	3
Huanzo	14°30'–15°01'	72°50'–73°15'	158	57	NW	5,445	Pacific-Atlantic	3
Chila	15°02'–15°26'	71°43'–72°37'	52	80	E	5,556	Pacific-Atlantic	2, 3
Ampato	15°24'–15°51'	71°51'–73°00'	105	140	E	6,426	Pacific	2, 3
Volcánica	16°07'–16°33'	71°12'–71°33'	15	50	NW	6,100	Pacific	2, 3
Barroso	16°51'–17°37'	69°45'–70°30'	20	110	NW	5,741	Pacific	2, 3
Huaytapallana	11°47'–11°56'	75°00'–75°05'	35	17	NW	5,720	Atlantic	3
Vilcabamba	13°10'–13°27'	72°30'–73°15'	173	85	E	6,271	Atlantic	3
La Raya	15°10'–15°26'	70°36'–71°14'	88	60	E	5,489	Pacific-Atlantic-Titicaca	2, 3
Huagaruncho	10°14'–10°19'	75°57'–76°03'	48	10	E	5,879	Atlantic	2, 3
Urubamba	13°08'–13°17'	71°58'–72°16'	23	30	NW	5,750	Atlantic	2, 3
Vilcanota	13°39'–14°29'	70°31'–71°20'	539	120	N, W	6,384	Atlantic	3
Carabaya	14°00'–14°22'	69°38'–70°19'		75	NW	5,780	Atlantic-Titicaca	2, 3
Apolobamba	14°35'–14°45'	69°14'–69°34'	100	35	E	5,852	Atlantic-Titicaca	2, 3
		Total	102					
			2,596					

1 Data from Peruvian glacier inventory. Source: vertical aerial photographs.
2 Data published in Revista Peruana de Andinismo.
3 Data from Landsat images.

Figure 2.—*Distribution of the 20 glacierized cordilleras of Perú shown in green and the location of some of the principal rivers. Abbreviation: R., Río.*

TABLE 2.—*Principal glaciers of Perú*

Cordillera	Name	Latitude south	Longitude west	Area (square kilometers)	Maximum length or diameter (kilometers)	Type of glacier
Vilcanota	*Quelccaya*	14°00'	70°46'	54.00	17.0	ice cap
Blanca	Copap	09°17'	77°20'	13.76	7.0	plateau
Huayhuash	Yerupaja	10°14'	76°55'	9.36	6.0	valley
Blanca	*Chopicalqui*	09°05'	77°36'	9.10	6.5	valley (debris-covered)
Blanca	*Pucahirca*	08°53'	77°35'	6.50	4.5	plateau
Blanca	*Artesonraju*	08°58'	77°38'	5.97	3.6	mountain
Central	Sullcon	11°52'	76°03'	5.43	5.3	valley
Blanca	Cook	09°02'	77°39'	5.39	4.6	valley (debris-covered)
Blanca	Safuna	08°51'	77°37'	4.69	3.6	valley
Raura	*Santa Rosa*	10°29'	76°44'	2.36	2.7	valley
Blanca	*Uruashraju*	09°35'	77°19'	2.15	2.5	valley
Blanca	*Yanamarey*	09°39'	77°16'	1.30	1.7	valley

Climatic Conditions

The glacierization of the cordilleras in Perú is directly related to the physical geography of the Andes, the elevation of the mountains, and the precipitation pattern. Generally speaking, the precipitation that falls on the glaciers comes from the Amazon and Paraná basins to the east of the mountains and falls as snow in the Andes because of the high elevations. The annual precipitation of snow in the highest cordillera is between 1,200 and 2,500 mm of water. This results in an annual accumulation of 2 to 3 m of snow between 5,000 and 6,000 m of elevation. The equilibrium line altitude that separates the accumulation area of glaciers from the lower ablation areas is between 4,800 and 5,100 m.

Hollin and Schilling (1981, p. 191) summarized the lowering of the snowline in the Peruvian Andes during the Pleistocene: "...the Pleistocene snowline was...4,000 m on the seaward side and 3,700 m on the landward side in northwest Perú; 4,300 m in central Perú; and 4,500 m in the southwest and 4,200 m in the northeast in a transect through Arequipa." Mercer and Palacios (1977) found evidence for a snowline of about 4,200 m for Nevado Auzangate in the Cordillera de Vilcanota in the last Wisconsinan and a snowline of 3,650 m for the coldest part of the Pleistocene; this compares with 4,600 m for the elevation of the modern glacier terminus. It is clear that the Andean mountains of tropical South America also experienced major climate cooling during the Pleistocene.

The Humboldt Current and the El Niño Current cause the unusual climatic conditions in Perú. The lowlands along the Pacific Coast have a hyperarid climate with infrequent rains and sparse to nonexistent annual precipitation. In contrast, the Andean highlands have alternating dry and rainy seasons and moderate precipitation. The eastern slopes of the Andes receive the greatest precipitation because of moisture from the vast Amazon basin, and precipitation continues throughout the year.

Because of these climatic variations, the flora and fauna in the arid coastal regions are completely dependent upon water from the Andean region (Dollfus, 1965). The glacierized areas in the Cordillera Occidental are very important as the unique sources of permanent water supply for the desertlike coastal areas of Perú.

Paleoclimatic Conditions

Studies of ice cores from the *Quelccaya ice cap* in southern Perú by Ohio State University, in cooperation with Electroperú, have provided new data about climatic conditions during the last 1,500 years. The studies included measurement of oxygen and other isotopes, as well as the study of conductivity and microparticles in the ice cores (Thompson and Dansgaard, 1975; Thompson, Hastenrath, and Morales Arnao, 1979; Thompson, 1980; Thompson, Bolzan, and others, 1982; Thompson, Mosley-Thompson, Grootes, and others, 1984; Thompson, Mosley-Thompson, and Morales Arnao, 1984; Thompson, Mosley-Thompson, Bolzan, and Koci, 1985; Thompson, Mosley-Thompson, Dansgaard, and Grootes, 1986; Thompson and Mosley-Thompson, 1987, 1989; Thompson, Davis, and others, 1988).

The results of such paleoclimate studies, including those of Hastenrath (1967), Nogami (1972), Mercer and Palacios (1977), and Wright and others (1989), together with present-day climatic data, will lead to a more accurate understanding of climatic variability in the region. This information also should be helpful in planning the most cost-effective development of the hydrological resources of Perú.

History of Glacier Studies

The presence of glaciers in Perú was first mentioned in 1532 by Miguel de Astete, who was one of the members of the Hernando Pizarro Expedition; they crossed the Cordillera Blanca while traveling from Cajamarca to *Pachacamac* (Lima) (fig. 2). The first noted major glacier-related catastrophe was in 1702, when an outburst flood from a glacier lake destroyed part of the city of Huaraz. In 1725, floods again caused damage in Huaraz, and on the same day, an ice avalanche destroyed the town of Ancash. Antonio Raymondi described glaciers of the Cordillera Blanca in 1866 (Raymondi, 1873).

Modern Glacier Studies

Glacier studies were begun in modern time by Ingeniero (Ing.) Jorge Broggi (Broggi, 1943, 1945) who, in 1927, commented on the influence of glaciers at the Raura Mines. Since 1932, several Austro-German expeditions led by P. Borchers and Professors Hans Kinzl and E. Schneider have surveyed and studied the Cordillera Blanca (Kinzl, 1935, 1942, 1964; Kinzl and Schneider, 1950) and Cordillera Huayhuash (Kinzl, Schneider, and Ebster, 1942; Kinzl, Schneider, and Awerzger, 1954); they made several accurate maps at scales of 1:200,000, 1:100,000, and 1:50,000 by using terrestrial photogrammetry. The expeditions also included observations of lakes and glaciers of the region (Kinzl, 1940).

In December 1941, a flood caused by the failure of a moraine dam at a lake in the Cordillera Blanca destroyed about 25 percent of the city of Huaraz. The catastrophe prompted the Instituto Geológico del Perú, under the direction of Ing. Jorge Broggi and the Commission of Cordillera Blanca Lakes, to begin a study and inventory of lakes and glaciers in the Cordillera Blanca. In addition, engineering projects were initiated to prevent or mitigate flood disasters caused by glacier-lake outbursts. This work has continued with some interruptions until the present (Fernandez Concha, 1957; Morales Arnao, B., 1969c).

Between 1944 and 1945, the Instituto Geológico del Perú extended its glacier studies to the Cordilleras *Central*, Vilcabamba, Carabaya, and *Apolobamba* (fig. 2). Between 1945 and 1972, the Corporación Peruana del Santa and the Regional Office of Electricity sponsored a number of studies that led to a series of reports on glaciers, glacial geology, and glacier lakes in the Cordillera Blanca: Oppenheim and Spann (1946), Heim (1947), Szepessy (1949, 1950), Trask (1952, 1953), Fernandez Concha (1957), Morales Arnao, B. (1962, 1966, 1969a, d), Petersen (1967), Ames (1969), Lliboutry (1977), Lliboutry, Morales Arnao, Pautre, and Schneider (1977), and Lliboutry, Morales Arnao, and Schneider (1977).

From 1966 to 1986, Ing. Benjamín Morales Arnao, initially with the Corporación Peruana del Santa and later with Electroperú, organized a special department of glacier studies (Kinzl, 1970); this department had as its primary objective the carrying out of studies of glaciers of the Cordillera Blanca and the planning of construction projects that would prevent catastrophic floods (Corporación Peruana del Santa, Electroperú, 1967–1995; Morales Arnao, B., 1969c, 1971; Schneider, 1969). The studies were begun in the northern part of the country. The Instituto de Geológia y Minería extended glacier studies to the entire country and had the goal of a complete inventory of glaciers and glacier lakes in Perú. The inventory was completed in 1988 (Hidrandina, 1988).

Starting in 1978, international agreements were signed with several institutions to support glacier studies, these included an arrangement with the Federal Institute of Technology, Zürich, Switzerland, to contribute Peruvian glacier data to the World Glacier Inventory Project, as well as cooperative research with Ohio State University on studies of paleoclimate from ice cores of the *Quelccaya ice cap* in the Cordillera de Vilcanota (Thompson, Mosley-Thompson, Grootes, and others, 1984) and from the Cordillera Blanca. More recently cooperative glacier studies have been established with the French Institute of Andean Studies and the Institute of Geography at the University of Innsbruck, Austria.

Peruvian Cordilleras

Cordillera Occidental

Cordillera Blanca

The Cordillera Blanca is the most extensive tropical ice-covered mountain range in the world and has the major ice concentration in Perú. It is part of the Cordillera Occidental and trends in a northwesterly direction for about 200 km between lat 8°08' and 9°58'S. and long 77°00' and 77°52'W. (figs. 2–5). It marks the continental divide; Río Santa on the west drains into the Pacific Ocean, whereas Río Marañón on the east drains into the Atlantic Ocean. The Cordillera Blanca has five of the most spectacular peaks above 6,000 m in the Peruvian Andes. The highest peak (Nevado Huascarán) rises to an elevation of 6,768 m asl. A total of 722 individual glaciers are recognized in the Cordillera Blanca, and these cover an area of 723.4 km^2. Most of these glaciers are on the western side of the ranges, where 530 glaciers cover an area of 507.5 km^2. On the eastern side are 192 glaciers that cover an area of 215.9 km^2; the lowest glacier terminus is at 4,200 m asl. Most of the glaciers, 91 percent of the total, are classified as mountain glaciers; they are generally short and have extremely steep slopes. The rest are classified as valley glaciers, except for one ice cap. Four are similar to rock glaciers (Kinzl, 1935, 1942, 1964; Kinzl and Schneider, 1950; Morales Arnao, C., 1964; Morales Arnao, B., 1969a, b; figs. 3 and 4; tables 1 and 2).

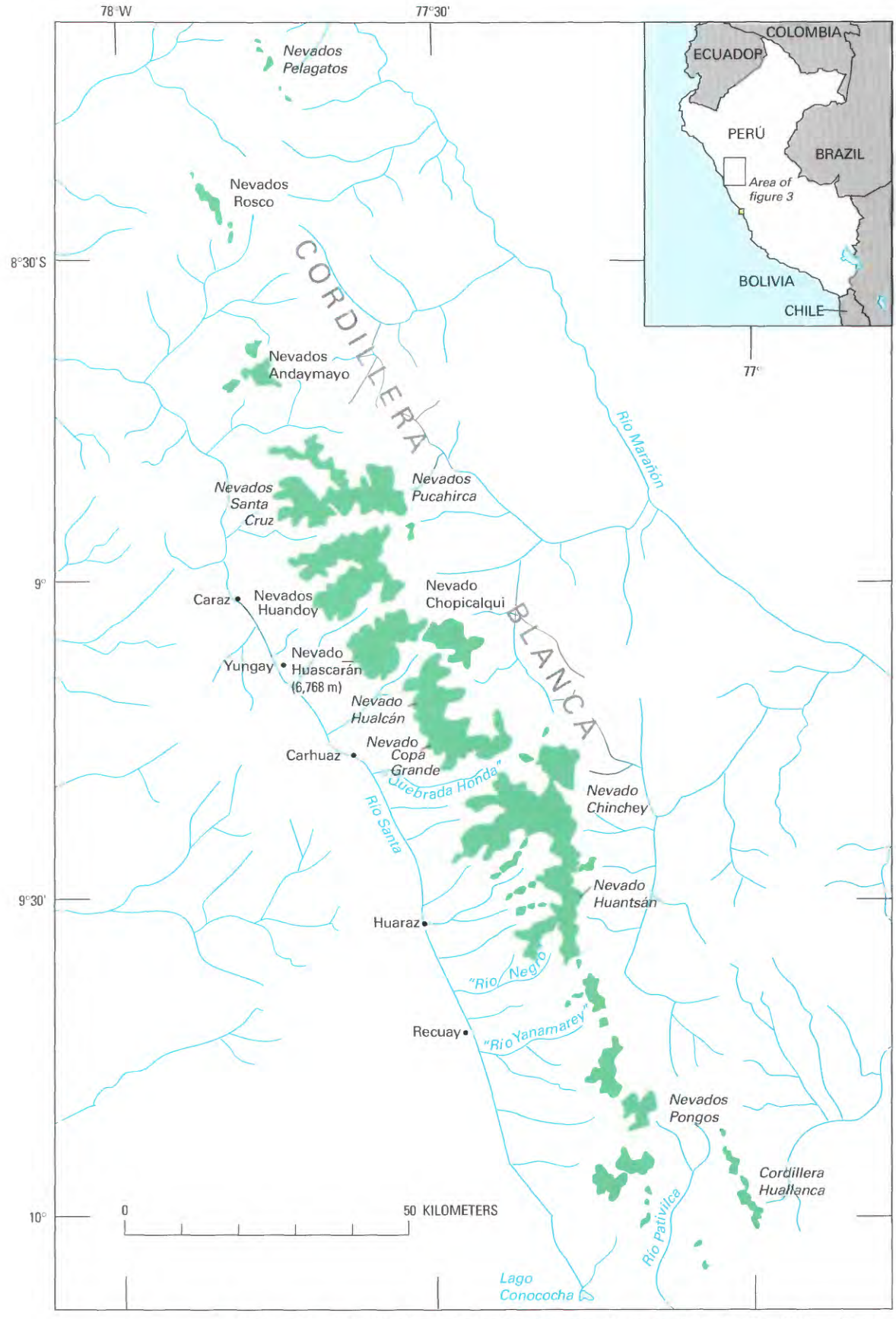

Figure 3.—*Distribution of glaciers (shown in green) in the Cordillera Blanca and* Cordillera Huallanca. *The Cordillera Blanca is the most extensive tropical ice-covered mountain range in the world and has the largest ice concentration in Perú.*

Cordillera Blanca on Landsat Imagery

By Stefan L. Hastenrath

Figure 4, the best available Landsat 1, 2, or 3 image of the Cordillera Blanca area, provides an excellent pictorial overview of the major glacierized areas. North of the main glacierized segment of the Cordillera Blanca can be seen the ice cover on *Nevados Pelagatos* and the Nevados Rosco. The great bend of the Río Santa valley (on the left center of the image) broadly marks the northern extremity of the Cordillera Blanca (fig. 4). The gross physiography of the area is dominated by this deep valley, as well as the Cordilleras Negra and Blanca on the west and east, respectively. It is possible to identify the separate glacierized areas on Nevados Andaymayo in the northwestern part of Cordillera Blanca.

Figure 4.—*Annotated Landsat 2 MSS false-color composite image (2194–14351; 4 August 1975; Path 8, Row 66) of the northern part of the Cordillera Blanca. Abbreviation: Q., Quebrada. Landsat 2 image from EROS Data Center, Sioux Falls, S. Dak.*

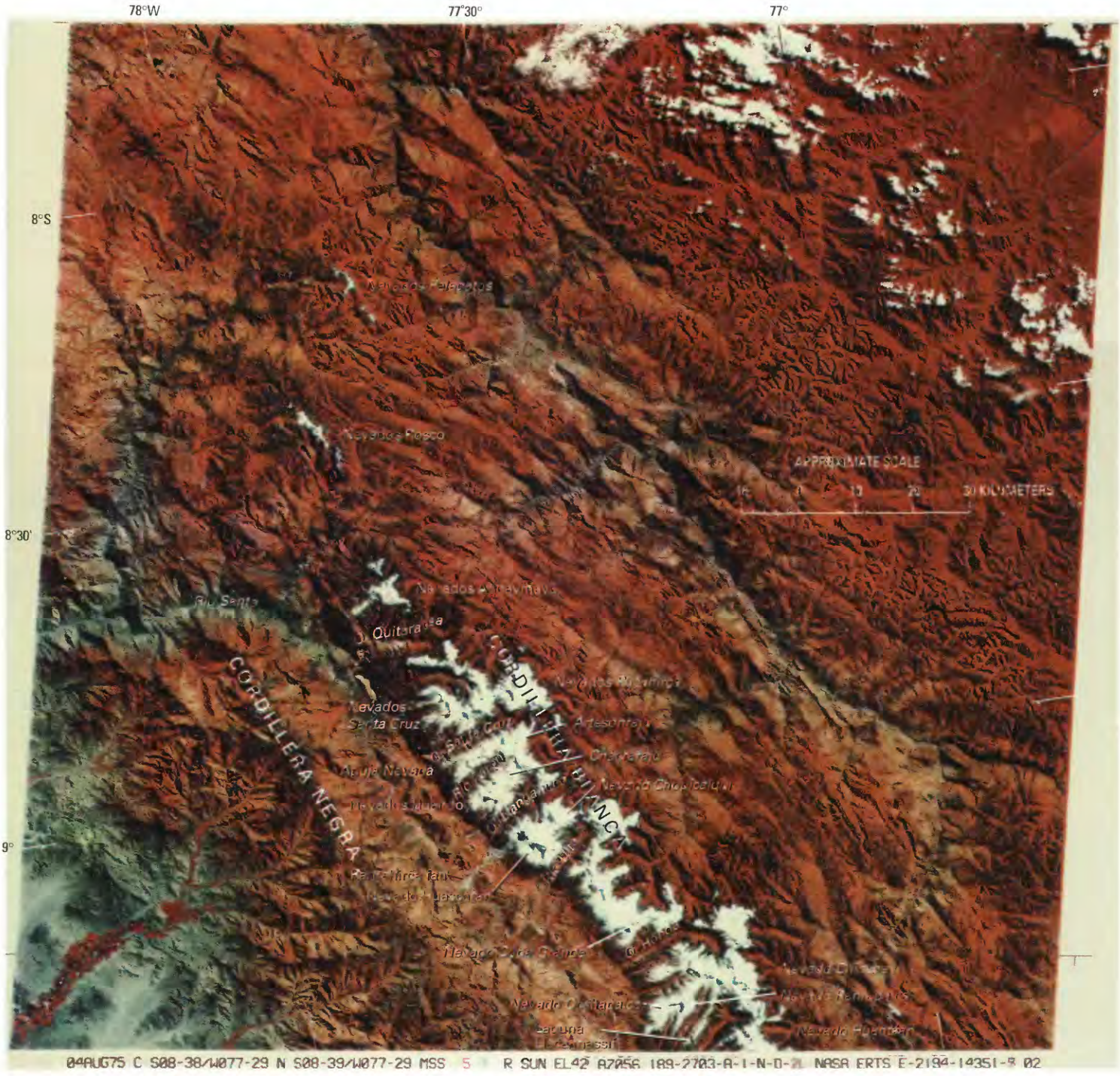

Two tributaries of Río Santa, *Quebrada Quitaracsa* and Quebrada Santa Cruz, bound the complex glacier system of the *Nevados Pucahirca* and *Nevados Santa Cruz* (fig. 4). The Quebrada Santa Cruz valley and *Quebrada Llanganuco* to the south delineate another glacier system, arranged in horseshoe form around *Río Parón*. Within this area are the mountain peaks *Aguja Nevada, Artesonraju, Chacraraju*, and Nevados Huandoy. These peaks can be seen in the panoramic view shown in figure 5. The *Quebrada Llanganuco* and the *Río Ulta* bound the Huascarán massif. The saddle between the north and south peaks of Nevado Huascarán can be seen in figure 4; particularly conspicuous are the scars of the catastrophic Huascarán debris avalanche of May 1970 (Welsch and Kinzl, 1970; Morales Arnao, B., 1971; Plafker and Ericksen, 1978) that originated on the west side of the north peak and completely destroyed the city of Yungay (see figs. 6 and 12).

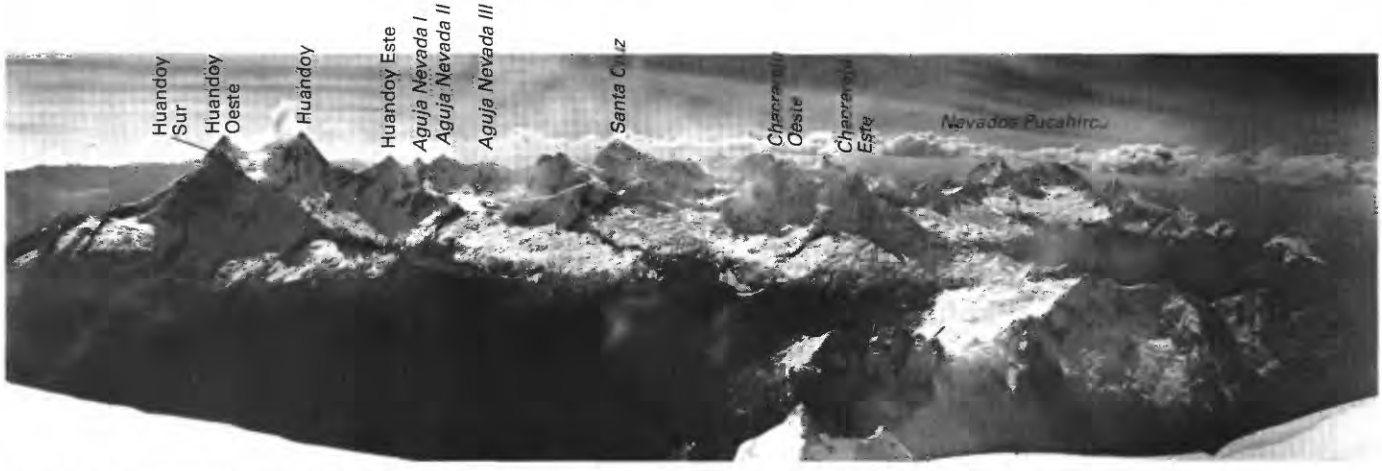

Figure 5.—*Panoramic view in the northern Cordillera Blanca taken from the summit of* Nevado Chopicalqui *looking from the northwest (left) to the north (right). Photograph by Leigh Ortenburger.*

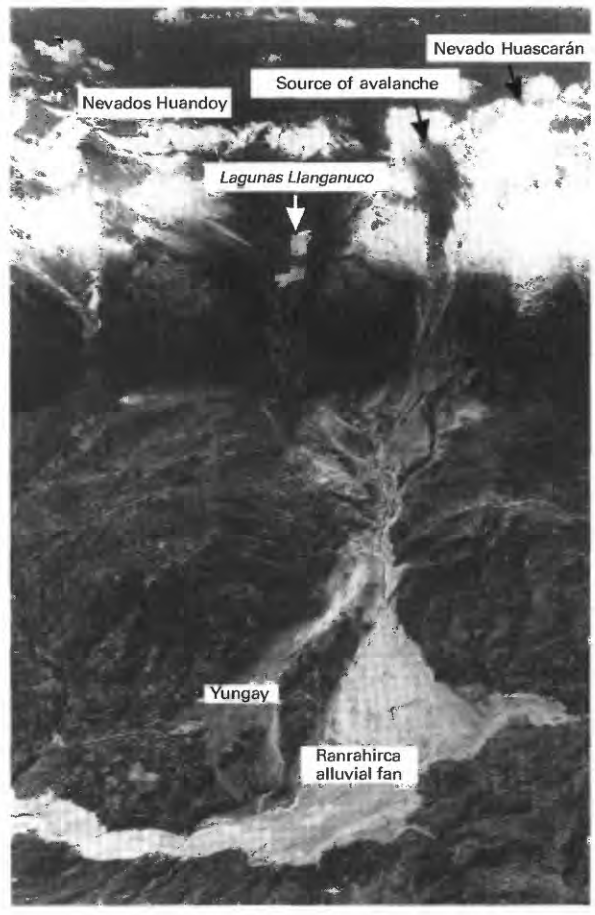

Figure 6.—*Oblique aerial photograph of the site of the former village of Yungay, which was completely destroyed 31 May 1970 by a massive ice-and-debris avalanche in the Cordillera Blanca. The avalanche originated from the west side of the north peak of the Huascarán massif. Photograph courtesy of Servicio Aerofotográfico Nacional (S.A.N.).*

Between *Río Ulta* on the north and *Quebrada Honda* on the south, a large glacierized area culminates in the *Nevado Copa Grande* (6,188 m). A large, continuous glacierized area extends from the *Quebrada Honda* southward to about the *Río Negro*, but only the northern two-thirds is depicted on the Landsat image (fig. 4). This extensive glacierized area includes the Nevados *Ocshapalca* and *Ranrapalca* and the *Laguna Llaca* mountain massif. The southern part of this glacierized region and three other glacierized areas in the southern part of the Cordillera Blanca are covered by another Landsat image further south (see table 7). Some maps of the Cordillera Blanca are listed in table 5.

Cordillera Huallanca

The *Cordillera Huallanca*, a small glacierized range between lat 9°52' and 10°03'S. and long 76°58' and 77°04'W., also is part of the Cordillera Occidental. The range is about 19 km long, and the glacierized area covers 22.41 km^2. It drains westward into Río Pativilca and the Pacific Ocean, as well as eastward into Río Marañón and the Atlantic Ocean. The highest peak reaches 5,480 m asl (figs. 2 and 3, table 1).

Cordillera Huayhuash

The Cordillera Huayhuash, between lat 10°11' and 10°26'S. and long 76°50' and 77°00'W., is part of the Cordillera Occidental of Perú. It is about 26 km long, and the glacierized area is 88.11 km^2. The highest peak is Cerro Yerupaja at an elevation of 6,634 m asl. Most of the glaciers are of the mountain type and drain into the Pacific and Atlantic Oceans by Río Pativilca and Río Marañón, respectively (fig. 2, table 1).

Cordillera Raura

The Cordillera Raura, also part of the Cordillera Occidental, lies between lat 10°21' and 10°31'S. and long 76°41' and 76°50'W. It trends northwesterly and is about 20 km long (fig. 2, table 1). The glacierized area is 57.03 km^2, and the glaciers are classified chiefly as mountain glaciers. The highest peak, *Cerro Santa Rosa*, rises to 5,727 m asl. The area drains into the Pacific Ocean by Río Pativilca and Río Huaura and into the Atlantic Ocean by Río Marañón and Río Huallaga.

Cordillera La Viuda

The *Cordillera La Viuda* is about 130 km long, trending northwesterly between lat 10°33' and 11°37'S. and long 76°07' and 76°42'W. It consists of small groups of ice-covered mountains (fig. 2, table 1). All of the glaciers are mountain glaciers and cover an area of 28.5 km^2. Drainage is westward into the Pacific Ocean by Río Huaura, *Río Chancay*, Río Chillón, and Río Rímac and eastward to the Atlantic Ocean by means of Río Huallaga and Río Mantaro. The highest peak in the range is the *Nevado Alcoy* at 5,780 m asl.

Cordillera Central

The *Cordillera Central* lies between lat 11°37' and 12°26'S. and long 75°30' and 76°18'W., trends northerly for 100 km, and is within the Cordillera Occidental (fig. 2, table 1). Glaciers are most prevalent in two areas totaling 176.3 km^2. They are mostly mountain glaciers, but a few valley glaciers are also present. Drainage is to the Pacific Ocean by Río Rímac and Río Cañete and to the Atlantic Ocean by Río Mantaro. The highest peak is the *Nevado Cotoni* at 5,817 m asl.

Cordillera de Chonta

The Cordillera de Chonta consists of a series of ice-capped peaks extending in a northerly direction for about 50 km between lat 12°37' and 13°07'S. and long 75°00' and 75°30'W. and is in the western branch of the Andes (fig. 2, table 1). The area of its glaciers, estimated from Landsat images, is 42 km^2. Several separate, small groups of glaciers exist. Drainage is to the west into the Pacific Ocean by Río Cañete and to the east into the Atlantic Ocean by Río Mantaro. The highest peak is *Nevado Palomo* at 5,305 m asl.

Cordillera de Huanzo

The Cordillera de Huanzo is a glacierized mountain range within the Cordillera Occidental that extends 57 km in a northwesterly direction between lat 14°30' and 15°01'S. and long 72°50' and 73°15'W. (fig. 2, table 1). The highest peak is the *Nevado Huaychahui* at 5,445 m asl. The glacierized area is estimated from Landsat images to be 158 km^2. Drainage is to the southwest by Río Ocoña into the Pacific Ocean and by Río Apurimac northward into the Atlantic Ocean.

Cordillera Chila

The *Cordillera Chila*, consisting of three mountain groups, is in the Cordillera Occidental between lat 15°02' and 15°26'S. and long 71°43' and 72°37'W. The range trends in an easterly direction for about 80 km. The glacierized area, estimated from Landsat images, is 52 km^2 (fig. 2, table 1). The highest peak is the Nevado Mismi at 5,556 m asl. Drainage is westward by Río Colca into the Pacific Ocean and northeastward by Río Apurimac. At the base of Nevado Quehuisha, the world's largest river, Río Amazonas, has its origin in the Río Apurimac.

Cordillera Ampato

The Cordillera Ampato consists of three different mountain groups, Nevados Ampato, Coropuna, and Solimana, and lies in the Cordillera Occidental between lat 15°24' and 15°51'S. and long 71°51' and 73°00'W. The range extends in an easterly direction for about 140 km (fig. 2, table 1). The glacierized area, estimated from Landsat images, is 105 km^2. The area lies entirely within the Pacific Ocean drainage and is drained by Río de Majes and Río Sihuas. The highest peak is the Nevado Coropuna at 6,426 m asl.

Cordillera Volcánica

The *Cordillera Volcánica* extends in a northwesterly direction parallel to the Pacific coast for about 50 km between lat 16°07' and 16°33'S. and long 71°12' and 71°33'W. (fig. 2, table 1). Small groups of ice-covered peaks have a glacierized area of 15 km^2, as estimated from Landsat images. The cordillera drains into the Pacific Ocean through Río Tambo and Río Vitor. The highest peak is Nevado Chachani at 6,100 m asl, but the most spectacular peak is Volcán Misti that towers over the city of Arequipa.

Cordillera del Barroso

The Cordillera del Barroso, volcanic in origin, is in the Cordillera Occidental between lat 16°51' and 17°37'S. and long 69°45' and 70°30'W. It trends northwesterly for about 110 km. The total area covered by glaciers is estimated from Landsat images to be 20 km^2 (fig. 2, table 1). Drainage is westward to the Pacific Ocean by Río Caplina, Río Sama, Río Locumba, and Río de Ilo and northeastward by Río Huenque into the Lago Titicaca basin. Volcán Tutupaca is the highest peak at 5,741 m asl. Figure 7, a Landsat image, clearly shows the glaciers and volcanic landforms of the Cordillera del Barroso area.

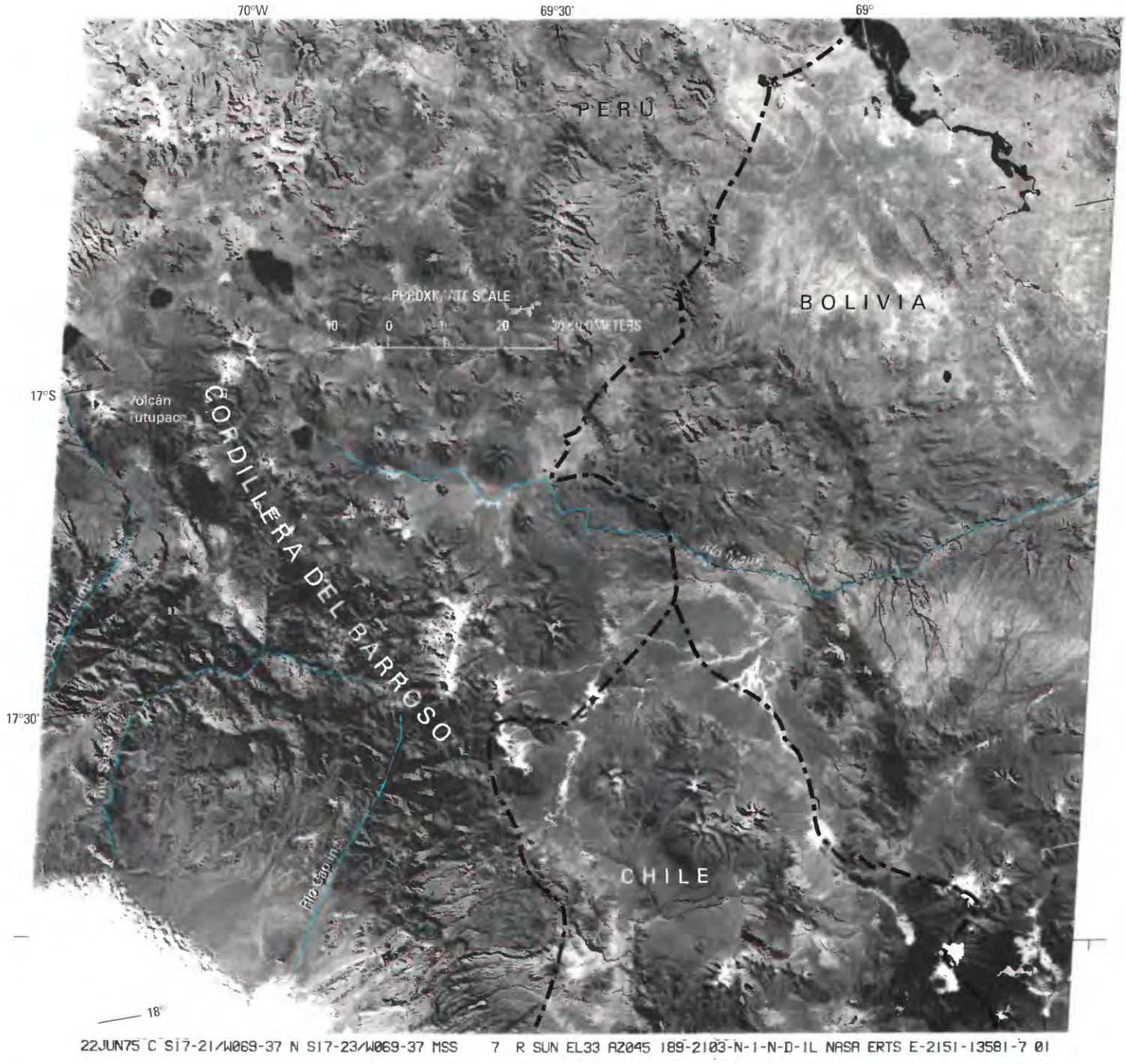

Figure 7.—*Section of an annotated Landsat image of the Cordillera del Barroso area. Both the glacierized area and the volcanic landforms are evident. Volcán Tutupaca is the highest peak in the region (5,741 m). Landsat 2 MSS image (2151–13581, band 7; 22 June 1975; Path 1, Row 72) from EROS Data Center, Sioux Falls, S. Dak.*

Cordillera Central

Cordillera Huaytapallana

The Cordillera Huaytapallana, a glacierized range in the Cordillera Central, lies between lat 11°47' and 11°56'S. and long 75°00' and 75°05'W. It is 17 km long and trends in a northwesterly direction (fig. 2, table 1). The glacierized area, estimated from Landsat images, covers 35 km^2. Drainage is into the Atlantic Ocean by the Río Mantaro. The highest peak is the *Nevado Lasuntay* at 5,720 m asl.

Cordillera de Vilcabamba

The Cordillera de Vilcabamba is a mountain range in the Cordillera Central between lat 13°10' and 13°27'S. and long 72°30' and 73°15'W. (fig. 2, table 1). It extends in an easterly direction for about 85 km. The glacierized area is estimated from Landsat images to be 173 km^2. Drainage is to the Atlantic Ocean by Río Apurimac and Río Urubamba. The highest peak is the Nevado Salccantay at 6,271 m asl.

Cordillera La Raya

The *Cordillera La Raya* is a mountain range situated northwest of the Peruvian altiplano between lat 15°10' and 15°26'S. and long 70°36' and 71°14'W. It extends about 60 km in an easterly direction, and the glacierized area is estimated from Landsat images to be 88 km^2 (fig. 2, table 1). Drainage is into the Atlantic Ocean, the Pacific Ocean, and the Lago Titicaca basin. *Chinchina*, the highest peak, is 5,489 m asl.

Cordillera Oriental

Cordillera Huagaruncho

The *Cordillera Huagaruncho*, a 10-km long, east-trending range, lies between lat 10°14' and 10°19'S. and long 75°57' and 76°03'W. (fig. 2, table 1). The glacierized area, estimated from Landsat images, is 48 km^2. It is drained by Río Huallaga into the Atlantic Ocean. The highest elevation is 5,879 m asl on *Nevado Huagaruncho*.

Cordillera Urubamba

The Cordillera Urubamba, a glacierized mountain range within the eastern cordillera, is between lat 13°08' and 13°17'S. and long 71°58' and 72°16'W. It trends in a northwesterly direction for about 30 km (fig. 2, table 1). The glacierized area is estimated from Landsat images to be 23 km^2. It drains to the Atlantic Ocean by Río Vilcanota and *Río Yanatile*. The highest peak is *Nevado Veronica* at 5,750 m asl.

Cordillera de Vilcanota

The Cordillera de Vilcanota has the second largest concentration of glaciers in Perú; it extends in a northerly direction for about 80 km and then in a westerly direction for about 40 km between lat 13°39' and 14°29'S. and long 70°31' and 71°20'W. (fig. 2, table 1). The glacierized area is 539 km^2, as estimated from Landsat images. Drainage is eastward to the Atlantic Ocean by Río Vilcanota, Río Paucartambo, Río Inambari, and Río Madre de Dios. The highest mountain is Nevado Auzangate at 6,384 m asl. Hollin and Schilling (1981, p. 191), referring to the work of Mercer and Palacios (1977), note that "on the north side of [Nevado] Auzangate (6,400 m) in the *Upismayo Valley*, the present glacier front is at about 4,600 m, while the late Wisconsin-Weichselian limit (sometime between 29,000 and 14,000 B.P.) was at about 4,200 m and the lowest Pleistocene limit at 3,650 m."

The *Quelccaya ice cap* (Zamora and Ames, 1977) is the largest single glacier in Perú (figs. 8 and 9). As previously mentioned, the Ohio State University's Institute of Polar Studies, in cooperation with the Government of Perú, carried out extensive paleoclimatic investigations from 1974 to 1984 of this low-latitude ice cap. In 1983, the project drilled two ice cores measuring 164 m and 154 m in length that contained a climatic record for the past 1,500 years. Figure 8 is a Landsat image of the Cordillera de Vilcanota area. Additional information about the *Quelccaya ice cap* is provided in the following separate section.

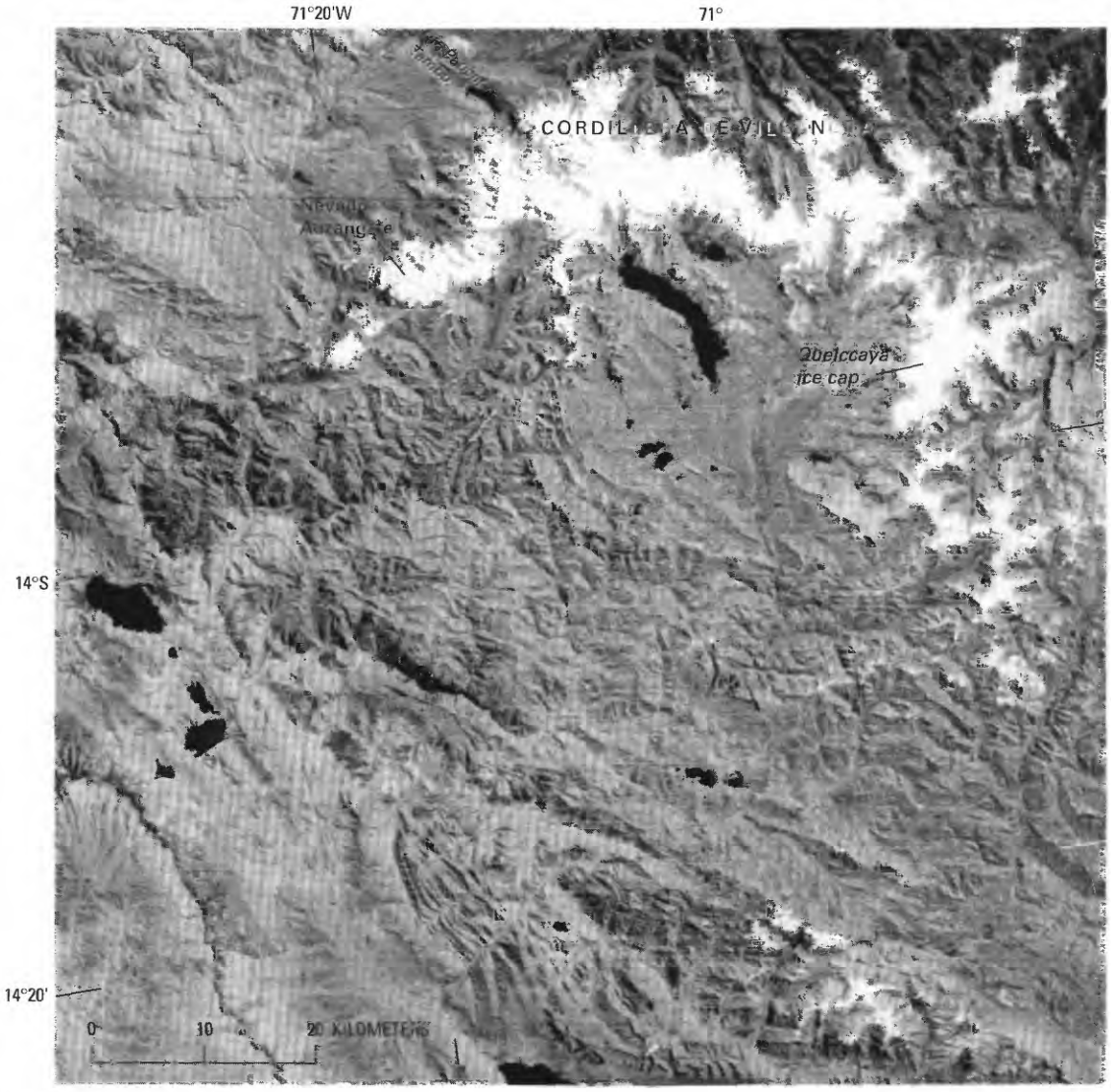

***Figure 8.**—Section of an annotated Landsat image of the Cordillera de Vilcanota.* Quelccaya ice cap, *the largest single glacier in Perú, is in this cordillera. Comparison of this image with figure 9 shows that the margin and structure of this ice cap are well represented here. Landsat 2 MSS image (2225–14074, band 5; 4 September 1975; Path 3, Row 70) from EROS Data Center, Sioux Falls, S. Dak.*

Quelccaya Ice Cap

By Stefan L. Hastenrath

The *Quelccaya ice cap* is situated in the Cordillera de Vilcanota in the eastern branch (Cordillera Oriental) of the Peruvian Andes. It is near the dropoff to the wet Amazon basin and is among the few large ice plateaus in the tropics (figs. 8, 9). It has an area of 54 km^2 and reaches a summit elevation around 5,650 m. Its rim is mostly formed by steep ice cliffs; it feeds only a few outlet glaciers, the largest of which descends to about 5,000 m on the western side of the ice cap.

The *Quelccaya ice cap* was the object of a multiyear field project aimed at the reconstruction of an estimated 1,500-year-long climatic record based on isotope and microparticle analysis of ice cores. Observations of the modern meteorological conditions and measurements related to the mass and heat budgets were also important components of the project. For additional details, refer to the work of Mercer and others (1975); Thompson and Dansgaard (1975); Hastenrath (1978); Thompson, Hastenrath, and Morales Arnao (1979); Thompson, Bolzan, and others (1982); Thompson, Mosley-Thompson, Grootes, and others (1984); Thompson, Mosley-Thompson, and Morales Arnao (1984); Thompson, Mosley-Thompson, Bolzan, and Koci (1985); Thompson, Mosley-Thompson, Dansgaard, and Grootes (1986); Thompson, Davis, and others (1988); Thompson (1980, 1988); Lyons and others (1985); Thompson and Mosley-Thompson (1987, 1989); and Grootes and others (1989).

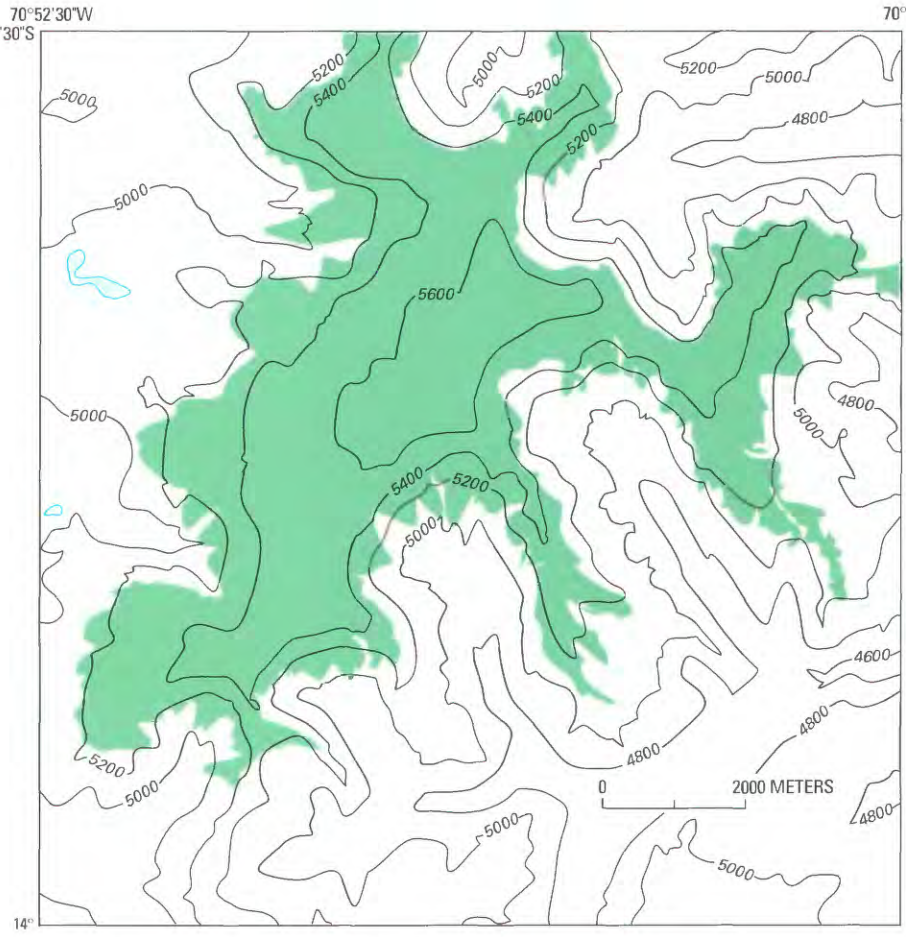

Figure 9.—Quelccaya ice cap *(green) in the Cordillera de Vilcanota showing the margin of the ice cap and elevation contours in meters. Map modified from Thompson (1980).*

The best map available of the *Quelccaya ice cap*, published in 1976, is at a scale of 1:25,000 and is based on 1962–63 aerial photography. It covers most of the ice cap except the highest parts (see table 5). Topographic contours on the summit plateau were completed in August 1976 and were based on traverses made with aneroid altimeters and a theodolite. In addition, an aerial photographic mosaic, based on the same aerial survey, was published in 1966 at a scale of 1:50,000 (table 6).

The *Quelccaya ice cap* and environs are clearly depicted on Landsat imagery (fig. 8). Comparison of the Landsat image and the map (fig. 9) shows that the margin and structure of this large ice body are remarkably well represented on the satellite image.

Cordillera de Carabaya

The Cordillera de Carabaya is in the Cordillera Oriental between lat 14°00' and 14°22'S. and long 69°38' and 70°19'W. It extends 75 km in a northwesterly direction (fig. 2, table 1). The glacierized area is estimated from Landsat images to extend for more than 100 km^2. Drainage is into the Titicaca basin to the south and into the Atlantic Ocean to the east by the Río Inambari. The highest peak is *Nevado Allincapac* at 5,780 m asl.

Cordillera Apolobamba

The *Cordillera Apolobamba* is at the northwestern end of the Bolivian Cordillera Real. In Perú, it extends about 35 km east between lat 14°35' and 14°45'S. and long 69°14' and 69°34'W. (fig. 2, table 1). The glacierized area, estimated from Landsat images, covers 102 km^2. The highest peak, *Nevado Ananea*, is at 5,852 m asl. The drainage is both south into the Titicaca basin and north into the Atlantic Ocean by Río Inambari. Figure 10 shows this area on a Landsat image.

TABLE 3.—*Mass-balance measurements of two glaciers in the Cordillera Blanca and one glacier in the Cordillera Raura*

Cordillera	Glacier	1977–78		1978–79		1979–80		1980–81	
		$\times 10^5$ m^3	ELA[1]	$\times 10^5$ m^3	ELA	$\times 10^5$ m^3	ELA	$\times 10^5$ m^3	ELA
Blanca	*Uruashraju*	−3.11	4,912	−3.25	4,912	−13.25	4,900	+5.31	4,909
Blanca	*Yanamarey*	−5.96	4,866	−12.07	4,795	−32.22	4,946	−3.64	4,790
Raura	*Santa Rosa*	−5.85	4,860	−17.61	4,936	−22.82	4,925	−3.18	4,900

[1] Equilibrium line altitude (ELA) in meters above mean sea level.

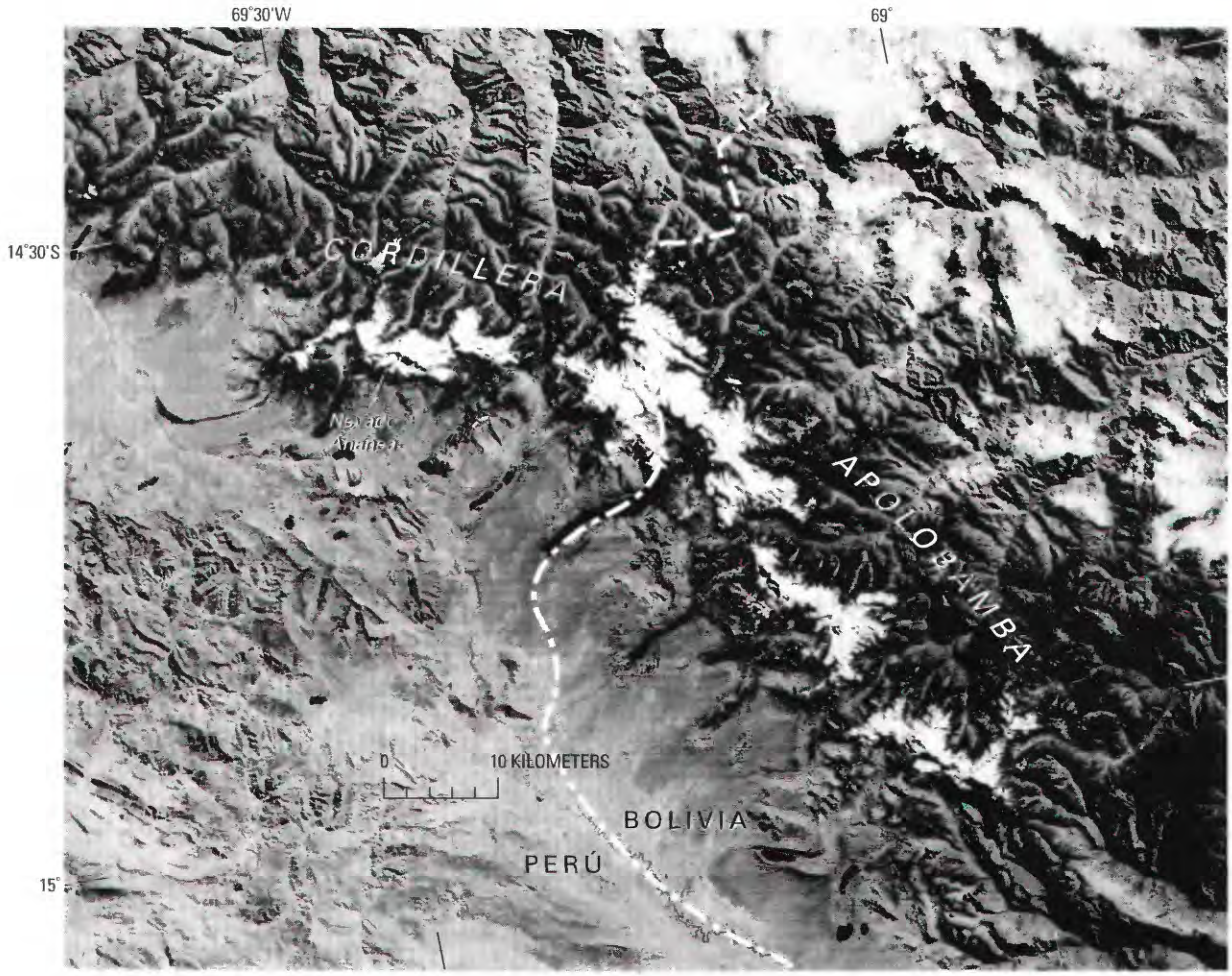

Figure 10.—*Section of an annotated Landsat image of the* Cordillera Apolobamba *area. The glacierized area, estimated from Landsat images, is 102 km^2. The cordillera continues into Bolivia as the Cordillera Real. Landsat 2 MSS image (2187–13565, band 7; 28 July 1975; Path 1, Row 70) from EROS Data Center, Sioux Falls, S. Dak.*

Glacier Mass Balance

In Perú, mass-balance measurements were begun in the Cordillera Blanca in 1966 by this author on the *Pucahirca Glacier*. Following that, mass-balance measurements were made between 1977 and 1983 by the glaciology department of Electroperú on three glaciers chosen for easy access: the *Uruashraju*, *Yanamarey*, and *Santa Rosa* (Dolores and others, 1980). Measurements for the years 1977–78, 1978–79, 1979–80, and 1980–81 are given in table 3. The measurements were made mainly in the ablation areas and only a few scattered measurements were made in the accumulation areas.

The mass-balance fluctuations were not random; during the 6 years of measurements, they show a similar pattern on all three glaciers (Morales Arnao, B., 1969a; Ames, 1985). Most of the measurements show negative mass balance, but the most dramatic ablation took place in 1979–80 and

1982–83. The accumulation values are estimated from precipitation recorded by rain gages at meteorological stations and from estimates of net annual accumulation determined on Nevado Huascarán by Thompson, Mosley-Thompson, Grootes, and others (1984). The rate of 0.91 m accumulation calculated by Thompson, Mosley-Thompson, Grootes, and others (1984) from an ice core at 5,990 m on Huascarán corresponds to a total accumulation of 1.255×10^6 m^3 a^{-1} over the 1.30 km^2 surface area of the *Yanamarey Glacier* and a water-equivalent loss of 1.62 m.

The length of *Yanamarey Glacier* decreased from 1.6 km in 1948 to 1.25 km in 1988; the loss of ice volume was 4×10^6 m^3 during that period. The volume remaining in 1988 was 25×10^6 m^3 (Hastenrath and Ames, 1995).

If the regimen of negative mass balance continues, the *Yanamarey Glacier* will establish a new equilibrium profile. If the glacier terminus recedes to 4,875 m, the surface area will decrease by a factor of two. The present reduction in glacier size is causing a marked increase in stream discharge in the area (Ames, 1985). The contribution of glacier meltwater to streams in the river basins has been very important (Fliri, 1980). It is probable that the importance of the glacier meltwater will diminish as the glacier decreases in size, as was observed in the French and Swiss Alps from 1940 to 1950. Unfortunately, the estimates of glacier mass balance in the above glaciers are based on limited data. More accurate results would have been possible if the observations had been made over a longer period of time and if more measurement locations had been available, particularly in the accumulation area. Monitoring of the discharge of *Río Querococha* also would have given a better idea of the contribution of the *Yanamarey Glacier* to the hydrology of the watershed.

The 6 years of mass-balance measurements have shown strong homogeneity in the variation in mass balance of the three glaciers. The glaciers seem to have had a similar response to the same average climatic conditions, as well as the same interannual variations. It is the first time that South America has had this kind of data, although this kind of regional response has been found in more temperate latitudes, such as in Scandinavia, the Alps, the Ural Mountains, Tien Shan, and the Caucasus Mountains.

If more intensive monitoring confirms that the glaciers in each watershed respond similarly, it will be possible to study more easily new glaciers or groups of glaciers in a watershed by making a few key measurements of ablation, accumulation, and stream discharge and then by comparing them with one well-studied glacier in the area, as in the technique used on *Yanamarey Glacier.*

Glacier Hazards

Since 1702, more than 22 catastrophic events have resulted from ice avalanches that have caused outburst floods from glacier lakes. The floods, known in Perú as aluviónes, come with little or no warning and are composed of liquid mud that generally transports large rock boulders and blocks of ice. The floods have destroyed a number of towns, and many lives have been lost (table 4). One of the hardest hit areas has been the Río Santa valley in northern Perú (fig. 11). Of these catastrophes, the most serious were the aluviónes that destroyed part of the city of Huaraz in 1725 and 1941, as well as the aluvión that resulted from the failure of *Lago Jancarurish* in 1950. In addition, two destructive, high-speed avalanches from the summit area of *Huascarán Norte* (6,655 m asl) in 1962 and 1970 destroyed several villages and caused the deaths of more than 25,000 inhabitants. Reports of these catastrophic glacier-related events include those by Morales Arnao, B., (1966, 1971), Chiglino (1950, 1971), Lliboutry

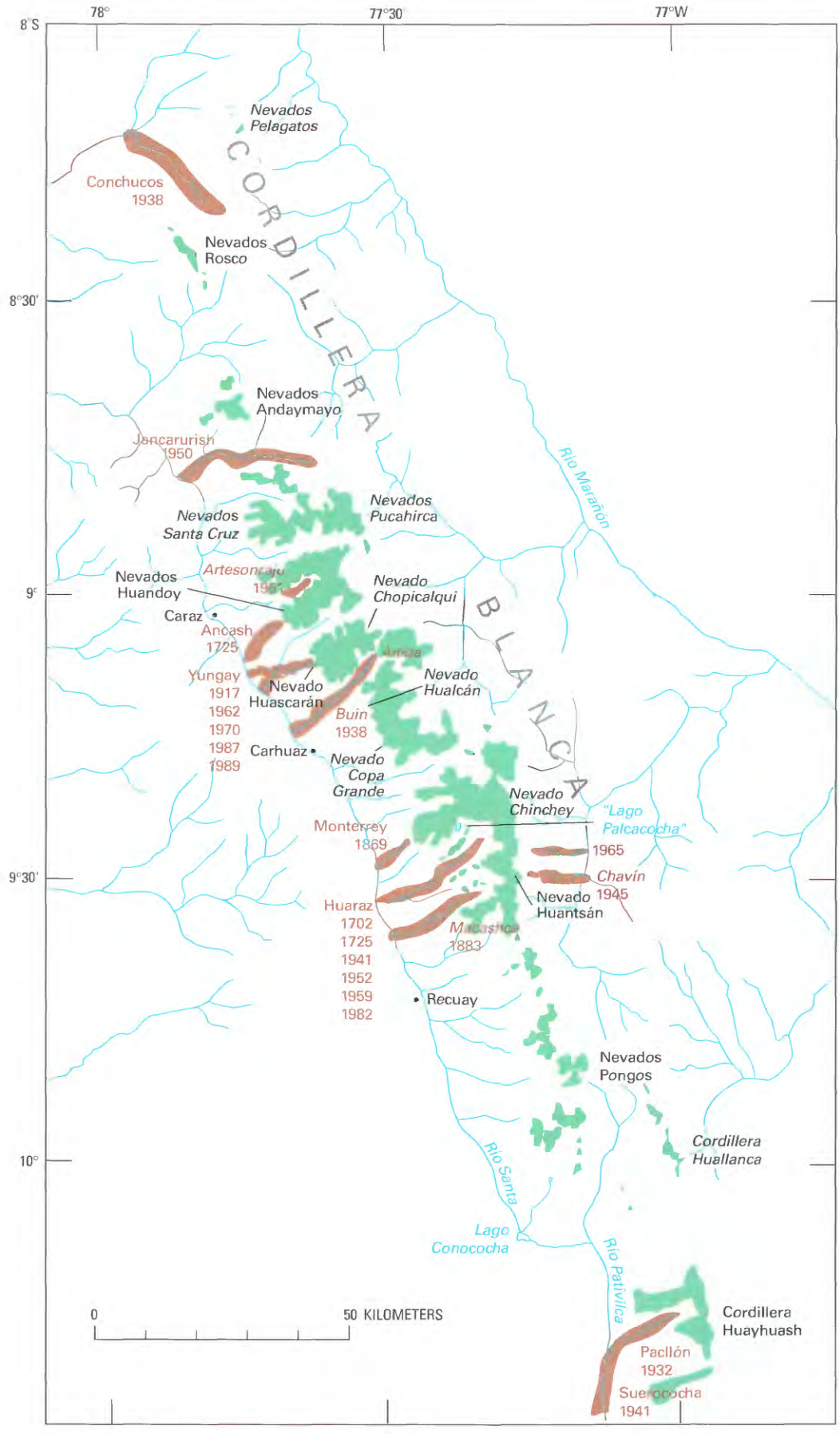

Figure 11.—*The locations of the many natural disasters, glaciological in origin, that have caused deaths or property damage in the Río Santa valley of Perú since 1702. See table 4 for additional information.*

(1975), Plafker and Ericksen (1978), and Hofmann and others (1983). Figures 6 and 12 give some idea of the effect of the Huascarán avalanches. Figure 13 shows the 1951 flood from *Lago Artesoncocha* into *Lago Parón*.

These catastrophes influenced the Government of Perú to establish an Oficina de Obras Seguridad (Security Works Office) to prevent or mitigate avalanches and floods from glacial lakes. Several glacial lakes have been drained by using two traditional methods, the first by excavating a channel through the morainic dam and the second by building tunnels through the moraine. Where the first method is employed, a channel through the top of the moraine is gradually and carefully excavated so that the water behind the dam is allowed to drain safely through the channel and into the stream below. When the water is drained to the desired level, a permanent concrete drainage pipe is constructed within the moraine. Next, the moraine is rebuilt to its original level by using compacted earth, which is covered in turn by rock and concrete. The permanent outlet provides drainage and a normally low water level, whereas the dam provides protection in case of

TABLE 4.—*Natural disasters in Perú that were glaciological in origin* (see fig. 11)

No.	Cordillera	Area	Description	Date
1	Blanca	Huaraz	Floods destroyed part of the city of Huaraz.	4 March 1702
2	Blanca	Huaraz	Earthquake, ice avalanche, and floods damaged the city of Huaraz. Approximately 1,500 people were reported missing; only 300 people were left alive.	6 January 1725
3	Blanca	Yungay	Avalanche from Nevados Huandoy. Floods destroyed the town of Ancash, and 1,500 people were reported to have perished. At the same time, an earthquake also took place.	6 January 1725
4	Blanca	Huaraz	Slides and floods affected the village of Monterrey, destroying houses and fields; 11 people missing.	10 February 1869
5	Blanca	Huaraz	Flood in the town of *Macashca*. Many people were reported to have died. *Rajucolla* levee was broken.	24 June 1883
6	Blanca	Yungay	Ice avalanche from Huascarán impacted Shacsha and Ranrahirca.	22 January 1917
7	Huayhuash	Bolognesi	Aluvión from *Lago Solteracocha* in the *Pacllón* basin.	14 March 1932
8	Blanca	Carhuaz	Aluvión from *Lago Arteza* (*Pacliashcocha*) into the *Quebrada Ulta* (*Río Buin*) near Carhuaz (Kinzl, 1940).	20 January 1938
9	Blanca	Pallasca	Aluvión from *Lago Magistral* affected the town of Conchucos.	1938
10	Huayhuash	Bolognesi	Aluvión from *Lago Suerococha* impacted Río Pativilca causing damage to agricultural fields and town of Sarapo.	20 April 1941
11	Blanca	Huaraz	Aluvión from *Lago Palcacocha* damaged the city of Huaraz. Approximately 5,000 people died. The new part of the city was destroyed.	13 December 1941
12	Blanca	Huari	Aluvión from *Lagos Ayhuinaraju* and *Carhuacocha* caused by an ice avalanche from the *Huantsan peak* damaged the town of *Chavín*. Many people died.	17 January 1945
13	Blanca	Huaylas	Aluvión from *Lago Jancarurish* above the *Los Cedros* drainage basin. Destruction of the Central Hidroeléctrica del Cañón del Pato, the highway, and part of the railway from Chimbote to *Huallanca*.	20 October 1950
14	Blanca	Huaylas	Aluvión from *Lago Artesoncocha* into *Lago Parón* (two events).	16 June and 28 October 1951
15	Blanca	Huaraz	Aluvión from *Lago Milluacochan* into the *Quebrada Ishinca* drainage basin.	6 November 1952
16	Blanca	Huaraz	Slides and flood from *Lago Tullparaju* affected Huaraz city.	8 December 1959
17	Blanca	Yungay	Avalanches and aluviónes from *Huascarán Norte*. About 4,000 people died; 9 towns were destroyed, one of which was Ranrahirca (Dollfus and Peñaherrera del Aguila, 1962; Morales Arnao, 1962).	10 January 1962
18	Blanca	Huari	Ice avalanche from *Nevado San Juan* above *Lago Tumarina* (*Quebrada Carhuascancha*, Huantar District); 10 people died in *Chavín*.	19 December 1965
19	Blanca	Yungay	Rock and ice avalanche from *Huascarán Norte* severely affected the city of Yungay. Approximately 23,000 people died. The same day another avalanche took place between *Lagunas Llanganuco*.	31 May 1970
20	Blanca	Huaraz	Small avalanche from *Toclla raju* near *Pallay* into *Lago Milluacocha*.	31 August 1982
21	Blanca	Yungay	Small ice avalanche from *Huascarán Norte* reached the Ranrahirca fan.	16 December 1987
22	Blanca	Yungay	Small ice avalanche from *Huascarán Norte* reached the Río Santa.	20 January 1989

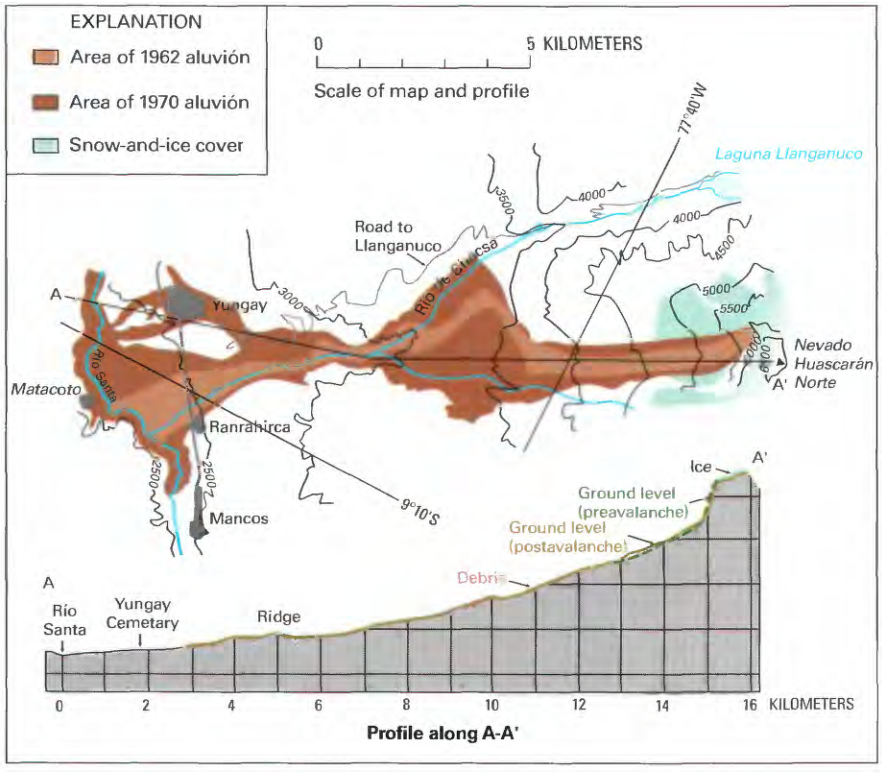

Figure 12.—*Sketch map and profile of the area affected by the 1962 and 1970 aluviónes from* Huascarán Norte *in the Cordillera Blanca (modified from Plafker and Ericksen, 1978). See also figure 6.*

Figure 13.—*Flood from* Lago Artesoncocha *(1951) into* Lago Parón *in the Cordillera Blanca near Caraz.*

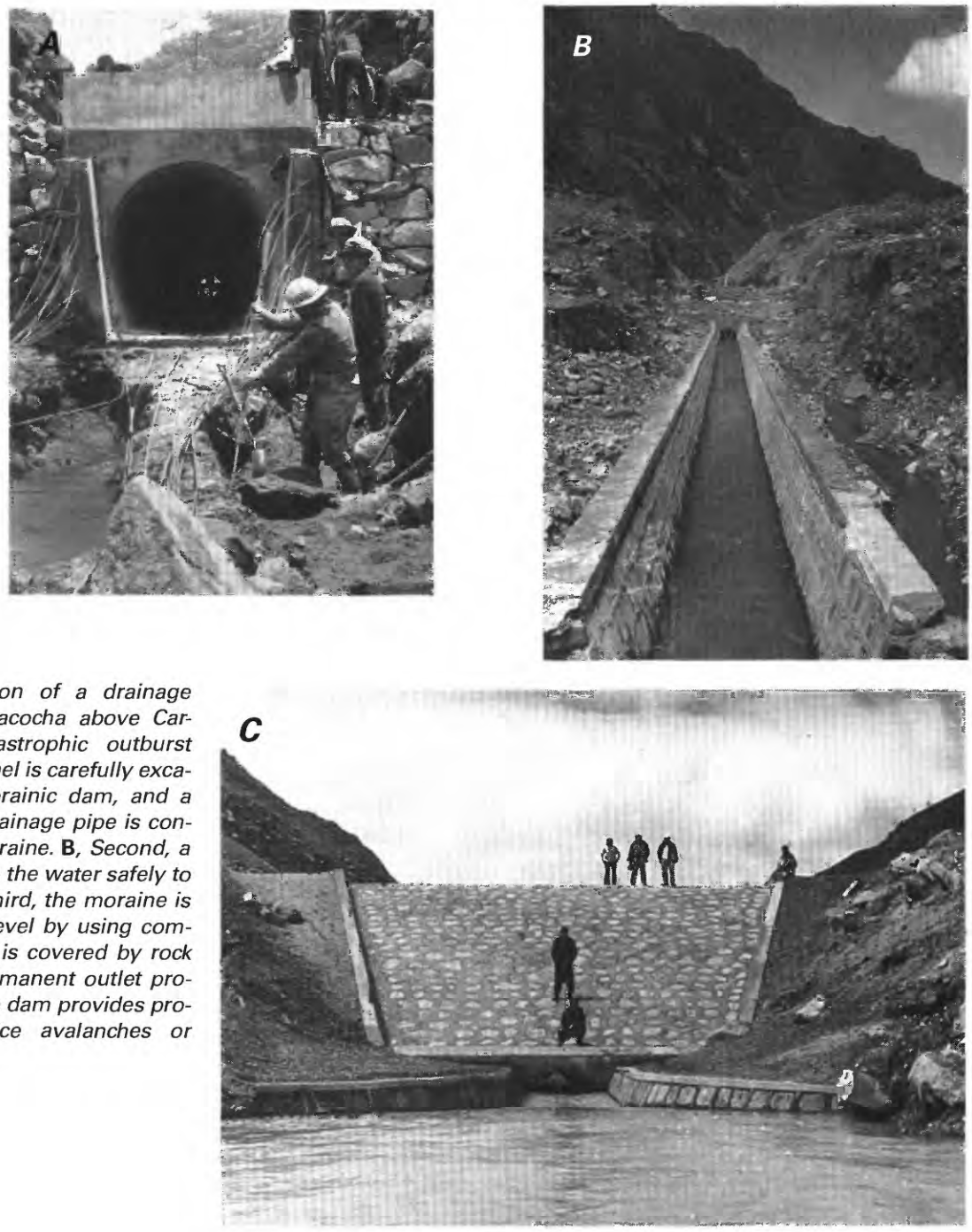

***Figure 14.**—Construction of a drainage outlet for Lago Hualcacocha above Carhuaz to prevent catastrophic outburst floods.* **A,** *First, a channel is carefully excavated through the morainic dam, and a permanent concrete drainage pipe is constructed within the moraine.* **B,** *Second, a channel is built to drain the water safely to the stream below.* **C,** *Third, the moraine is rebuilt to its original level by using compacted earth, and this is covered by rock and concrete. The permanent outlet provides drainage, and the dam provides protection in case of ice avalanches or morainic rock slides.*

avalanches and floods. The second method digs or drills tunnels through the morainic dams or surrounding rock; the tunnels are left open to prevent the glacier lakes from forming in the future. In both methods, great care must be taken to prevent uncontrolled drainage of the lake because of the possibility of catastrophic flooding. Construction is difficult because most sites are situated at elevations of 4,000 m or higher.

The first method was used successfully on *Lago Llaca* and Lago Shallap above Huaraz and on Lago Hualcacocha above Carhuaz (figs. 3, 14). The second method was used on the moraines of *Lago Tullparaju* above Huaraz and Lago Safuna, northwest of *Nevados Pucahirca*, and in the drilling of the Parón Tunnel above Caraz through granitic rock 50 m below the water surface, as well as the tunnels on 513 lakes above Carhuaz (fig. 3).

After more than 30 years of continuous work, the program appears to be successful because no destructive floods resulting from the breakout of glacial lakes have occurred in the Cordillera Blanca since 1972.

Glacier Surveying and Mapping

In Perú, detailed field studies and surveys have been carried out at various times in response to the occurrence of hazards associated with glaciers and glacier lakes. Between 1932 and 1940, Austro-German expeditions carried out excellent surveys and produced maps by using terrestrial photogrammetry of the Cordilleras Blanca and Huayhuash at scales of 1:200,000, 1:100,000, 1:50,000, and 1:25,000 (table 5).

Subsequent to this European effort and because of the catastrophic glacier flood in 1941, the Peruvian government, through a special legislative act, began the first inventory of glacier lakes and glaciers, which was based on the interpretation of aerial photographs. In 1967, the Corporación Peruana del Santa contracted specifically to have maps made of the entire Cordillera Blanca at a scale of 1:25,000 by using aerial photogrammetry (Corporación Peruana del Santa, 1967–1995). In 1970, because of an earthquake

TABLE 5.—*Selected maps of the glacierized areas of Perú*

Glacierized area	Name of map	Scale	Date	Publisher or author
Cordillera Blanca	Departamento de Ancash	1:200,000	1976	Instituto Geográfico Militar, Lima
Cordillera Blanca	Carta Nacional sheets: Corongo 18–h Pomabamba 18–i Carhuas 19–h Huari 19–i Huaraz 20–h Recuay 20–i Chiquian 21–i Yanahuanca 21–j	1:100,000	1971–76	Instituto Geográfico Militar, Lima
Cordillera Blanca	Cordillera Blanca (southern part)	1:100,000	1949	Map accompanies Kinzl (1949)
	Cordillera Blanca (from lat 8°40'S. to 9°30'S.)	1:100,000	pre-1955	Klein and Volbert, Munich (publisher)
	Cordillera Blanca (southern part)	1:100,000	1964	Kinzl (author)
			1972	Kinzl (author)
Cordillera Blanca	Cordillera Blanca (sketch map, 4 sheets)	1:100,000	1977	Alpine Club of Canada and American Alpine Club in Yuraq Janka by John F. Ricker
Cordillera Blanca	Proyecto	1:25,000	1968	Servicio Aerofotográfico Nacional
Cordillera Huayhuash	Cordillera de Huayhuash	1:50,000	1939	Deutscher Alpenverein (accompanies Kinzl, Schneider, and Ebster, 1942)
			1942	Kinzl-Schneider (authors)
			1954	Kinzl-Schneider (authors)
Cordillera Raura	Cordillera Raura (sketch map)	1:133,333	1974	American Alpine Club, American Alpine Journal, v. 19, no. 48, p. 107
Cordillera Central	Proyecto 9221–A–190	1:10,000	1957	Servicio Aerofotográfico Nacional
Cordillera de Chonta	23 sheets	1:50,000	1948	Dirección General de Ferrocarriles and Ministerio de Fomento y Obras Públicas
Quelccaya ice cap	Sicuani, hoja 14j (Carta Nacional)	1:200,000	1973	Instituto Geográfico Militar, Lima
	Nuñoa	1:200,000	1973	Instituto Geográfico Militar, Lima
Quelccaya ice cap	Nuñoa, hoja 28u–III–SE	1:25,000	1976	Ministerio de Agricultura, Oficina de Catastro Rural

and avalanche from the summit of Huascarán, the National Aeronautics and Space Administration carried out an aerial reconnaissance of part of the Cordillera Blanca that produced false-color infrared aerial photographs.

In 1972, Dr. Walter Welsch of Munich, Germany, using photogrammetric methods, compiled a map of Huascarán and the avalanche zone at scales of 1:25,000 and 1:15,000 (Welsch and Kinzl, 1970). In other parts of the country, the Instituto Geográfico Militar has compiled maps at scales of 1:100,000 and 1:250,000 by the use of aerial photographs. Between 1970 and 1974, photogrammetric maps of most of Perú were prepared at a scale of 1:25,000 as part of the Reforma Agraría programs.

The climatic conditions of the Cordillera Oriental, which include frequently cloudy weather, make it difficult to conduct aerial surveys and to acquire the vertical aerial photography needed to prepare maps. In order to avoid delays and the other problems caused by the cloudy conditions, the Government of Perú carried out an aerial survey between 1974 and 1977 that used side-looking airborne radar (SLAR) of the entire Cordillera Oriental of Perú from Ecuador in the north to Bolivia in the south. The SLAR survey also included parts of the Cordillera Central and Cordillera Occidental.

The information from the glacier and glacier lake inventory conducted by Electroperú has been plotted on the 1:25,000-scale photogrammetric maps produced for Reforma Agraría. The best examples of large-scale maps of glaciers of Perú are the 1:5,000-scale topographic maps prepared by Electroperú of five different types of glaciers in the Cordillera Blanca and Cordillera Raura. In addition, Cesar Morales Arnao and Grocio Escudero constructed an 11-m model of the Cordillera Blanca at the scales of 1:25,000 and 1:12,500. Other regions of Perú have few large-scale maps that are useful for studies of glaciers. For example, no accurate maps exist for the Cordillera Vilcabamba and Cordillera Urubamba in the southern part of the country. Tables 5 and 6 list a selected group of maps and aerial photographs of the glacierized areas of Perú. A good listing of early sketch maps of glacierized areas of Perú is found in Mercer (1967).

Landsat Imagery

Good quality, cloud-free Landsat imagery is available for many of the glacierized areas of Perú (table 7 and fig. 15). However, the use of satellite imagery is somewhat limited for studying small mountain-type glaciers or areas that are obscured by shadows in high-relief regions. Where available, satellite imagery acquired during dry periods at the end of the melt season is particularly useful because it shows glacier margins that are not masked by snowpack.

Landsat images have been used to make a general inventory of the glaciers of Perú on which this report is based. Photographic prints at a scale of 1:1,000,000 or enlarged to a scale of 1:250,000 were used to estimate the glacier area and were especially useful for several cordilleras that are not covered by aerial photography (table 1). Newer satellite systems that have increased resolution will provide even more accurate information in the future.

TABLE 6.—*Selected aerial photographs of the glacierized areas of Perú*

Aerial photographs				
Glacierized area	Scale	Date	Project or photograph identification	Archive
Chonta, Huanzo, *Chila*, Ampato, *Volcánica*, Barroso, *La Raya*	1:60,000	1955–56		IGM[1]
Blanca, *Huallanca*, Huayhuash, Raura, *La Viuda, Central*, Chonta, Huaytapallana, *La Raya, Huagáruncho*, Urubamba, Vilcanota, Carabaya, *Apolobamba*	1:50,000–1:60,000	1961	Topographic mapping	IGM
Vilcabamba	1:40,000	–	Proyecto 66–60–A	SAN[2]
Carabaya and *Apolobamba*	1:40,000	1961–62	Proyecto 70–60–A	SAN
La Viuda	1:35,000	1955	Proyecto 7500–22	SAN
Huaytapallana		1961		Hunting Survey Corp.
Huagaruncho		1956–58		The Peruvian Corp.
Blanca	1:20,000	1948	Proyecto 2524	SAN
Urubamba	1:20,000	1956	Proyecto 8485	SAN
Volcánica	1:20,000	1961		
Huallanca	1:15,000	1954	Proyecto 6900–5	SAN
Barroso	1:15,000	1954		SAN
Ampato	1:10,000	1950	Proyecto 3800	SAN
Urubamba	1:10,000	1956	Proyecto 8485A	SAN
La Viuda	1:8,000	1951	Proyecto 5460	SAN
Quelccaya ice cap		Nov 1962	AF 60, frames 33804–33807, 33011–33012	
		May 1963	AF 60, frames 40796–40799	
		Jul 1963	AF 60, frames 48223–48224	

Photomosaic				
Glacierized area	Name	Scale	Date	Publisher
Quelccaya ice cap	Marcapata, hoja 28–III (Fotocarta Nacional)	1:50,000	1966	IGM

[1] IGM, Instituto Geográfico Militar, Lima.

[2] SAN, Servicio Aerofotográfico Nacional.

TABLE 7.—*Optimum Landsat 1, 2, and 3 images of the glaciers of Perú*

[See fig. 15 for explanation of symbols used in "code" column]

Path-Row	Nominal scene center (lat-long)	Landsat identification number	Date	Solar elevation angle (degrees)	Code	Cloud cover (percent)	Remarks
1–70	14°26'S. 68°52'W.	2187–13565	28 Jul 75	37	●	0	*Cordillera Apolobamba*. Image used for figure 10
1–72	17°19'S. 69°34'W.	2151–13581	22 Jun 75	33	●	0	Cordillera del Barroso. Image used for figure 7
1–72	17°19'S. 69°34'W.	277216–13350	04 Aug 77	32	●	0	Archived in Brazil
2–69	12°59'S. 69°57'W.	2188–14021	29 Jul 75	38	◑	20	Band 6
2–70	14°26'S. 70°18'W.	2188–14024	29 Jul 75	37	◕	10	Cordillera de Vilcanota
2–71	15°52'S. 70°39'W.	2170–14032	11 Jul 75	34	●	0	*Cordillera La Raya*
2–72	17°19'S. 71°00'W.	2206–14025	16 Aug 75	38	●	0	Nevado Arundane, Cordillera del Barroso
2–72	17°19'S. 71°00W.	31183–13584, Subscene B	31 May 81	33	●	0	Landsat 3 RBV, Nevado Arundane, Cordillera del Barroso. Image archived by USGS-GSP*
3–69	12°59'S. 71°23'W.	2531–14012	06 Jul 76	35	◑	30	
3–70	14°26'S. 71°44'W.	2135–14085	06 Jun 75	36	●	0	Cordillera de Vilcanota, Cordillera de Huanzo
3–71	15°52'S. 72°05'W.	2279–14073	28 Oct 75	55	●	0	Nevado Ampato and *Cordilleras Chila* and *Volcánica*
4–69	12°59'S. 72°49'W.	2190–14134	31 Jul 75	38	◕	10	Cordilleras Vilcabamba and Urubamba
4–70	14°26'S. 73°10'W.	22116–14134	07 Nov 80	55	●	0	Cordillera de Huanzo
4–71	15°52'S. 73°31'W.	22116–14141	07 Nov 80	55	●	0	Nevado Ampato
6–68	11°33'S. 75°21'W.	2156–14251	27 Jun 75	37	◑	30	*Cordillera Central* area
6–69	12°59'S. 75°51'W.	2156–14254	27 Jun 75	36	●	0	Southern *Cordillera Central*, Cordillera de Chonta
7–67	10°06'S. 76°27'W.	2445–14254	11 Apr 76	45	◑	30	Cordilleras Huayhuash, Raura, *Huagaruncho*
7–68	11°33'S. 76°47'W.	2175–14304	16 Jul 75	38	◑	30	Southern part of *Cordillera La Viuda* and western *Cordillera Central*
7–68	11°33'S. 76°47'W.	2139–14310	10 Jun 75	38	●	0	
7–68	11°33'S. 76°47'W.	31224–14271, Subscene B	11 Jul 81	37	○[B]	0	Landsat 3 RBV. Image archived by USGS-GSP*
8–66	08°40'S. 77°32'W.	2194–14351	04 Aug 75	42	●	0	Cordillera Blanca. Image used for figure 4
8–67	10°06'S. 77°53'W.	2518–14294	23 Jun 76	37	●	0	Southern Cordillera Blanca

*USGS-GSP is the U.S. Geological Survey-Glacier Studies Project.

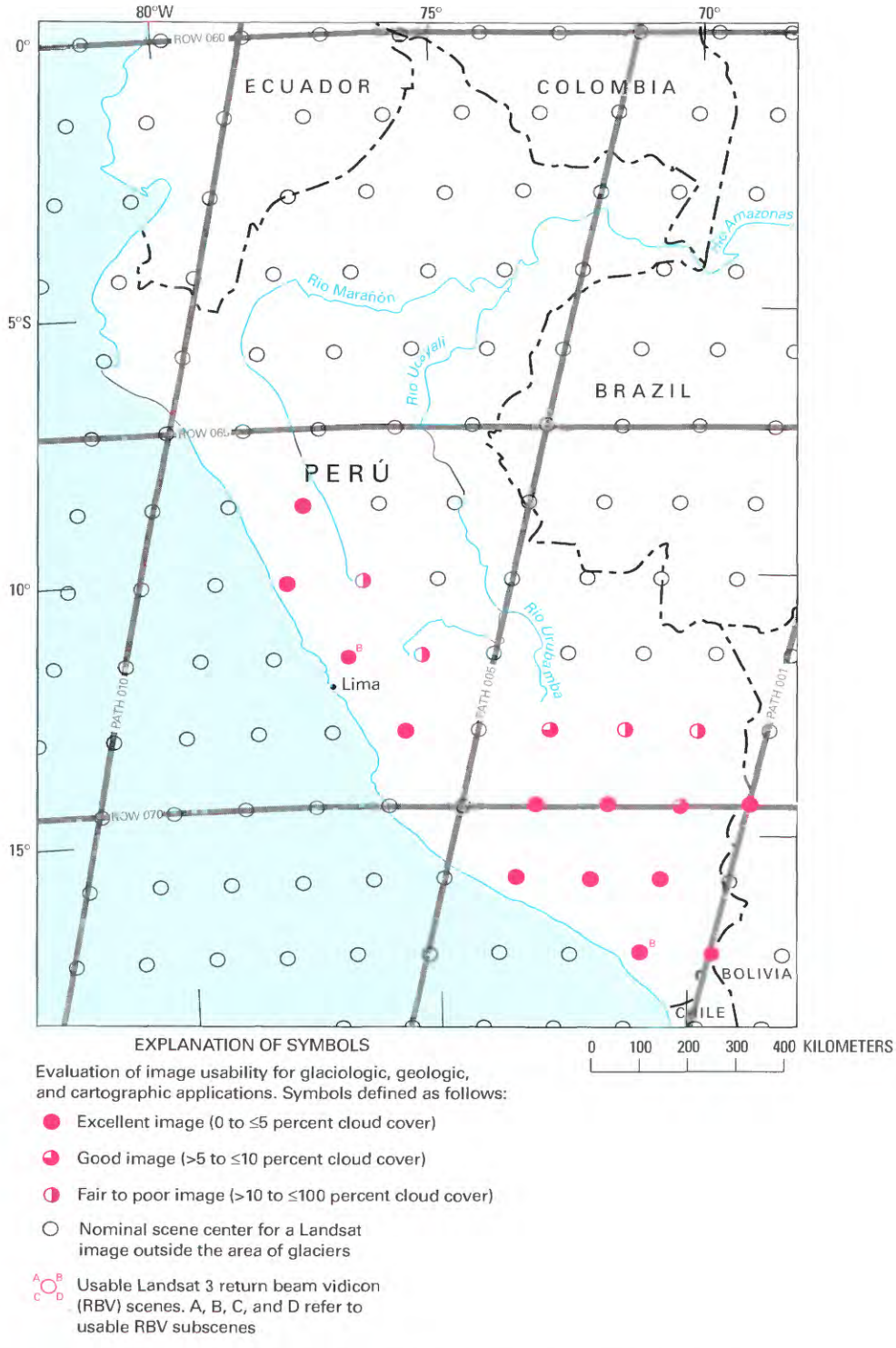

Figure 15.—*Optimum Landsat 1, 2, and 3 images of the glaciers of Perú.*

References Cited

Ames, Alcides, 1969, Control topografico del movimiento glaciar en el Pucahirca norte y el Uruashraju [Topographic control of glacier movement on north Pucahirca and Uruashraju]: Revista Peruana de Andinismo y Glaciología, 1966–1967–1968, no. 8, p. 58–59.

———1985, Variación y balance de masas de los glaciares y su contribución en el caudal de las cuencas [Variation and mass balance of the glaciers and their contribution to the streamflow of the watershed]: Laboratorio de Glaciología, Université de Grenoble Publicación no. 457, p. 1–80.

Broggi, J.A., 1943, La desglaciación Andina y sus consecuencias [The Andean deglaciation and its consequences]: Lima, Revista de Ciencias, v. 45, p. 159–173.

———1945, La desglaciación actual de los Andes del Perú [Present deglaciation of the Andes of Peru]: Lima, Universidad de San Marcas, Museo de Historia Natural "Javier Prado" Boletín no. 35, p. 222–248.

Chiglino, L.A., 1950, Informe sobre el aluvión de Los Cedros [Report on the alluvión of Los Cedros]: Corporación Peruana del Santa Internal Report, 10 p.

———1971, Alud de Yungay y Ranrahirca del 31.05.70 [The Yungay and Ranrahirca avalanche of 31 May 1970]: Revista Peruana de Andinismo y Glaciología, no. 9, p. 84–88.

Corporación Peruana del Santa, Electroperú, 1967–95, Informes internos sobre estudios de glaciares y lagunas de Cordillera Blanca y otras la cordilleras del Perú [Internal reports about glaciers and lakes of the Cordillera Blanca and other cordilleras of Peru]: Unidad de Glaciología y Seguridad de Lagunas Internal Reports [variously paged].

Dollfus, Olivier, 1965, Les Andes Centrales du Perou et leurs piemonts (entre Lima et le Perene) [The central Andes of Peru and their piedmonts (between Lima and Río Perene)]: Lima, Peru, Travaux de l'Institut Français d'Études Andines, v. 10, 404 p.

Dollfus, Olivier, and Peñaherrera del Aguila, Carlos, 1962, Informe de la Comisión Peruana de Geomorfología sobre la catástrofe ocurrida en el Callejón de Huaylas el 10 de Enero 1962 [Report of the Peruvian Commission of Geomorphology on the catastrophe that occurred in Callejón de Huaylas on January 10, 1962]: Sociedad Geográfica de Lima Boletín, v. 79, p. 3–18.

Dolores, Santiago, Ames, Alcides, and Valverde, Augusto, 1980, Estudios glaciológicos realizados en los glaciares Broggi, Uruashraju, Yanamarey, Santa Rosa y otras 1979–1980 [Glacial studies produced of the Broggi, Uruashraju, Yanamarey, Santa Rosa and other glaciers 1979–1980]: Ingemmet Internal Report, p. 2–74.

Fernandez Concha, Jaime, 1957, El problema de las lagunas de la Cordillera Blanca [The problem of the lakes of the Cordillera Blanca]: Sociedad Geológica del Perú Boletín, v. 32, p. 87–95.

Fliri, Franz, 1980, Beitrage zur Hydrologie der Cordillera Blanca, Perú [Contributions on the hydrology of the Cordillera Blanca, Peru]: Innsbruck, Herausgeber-Universität, p. 25–52.

Francou, Bernard, 1984, Données préliminaires pour l'étude des processus périglaciares dans les hautes Andes du Pérou [Preliminary data for the study of periglacial processes in the high Andes of Peru]: Revue de Géomorphologie Dynamique, v. 33, p. 113–126.

Grootes, P.M., Stuiver, Minze, Thompson, L.G., and Mosley-Thompson, Ellen, 1989, Oxygen isotope changes in tropical ice, Quelccaya, Peru: Journal of Geophysical Research, v. 94D, no. 1, p. 1187–1194.

Hastenrath, Stefan, 1967, Observations on the snowline in the Peruvian Andes: Journal of Glaciology, v. 6, p. 541–550.

———1978, Heat-budget measurements on the Quelccaya ice cap, Peruvian Andes: Journal of Glaciology, v. 20, no. 82, p. 85–97.

Hastenrath, Stefan, and Ames, Alcides, 1995, Recession of Yanamarey Glacier in Cordillera Blanca, Peru, during the 20th century: Journal of Glaciology, v. 41, no. 137, p. 191–196.

Heim, Arnold, 1947, Observaciones glaciológicas en la Cordillera Blanca-Perú [Glaciological observations in the Cordillera Blanca-Perú]: Sociedad Geológica del Perú Boletín, v. 20, p. 119–122.

Hidrandina, S.A., 1988/1989, Inventario de glaciares del Perú [Glacier inventory of Peru]: Huaraz, Hidrandina, S.A., Unidad de Glaciología e Hidrología, Part 1, 1988, 173 p; Part 2, 1989, 105 p.

Hofmann, W., Kurner, H., Schneider, Erwin, Stadelmann, J., and Welsch, Walter, 1983, Die berg und gletschersturze von Huascaran, Cordillera Blanca, Perú [The mountain and glacier avalanche of Huascaran, Cordillera Blanca, Peru]: Innsbruck, Universitätsverlag Wagner, v. 6, 110 p.

Hollin, J.T., and Schilling, D.H., 1981, Late Wisconsin-Weichselian mountain glaciers and small ice caps, *in* Denton, G.H., and Hughes, T.J., eds., The last great ice sheets: New York, John Wiley and Sons, p. 179–206.

Kinzl, Hans, 1935, Gegenwartige und eiseitliche Vergletscherung in der Cordillera Blanca (Perú) [Present and Pleistocene glaciation in the Cordillera Blanca (Peru)]: Bad Nauheim, Germany, Verhandlungen des Deutschen Geographentages, 1934, p. 41–56.

———1940, La ruptura del lago glacial en la Quebrada de Ulta en el año 1938 [The break out from the Quebrada de Ulta glacier lake in 1938]: Lima, Universidad de San Marcas, Museo de Historia Natural "Javier Prado" Boletín, v. 4, no. 13, p. 153–167.

———1942, Gletscherkundliche Begleitworte zur Karte der Cordillera Blanca [Glaciological explanation on the map of the Cordillera Blanca]: Zeitschrift für Gletscherkunde, v. 28, no. 1–2, p. 1–19.

———1949, Die Vergletscherung in der Südhalfte der Cordillera Blanca (Peru): Zeitschrift für Gletscherkunde und Glazialgeologie, v. 1, no. 1, p. 1–28.

———1964, ed., Begleitworte zur Karte 1:100,000 der Cordillera Blanca (Perú) Sud Teil [Explanation on the 1:100,000-scale map of the Cordillera Blanca (Peru) southern sheet]: Wissenschaftliche Alpenvereinsheft, no. 17, 48 p.

———1968, La glaciación actual y Pleistocénica en los Andes Centrales [The present and Pleistocene glaciation in the Central Andes]: Bonn, Colloquium geographicum, v. 9, p. 77–90.

———1970, Gründung eines glaziologischen institutes in Perú [The establishment of a glaciological institute in Peru]: Zeitschrift für Gletscherkunde und Glazialgeologie, v. 6, no. 1–2, p. 245–246.

Kinzl, Hans, and Schneider, Erwin, 1950, Cordillera Blanca: Innsbruck, Universitätsverlag Wagner, Tiroler Graphic GmbH, 167 p.

Kinzl, Hans, Schneider, Erwin, and Awerzger, A., 1954, Cordillera Huayhuash, Perú: Ein Bildwerk über ein trapisches Hochgebirge Verlag [Cordillera Huayhuash, Peru: Imagery across a high volcanic mountain range]: Innsbruck, Tiroler Graphik GmbH, p. V–XLII, and photographs 1–63.

Kinzl, Hans, Schneider, Erwin, and Ebster, F., 1942, Die Karte der Kordillere von Huayhuash (Perú) [The map of Cordillera Huayhuash (Peru)]: Zeitschrift der Gesellschaft für Erdkunde zu Berlin, p. 1–35.

Lliboutry, L.A., 1975, La catastrofe de Yungay (Pérou) [The catastrophe of Yungay (Peru)]: International Association of Hydrological Sciences-Association Internationale des Sciences Hydrologiques Publication no. 104, p. 353–363.

———1977, Glaciological problems set by the control of dangerous lakes in Cordillera Blanca, Perú, II: Movement of a covered glacier embedded within a rock glacier: Journal of Glaciology, v. 18, no. 79, p. 255–273.

Lliboutry, L.A., Morales Arnao, Benjamín, Pautre, A., and Schneider, B., 1977, Glaciological problems set by the control of dangerous lakes in Cordillera Blanca, Perú, I: Historical failures of morainic dams, their causes and prevention: Journal of Glaciology, v. 18, no. 79, p. 239–254.

Lliboutry, L.A., Morales Arnao, Benjamín, and Schneider, B., 1977, Glaciological problems set by the control of dangerous lakes in Cordillera Blanca, Perú, III: Study of moraines and mass balances at Safuna: Journal of Glaciology, v. 18, no. 79, p. 275–290.

Lyons, W.B., Mayewski, P.A., Thompson, L.G., and Allen, B., III, 1985, The glaciochemistry of snow-pits from Quelccaya ice cap, Peru, 1982: Annals of Glaciology, v. 7, p. 84–88.

Mercer, J.H., 1967, Glaciers of Peru, in Southern Hemisphere glacier atlas: U.S. Army Natick Laboratories, Earth Sciences Laboratory, Series ES–33, Technical Report 67–76–ES, p. 23–64.

Mercer, J.H., and Palacios, M. Oscar, 1977, Radiocarbon dating of the last glaciation in Peru: Geology, v. 5, no. 10, p. 600–604.

Mercer, J.H., Thompson, L.G., Marangunic, C., and Ricker, J.F., 1975, Peru's Quelccaya ice cap: Glaciological and glacial geological studies, 1974: Antarctic Journal of the United States, v. 10, no. 1, p. 19–24.

Morales Arnao, Benjamín, 1962, Observaciones sobre el alud de Ranrahirca [Observations about the Ranrahirca avalanche]: Revista Peruana de Andinismo y Glaciología, no. 5, p. 81–85.

———1966, The Huascarán avalanche in the Santa Valley, Perú: Association Internationale d'Hydrologie Scientifique Publication no. 69, p. 304–315.

———1969a, Estudios de ablación en la Cordillera Blanca [Studies of ablation in the Cordillera Blanca]: Revista Peruana de Andinismo y Glaciología, 1966–1967–1968, no. 8, p. 111–116.

———1969b, Estudio de la evolución de la lengua glaciar del Pucahirca y de la laguna Safuna [Study of the evaluation of the glacier tongue of Pucahirca and Safuna Lake]: Revista Peruana de Andinismo y Glaciología, 1966–1967–1968, no. 8, p. 89–96.

———1969c, Las lagunas y glaciares de la Cordillera Blanca y su control [The lakes and glaciers of the Cordillera Blanca and their control]: Revista Peruana de Andinismo y Glaciología, 1966–1967–1968, no. 8, p. 76–79.

———1969d, Perforaciones en los glaciares de la Cordillera Blanca [Drillings from the glaciers of the Cordillera Blanca]: Revista Peruana de Andinismo y Glaciología, 1966–1967–1968, no. 8, p. 103–110.

———1971, El día más largo en el Hemisferio Sur [The longest day in the Southern Hemisphere]: Revista Peruana de Andinismo y Glaciología, Publicaciones Especiales por el Terremoto 1970, no. 9, p. 63–71.

Morales Arnao, Cesar, 1953–1995, Articulos y mapas sobre cordilleras del Perú [Articles and maps concerning the cordilleras of Peru]: Revistas Bianuales de Andinismo y Glaciología [variously paged].

———1964, Los Andes Peruanos tienen 20 Cordilleras [The 20 cordilleras of the Peruvian Andes]: Revista Peruana de Andinismo y Glaciología, no. 6, p. 70–78.

Nogami, M., 1972, The snowline and climate during the last glacial period in the Andes mountains: Quaternary Research, no. 11, p. 71–80 (in Japanese).

Oppenheim, Victor, and Spann, H.J., 1946, Investigaciones glaciológicas en el Perú 1944–1945 [Glaciological investigations in Peru 1944–1945]: Instituto Geológico del Perú Boletín no. 5, 70 p.

Petersen B., Ulrich, 1958, Structure and uplift of the Andes of Perú, Bolivia, Chile and adjacent Argentina: Sociedad Geológica del Perú Boletín, v. 33, p. 57–129.

———1967, El glaciar Yanasinga—19 años de observaciones instrumentales [The Yanasinga Glacier—19 years of instrumental observations]: Sociedad Geológica del Perú Boletín, v. 40, p. 91–97.

Plafker, George, and Ericksen, G.E., 1978, Nevados Huascarán avalanches, Peru, in Voight, Barry, ed., Rockslides and avalanches v. 1: Amsterdam, Elsevier Scientific Publishing Company, p. 277–314.

Raimondi, Antonio, 1873, El Departamento de Ancash [Ancash Department]: published by Enrique Meiggs, imprint of El Nacional.

Ricker, J.F., 1977, Yuraq Janka: Guide to the Peruvian Andes: Banff, Alberta, Alpine Club of Canada, 180 p.

Schneider, B., 1969, Levantamiento de batimetria en la Cordillera Blanca [The rise in bathymetry in the Cordillera Blanca]: Revista Peruana de Andinismo y Glaciología, 1966–1967–1968, no. 8, p. 67–75.

Szepessy, Ali, 1949, Contribución al conocimiento de las lagunas glaciares en la Cordillera Blanca [Contribution to the knowledge of the glacial lakes of the Cordillera Blanca]: Sociedad Geológica del Perú Boletín, v. Jubilar, pt. 2, f. 10, 5 p.

———1950, Monográfica preliminar de la Cordillera Blanca [Preliminary monograph on the Cordillera Blanca]: Corporación Peruana del Santa Internal Report, p. 2–64.

Thompson, L.G., 1980, Glaciological investigations of the tropical Quelccaya ice cap, Peru: Journal of Glaciology, v. 25, no. 91, p. 69–84.

———1988, 1500 años de variabilidad climática registrada en testigos de hielo procedentes de los Andes del Sur del Perú [1500 years of climatic variability recorded in ice cores obtained from the Andes Mountains of southern Peru]: Columbus, Ohio, Ohio State University, Byrd Polar Research Center, 3 p.

Thompson, L.G., Bolzan, J.F., Brecher, H.H., Kruss, P.D., Mosley-Thompson, Ellen, and Jezek, K.C., 1982, Geophysical investigations of the tropical Quelccaya ice cap, Peru: Journal of Glaciology, v. 28, no. 98, p. 57–69.

Thompson, L.G., and Dansgaard, W., 1975, Oxygen isotope and micro particle studies of snow samples from Quelccaya ice cap, Peru: Antarctic Journal of the United States, v. 10, no. 1, p. 24–26.

Thompson, L.G., Davis, M.E., Mosley-Thompson, Ellen, and Liu, K-b, 1988, Pre-Incan agricultural activity recorded in dust layers in two tropical ice cores: Nature (London), v. 336, no. 6201, p. 763–765.

Thompson, L.G., Hastenrath, Stefan, and Morales Arnao, Benjamín, 1979, Climatic ice core records from the tropical Quelccaya ice cap: Science, v. 203, no. 4386, p. 1240–1243.

Thompson, L.G., and Mosley-Thompson, Ellen, 1987, Evidence of abrupt climatic change during the last 1,500 years recorded in ice cores from the tropical Quelccaya ice cap, Peru, in Berger, W.H., and Labeyrie, L.D., eds., Abrupt climatic change: Dordrecht-Boston, D. Reidel Publishing Company, p. 99–110.

———1989, One-half millenia of tropical climate variability as recorded in the stratigraphy of the Quelccaya ice cap, Peru, *in* Peterson, D.H., ed., Aspects of climate variability in the Pacific and western Americas: American Geophysical Union Geophysical Monograph 55, p. 15–31.

Thompson, L.G., Mosley-Thompson, Ellen, Bolzan, J.F., and Koci, B.R., 1985, A 1500-year record of tropical precipitation in ice cores from the Quelccaya ice cap, Peru: Science, v. 229, no. 4714, p. 971–973.

Thompson, L.G., Mosley-Thompson, Ellen, Dansgaard, W., and Grootes, P.M., 1986, The Little Ice Age as recorded in the stratigraphy of the tropical Quelccaya ice cap: Science, v. 234, no. 4774, p. 361–364.

Thompson, L.G., Mosley-Thompson, Ellen, Grootes, P.M., Pourchet, M., and Hastenrath, Stefan, 1984, Tropical glaciers: Potential for ice core paleoclimatic reconstructions: Journal of Geophysical Research, v. 89D, no. 3, p. 4638–4646.

Thompson, L.G., Mosley-Thompson, Ellen, and Morales Arnao, Benjamín, 1984, El Niño-Southern Oscillation events recorded in the stratigraphy of the tropical Quelccaya ice cap, Peru: Science, v. 226, no. 4670, p. 50–53.

Trask, P.D., 1952, The alluvión problem in the Cordillera Blanca of Peru: Berkeley, California, University of California, Department of Engineering, 86 p.

———1953, El problema de los aluviones de la Cordillera Blanca [The alluvión problem in the Cordillera Blanca of Peru]: Sociedad Geográfica de Lima Boletín, v. 70, p. 1–75.

U.S. Board on Geographic Names, 1989, Gazetteer of Peru: Washington, D.C., Defense Mapping Agency, 869 p.

Welsch, Walter, and Kinzl, Hans, 1970, Der Gletschersturz vom Huascarán (Perú) am 31 Mai 1970, die grosste Gletscherkatastrophe der Geschichte [The glacier avalanche from Huascarán (Peru) on 31 May 1970, the biggest glacial catastrophe in history]: Zeitschrift für Gletscherkunde und Glazialgeologie, v. 6, no. 1–2, p. 181–192.

Wright, H.E., Jr., Seltzer, G.O., and Hansen, B.C.S., 1989, Glacial and climatic history of the central Peruvian Andes: National Geographic Research, v. 5, no. 4, p. 439–445.

Zamora, Marino, and Ames, Alcides, 1977, Investigaciones glaciológicas en el Glaciar Quelccaya de la Cordillera Carabaya [Glaciological investigations of the Quelccaya ice cap, Cordillera Carabaya]: Revista Peruana de Andinismo y Glaciología, no. 12, p. 127–132.

Glaciers of South America–

GLACIERS OF BOLIVIA

By EKKEHARD JORDAN

SATELLITE IMAGE ATLAS OF GLACIERS OF THE WORLD

Edited by RICHARD S. WILLIAMS, Jr., *and* JANE G. FERRIGNO

U.S. GEOLOGICAL SURVEY PROFESSIONAL PAPER 1386–I–5

Bolivia has a total glacier-covered area of more than 560 square kilometers. A few crater glaciers, small summit ice caps, and outlet glaciers (about 10 square kilometers) are located on the extinct volcanoes of the Cordillera Occidental of northern Bolivia. Most of the ice (more than 550 square kilometers) is found as ice caps, valley glaciers, and mountain glaciers on the highest peaks of the Cordilleras Apolobamba, Real, and Tres Cruces *and Nevado Santa Vera Cruz of the Cordillera Oriental*

CONTENTS

GLACIERS OF SOUTH AMERICA–

GLACIERS OF BOLIVIA

By EKKEHARD JORDAN[1]

Abstract

Present-day glaciers of Bolivia are restricted to the highest peaks of the Andes Mountains. In the Cordillera Occidental, the glaciers are found as crater glaciers, small summit ice caps, and outlet glaciers on the extinct volcanoes in the northern part of the country. Their total surface area is about 10 square kilometers. Most of the glaciers are located in the Cordillera Oriental in the Cordilleras Apolobamba, Real, and *Tres Cruces* and in Nevado Santa Vera Cruz[2] as ice caps, valley glaciers, and mountain glaciers. Their surface area covers more than 550 square kilometers. Because of the limited precipitation, no glaciers exist in southern Bolivia.

During the Pleistocene, glacierization was much more extensive. Presently glacierized areas were larger, and glaciers were also found in areas that no longer support permanent ice. In the Cordillera Occidental, terminal moraines have been found below the 4,500-meter elevation, and in the Cordillera Oriental, at slightly above 3,000 meters. In between, in the Altiplano, traces of glaciation rise 100–200 meters higher from the center to the margin of that area.

The location, distribution, and mass-balance of Bolivian glaciers are the result of the climate and the orientation and elevation of its mountain ranges. In contrast to extratropical glaciers, accumulation takes place during the summer, and ablation takes place during the winter and interseasonal periods. The daily cloud-cover cycle, which leaves the glaciers exposed to morning solar radiation from the north and east and protects the western slopes in the afternoon, results in a substantially lower snowline on the western and southern slopes (100 to 300 meters lower).

The glaciers of Bolivia are covered by maps, aerial photographs, and satellite images of varying degrees of usefulness. Accurate maps at 1:50,000 scale cover the Cordillera Real. Vertical aerial photographs having scales between 1:30,000 and 1:80,000 cover all the glacierized areas of Bolivia and range in quality from good to satisfactory. Satellite images with resolutions ranging from 5 to 79 meters are also available, and although they may be limited by resolution, cloudiness, shadowing, or spectral discrimination, they offer a useful tool for frequently monitoring glacier variation.

Occurrence and Distribution of Glaciers in Bolivia

Because Bolivia lies completely within the tropics, glaciers can be found only at the highest elevations (Francou, 1993). Hence, glaciers are restricted to the highest mountain peaks in the Andean region of Bolivia.

Annual precipitation within Bolivia is variable, decreasing to less than 200 mm a^{-1} in the southwest. As a consequence, even the highest peaks of the Andes Mountains at 6,000 m and above cannot sustain glaciers south of lat 18°30' S. and have only temporary snow patches (see table 1 and fig. 1). No glaciers exist anywhere in southern Bolivia. The southern limit of glaciers in Bolivia is roughly equivalent to the northern line of the large salars, such as Salar de Coipasa and Salar de Uyuni, in the central plateau (Altiplano) of the Andes.

Manuscript approved for publication 18 March 1998.

[1] Lehrstuhl für Physische Geographie, Heinrich-Heine-Universität, Universitätstrasse 1, 40225 Düsseldorf, Germany.

[2] The names in this section conform to the usage authorized by the U.S. Board on Geographic Names in its Gazetteer of Bolivia (U.S. Board on Geographic Names, 1992), varient names and names not listed in the gazetteer are shown in italics.

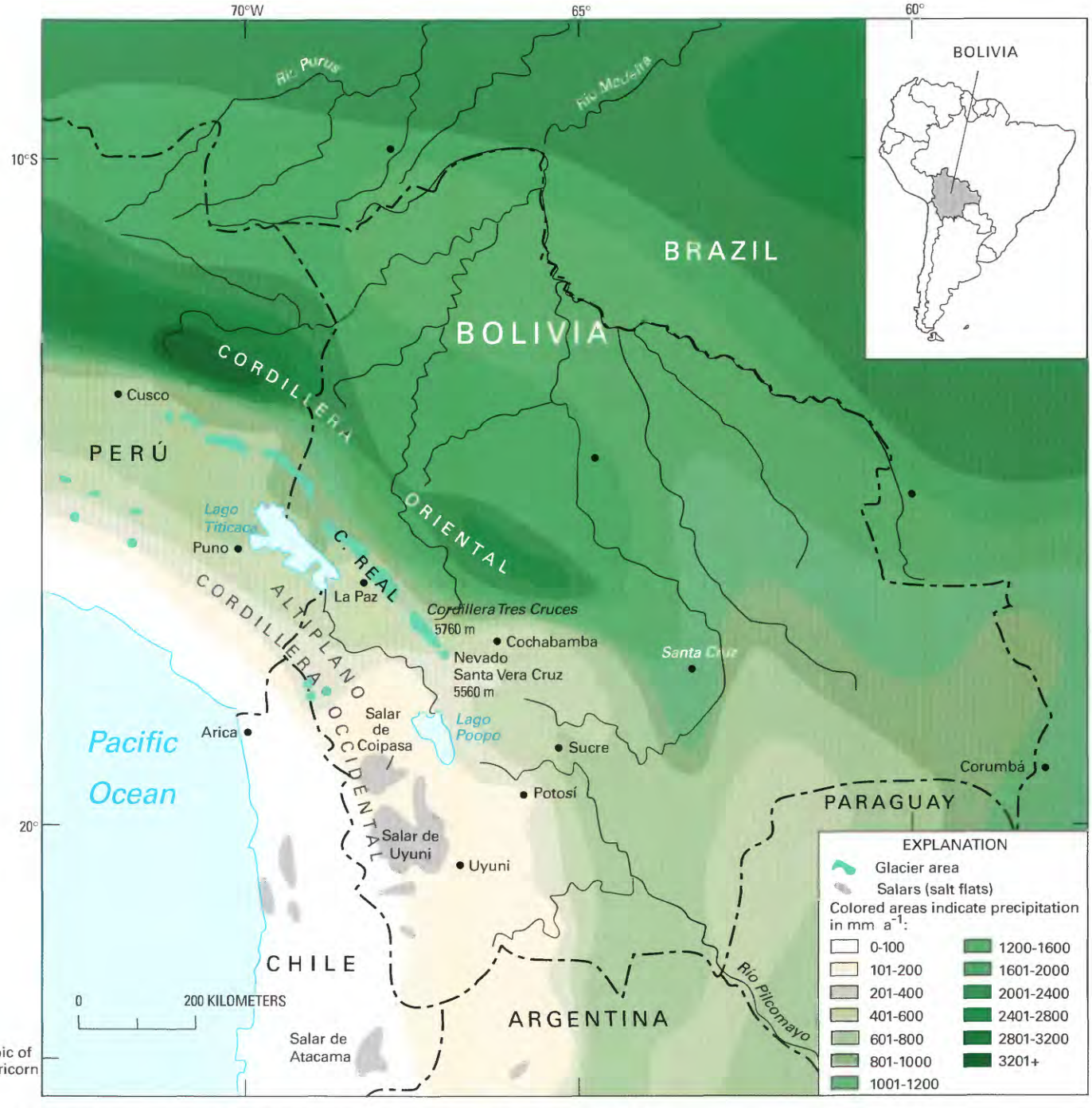

Figure 1.—*Glacierized areas of Bolivia showing location of glaciers and distribution and amount of precipitation. It is evident that the southwestern part of the country does not receive enough precipitation to maintain glaciers on even the highest peaks. The location of present glaciers is shown with a tint. Information about the area, number, and elevation of the glaciers in each glacierized region is given in table 1.*

TABLE 1.— *Glaciers of the Bolivian Andes on 1 November 1984*

[Taken from Jordan, 1991, table 10. Leaders (–) not known]

Mountain group	Latitude (south)	Longitude (west)	Glacier				Highest elevation (meters)	Lowest glacier terminus (meters)
			Area square kilometers[1]	Percent	Number	Percent		
CORDILLERA ORIENTAL								
CORDILLERA ORIENTAL	14°37'–17°04'	67°13'–69°14'	**591.600 (including 35.590 in Perú)**	**100**	**1826**	**100**	6,436	4,311
CORDILLERA APOLOBAMBA	14°37'–15°04'	68°58'–69°14'	**219.804**	**37.2**	**652**	**36**	6,059	4,311
Chaupi Orko	14°40'	69°10'	129.357	21.9	346	19	6,059	4,365
Cololo	14°50'	69°06'	43.072	7.3	135	7.5	5,774	4,311
Ulla Khaya	15°00'	69°03'	47.375	8	171	9.5	5,669	4,390
CORDILLERA DE MUÑECAS	15°20'–15°38'	68°33'–68°55'	**.684**	**.1**	**16**	**1**	5,237	4,828
Morocollu	15°20'	68°55'	.148	.03	8	.5	5,156	4,828
Cuchu	15°38'	68°33'	.536	.1	8	.5	5,237	4,886
CORDILLERA REAL	15°45'–16°40'	67°40'–68°34'	**323.603**	**54.7**	**964**	**53**	6,436	4,420
NORTHERN CORDILLERA REAL	15°45'–16°20'	68°01'–68°34'	**262.766**	**44.4**	**784**	**43**	6,436	4,420
Illampu-Ancohuma	15°50'	68°30'	103.099	17.4	147	8	6,436	4,438
Calzada-Chiaroco-Chachacomani	16°00'	68°20'	94.072	15.9	251	14	6,127	4,676
Nigruni-Condoriri	16°08'	68°15'	40.868	6.9	241	13	5,752	4,420
Saltuni-Huayna Potosí	16°15'	68°08'	14.504	2.5	50	3	6,088	4,804
Zongo-Cumbre-Chacaltaya	16°18'	68°05'	10.223	1.7	95	5	5,519	4,578
SOUTHERN CORDILLERA REAL	16°20'–16°40'	67°40'–67°58'	**60.837**	**10.3**	**180**	**10**	6,414	4,499
Hampaturi-Taquesi	16°26'	67°52'	11.685	2	70	4	5,548	4,723
Mururata	16°30'	67°47'	17.207	2.9	75	4	5,836	4,592
Illimani	16°38'	67°44'	31.945	5.4	35	2	6,414	4,499
CORDILLERA TRES CRUCES (QUIMSA CRUZ)	16°47'–16°09'	67°22'–67°32'	**45.276**	**7.7**	**177**	**9.5**	5,760	4,708
Choquetanga	16°54'	67°22'	6.992	1.2	21	1	5,541	4,812
High region of *Tres Cruces*	16°56'	67°24'	38.284	6.5	156	8.5	5,760	4,708
NEVADO SANTA VERA CRUZ	17°03'–17°04'	67°13'–67°14'	2.233	**.4**	**17**	**1**	5,560	4,853
CORDILLERA OCCIDENTAL								
CORDILLERA OCCIDENTAL	18°03'–18°25'	68°53'–69°09'	**10**	**100**	–	–	6,542	5,100
Nevado Sajama	18°06'	68°53'	4	40	–	–	6,542	5,100
Nevados Payachata	18°09'	69°09'	4	40	–	–	6,222	5,500
Cerros Quimsachata	18°23'	69°03'	2	20	–	–	6,032	5,500

[1] Glacier areas based on analysis of 1975 aerial photographs and 1984 field measurements.

Glaciers in Bolivia are found in two main ranges of the Andes, the Cordillera Occidental along the western border with Chile and the Cordilleras Apolobamba, Real, and *Tres Cruces* and Nevado Santa Vera Cruz, which are the southern extension of the Cordillera Oriental in Perú. Between the Cordillera Apolobamba and Cordillera Real lies the Cordillera de Muñecaus, which has two very small glacierized areas containing 16 small glaciers that have a total area of 0.1 km^2 (table 1). The approximately 200-km-wide Altiplano between these two main ranges is no longer glacierized because it does not have sufficient elevation and (or) precipitation.

The type and areal extent of glaciers in the Cordillera Occidental and in the Cordilleras Apolobamba, Real, and *Tres Cruces* and Nevado Santa Vera Cruz are very diverse. The Cordillera Occidental consists exclusively of extinct volcanoes, and glaciers are limited to Nevado Sajama (6,542 m) and its neighboring volcanoes (fig. 2). In addition to crater glaciers, small summit ice caps commonly occur that have several outlet glaciers that terminate

downslope (fig. 3). Their extent and total surface area are very small and scarcely amount to 10 km^2 in Bolivia and northern (tropical) Chile. However, these are the glaciers that have the highest minimum elevation on Earth (table 1), except for the small icefield of the Chilean-Argentine stratovolcano Cerro/Volcán Llullaillaco (6,739 m) (Messerli and others, 1992, p. 262).

Substantially more significant, on the other hand, is the glacierization of the Cordilleras Apolobamba (figs. 4 and 5), Real (fig. 6), and *Tres Cruces* (fig. 7) and of Nevado Santa Vera Cruz (fig. 7) in the Cordillera Oriental. From a geological viewpoint, these cordilleras are strongly elevated intrusions whose slaty covers have been exposed by erosion and covered by

***Figure 2.**—Cordillera Occidental of Bolivia and Chile.* **A,** *Annotated Landsat 1 MSS image showing area from Nevado Condoriri to Salar de Coipasa. The scene includes the glacierized areas of Nevados Payachata and Sajama, as well as Cerros Quimsachata and several volcanoes on the Bolivian Altiplano. Landsat 1 MSS image (1100–14043; band 7; 31 October 1972; Path 251, Row 73) from the EROS Data Center, Sioux Falls, S. Dak.* **B, C,** *See facing page.*

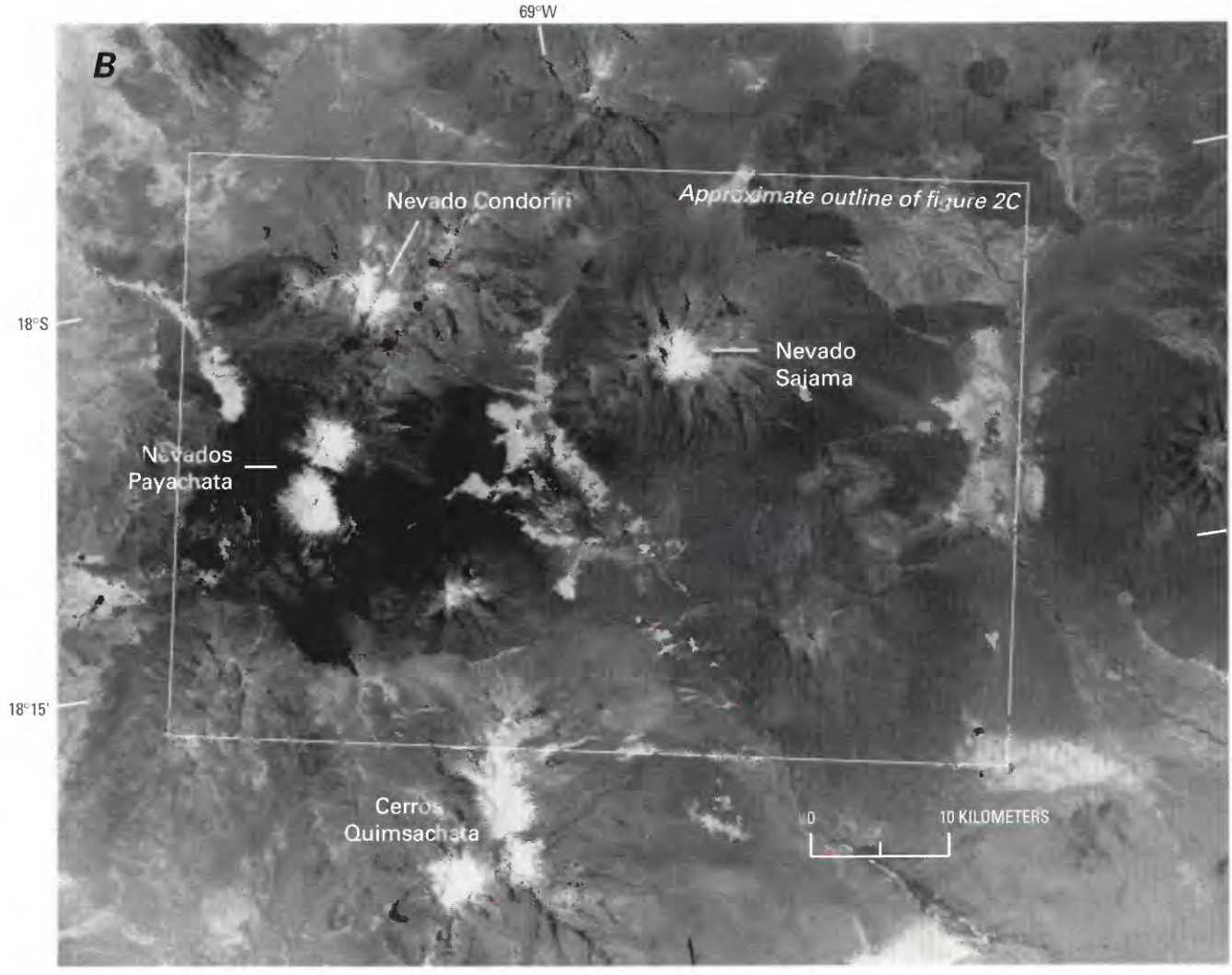

Figure 2B.—*Annotated 1:500,000-scale enlargement of part of the Landsat 1 MSS satellite image shown in* A. *The snow-and-ice cover of the three glacier complexes in the central Cordillera Occidental is evident. These glaciers are the southernmost in Bolivia; no volcanoes located south of the Quimsachata group have an ice cap. At the time the image was acquired on 31 October 1972, the transient snowline elevation was average.*

C, *Landsat 5 TM false-color composite image of the Nevados Payachata and Sajama area acquired on 17 July 1993. The color composite was created by using bands 3, 5, and 4, and snow-and-ice areas appear pink. Comparison of* B *and* C *shows a much smaller amount of snow-and-ice cover on the later image, although shadows conceal part of the glacierized areas on the southwestern slopes of the volcanoes in* C.

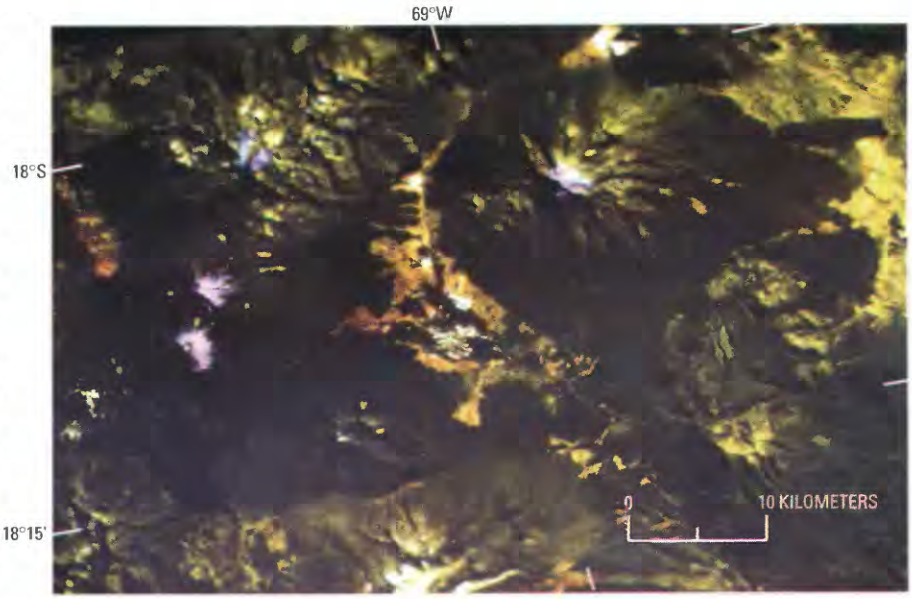

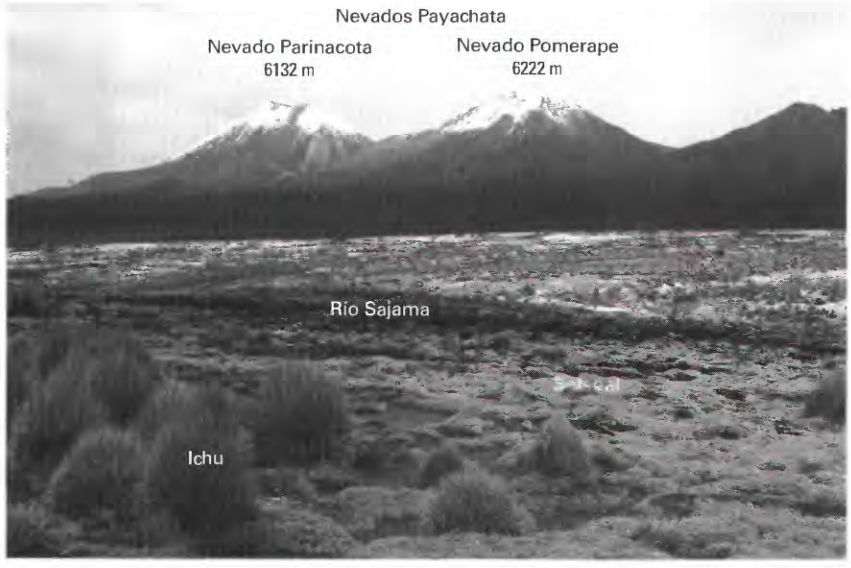

Figure 3.—*Nevados Payachata of the Cordillera Occidental. The photograph is looking west from the foot of Nevado Sajama (lat 18°6'05"S., long 68°58'10" W.) at an elevation of 4,260 m at the end of the dry season. The snow has largely dissipated, and small glacier areas appear. In the center, extending across the entire picture are white salt efflorescences. The foreground is marked by thickets of Ichu grass on a hard cushion bog (Bofedal). Photographed by Ekkehard Jordan on 5 September 1980.*

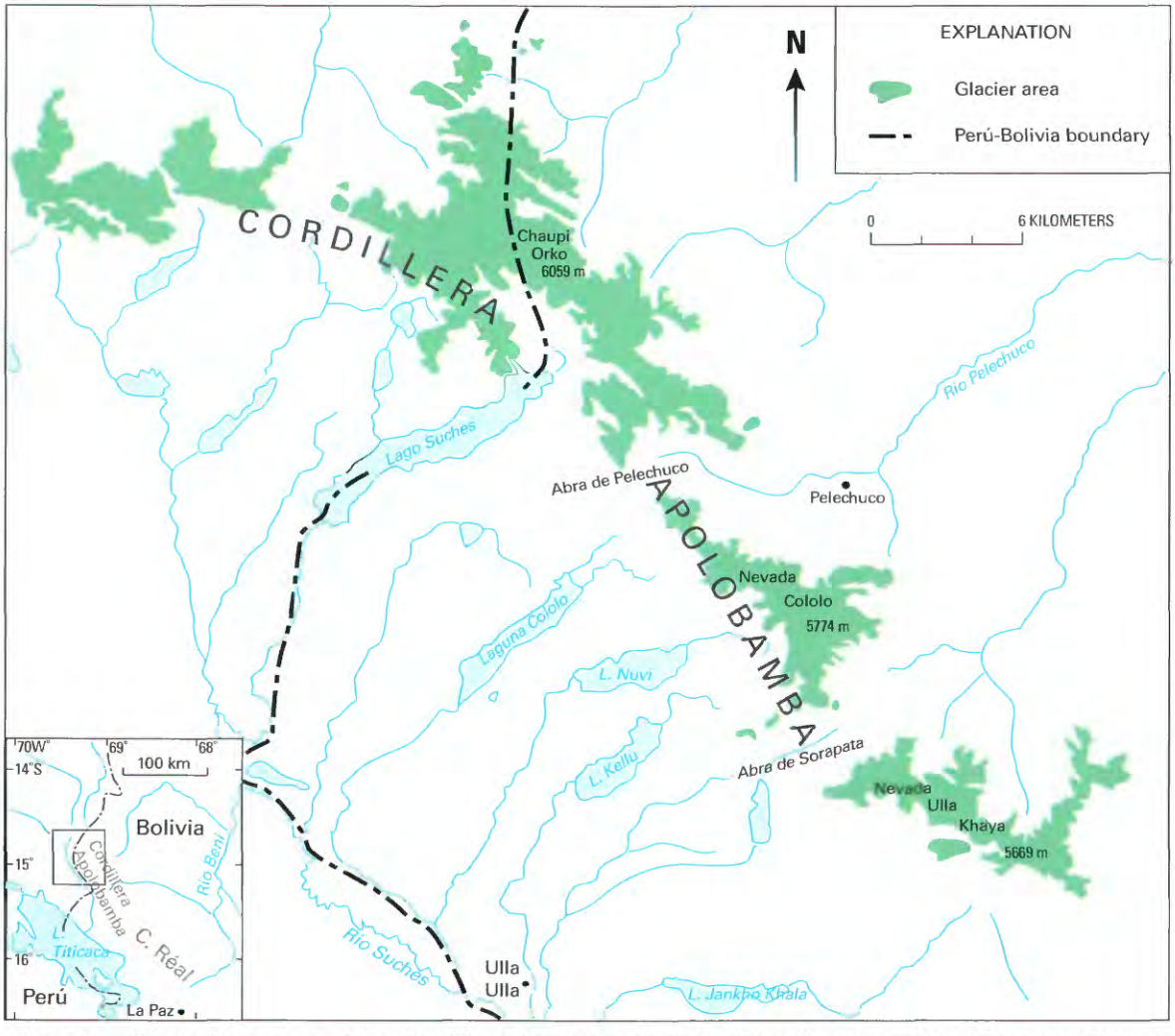

Figure 4.—*Glacierized areas of the Cordillera Apolobamba in the Cordillera Oriental of Perú and Bolivia. This map is modified from a more detailed map by the author that was based on satellite images, aerial photographs, route drawings, and maps. Abbreviation: L., Lago/Laguna.*

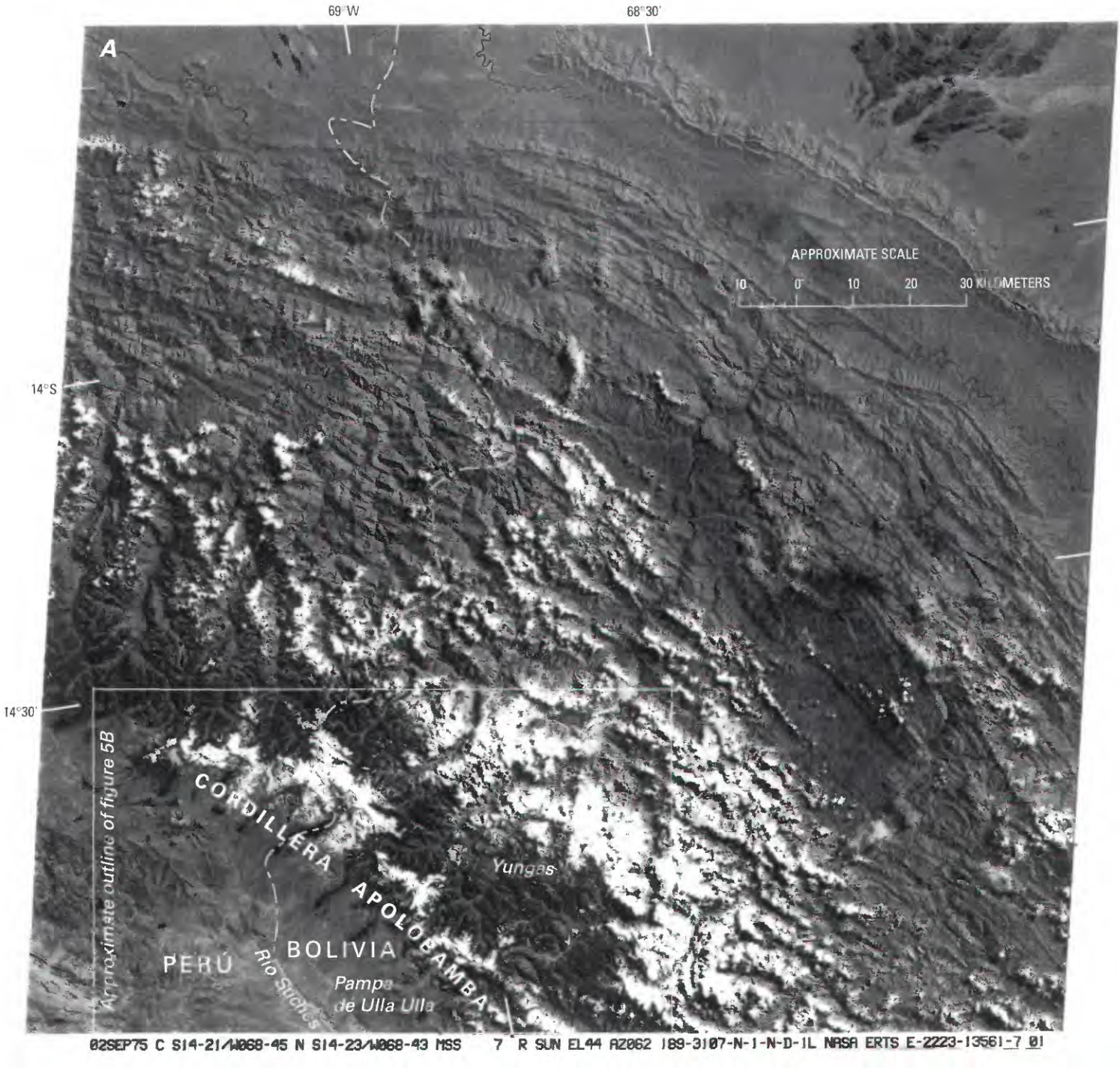

Figure 5.—*Cordillera Apolobamba in Perú and Bolivia.* **A**, *Landsat 2 MSS image of the cordillera acquired when substantial amounts of snow cover were present. Contrast with figure 8. The white spots located east of the glaciated mountain chain are not snowfields, but cloudfields that, as a rule, reach the glacier areas by noon and protect them from direct solar radiation. Landsat image (2223–13561, band 7; 2 September 1975; Path 1, Row 70) from the EROS Data Center, Sioux Falls, S. Dak.*
B, *Landsat 5 TM false-color composite image of the Cordillera Apolobamba acquired 21 August 1991. The color composite was generated by using bands 3, 5, and 4 and shows the sharply defined glacierized areas in pink (see* A *for approximate location of* B*). Also, it is possible to see Pleistocene moraines around the "finger lakes."*

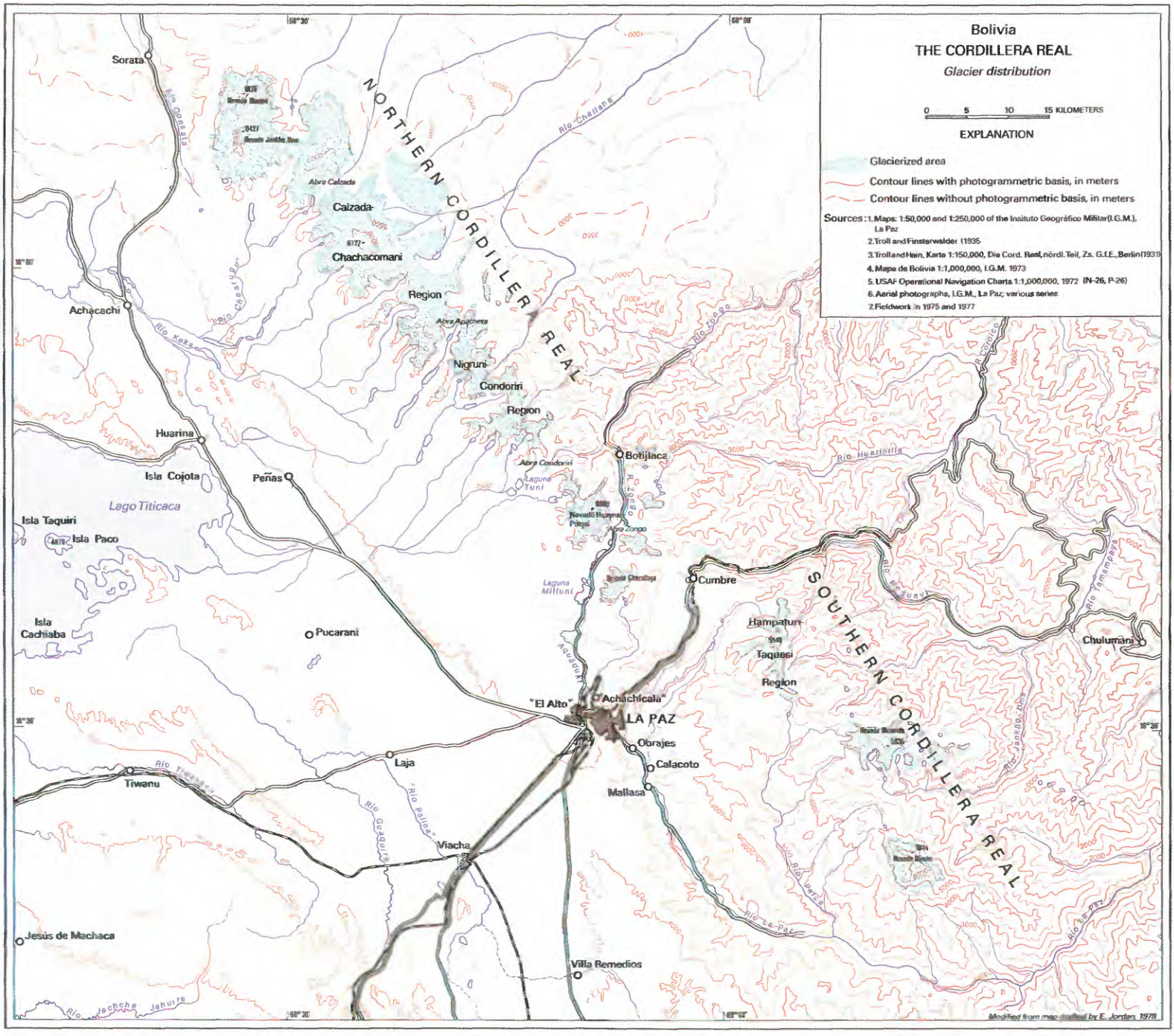

Figure 6.—*Glacier distribution in the Cordillera Real. The map, drawn by the author, is based on field studies, aerial photographs, and various topographic maps. Compare with Landsat image of the Cordillera Real in figure 8.*

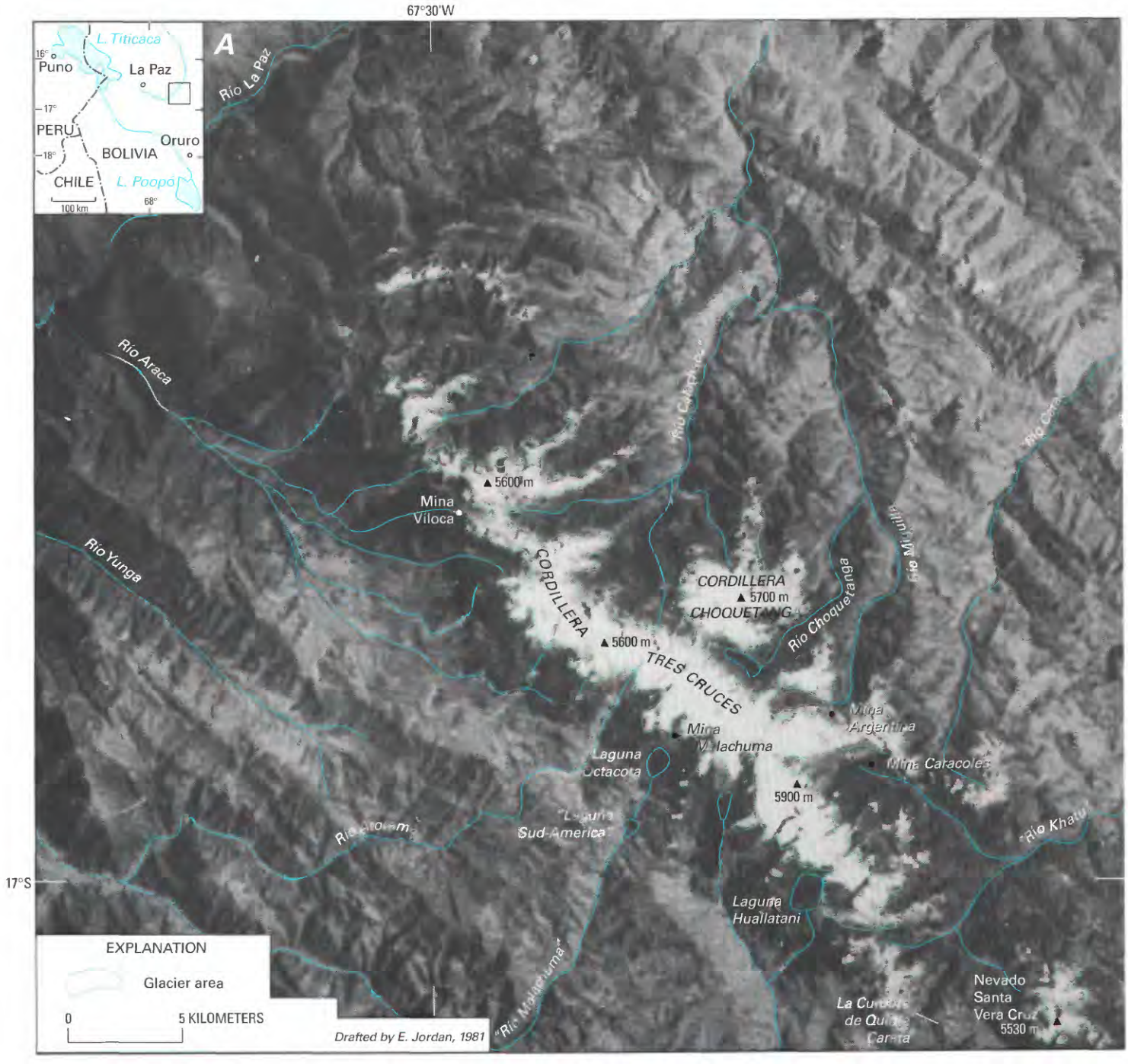

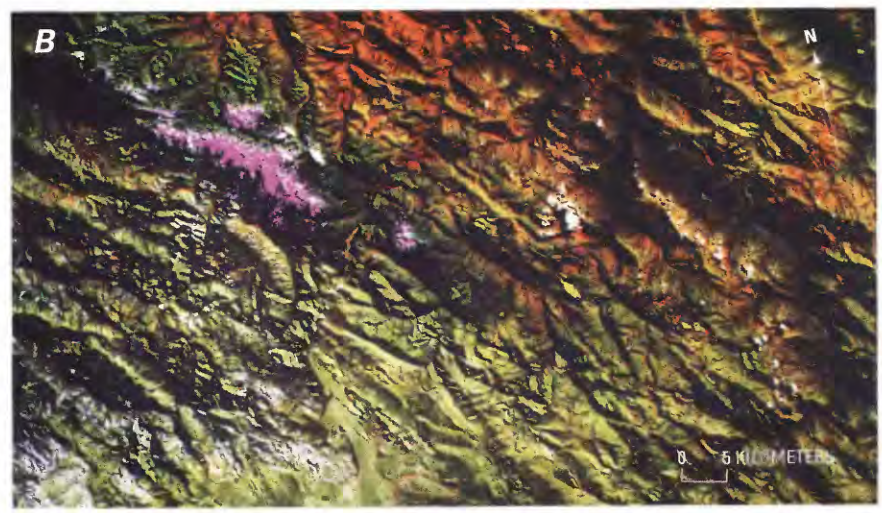

Figure 7.—*Glacierized regions of the* Cordillera Tres Cruces *and Nevado Santa Vera Cruz.* **A**, *Annotated enlargement of part of a Landsat 2 MSS image and overlay based on topographic maps, field studies, aerial photographs, and satellite images. Landsat image (2276–13505, band 7; 25 October 1975; Path 251, Row 72) from the EROS Data Center, Sioux Falls, S. Dak. [Approximate scale, 1:250,000.] Abbreviation: L., Laguna.*

B, *Landsat 5 TM false-color composite image of the same area, acquired 7 May 1993. The color composite was generated by using bands 3, 5, and 4 and shows the glacierized areas in pink.*

glaciers. The nearly 600 km^2 of glacier surface area is distributed over the four mountain groups of the Cordillera Oriental (fig. 8), whose characteristics are presented in table 1. Almost all types of glaciers are represented, including ice caps, valley glaciers, and mountain glaciers; the large variety of glacier types shows some similarity to the classic glacierized areas of the European Alps (see fig. 10). The similarity of topography has been thought to correspond to similar glacial phenomena. In the following discussion, however, emphasis will be placed on relating glacier type to climate.

As is true elsewhere in the world, the mountains of Bolivia provide evidence of a substantially greater glaciation during the "Ice Age," which can be demonstrated on satellite images. However, because tectonic uplift of the Central Andes continued into the Quaternary Period (Troll and Finsterwalder, 1935) and the mountains reached their current elevation only in

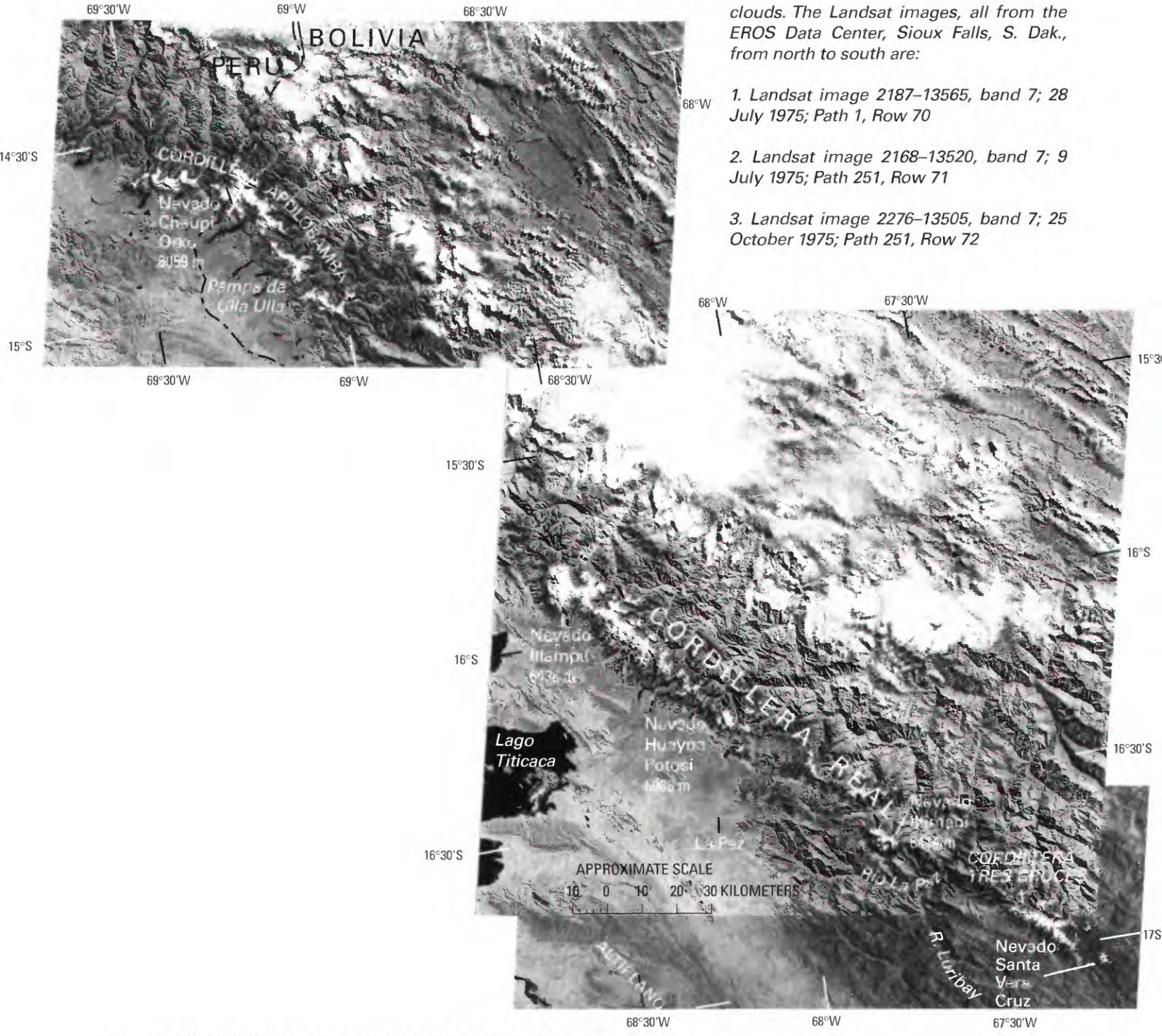

Figure 8.—*Annotated Landsat 2 MSS image mosaic of glacierized regions of the Cordilleras Apolobamba, Real,*Tres Cruces, *and of Nevado Santa Vera Cruz of Bolivia. The satellite mosaic gives an excellent view of the geographical arrangement of the glaciers of the region. The images showing minimum snow cover were chosen. The white areas in the northeast corner of the mosaic are not snowfields, but clouds. The Landsat images, all from the EROS Data Center, Sioux Falls, S. Dak., from north to south are:*

1. Landsat image 2187–13565, band 7; 28 July 1975; Path 1, Row 70

2. Landsat image 2168–13520, band 7; 9 July 1975; Path 251, Row 71

3. Landsat image 2276–13505, band 7; 25 October 1975; Path 251, Row 72

the middle of the Quaternary Period, only the two latest Pleistocene glaciations are documented by glacial deposits. During the Pleistocene glaciation, the presently glacierized regions were significantly expanded, and a large number of mountain massifs and volcanoes, which no longer have glaciers, supported ice caps (fig. 9). This is true of the Cordillera Occidental, where terminal moraines extend below the 4,500-m elevation, and of the Cordilleras Apolobamba, Real, and *Tres Cruces* and Nevado Santa Vera Cruz in the Cordillera Oriental, where it is possible to identify moraines below 3,500 m in elevation (Schulz, 1992). The author independently documented these moraines along the eastern escarpment up to slightly higher than 3,000 m. According to studies by Hastenrath (1967, 1971a, b), Nogami (1976), and Graf (1975, 1981) and the author's observations and analyses of aerial photographs, evidence of the lower elevation of more extensive Pleistocene glaciation in the Cordillera Occidental rises 100–200 m toward the south and from the center to the margin of the Altiplano. In contrast to the field evidence in the Cordillera Occidental, conditions in the mountain ranges to the east of the Altiplano are more complicated; no general pattern of Pleistocene glacier distribution can be recognized (Jordan and others, 1994). This is because of the much greater dissected relief in this region, which is seen in the cross-cutting valleys of Río Consata, Río La Paz, and Río Pilcomayo, that reach the border of the Altiplano. The position of mountain ranges within atmospheric circulation systems and the windward-leeward orientation and exposure play an important role in glacier development. The presence of a much colder climate during the Pleistocene has been confirmed by ice cores from Nevado Sajama (Thompson and others, 1998).

Figure 9.—*Part of a Landsat 2 MSS false-color composite image enlarged to 1:500,000-scale showing traces of Pleistocene glaciation in the Cerro Potosí. The Cerro Potosí is one of the largest continuous areas of Pleistocene glaciation in the southeastern Bolivian highland, which today is not glacierized. The diversity of glacial forms can be distinguished on the satellite image; they extend from the highest pyramidal peak south of the mountain massif, which has an elevation slightly above 5,000 m (Cerro Cunurana, 5,056 m), to below 4,000 m, and they have even produced a small foreland glaciation in the southwest. During the glacial maximum, the glacierized area of this mountain range alone reached an extent larger than the total areal extent of the modern glacierization. It covered 700–800 km^2 in the form of an ice-stream network. The eye-catching cone- or trumpet-shaped, typically glacially carved valleys tend to diverge radially and show the extreme relief of immense side moraines in the former terminus region. These are adjoined, particularly from the northwest to west to southwest, by immense alluvial cones descending to below 3,000 m. Because of its excellent water supply, the alluvial material is used intensively for agricultural purposes. The false-color composite image shows this indirectly by the distinctive red coloration of the chlorophyll-rich vegetation. The vegetation covers the land surface far into the dry season in these areas because of surface irrigation. The glacial lakes, which are numerous in the erosion area, as well as in the terminus region, of the Pleistocene glaciers, are proof of the rich water resources of the mountain range. These lakes represent natural, glacially supplied water reservoirs that have provided the mines and the former industrial center, Potosí, with drinking and municipal water. Directly south of Potosí the pronounced cone-shaped Cerro Rico (silver mountain) has lost its glacial shape as a result of undercutting by underground mining activity during the past centuries. This mountain, reaching an elevation of 4,824 m, was previously covered by a considerable ice cap. The Landsat image (2148–13415; 19 June 1975; Path 249, Row 74) is from the EROS Data Center, Sioux Falls, S. Dak.*

Climate and Glaciers in Bolivia: The Special Mass-Balance Situation

Bolivia's glaciers, situated between lat 14°37' and 18°23' S. on the southern edge of the tropical zone of the Southern Hemisphere, are affected by the change between intertropical circulation in the summer and southeast trade winds in the winter. During the southern summer, this generally means precipitation that decreases in amount and duration from north to south. This author believes that the term "summer" is appropriate for the rainy season in Bolivia, in contrast to the central tropics of Venezuela, Colombia, and Ecuador, even though Schubert (1992) gives a different view. Inhabitants of these countries, however, seldom refer to summer or winter; they speak of dry and rainy seasons. The dual climatic situation and the orientation and elevation of its mountain ranges are the determining factors in the occurrence and distribution of Bolivia's glaciers (fig. 1).

In contrast to extratropical glaciers, the fundamental difference in glacier formation lies in the fact that the tropical snow reserves must be established during the summer. They cannot be established during the coldest period of the year because during the winter, as a rule, little to no precipitation falls. Ablation, on the other hand, takes place during the interseasonal periods and the winter when solar radiation is intense, as well as during summertime dry periods. This results in a completely different kind of mass-balance situation over the budget year, which is further complicated by irregularities in the annual precipitation cycle (Jordan, 1979). During the summer, the maintenance of a glacier is a delicate balance between the accumulation of snow reserves and the ablation from radiation at an increased temperature. Data from mass-balance measurements give more exact information (Jordan, 1992; Francou and others, 1995). Ribstein and others (1995) discuss the results of a 2-year study of the hydrology of a 3-km^2 basin in the Cordillera Real that is 77 percent glacierized. In this area, accumulation and melt periods coincide during the rainy season, but the amount of melt often exceeds precipitation, which is resulting in the rapid recession of the glacier termini.

Because of the year-round high position of the Sun in the tropics, north-south exposure differences are less apparent than they are outside the tropics. In the Southern Hemisphere, the effect of the Sun increases in importance toward the south, however, and the cycle of cloud formation during the day must then be taken into consideration with respect to the exposure differences that affect the mass balance of a glacier. Because cloud cover descends very regularly at night to a level of 3,500 to 4,000 m, the glaciers are fully exposed to the morning Sun even during the rainy season. The cloudiness that develops during the forenoon protects the glaciers from radiation during the rest of the day (see fig. 10). Because the Sun shines on the eastern slopes in the early morning and because the northern slopes have greater solar radiation in the Southern Hemisphere, the east-to-north slope exposures have comparably smaller glacierization. The snowline is lower on the western and southern slopes and rises substantially (100 to 300 m) on the eastern and northern slopes (see figs. 11–13; Jordan, 1985). The solar-radiation effect increases toward the arid regions to the south. Combined with the extreme dryness of the air, solar radiation produces a peculiar phenomenon on firn and glacier surfaces, the intensified development of snow and ice penitents (Troll, 1942). The penitents phenomenon is also very dependent on the slope and radiation exposure and the annual climate cycle; these factors produce large differences, both with respect to time and space, in shaping the penitents (fig. 14). As a result of this differential surface ablation, which

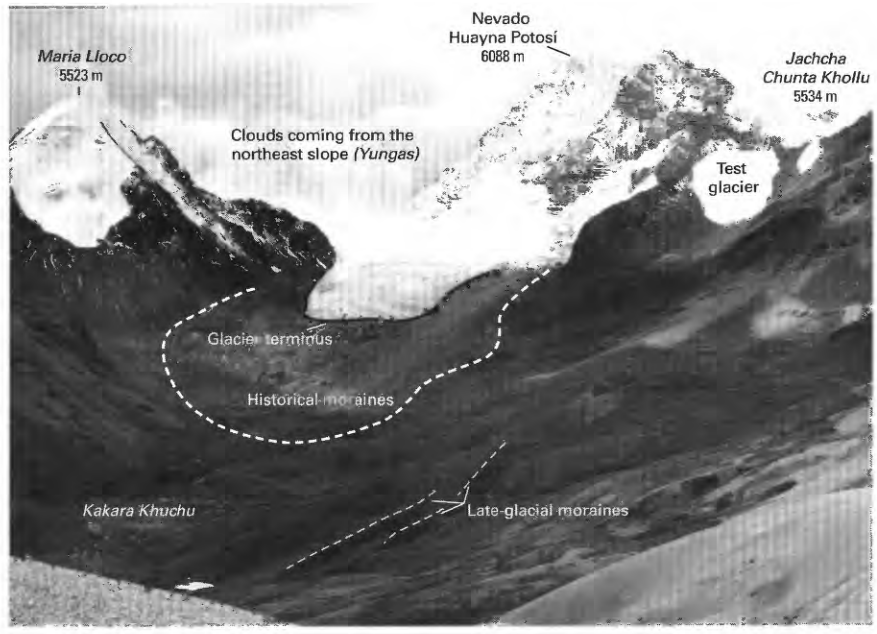

Figure 10.—*Nevado Huayna Potosí (6,088 m) in the northern Cordillera Real. The annotated terrestrial photograph shows the west side of the Nevado Huayna Potosí (also called Caca-aca) and the surrounding landscape, which is similar to the European Alps. The slope glaciers join together into a short valley glacier at about 5,200 m elevation in the center of the photograph. The Holocene Epoch (labeled historical) and Pleistocene Epoch (late-glacial) moraines can be seen clearly. To their left and right are smaller slope and cirque glaciers. Toward noon, the clouds of the northeast slope (Yungas) move up across the pass as far as the peaks of the cordillera, where they protect the glaciers from solar radiation. Photographed by Ekkehard Jordan on 15 May 1980 from the road between Milluni and La Unión looking east (elevation, 4,900 m; lat 16°17'42"S., long 68°12'14"W.).*

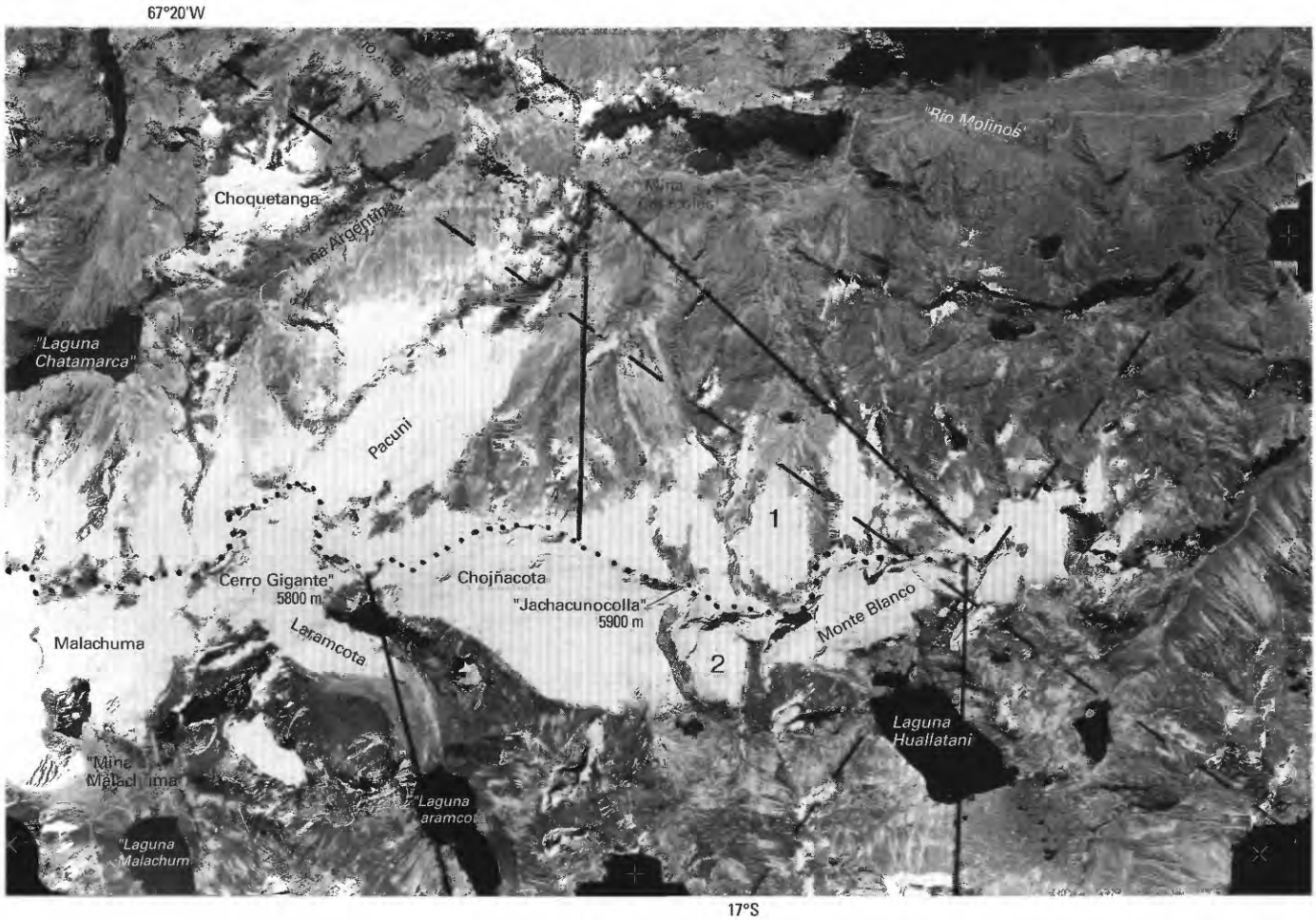

Figure 11.—*Annotated vertical aerial photograph of the southern part of* Cordillera Tres Cruces. *The watershed divide is shown by a dotted line. The two sections marked 1 and 2 show the locations of two ground photographs (figs. 12 and 13). The solid black lines indicate limits of coverage of each photograph. The aerial photograph and two ground photographs clearly illustrate the different degree of glacierization on the northeast escarpment (fig. 12) in contrast to that on the southwest escarpment (fig. 13) of the mountain range. Aerial photograph from Instituto Geográfico Militar, La Paz, taken 29 July 1975 [scale about 1:60,000].*

Figure 12.—*Northeast-facing escarpment of the southern* Cordillera Tres Cruces *(also called Quimsa Cruz). The terrestrial photograph shows the high lower limit of the glacier in the region of the Caracoles mine toward the end of the rainy season. The large white spots in the lower sector of the cirque walls are remnants of snow. In the foreground, Holocene Epoch moraines are visible. The location of the photograph is shown in figure 11 as number 1 between the solid black lines. Photographed by Ekkehard Jordan on 8 April 1977 from above Caracoles at an elevation of 4,800 m; lat 16°56'30"S., long 67°19'30"W.*

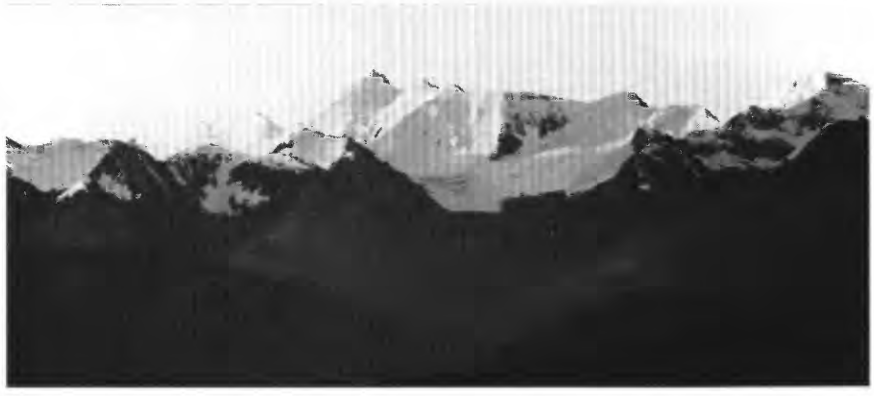

Figure 13.—*Southwest-facing escarpment of the southern* Cordillera Tres Cruces *showing the strong extent of glacierization of the western slope in the sector between Laguna Laramcota and Laguna Huallatani. The location of the ground telephotograph is shown in figure 11 as number 2 between the solid black lines. Photographed by Ekkehard Jordan on 12 May 1977 from the northern foot of Cerro Punaya; view to the east (elevation, 4,155 m; lat 17°21'50"S., long 67°24'30"W.).*

Figure 14.—*Ice penitents on the Glaciar Laramcota, western slope of the* Cordillera Tres Cruces. *During the dry season, 50- to 80-cm-high ice penitents develop in several sectors of the tongue of the Glaciar Laramcota at an elevation of 4,900 m. Photographed by Ekkehard Jordan on 23 August 1980; lat 16°57'15"S., long 67°22'30"W.*

is typically a subtropical-tropical phenomenon, glaciers and snow patches become especially difficult to traverse toward the end of the dry season.

A further manifestation of the distinctive daytime climate of high mountains on the southern edge of the tropics is the presence of glaciers with a high accumulation of debris. In addition, rock glaciers are found at elevations of 4,800 m and above, south of the actual occurrence of glaciers (fig. 15). Their exact classification is the subject of scientific controversy (see section on Rock Glaciers in this volume), and their exact areal distribution is not elaborated in this section because the author is inclined to characterize them, on the basis of their typical slope, as a periglacial permafrost phenomenon. Also, because of their modest size, they are not discernible on satellite images.

Observation and Mapping of Glaciers

First reports about glaciers in Bolivia are available from the last century (d'Orbigny, 1835–1847). Although no records by the native Indian population exist, the mountain land up to the glacier tongues has been used for many centuries for cattle and by vicuñas, llamas, and alpacas. The lack of records stems primarily from the fact that the Indian population had no writing system. Their verbal history of the glaciers and mountain peaks was based on myths. For the Indians, the glaciers and mountain peaks are inviolably divine.

At the beginning of the 20th century, a wave of glacier exploration took place. It was a time devoted to eliminating blank places on maps of the Earth. This period also produced the first sketches and maps of Bolivia's glacierized mountains. In terms of scientific content, the research was directed at snowline and glacier terminus locations and glacier morphology and distribution. Names such as Conway (1900), Hauthal (1911), and Herzog (1913, 1915) bear witness to this period of research activity. During this period and immediately following, a variety of mountain-climbing expeditions often included scientists. Most successful with respect to cartography and glacier exploration was that of the German-Austrian Alpine Association expedition in 1927–28 led by Carl Troll. His precise field photographs and triangulation measurements formed the basis for a number of good route drawings. He produced accurate general maps and a precise topographic map of the northern Cordillera Real (Illampu area) (Troll and Finsterwalder, 1935) at a scale of 1:50,000, which was based on terrestrial photogrammetric methods. Their precision and cartographic perfection were never equaled by any other map of glacierized regions in Bolivia. A

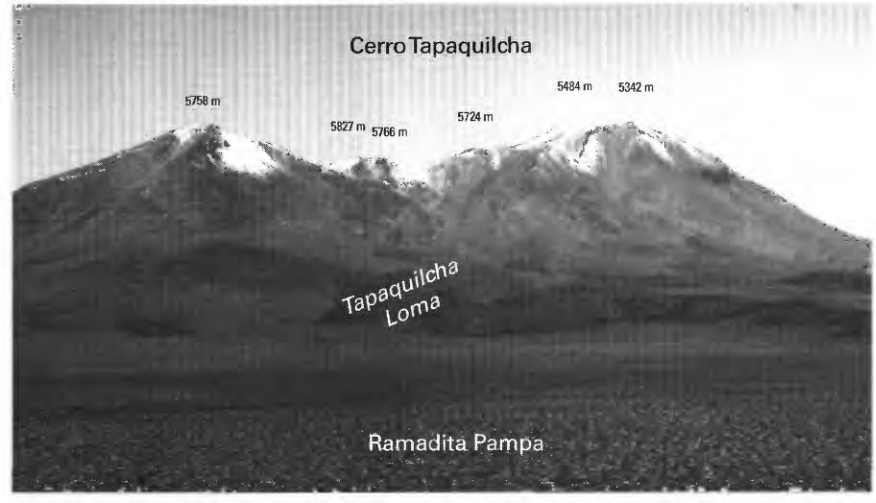

Figure 15.—*Cerro Tapaquilcha (5,827 m) in the southern Cordillera Occidental. In the upper slope region of the Tapaquilcha volcano complex, it is possible to see solifluction lobes and a light snow cover at the end of the rainy season, but glaciers are not present. The location of the annotated ground photograph is shown in figure 19. Photographed by Ekkehard Jordan on 10 April 1980 from Ramadita Pampa south of the Cerro Tapaquilcha looking north (elevation, 4,550 m; lat 21°40'03"S., long 67°57'W.).*

period of relative quiet followed this high point of cartographic-glacier exploration and research at the end of the 1920's, but later alpine expeditions produced route drawings. Geological studies in the high mining regions of the *Cordillera Tres Cruces* by Federico Ahlfeld resulted in a general map of this massif (Ahlfeld, 1946), which sketches the general distribution of glaciers. A recent topographic map of the Illampu area has been made by using aerial photos taken in 1963 and 1975 (Finsterwalder, 1987). Because of the accuracy of Troll and Finsterwalder's 1935 topographic map, it has been possible to quantify the ice loss by comparing that map with Finsterwalder's 1987 map. An accurate cartographic map of the southern Cordillera Real (Illimani area) has also been published at a scale of 1:50,000 (Finsterwalder, 1990; Jordan and Finsterwalder, 1992).

Official mapping of Bolivia was started in the 1940's with assistance from the U.S. Army Map Service. The work was based on vertical aerial photographs and is being completed and updated by the Instituto Geográfico Militar (IGM) in La Paz. The maps have scales of 1:50,000 and 1:250,000 (fig. 16). To date, only part of the glacierized regions in the environs of La Paz and the Cordillera Occidental has been covered by published maps. Unfortunately, no distinction is made between snow patches and glaciers on these maps. Thus, the maps show the snow cover prevailing at the time that the vertical aerial photograph was made and do not show the actual glacier distribution. Although the snow patches and glaciers on these maps are depicted by blue contour lines, they are nonetheless unsuitable for glacier studies. It is almost always necessary to analyze the vertical aerial photographs.

Later, a survey of the glaciers of Bolivia was conducted by Mercer (1967). Since 1975, the author has carried out modern glaciological and glacial-hydrologic studies in Bolivia by using mass-balance data and energy records; his studies include measurements of ice movement, precipitation, temperature, evaporation, ablation, and glacier runoff. He has taken terrestrial photogrammetric photographs of reference glaciers and has surveyed the location of glacier termini. He also has undertaken the compilation of a glacier inventory for Bolivia (Jordan and others, 1980). For this purpose, aerotriangulations of Bolivia's glacierized regions, which up to now had not been recorded on official maps, were carried out from the northern Cordillera Real across the Cordillera Apolobamba to the Peruvian border. This work has been published in two volumes (text and maps and illustrations) and contains the maps of all glacierized areas of Bolivia (Jordan, 1991; Herrmann, 1993). The data are also part of the "World Glacier Inventory" of the United Nations Environment Programme/United Nations Educational, Scientific, and Cultural Organization/International Commission on Snow and Ice (UNEP/UNESCO/ICSI) [now part of the World Glacier Monitoring Service, Zürich, Switzerland].

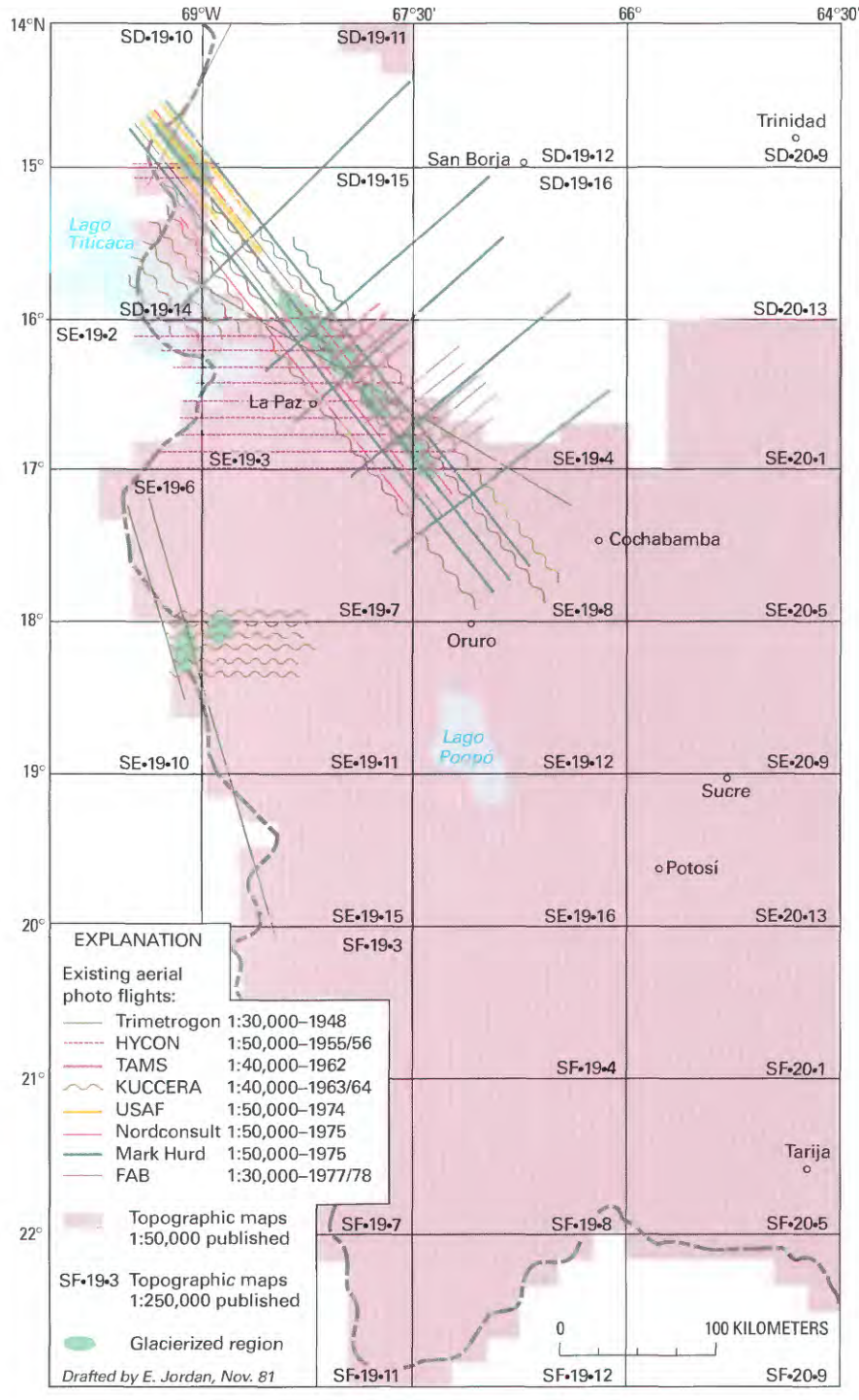

Figure 16.—*Aerial photographs and topographic maps of the glacierized regions of Bolivia. The photograph and map summary shows the status of photogrammetric flights having scales from 1:30,000 to 1:50,000, and the published topographic maps having scales of 1:50,000 and 1:250,000. In order to keep the index legible, only the photographic flights that record Holocene glaciers are plotted.*

Glacier Imagery

Aerial Photographs

Through the development of analytical techniques using vertical aerial photographs and more recently using satellite images, a new era in glacier studies began. The use of these two technologies means that no glacierized regions in Bolivia should remain unknown to us today. The analysis of satellite images provided, for the first time, an assessment of glacier distribution in the different cordilleras. Although the quantitative results are not as accurate as those derived from precise photogrammetric measurements of aerial photographs (table 1), satellite imagery provides the capability for more accurately monitoring Bolivia's glaciers. The frequently acquired satellite data will give more up-to-date information and permit observation of the substantial recession of these tropical glaciers.

The first aerial mapping surveys using photogrammetric quality metric cameras were begun by the U.S. Army Air Force in 1942 and employed trimetrogon aerial photography. The aerial surveys were continued until 1948. After World War II, aerial navigation and photographic technologies improved rapidly. Beginning in 1952, at the Government of Bolivia's request, a new series of aerial surveys acquired vertical aerial photographs for use in various photogrammetric plotting instruments (for example, Multiplex and Kelsh) to compile modern maps of Bolivia. It was 1975, however, before all glacierized regions in Bolivia were covered by vertical aerial photographs (fig. 16). The quality of the photographs ranges from good to satisfactory, but a number of disadvantages is inherent in the available data. A major disadvantage is the fact that several different organizations carried out a variety of aerial surveys, using different cameras, lenses, and survey altitudes during different seasons over an extended period of years. Therefore, synoptic comparisons of glaciers are not possible. Because some areas covered by the different surveys overlap, it is sometimes possible to quantify the disappearance of glaciers during the intervals of aerial photographic coverage.

The available aerial photographic scales for Bolivia range from 1:30,000 to 1:80,000. On the basis of the aerial photographs, official maps of Bolivia are being compiled by IGM. During the past several years, most of the surveys have been carried out by the Fuerza Aérea Boliviana (Bolivian Air Force). The new maps compiled under the direction of Finsterwalder (1987, 1990) by using modern cartographic techniques are good examples of maps that give more precise information about the location and size of glaciers.

Satellite Photographs and Images

The first significant photograph of Bolivian glaciers from space comes from the *Gemini 9* manned space flight in early June 1966. It is an oblique photograph that shows Lago Titicaca in the center; in the foreground are the glaciers of the Cordillera Apolobamba and the entire Cordillera Real as far as Illimani, the majestic panoramic massifs around the capital city La Paz (fig. 17).

Earlier polar-orbiting meteorological satellites, and even the more advanced ones operating at present, have virtually no value for analysis of tropical glaciers because the spatial resolution is far too coarse. Picture elements (pixels) are generally 1 km, so the imagery vaguely suggests the mountain topography and the regional snow cover when no cloud cover

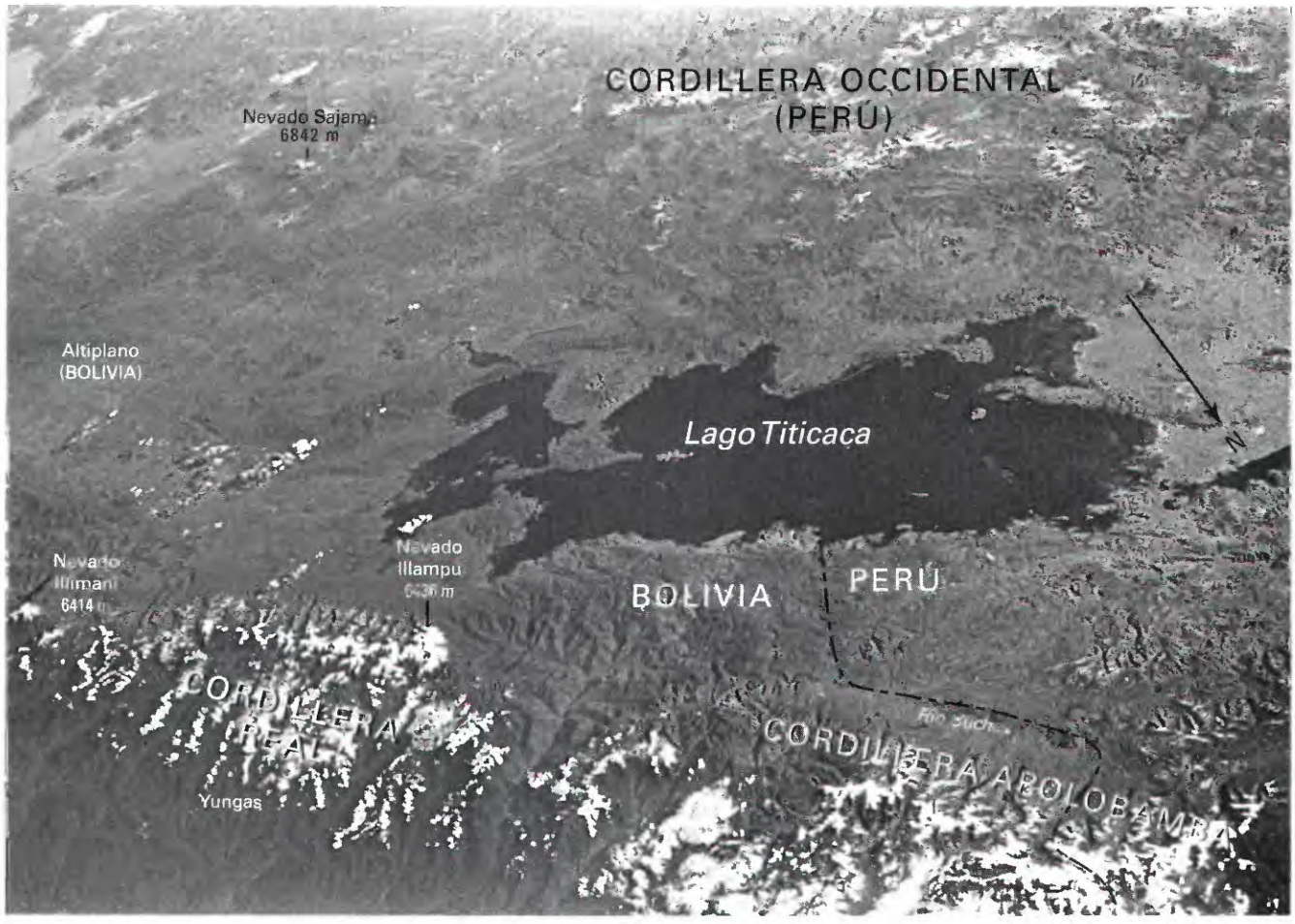

***Figure 17.**—Annotated oblique satellite photograph taken from the* Gemini 9 *spacecraft looking west at the glacierized Cordillera Oriental. The photograph, which originally was in color, shows Lago Titicaca in the center, Cordillera Apolobamba in the right foreground, and the Cordillera Real to the left. In the immediate foreground, above the escarpment to the lowland, are some clouds. Photograph taken June 1966 by using a Zeiss-Biogon 1:4.5/38 mm Hasselblad camera. Approximate scale, 1:1,800,000.*

interferes. Their only advantage lies in the frequent orbital passage that permits monitoring of general variations in the temporal and seasonal snow cover and elevation of the snowline in the glacierized regions of the tropics. However, with the first of the series of Earth Resources Technology Satellites (ERTS–1, later renamed Landsat 1) launched on 22 July 1972, it became possible to analyze images that had a pixel resolution of 79 m and were suitable for glacier studies on a scale suited to tropical glaciers. Because of the 18-day repeat cycle of the Landsat 1, 2, and 3 satellites (16-day cycle for Landsats 4 and 5), a large number of satellite images have been acquired, although most of the images either are not suited for glaciological studies or have only limited value because of persistent cloudiness. The images found to be useful are listed in table 2, and their locations are shown in figure 18. Specialized studies using advanced techniques for analyzing satellite images of glaciers have not been done on Bolivian glaciers yet, but general observations of glaciological applications will be discussed in the following section, which also includes discussion of the interpretation of glaciological features on Landsat images acquired in different seasons using different spectral bands. Remote sensing systems that have higher resolution sensors, such as Landsat 4 and 5 Thematic Mapper (TM) (30 m), Satellite Pour l'Observation de la Terre (SPOT) (10–20 m), and Modular Optoelectronic Multispectral Scanner (MOMS) (up to 5 m), have limitations, even though the satellites allow more detailed observation of the small tropical glaciers. Landsat data and SPOT data are quite expensive. The MOMS system has the disadvantage that it is still not an operational system; it has only been tested on Space Transportation System (Shuttle) flights. However, SPOT and MOMS have the advantage of stereoscopic interpretation capability.

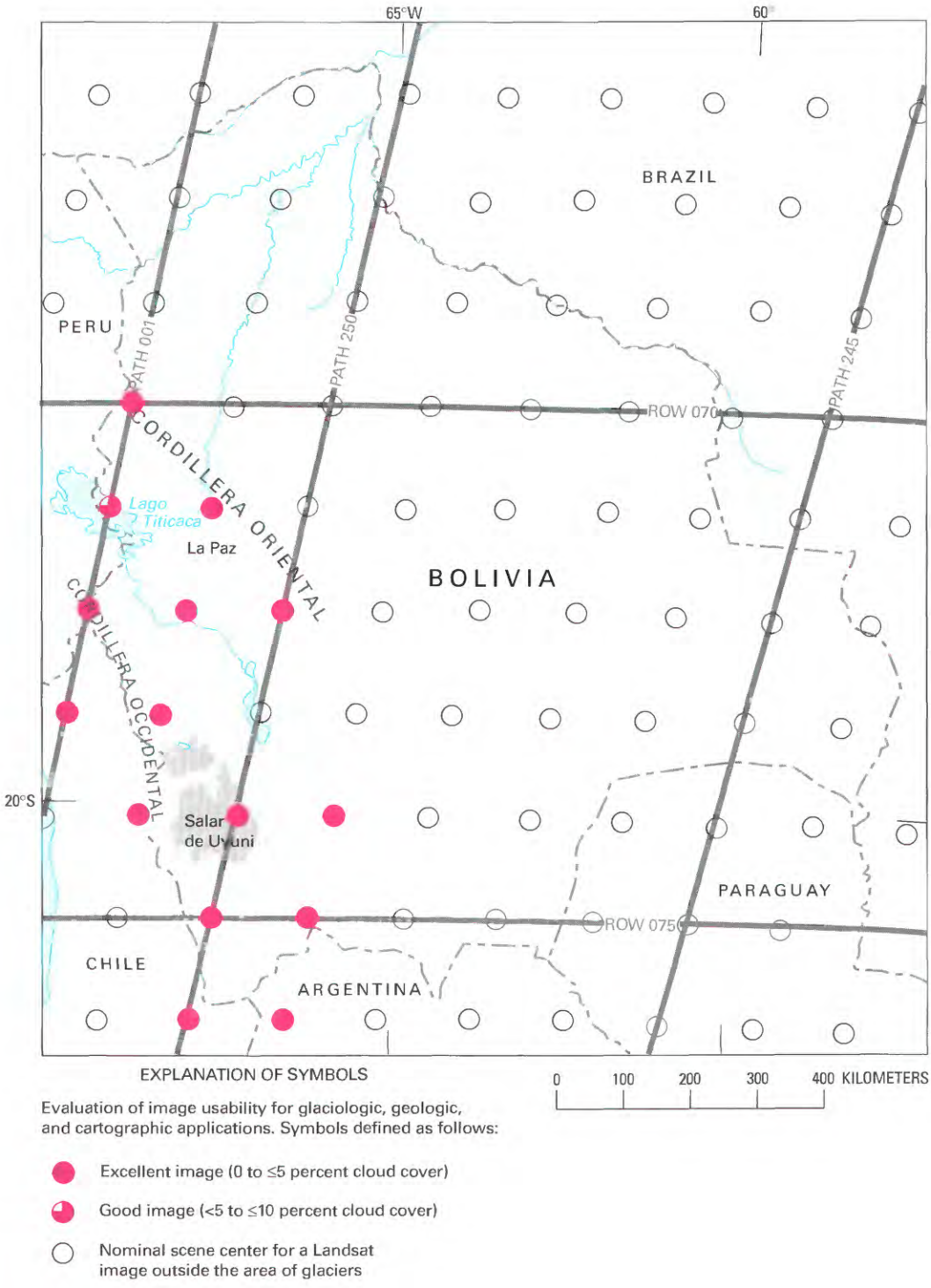

Figure 18.—*Optimum Landsat 1, 2, and 3 images of the glaciers of Bolivia.*

TABLE 2.—*Optimum Landsat 1, 2, and 3 images of the glaciers of Bolivia*

[See fig.18 for explanation of symbols used in "code" column]

Path-Row	Nominal scene center (lat-long)	Landsat identification number	Date	Solar elevation angle (degrees)	Solar azimuth angle (degrees)	Code	Cloud cover (percent)	Remarks (image archived by U.S. Geological Survey EROS Data Center, Sioux Falls, S. Dak., unless otherwise noted)
249–74	20°11'S. 65°59'W.	2148–13415	19 Jun 75	30	44	●	0	No Holocene, only Pleistocene glacier areas; image used for figure 9
249–75	21°38'S. 66°21'W.	2418–13382	15 Mar 76	42	71	●	0	Bolivia-Argentina; no Holocene, only Pleistocene glacier areas; moderate snow cover; image used for figure 20*C*
249–75	21°38'S. 66°21'W.	2148–13421	19 Jun 75	29	44	●	0	Bolivia-Argentina; no Holocene, only Pleistocene glacier areas; moderate snow cover; image used for figure 20*E*, *F*
249–75	21°38'S. 66°21'W.	2310–13401	28 Nov 75	54	96	●	0	Bolivia-Argentina; no Holocene, only Pleistocene glacier areas; minimal snow cover; image used for figure 20*A*, *B*
249–76	23°04'S. 66°44'W.	2256–13411	05 Oct 75	48	69	●	0	Argentina-Bolivia-Chile; no Holocene, only Pleistocene glacier areas; minimal snow cover
250–72	17°19'S. 66°42'W.	2149–13464	20 Jun 75	33	45	●	0	*Cordilleras Tres Cruces* - Nevado Santa Vera Cruz; moderate snow cover
250–74	20°11'S. 67°25'W.	1243–13595	23 Mar 73	46	65	●	0	Bolivia-Chile, Cordillera Occidental
250–75	21°38'S. 67°48'W.	1243–14001	23 Mar 73	45	64	●	0	Bolivia-Chile, Cordillera Occidental; minimal snow cover; image used for figure 19
250–76	23°04'S. 68°10'W.	2401–13450	27 Feb 76	44	78	●	0	Chile-Bolivia; moderate snow cover
250–76	23°04'S. 68°10'W.	1243–14004	23 Mar 73	44	63	●	0	Excellent with minimal snow cover on mountain peaks; no Holocene glaciers
250–76	23°04'S. 68°10'W.	2257–13470	06 Oct 75	48	70	●	0	Excellent but with considerable snow cover in the cordillera; no Holocene glaciers
251–71	15°52'S. 67°47'W.	2168–13520	09 Jul 75	34	47	●	0	Cordillera Real; minimal snow cover, image used for figure 8
251–72	17°19'S. 68°08'W.	2276–13505	25 Oct 75	54	86	●	0	Southern Cordilleras Real and *Tres Cruces*, and Nevado Santa Vera Cruz; moderate snow cover; image used for figures 7 and 8
251–72	17°19'S. 68°08'W.	1100–14041	31 Oct 72	58	89	●	0	Southern Cordilleras Real and *Tres Cruces* and Nevado Santa Vera Cruz; minimal snow cover
251–73	18°45'S. 68°30'W.	1100–14043	31 Oct 72	57	87	●	0	Bolivia-Chile, Cordillera Occidental; minimal snow cover; image used for figure 2*A*, *B*
251–74	20°11'S. 68°51'W.	1244–14053	24 Mar 73	46	65	●	0	Chile-Bolivia, Cordillera Occidental
1–70	14°26'S. 68°52'W.	2223–13561	02 Sep 75	44	62	●	0	Bolivia-Perú, Cordillera Apolobamba; substantial snow cover; image used for figure 5*A*
1–70	14°26'S. 68°52'W.	2187–13565	28 Jul 75	37	51	●	0	Bolivia-Perú, Cordillera Apolobamba; minimal snow cover; image used for figure 8
1–70	14°26'S. 68°52'W.	277108–133941	18 Apr 77	39	62	●	10	Bolivia-Perú, Cordillera Apolobamba; marginal cloud cover; excellent glacier without snow cover; image source: Brazil
1–71	15°52'S. 69°13'W.	277108–134006	18 Apr 77	38	61	◕	10	Bolivia-Perú, Northern Cordillera Real, Lake Titicaca; excellent glacier; image source: Brazil
1–72	17°19'S. 69°34'W.	1065–14091	26 Sep 72	52	69	●	0	Perú-Bolivia-Chile, Cordillera Occidental; minimal snow cover
1–72	17°19'S. 69°34'W.	277108–134031	18 Apr 77	38	60	●	0	Perú-Bolivia-Chile, Cordillera Occidental; image source: Brazil
1–73	18°45'S. 69°56'W.	2061–13583	24 Mar 75	44	68	●	0	Chile-Bolivia-Perú, Cordillera Occidental; glaciers masked by snow cover

Capabilities and Limitations of Interpreting Glaciological Phenomena from Satellite Images of Bolivia's Semitropical Glaciers

The following discussion is limited to the manual-optical analysis of 1:1,000,000-scale satellite images from the Landsat series. Because of the scanning element (pixel) size of 79×79 m in Landsat multispectral scanner (MSS) images, certain limits are set for interpretation. Yet these limits are not only determined by the pixel resolution but also by the discrimination of various materials within the spectral ranges of the images, by the seasonal and climatic conditions during imaging, and finally, by the characteristics of tropical glaciers. In this section, the occurrence of the Bolivian glaciers will be examined, including a discussion of the limitations just mentioned. The facts are essentially the same for the increased resolution of Landsat TM, SPOT, and MOMS images.

Initial difficulties emerge in the general determination of glacier distribution. Distinguishing between ice and snow and salt areas, and also cloud cover, is difficult. It is made easier with the proper selection of the available multispectral images, especially by using MSS spectral band 7.

The glaciers of the Cordillera Occidental have a spectral reflectance that is similar to salt efflorescences and salars (figs. 2, 3, and 19). As a rule, the latter are located in intermontane basins, whereas snow and glaciers cover the volcanic peaks. Stereoscopic observation capability, therefore, makes differentiation possible with absolute certainty. Since 1986, SPOT has provided this capability, as have the 1983–84 and 1993 MOMS test series images. Landsat imagery does not have true stereoscopic quality. However, the azimuth and orientation of the Sun at the time of imaging give the terrain the appearance of substantial relief so that, except for some borderline cases, it is possible to differentiate between ice and snow and salt areas with fair certainty.

On the other hand, the difficulty of spectrally separating and therefore delineating areas of snow, firn, glacier ice, and glacier ice covered with snow and firn is much more important. For example, snow cover gives the false impression that many of the volcanic cones of the Cordillera Occidental and the Cordillera de Lípez are covered by glaciers (figs. 2, 19, and 20). However, only a few volcanoes (table 1) are actually capped by ice; all the others have only a temporary firn cap, which may persist, in part, for several years, with an especially strong definition after the rainy season in March and April (see fig. 20).

In the case of extratropical glaciers, definite accumulation and ablation phases exist, and in the fall, the highest snow and firn lines can be noted. In the tropics, these phases cannot be so clearly defined (fig. 20). Thus, a specific time of year cannot be selected for the optimum analysis of glacier areas. Therefore, analysis of satellite images of Bolivia is always accompanied by the uncertainty of having included in the peripheral areas some large firn and snow-covered areas—as has obviously happened with the "Mapa de cobertura y uso actual de la tierra Bolivia" (Brockmann, 1978).

A further difficulty in analyzing satellite images results from the size of the glaciers. The total extent of the glaciers, about 600 km^2, is substantial. However, the glacierized area includes many small glaciers, strongly segmented recharge areas, fragmented glaciers, and steep cliff glaciers and glacier tongues. As a rule, these small glacier areas are generally less than 1 km^2 in size. Because of the limitation of the resolution of Landsat imagery, these areas are hard to delineate.

The abundance of small, steep glaciers is also difficult to discern owing to the strong shadows on the slopes oriented toward the southwest (figs. 2

Figure 19.—*Annotated Landsat 1 MSS false-color composite image of the Cordillera Occidental in southern Bolivia and northeastern Chile. The image shows a large number of snow-capped volcanic peaks. However, none of the high mountains has a glacier, and the white snow patches were caused by the abundant precipitation during the just completed rainy season. The snow patches as a rule disappear again at the end of the dry season, mostly through sublimation. The concentration of red color in the lowlands and middle slope regions of the volcanoes, which indicates a strong spectral response in the near-infrared part of the electromagnetic spectrum, also documents the abundant precipitation in the year that the image was acquired. The red coloration in this case represents good plant growth and intensive formation of chlorophyll. The abundant precipitation is further attested to by the extended surface water in the region of the salars. The location of figure 15 is shown. Landsat image (1243–14001; 23 March 1973; Path 250, Row 75) is from the EROS Data Center, Sioux Falls, S. Dak.*

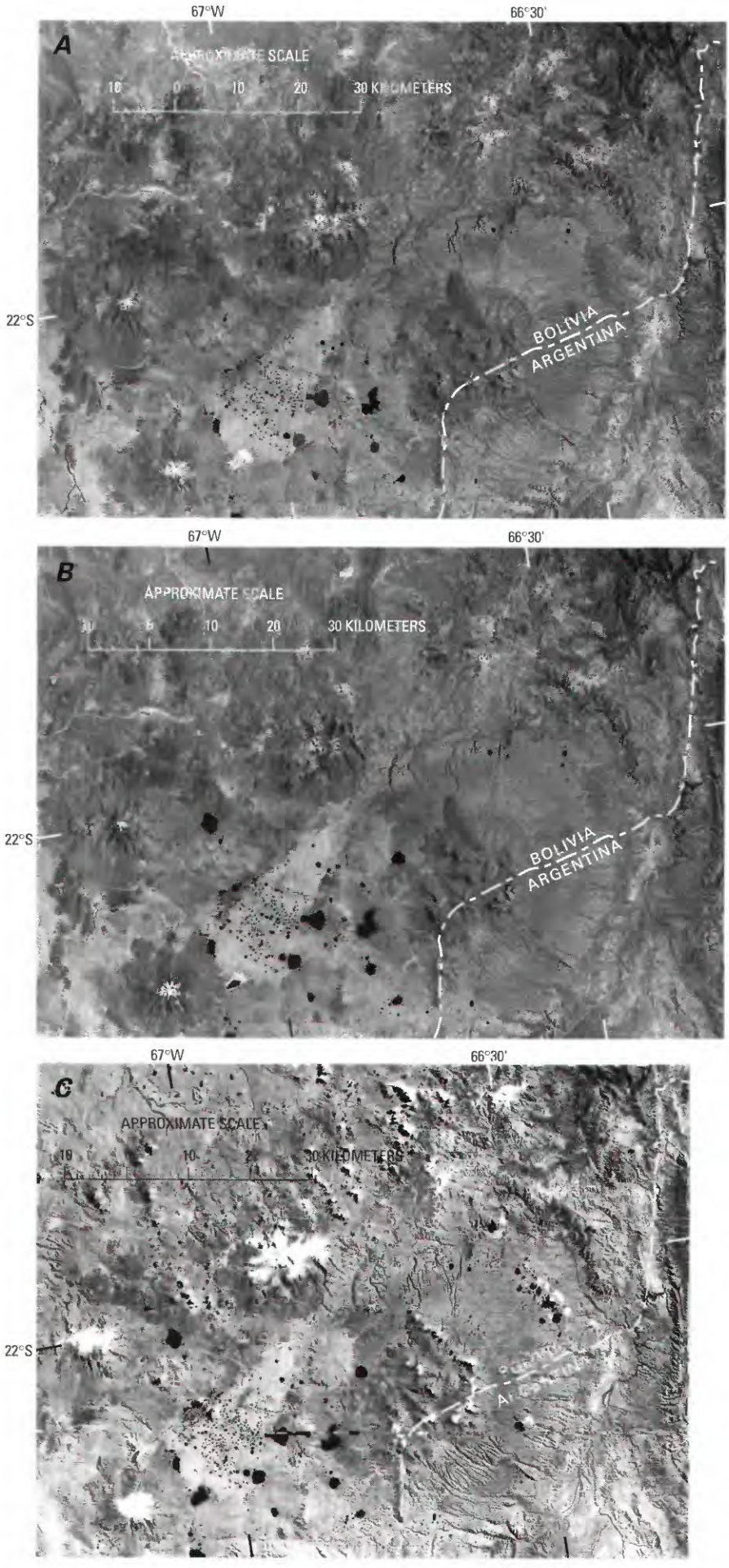

Figure 20.—*Parts of six 1:1,000,000-scale Landsat 2 MSS images showing the seasonal cycle of snow and firn fields in the Cordillera de Lípez.*

A, *Landsat image 2310–13401, band 5; 28 November 1975; Path 249, Row 75.*

B, *Landsat image 2310–13401, band 7; 28 November 1975; Path 249, Row 75.*

C, *Landsat image 2418–13382, band 7; 15 March 1976; Path 249, Row 75.*

D, *Landsat image 2058–13421, band 7; 21 March 1975; Path 249, Row 75.*

E, *Landsat image 2148–13421, band 5; 19 June 1975; Path 249, Row 75.*

F, *Landsat image 2148–13421, band 7; 19 June 1975; Path 249, Row 75.*

The satellite images show a section of the Cordillera de Lípez in the extreme south of Bolivia at the boundary with Argentina. The area encompasses the highest peaks of southern Bolivia, which, according to official survey data, include several peaks more than 5,000 m high and one peak, in the Uturunco massif, that exceeds 6,000 m in elevation. In spite of these high elevations, no recent glacierization exists, only some firn patches, which can be seen in A *and* B *acquired 28 November toward the end of the dry season. Beginning in November, snowfields normally increase in size and reach their greatest extent toward the end of the rainy season in March and April, as shown in* C *and* D. *At this time, the snow cover may completely cover the high peaks and upper basins for several days. Below 5,000 m, the temperatures are high enough so that the snow cover melts quickly. At the greater elevation of the higher peaks, the ablation process proceeds very slowly because of decreasing temperatures during the dry season, as can be seen in an image acquired in June (*E *and* F*).*

The snow patches show their smallest extent at the beginning of the rainy season in early summer. This is the time of formation of the most pronounced penitent forms. Residual firn patches often can be found at the highest elevations or in sheltered areas. The snow completely disappears in all locations only during irregular cycles of about 3–10 years' duration. The great variability of precipitation in the individual years is naturally reflected by a variability of snow thickness and snow cover extent, as documented by the comparison of the two March images of 1975 and 1976 (C and D). The results of the annual radiation cycle at this location a little north of the Tropic of Capricorn (lat 23.5°S.) can also be distinguished on the images. A comparison of the November images (A and B) near the annual zenith position of the Sun with the June images (E and F), taken at the astronomically lowest angle of solar radiation, shows that the greater effect of shadowing of the June image is quite pronounced. This, naturally, favors snow preservation in southern exposures. The varying response of the surface materials in spectral bands 5 and 7 is noticeable in several areas, including the location of the numerous lakes. Also, particularly in the November image, the white snow-capped peak appears larger in band 5 than in band 7; however, without knowledge of the local conditions (ground truth), one cannot distinguish whether one is looking at wet snow, which responds differently in bands 5 and 7, at old "dirty" snow, or possibly at sulfur efflorescence of craters in volcanically active regions.

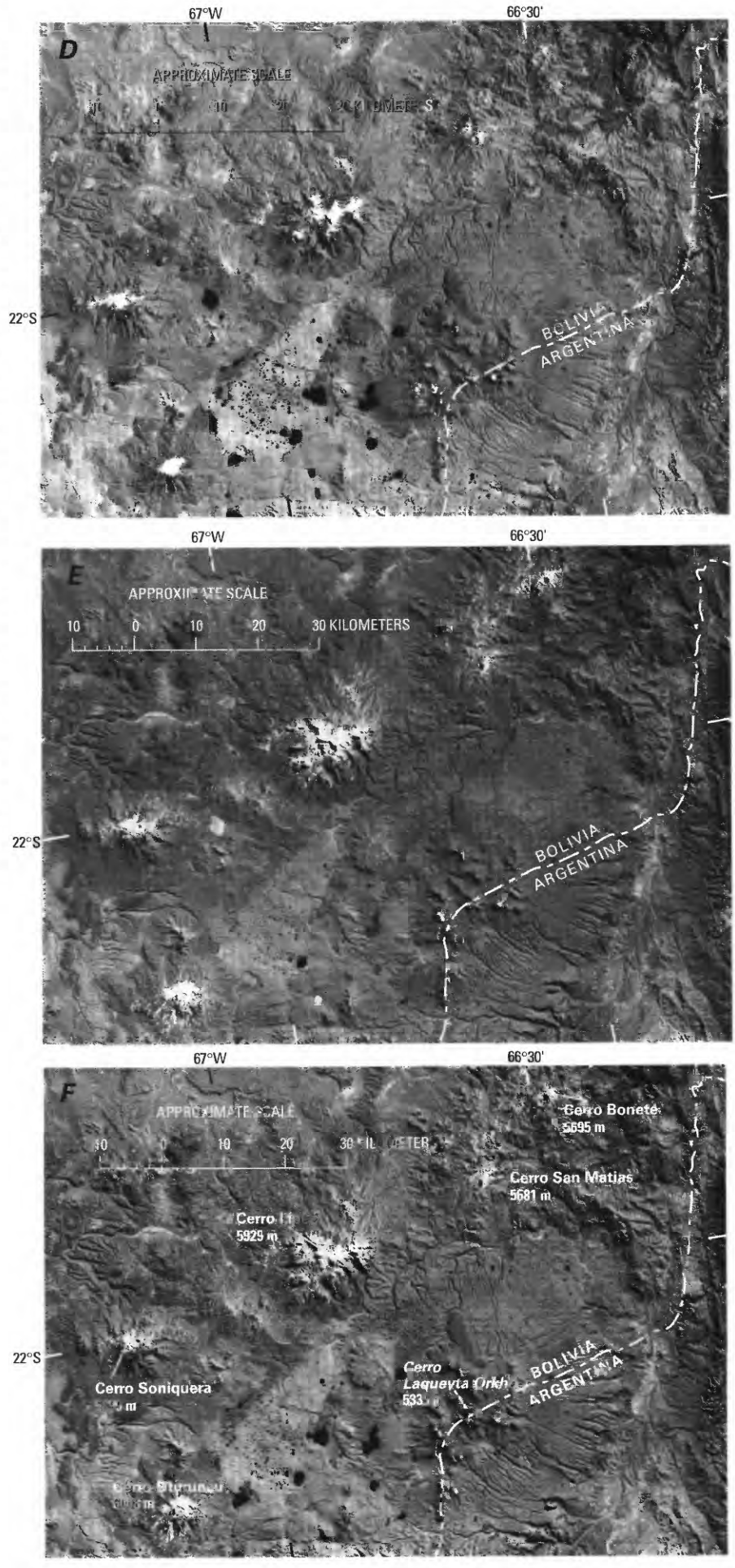

and 8). The shadows are caused by the low, early morning position of the Sun at the time of imaging because of the Equatorial crossing time of 0930 h. On the northern and eastern sides of the slopes, the casting of shadows has an advantage when differentiating between snow or glaciers and clouds. The clouds can be more easily distinguished under certain conditions from similarly reflective materials because of the presence of a cloud shadow. Of course, this ability to distinguish clouds and ice is more difficult if the cloud level itself is located at the height of the glacier and snow fields.

The shadows resulting from the low Sun angle also cause a systematic faulty evaluation of the actual glacier area, especially during the southern winter. The shadows at these latitudes, which are especially dark because of the small diffuse amount of radiation at the tropical heights, cause primarily the steep west to southwest mountain slopes to appear very dark. As a result, their glacierization is partially obscured, whereas the glaciers on the east side, which are lit up in the sunlight, are especially well illuminated. On the other hand, the early time of imaging gives the impression that the west side of the Cordillera Oriental is the preferred snowfall region because the snow that fell in the afternoon and night hours on this side of the cordillera has not yet thawed. This is because of the daily climate cycle that includes cloud cover that protects the snowfields on the western slopes from the Sun's radiation in the afternoon (figs. 5 and 8).

Small-scale glacier surface phenomena are seldom visible on Landsat imagery. These include glacier-flow structures and ablation forms of all kinds, such as penitents, old snow areas, and bare ice surfaces, as well as changes in proglacial lake levels. The same lack of visibility is true for the small, short-term advance and recession of glaciers, which result in small surges that are climatically conditioned response mechanisms. However, historic and Pleistocene glacier fluctuations can be interpreted by clearly identifiable moraine stands on the satellite images.

Landsat 1, 2, and 3 MSS images, and more recently Landsat 4 and 5 TM, SPOT, and finally MOMS images, have proved to be useful for glaciological studies in Bolivia. However, the development in the direction of higher resolution satellite imaging systems will continue to provide significant improvements for the observation and surveillance of these semitropical glaciers in the future. The availability of a wide variety of remotely sensed data will make it possible to select particular sensors or wavelengths of the electromagnetic spectrum depending on the specific glaciological application.

References Cited

Ahlfeld, Federico, 1946, Geología de Bolivia [Geology of Bolivia]: La Plata, Universidad Nacional Museo Revista, Sección Geológica, new series, v. 3, no. 19, 370 p., color geologic map at a scale of 1:1,212,000.

Brockmann, H.C.E., 1978, Mapa de cobertura y uso actual de la tierra Bolivia memoria explicatia [Land-cover and present-day land-use map of Bolivia]: La Paz, Servicio Geológico de Bolivia, Programa del Satélite Tecnológico de Recursos Naturales, Serie Sensores Remotos, no. 2, 116 p., color land-use maps at a scale of 1:1,000,000.

Conway, Martin, 1900, Notes on a map of part of the Cordillera Real of Bolivia: Geographical Journal, v. 15, no. 5, p. 528–529, color map (1898) at a scale of 1:500,000.

d'Orbigny, A.D., 1835–1847, Voyage dans l'Amérique Méridionale (le Brésil, la République orientale de l'Uruguay, la République Argentine, la Patagonie, la République du Chili, la République de Bolivia, la République du Pérou), executé pendant les années 1826, 1827, 1828, 1829, 1830, 1831, 1832 et 1833 [Voyage to South America (Brazil, Uruguay, Argentina, Patagonia, Chile, Bolivia, Perú), carried out during the years 1826–1833]: Paris, Pitois-Levrault and Company, 9 v.

Finsterwalder, Rüdiger, dir., 1987, Map of the Cordillera Real Nord (Illampu): München, Deutsche Alpenverein, scale 1:50,000.

———1990, Map of the Cordillera Real Süd (Illimani): München Deutsche Alpenverein, scale 1:50,000.

Francou, Bernard, 1993, Une représentation factorielle des cryosphères d'altitude dans le monde *in* Géomorphologie et aménagement de la montagne—melanages in hommage à P. Gabert [A quantitative description of the high-altitude cold regions in the world *in* Geomorphology and development of the mountain—a series of papers dedicated to Pierre Gabert]: Centre National de la Recherche Scientifique, Centre de Geomorphologie de Caen, Bulletin, v. 42, p. 75–86.

Francou, Bernard, Ribstein, Pierre, Saravia, Ronald, and Tiriau, Eric, 1995, Monthly balance and water discharge of an intertropical glacier: Zongo Glacier, Cordillera Real, Bolivia, 16° S: Journal of Glaciology, v. 41, no. 137, p. 61–67.

Graf, Kurt, 1975, Estudios geomórficos en los Andes y el Altiplano Bolivianos [Geomorphological studies in the Bolivian Andes and Altiplano]: Sociedad Geológica Boliviana Boletín, no. 21, p. 3–23.

———1981, Zum Höhenverlauf der Subnivalstufe in den tropischen Anden, insbesondere in Bolivien und Ecuador [Altitudinal traces of the periglacial zone in the tropical Andes, particularly in Bolivia and Ecuador]: Zeitschrift für Geomorphologie, Neue Folge, Ergänzungshefte [Supplement], v. 37, p. 1–24.

Hastenrath, S.L., 1967, Observations on the snow line in the Peruvian Andes: Journal of Glaciology, v. 6, no. 46, p. 541–550.

———1971a, Beobachtungen zur klima-morphologischen Höhenstufung der Cordillera Real (Bolivien) [Observations on the climate-morphological altitudinal gradations of the Cordillera Real (Bolivia)]: Erdkunde, v. 25, no. 2, p. 102–108.

Hastenrath, S.L., 1971b, On the Pleistocene snow-line depression in the arid regions of the South American Andes: Journal of Glaciology, v. 10, no. 59, p. 255–267.

Hauthal, R.J.F., 1911, Reisen in Bolivien und Peru, ausgeführt 1908 [Travels in Bolivia and Perú, taken in 1908): Leipzig, Duneker and Humbolt, 247 p.

Herrmann, Andreas, 1993, Review of Jordon, Ekkehard, 1991, The glaciers of the Bolivian Andes, a photogrammetric-cartographical inventory of the Bolivian glaciers as a basis for climatic interpretation and potential economic use: Catena, v. 20, no. 3, p. 351–353.

Herzog, Theodor, 1913, Vom Urwald zu den Gletschern der Kordillere; 2 Forschungsreisen in Bolivien [From the jungle to the glaciers of the Cordillera; two research trips in Bolivia]: Stuttgart, Strecker and Schroder, 270 p.

———1915, Beiträge zur Kenntnis von Tektonik und Glazial der bolivischen Ostkordillere [Contributions to the knowledge of tectonics and glacial features of the Bolivian Eastern Cordillera]: Geologische Rundschau, v. 5 (1914), p. 353–371.

Jordan, Ekkehard, 1979, Grundsätzliches zum Unterschied zwischen tropischem undaussertropischem Gletscherhaushalt unter besonderer Berücksichtigung der Gletscher Boliviens [Fundamental information on the difference between tropical and extratropical glacier mass-balance with special consideration of Bolivia's glaciers]: Erdkunde, v. 33, no. 4, p. 297–309.

———1985, Recent glacier distribution and present climate in the Central Andes of South America: Zeitschrift für Gletscherkunde und Glazialgeologie, v. 21, p. 213–224.

———1991, Die Gletscher der bolivianischen Anden, eine photogrammetrisch-kartographische Bestandsaufnahme der Gletscher Boliviens als Grundlage für klimatise Deutungen und Potential für die wirtschaftliche Nutzung [The glaciers of the Bolivian Andes, a photogrammetric-cartographical inventory of the Bolivian glaciers as a basis for climatic interpretation and potential for economic use]: Stuttgart, Franz Steiner Verlag, 401 p., maps.

———1992, The recent development of the tropical andean glaciers in comparison to those in the European Alps and first indications of a climate change: Sociedad Geográfica de Lima Boletín, Segundo Congreso Internacional de Geografía de las Américas, v. 105, p. 289–310.

Jordan, Ekkehard, Brockman, Carlos, Fernandez, A., Alvarez, R., and Jacobsen, K., 1980, The glacier inventory of Bolivia *in* World glacier inventory, proceedings of the Riederalp (Switzerland) workshop: International Association of Hydrological Sciences, IAHS–AISH Publication no. 126, p. 25–32.

Jordan, Ekkehard, and Finsterwalder, Rüdiger, 1992 [1993?], Observaciones respecto al mapa Cordillera Real Norte (Illampú) 1:50,000—una contribución a la representación cartográfica y a la glaciología e historia de los glaciares de los Andes bolivianos [Explanatory notes to the map Cordillera Real North (Illampu) 1:50,000—A contribution to the cartographic representation, glaciology, and glacial history of the Bolivian Andes]: La Paz, Instituto Geográfico Militar, 178 p. [In Spanish, German, English, and French.]

Jordan, Ekkehard, Reuter, Gerhard, Leinweber, Peter, Alfaro, Hernan, Condo, Angel, Geyh, M.A., 1994, Pleistocene moraine sequences in different areas of glaciation in the Bolivian Andes: Zentralblatt für Geologie und Paläontologie, pt. 1, v. 1993, no. 1–2, p. 455–470.

Mercer, J.H., 1967, Glaciers of Bolivia and of Chile north of latitude 23°S; *in* Southern Hemisphere glacier atlas: U.S. Army Natick Laboratories, Earth Sciences Laboratory, Series ES–33, Technical Report 67–76–ES, p. 65–81.

Messerli, Bruno, Grosjean, Martin, Graf, Kurt, Schotterer, Velli, Schreier, Hans, and Vuille, Mathias, 1992, Die Veränderungen von Klima und Umwelt in der Region Atacama (Nordchile) seit der letzten Kaltzeit [Climate and environmental change in the Atacama region (northern Chile) since the last ice age]: Erdkunde, v. 46, p. 257–272.

Nogami, M., 1976, Altitude of the modern snowline and Pleistocene snowline in the Andes: Tokyo Metropolitan University, Geographical Reports, no. 11, p. 71–86.

Ribstein, Pierre, Tiriau, Eric, Francou, Bernard, and Saravia, Ronald, 1995, Tropical climate and glacier hydrology; a case study in Bolivia: Journal of Hydrology, v. 165, no. 1–4, p. 221–234.

Schubert, Carlos, 1992, The glaciers of the Sierra Nevada de Mérida (Venezuela), a photographic comparison of recent deglaciation: Erdkunde, v. 46, p. 58–64.

Schulz, Georg, 1992, Schlüsselpositionen für die pleistozäne Schneegrenzableitung über Karböden zwischen 3300 und 4200 m ü.d.M. aus Peru und Bolivien [Key locations for determining the Pleistocene snowline by means of cirque floors between 3,300 and 4,200 m in Perú and Bolivia]: Zentralblatt für Geologie und Paläontologie, pt. 1, v. 1991, no. 6, p. 1723–1736.

Thompson, L.G., Davis, M.E., Mosley-Thompson, Ellen, Sowers, T.A., Henderson, K.A., Zagorodnov, V.S., Lin, P.-N., Mikhalenko, V.N., Campen, R.K., Bolzan, J.F., Cole-Dai, J., Francou, Bernard, 1988, A 25,000-year tropical climate history from Bolivian ice cores: Science, v. 282, no. 5385, p. 1858–1864.

Troll, Carl, 1942, Büsserschnee (Nieve de los Penitentes) in den Hochgebirgen der Erde [Snow penitents in the high mountains of the Earth]: Petermanns Geographische Mitteilungen, Ergänzungshefte [Supplement] no. 240, 103 p.

Troll, Carl, and Finsterwalder, Richard, 1935, Die Karten der Cordillera Real und des Talkessels von La Paz and die Diluvialgeschichte der zentralen Anden [The maps of the Cordillera Real and the valley of La Paz and the Pleistocene history of the Central Andes]: Petermanns Geographische Mitteilungen, v. 81, no. 11, p. 393–399, and no. 12, p. 445–455.

U.S. Board on Geographic Names, 1992, Gazetteer of Bolivia (2d ed.): Washington, D.C., Defence Mapping Agency, 719 p.

Glaciers of South America–

GLACIERS OF CHILE AND ARGENTINA

By LOUIS LLIBOUTRY

INTRODUCTION
By LOUIS LLIBOUTRY

GLACIERS OF THE *DRY ANDES*
By LOUIS LLIBOUTRY

With a section on
ROCK GLACIERS
By ARTURO E. CORTE

GLACIERS OF THE *WET ANDES*
By LOUIS LLIBOUTRY

SATELLITE IMAGE ATLAS OF GLACIERS OF THE WORLD

Edited by RICHARD S. WILLIAMS, Jr., *and* JANE G. FERRIGNO

U.S. GEOLOGICAL SURVEY PROFESSIONAL PAPER 1386-I-6

Numerous glaciers are found along the more than 4,000-km length of the Andes Mountains and range in size from very small snow patches and glacierets in northern Chile to the 13,000-km^2 Southern Patagonian Ice Field in Chile and Argentina, the largest glacier outside Antarctica in the Southern Hemisphere. The ice fields and glaciers of Patagonia are akin to those of southern Alaska. The 2,200 km^2 of glaciers in the Central Andes *between Santiago and Mendoza are unique*

CONTENTS

GLACIERS OF SOUTH AMERICA–

GLACIERS OF CHILE AND ARGENTINA

By LOUIS LLIBOUTRY[1]

With a section on ROCK GLACIERS

By ARTURO E. CORTE

Introduction

Occurrence of Glaciers

The glaciers of Chile and Argentina appear as glacierets, mountain glaciers, valley glaciers, cirque glaciers, outlet glaciers, piedmont glaciers, ice caps, and ice fields along the more than 4,000-km length of the Andes Mountains in these countries. Here, the glaciers extend from the southern border of Perú at lat 17°30'S. to the southern tip of South America at lat 55°S. They range in size from very small glacierets or snow patches found on the isolated volcanoes of northern Chile (Lliboutry and others, 1958) to the 13,000-km^2 Southern Patagonian Ice Field at lat 49°S.

The climate and topography vary along the length of the Andes Mountains, creating different environments for the formation of glaciers. For this reason, the discussion of the glacierized areas is divided into the *Dry Andes*[2], covering the region from lat 17°30'S. to 35°S., and the *Wet Andes*, covering the region south of lat 35°S. The *Dry Andes* section has been further divided into the *Desert Andes* from lat 17°30'S. to 31°S. and the *Central Andes* from lat 31° to 35°S. (fig. 1). The *Wet Andes* section has been further divided into two parts north and south of lat 45°30'S. The northern part includes the Región de los Lagos (Lakes Region) but extends farther north and south. The southern part is now called the *Patagonian Andes*. (Historical Patagonia was all the land south of lat 37°S.)

In the *Desert Andes*, arid conditions limit the ice-and-snow formation to small patches on the highest peaks (Lliboutry and others, 1958). North of lat 28°S., these ice-and-snow patches are found on individual volcanoes, some of which are more than 6,000 m in elevation (González-Ferrán, 1995). South of lat 28°S., isolated volcanoes do not exist. Here, most of the small ice-and-snow areas are found on the main range, which is the border between Argentina and Chile. Farther south, in the *Central Andes* between lat 31° and 35°S., true glaciers flowing at the head of valleys exist because of higher mountains and greater precipitation. The total area of uncovered and debris-covered glaciers here is about 2,200 km^2.

The *Wet Andes* south of lat 35°S. have a much greater amount of precipitation. Between lat 35° and 45°30'S., west of the continuous range that

Manuscript approved for publication 18 March 1998.

[1] 3, Avenue de la Foy, 38700 Corenc, France.

[2] Geographic place-names in this section conform to the usage recommended by the U.S. Board on Geographic Names in the gazetteers of Argentina (1992a), Chile (1967, 1992c), Peru (1989), and Bolivia (1992b). Where a feature on the border of Argentina and Chile has a different name in each country, both names are given separated by a slash, the Argentine name listed first. Names not listed in the gazetteer for any of the countries are shown in italics, or in quotation marks if the place-name is already italicized in an illustration.

Figure 1.—*Chile and Argentina showing the occurrence of glaciers in the* Dry Andes (Desert Andes *and* Central Andes) *and in the* Wet Andes (Lakes Region *and* Patagonian Andes) *and location of towns and cities near the glacierized areas that have airports.*

forms the water divide and the border, more than 35 isolated volcanoes have elevations high enough to support glacier ice. However, owing to a decrease in the elevation of the main cordillera, no cirque glaciers are present in this range until about lat 41°S. South of lat 41°S., a few cirque glaciers appear and then become numerous. It is not until about lat 44°25'S. that they are large enough to be delineated on Landsat multispectral scanner (MSS) images. South of lat 45°30'S. in the *Patagonian Andes*, a very large number of mountain glaciers, outlet glaciers, and ice fields are located, including the 4,200-km^2 Northern Patagonian Ice Field, the 13,000-km^2 Southern Patagonian Ice Field, and the 2,300-km^2 ice field of Cordillera Darwin in the southwest corner of Tierra del Fuego.

Climatic Setting

The variation in the size and occurrence of glaciers in Chile and Argentina is a result of the interaction of topography and climate. As seen in figure 2, the lowering of the equilibrium line altitude (ELA) going southward is progressive, whereas the Andes Mountains are very much lower south of lat 35°S. Therefore, large glaciers are found in the *Central Andes* (lat 31° to 35°S.), but between lat 35° and 42°S., ice is found only on isolated volcanoes, which are the highest summits there. Moreover, in the *Central Andes*, because all humidity comes from the Pacific Ocean, the ELA at a given latitude rises by about 1,500 m from west to east (see fig. 6).

In the most frequent, "normal" meteorological situation, a belt of stationary high pressure extends across South America at about lat 35°S., which thereby prevents any intrusion of moisture-laden airmasses into the continent. One anticyclone (atmospheric high pressure system with winds blowing spirally outward; in the Southern Hemisphere, the winds travel in a

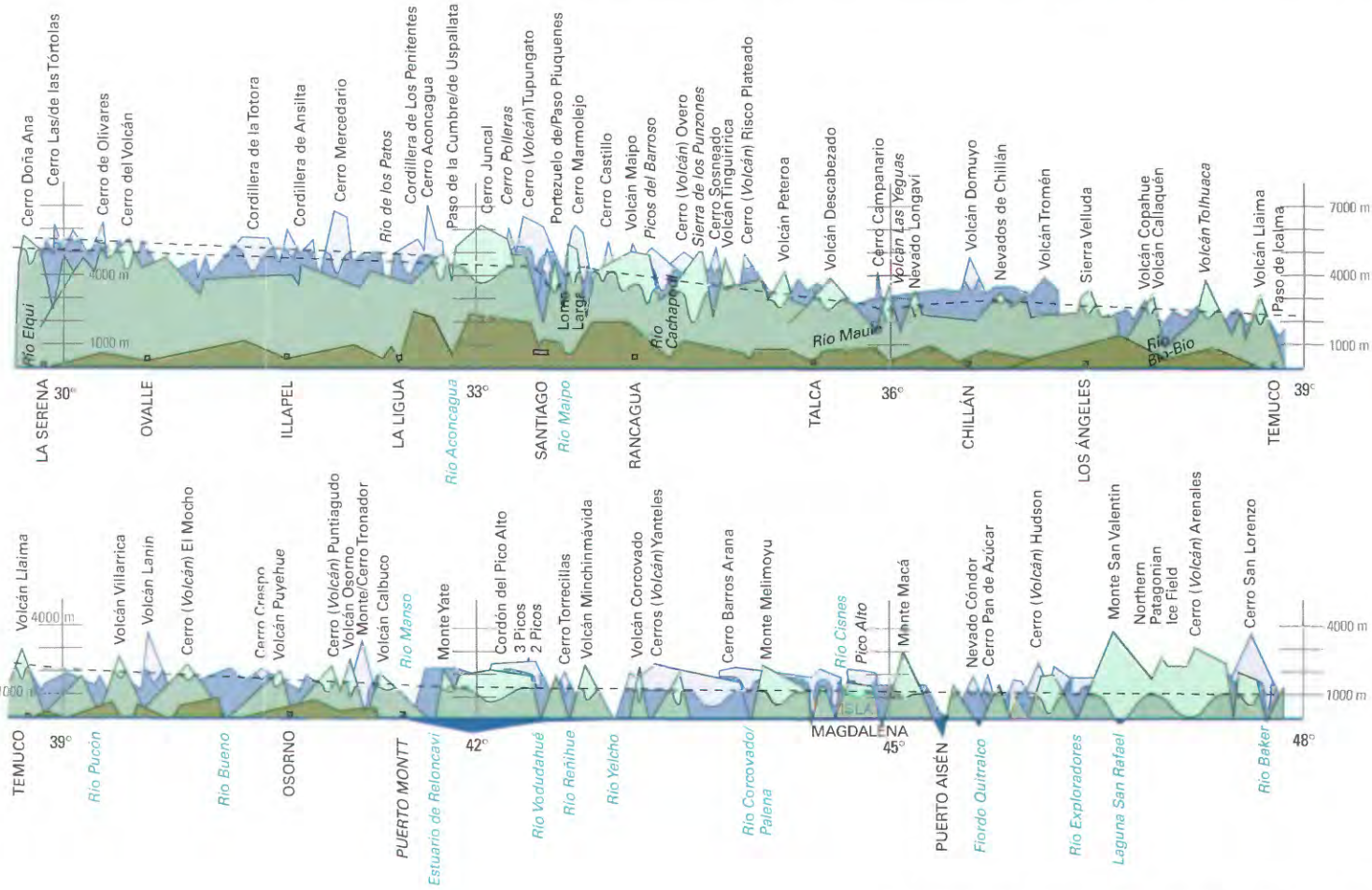

Figure 2.—*Southern Andes seen from the west. Green-tinted low area is the Coast Range (Cordillera de la Costa). The dashed line represents the glaciation level. Mountain summits above the glaciation level are shown in a lighter tint, although in the* Central Andes *(lat 31°S. to lat 35°S.) they are not totally ice covered. The lighter tinted areas have also been extended down to the elevation reached by the main glaciers (modified from Lliboutry, 1956).*

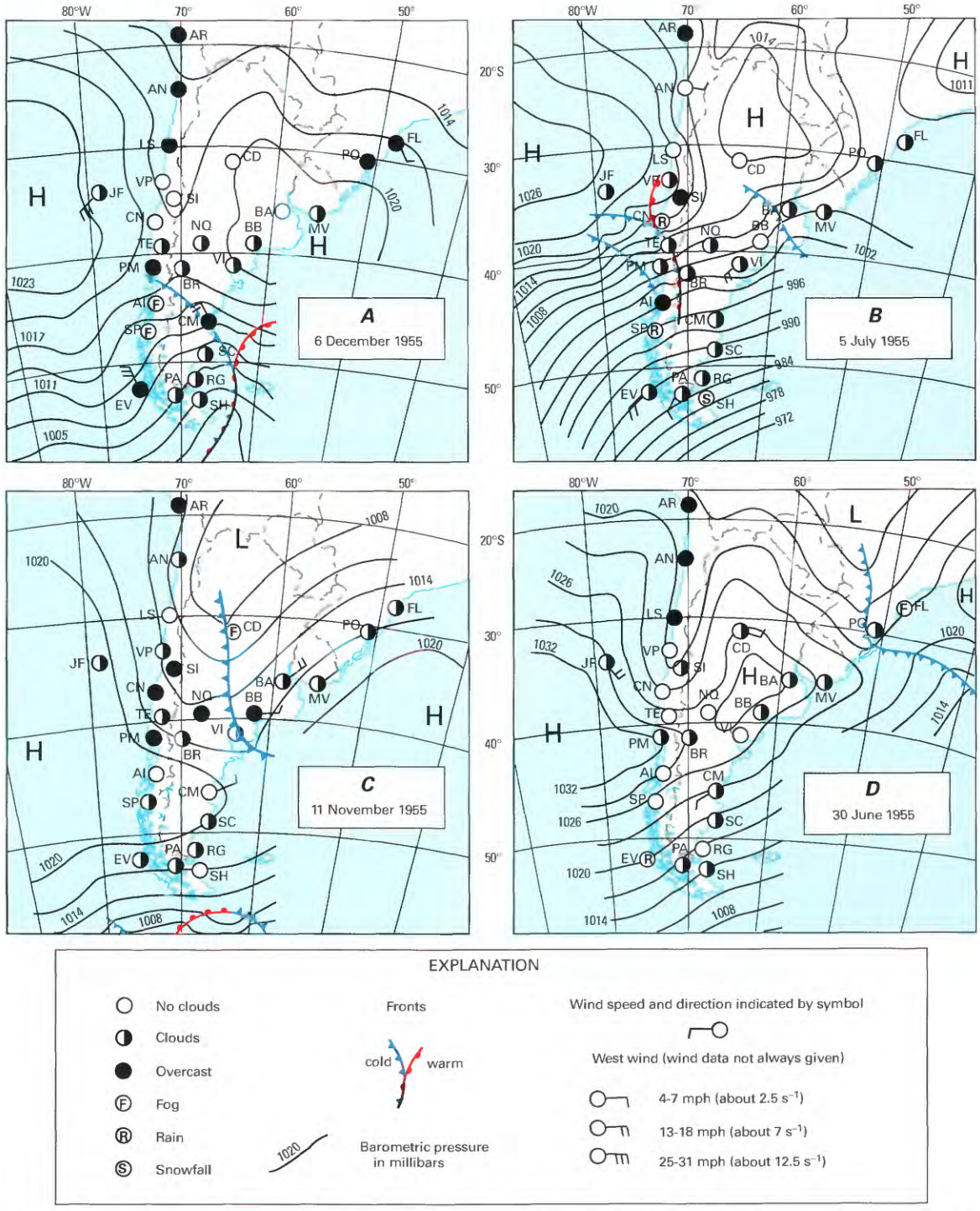

Figure 3.—*Selected synoptic meteorological charts of southern South America as published in "El Mercurio" (Santiago):* **A**, *The most frequent meteorological conditions: high-pressure systems (H) located at about lat 35°S. prevent moisture from reaching the central and northern parts of the Andes but allow moisture-laden winds over Patagonia in the south;* **B**, *High-pressure systems located farther north permit moisture-laden air from the southwest to reach the* Central Andes *(lat 31°S. to lat 35°S.);* **C**, *Sudestada (southeasterly wind regime) in Provincia del Neuquén, and an area of high pressure over Patagonia. Moisture coming from the northeast can reach as far as lat 25°S.; and* **D**, *Sudestada in northern Argentina. No precipitation is found in the* Central Andes. *Regions of low pressure are indicated with an L.*

Meteorological stations and their abbreviations shown on the synoptic charts:

AI, Puerto Aisén
AN, Antofagasta
AR, Arica
BA, Buenos Aires
BB, Bahía Blanca
BR, Bariloche
CD, Córdoba
CM, Comodoro Rivadavia
CN, Concepción
EV, Islas Evangelistas
FL, Florianopolis
JF, Juan Fernandez
LS, La Serena
MV, Montevideo
NQ, Neuquén
PA, Punta Arenas
PM, Puerto Montt
PO, Porto Alegre
RG, Río Gallegos
SC, Santa Cruz
SH, Springhill
SI, Santiago
SP, Isla San Pedro
TE, Temuco
VI, Viedma
VP, Valparaíso

counter-clockwise direction) is situated permanently on the west coast over the Pacific Ocean and another on the Atlantic coast. To the south, a steep north-south atmospheric-pressure gradient induces strong, moisture-laden westerly winds to flow over Patagonia (south of lat 45°30'S. in fig. 3*A*). Consequently, western Patagonia has heavy precipitation, whereas the northern part of Chile is a hyperarid desert.

During the year, the anticyclones fluctuate in latitudinal position. Normally from May to September, they are located at lower latitudes, which allows moist air masses from the southwest to reach the Andes Mountains and results in some very heavy snowfalls (fig. 3*B*). This influence can extend northward as far as lat 28°S. North of lat 24°S. on the very high *Puna*, local convection provides some storms with snowfall, however.

From October to April, as a rule, the anticyclones are found at higher latitudes. Moisture from the Amazon basin reaches Perú and the Cordillera Oriental of Bolivia. Some precipitation coming from the northeast can also reach the Altiplano (the very high, semiarid plateau) as far as lat 25°S. The Pacific anticyclone can even extend over Patagonia, which results in a south wind, fine weather, and a cloudless sky over the *Patagonian Andes*, a rare event (fig. 3*C*).

Other synoptic weather patterns are also possible. In particular, between the Pacific and Atlantic anticyclones, cool and humid Atlantic maritime airmasses can invade central Argentina, a situation called Sudestada (southeasterly wind regime). Figures 3*C* and 3*D* illustrate two extreme cases. In the first, rain in the lowlands and snow in the Andes are found in Provincia del Neuquén (between the Provincia de Mendoza and Lago Nahuel Huapí) (about lat 36° to 40°S.). In this case, the *Central Andes* only have light snowfall. In the second case, the Sudestada wind pattern extends over Uruguay as far as the Provincia de Tucumán, especially affecting the Nevados de Aconquija at about lat 27°S. Under these meteorological conditions, no precipitation results in the *Central Andes*.

The three possible sources of moisture to the *Dry Andes,* in decreasing order, are the southwest, southeast, and northeast. This explains why the driest Andes are found on the west border of the Altiplano between lat 20° and 28°S.

Application of Remote Sensing

As a rule, the Andes Mountains of Chile and Argentina have neither inhabitants nor roads. This fact, combined with the very high elevations of the *Dry Andes* and the very bad weather and often impenetrable rain forest of most of the *Wet Andes*, makes the study of their glaciers very difficult. Under such conditions, remotely sensed data provide a valuable tool to aid in the monitoring of glacierized areas. Remotely sensed data, and particularly Landsat data, can be used to determine the occurrence of glaciers in some areas, to delineate areal extent, where not obscured by debris cover, and to monitor snowline variation, glacier surges, and volcanic events that affect glacier areas. Figure 4 and table 1 show the optimum Landsat 1, 2, and 3 MSS and return beam vidicon (RBV) images that have been evaluated for glaciological applications and are available from the U.S. archive at the EROS Data Center, Sioux Falls, S. Dak. More recent Landsat data are also available from the EROS Data Center and from receiving stations in South America.

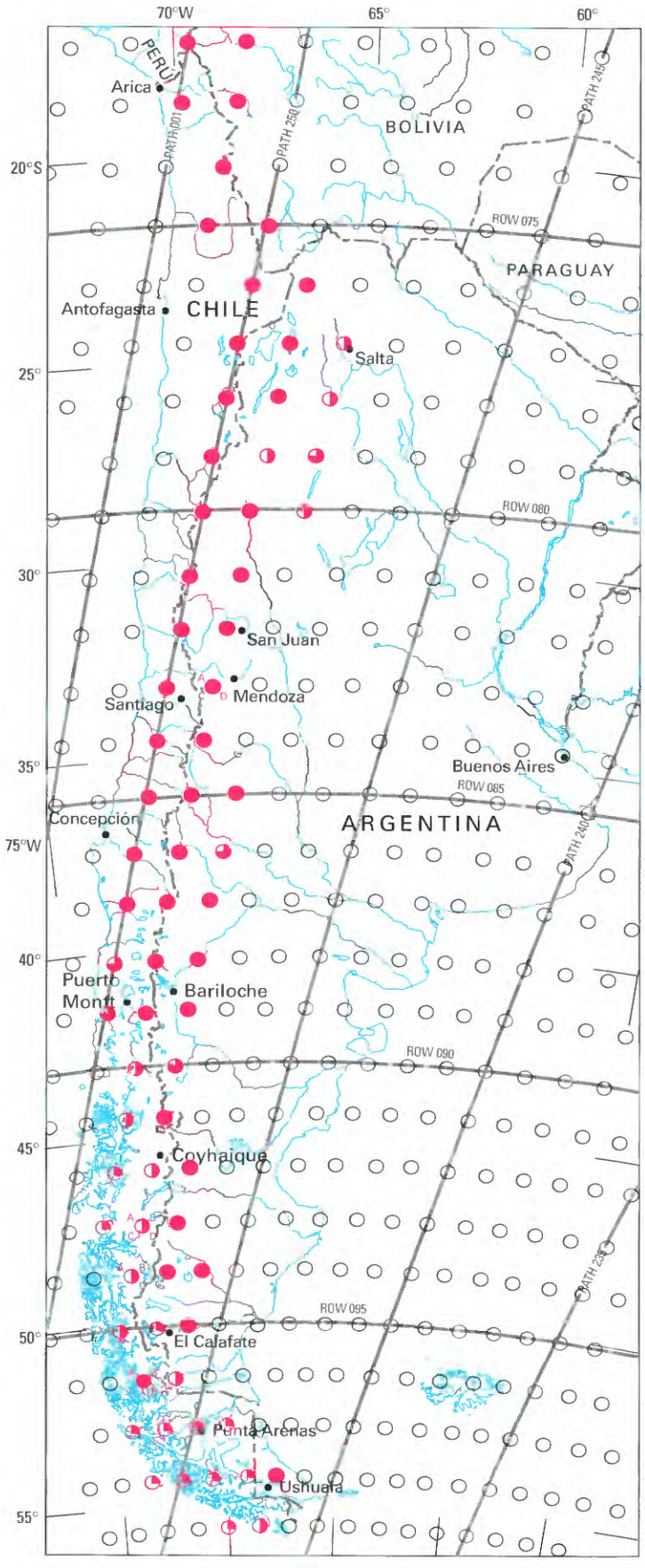

Figure 4.—*Optimum Landsat 1, 2, and 3 images of the glaciers of Chile and Argentina.*

0 400 KILOMETERS

EXPLANATION OF SYMBOLS

Evaluation of image usability for glaciologic, geologic, and cartographic applications. Symbols defined as follows:

- Excellent image (0 to ≤5 percent cloud cover)
- Good image (>5 to ≤10 percent cloud cover)
- Fair to poor image (>10 to <100 percent cloud cover)
- Unusable image (100 percent cloud cover)
- No image available
- Nominal scene center for a Landsat image outside the area of glaciers
- Usable Landsat 3 RBV scenes. A, B, C, and D refer to usable RBV subscenes

TABLE 1.—*Optimum Landsat 1, 2, and 3 images of the glaciers of Chile and Argentina*[1]

[See fig. 4 for explanation of symbols used in "code" column]

Path-Row	Nominal scene center (lat-long)	Landsat identification number	Date	Solar elevation angle (degrees)	Code	Cloud cover (percent)	Remarks
242–98	54°22'S. 67°54'W.	30380–13120	20 Mar 79	21	●	0	Beagle Channel; multiple scan lines missing
242–99	55°45'S. 68°42'W.	1397–13225	24 Aug 73	11	◑	90	
243–98	54°22'S. 69°21'W.	No usable data			◔		
243–99	55°45'S. 70°09'W.	No usable data			◔		
244–97	52°58'S. 70°02'W.	No usable data			◔		
244–98	54°22'S. 70°47'W.	No usable data			◔		
245–97	52°58'S. 71°28'W.	No usable data			◔		
245–98	54°22'S. 72°13'W.	No usable data			◔		
246–94	48°44'S. 70°52'W.	21441–13193	02 Jan 79	41	●	0	
246–95	50°09'S. 71°30'W.	21441–13200	02 Jan 79	41	●	0	Lagos Viedma and Argentino
246–96	51°34'S. 72°11'W.	30060–13331	04 May 78	10	◑	50	Thin cloud, snow cover
246–96	51°34'S. 72°11'W.	21441–13202	02 Jan 79	40	◑	50	
246–97	52°58'S. 72°54'W.	No usable data			◔		
246–98	54°22'S. 73°39'W.	No usable data			◔		
247–92	45°55'S. 71°06'W.	1474–13470	09 Nov 73	45	●	0	Snow cover
247–93	47°20'S. 71°41'W.	1474–13473	09 Nov 73	44	●	0	Snow cover
247–94	48°44'S. 72°18'W.	1474–13475	09 Nov 73	44	●	0	Snow cover
247–95	50°09'S. 72°56'W.	No usable data			◔		
247–96	51°34'S. 73°37'W.	30385–13400 A,B,C,D	25 Mar 79	22	A B C D	A=20 B=0 C=20 D=0	Landsat 3 RBV; Archived by USGS GSP[2]
247–97	52°58'S. 74°20'W.	No usable data			◔		
248–77	24°31'S. 65°40'W.	1223–13493	03 Mar 73	46	◑	50	
248–78	25°56'S. 66°03'W.	1223–13495	03 Mar 73	46	◑	60	
248–79	27°23'S. 66°27'W.	2417–13342	14 Mar 76	40	◕	10	

TABLE 1.—*Optimum Landsat 1, 2, and 3 images of the glaciers of Chile and Argentina*[1]—Continued

[See fig. 4 for explanation of symbols used in "code" column]

Path-Row	Nominal scene center (lat-long)	Landsat identification number	Date	Solar elevation angle (degrees)	Code	Cloud cover (percent)	Remarks
248–80	28°49'S. 66°51'W.	2039–13384	02 Mar 73	42	◑	20	
248–85	35°58'S. 68°58'W.	2363–13381	20 Jan 76	45	●	0	
248–86	37°24'S. 69°26'W.	2363–13383	20 Jan 76	45	◕	10	
248–87	38°49'S. 69°54'W.	2399–13381	25 Feb 76	37	●	0	
248–88	40°14'S. 70°24'W.	2399–13383	25 Feb 76	36	●	0	
248–89	41°40'S. 70°54'W.	2417–13383	14 Mar 76	31	●	0	
248–90	43°05'S. 71°25'W.	2417–13385	14 Mar 76	30	◕	10	
248–91	44°30'S. 71°58'W.	21515–13324	17 Mar 79	29	●	0	Montes Melimoyu and Mentolat, image used for fig. 24
248–92	45°55'S. 72°32'W.	2399–13401	25 Feb 76	33	◑	25	Montes Macá and Cay; image used for fig. 25
248–93	47°20'S. 73°07'W.	2399–13404	25 Feb 76	32	◑	30	Northern Patagonian Ice Field
248–93	47°20'S. 73°07'W.	30368–13444	08 Mar 79	30	◑	20	Northern Patagonian Ice Field; image used for fig. 42
248–93	47°20'S. 73°07'W.	30368–13444 A,B,C,D	08 Mar 79	30	A B C D	A=50 B=50 C=50 D=30	Landsat 3 RBV images; archived by USGS GSP
248–94	48°44'S. 73°44'W.	2399–13410	25 Feb 76	31	◑	35	Northern part of Southern Patagonian Ice Field; image used for fig. 33
248–94	48°44'S. 73°44'W.	30368–13450	08 Mar 79	29	◑	40	Image used for fig. 51
248–94	48°44'S. 73°44'W.	30368–13450 B,C,D	08 Mar 79	29	B C D	B=40 C=80 D=70	Landsat 3 RBV images. Subscene B used for fig. 50; subscene D used for fig. 49. Archived by USGS GSP
248–95	50°09'S. 74°22'W.	30368–13453	08 Mar 79	28	◑	60	Southern part of Southern Patagonian Ice Field
249–76	23°04'S. 66°44'W.	1008–13533	31 Jul 72	33	●	0	
249–77	24°31'S. 67°06'W.	1008–13540	31 Jul 72	32	●	0	
249–78	25°56'S. 67°29'W.	2418–13393	15 Mar 76	40	●	0	
249–79	27°23'S. 67°53'W.	2418–13400	15 Mar 76	39	◑	15	
249–80	28°49'S. 68°17'W.	2418–13402	15 Mar 76	39	◕	10	
249–80	28°49'S. 68°17'W.	2040–13443	03 Mar 75	42	●	0	Nevado de Famatina
249–81	30°15'S. 68°41'W.	2040–13445	03 Mar 75	41	●	0	
249–82	31°41'S. 69°06'W.	2040–13452	03 Mar 75	40	●	0	

TABLE 1.—*Optimum Landsat 1, 2, and 3 images of the glaciers of Chile and Argentina*[1]—Continued

[See fig. 4 for explanation of symbols used in "code" column]

Path-Row	Nominal scene center (lat-long)	Landsat identification number	Date	Solar elevation angle (degrees)	Code	Cloud cover (percent)	Remarks
249–83	33°07'S. 69°32'W.	2022–13455	13 Feb 75	43	●	0	
249–83	33°07'S. 69°32'W.	2418–13414	15 Mar 76	36	●	0	Cerro (*Volcán*) Tupungato, Cerros Chimbote and Aconcagua; image used for fig. 9
249–83	33°07'S. 69°32'W.	30675–13415 A,C,D	09 Jan 80	48	A ○ C D	A=20 C=15 D=50	Landsat 3 RBV images; Volcán Maipo and Cerro (*Volcán*) El Palomo. Archived by USGS GSP
249–84	34°32'S. 69°58'W.	2022–13461	13 Feb 75	42	●	0	
249–84	34°32'S. 69°58'W.	2418–13420	15 Mar 76	35	●	0	Volcán Maipo and Cerro (*Volcán*) El Palomo; image used for fig. 10
249–85	35°58'S. 70°24'W.	2418–13423	15 Mar 76	34	●	0	Volcán Domuyo
249–86	37°24'S. 70°52'W.	2382–13440	08 Feb 76	41	●	0	Volcanes Antuco, Copahue, and Callaquén, Sierra Velluda
249–87	38°49'S. 71°20'W.	2382–13442	08 Feb 76	41	●	0	Volcanes Llaima, Villarrica, and Quetrupillán, Nevados de Sollipulli
249–88	40°14'S. 71°50'W.	2436–13431	02 Apr 76	27	●	0	
249–89	41°40'S. 72°20'W.	2436–13433	02 Apr 76	26	●	0	Monte/Cerro Tronador; image used for fig. 21
249–90	43°05'S. 72°51'W.	21516–13380	18 Mar 79	28	◑	50	Volcán Minchinmávida
249–91	44°30'S. 73°24'W.	2130–13485	01 Jun 75	11	◑	15	Montes Melimoyu, Mentolat, Cay, and Macá; snow cover
249–92	45°55'S. 73°58'W.	No usable data			◔		
249–93	47°20'S. 74°33'W.	No usable data			◔		
250–75	21°38'S. 67°48'W.	1243–14001	23 Mar 73	45	●	5	
250–76	23°04'S. 68°10'W.	1243–14004	23 Mar 73	44	●	5	
250–77	24°31'S. 68°33'W.	1243–14010	23 Mar 73	43	●	0	
250–78	25°56'S. 68°55'W.	1243–14013	23 Mar 73	42	●	0	
250–78	25°56'S. 68°55'W.	2401–13455	27 Feb 76	43	●	0	
250–79	27°23'S. 69°19'W.	1243–14015	23 Mar 73	41	●	0	
250–80	28°49'S. 69°43'W.	1243–14022	23 Mar 73	40	●	0	
250–81	30°15'S. 70°07'W.	1243–14024	23 Mar 73	39	●	0	Cerro de Olivares
250–82	31°41'S. 70°33'W.	1243–14031	23 Mar 73	38	●	0	
250–83	33°07'S. 70°58'W.	2419–13472	16 Mar 76	36	●	0	

TABLE 1.—*Optimum Landsat 1, 2, and 3 images of the glaciers of Chile and Argentina*[1]—Continued

[See fig. 4 for explanation of symbols used in "code" column]

Path-Row	Nominal scene center (lat-long)	Landsat identification number	Date	Solar elevation angle (degrees)	Code	Cloud cover (percent)	Remarks
250–84	34°32'S. 71°24'W.	2365–13491	22 Jan 76	46	●	0	
250–85	35°58'S. 71°51'W.	2059–13521	22 Mar 75	34	●	0	Volcán Descabezado
250–86	37°24'S. 72°18'W.	2365–13500	22 Jan 76	45	●	0	Nevados de Chillán, Volcán Antuco, and Sierra Velluda
250–87	38°49'S. 72°46'W.	2383–13501	09 Feb 76	40	●	0	
250–88	40°14'S. 73°16'W.	2383–13503	09 Feb 76	40	◕	10	
250–89	41°40'S. 73°46'W.	2383–13510	09 Feb 76	39	◕	10	
251–72	17°19'S. 68°08'W.	1100–14041	31 Oct 72	58	●	0	
251–73	18°45'S. 68°30'W.	1010–14035	02 Aug 72	36	◕	10	
251–73	18°45'S. 68°30'W.	1100–14043	31 Oct 72	57	●	0	
251–74	20°11'S. 68°51'W.	1100–14050	31 Oct 72	56	●	0	
251–74	20°11'S. 68°51'W.	1244–14053	24 Mar 73	46	●	0	
251–75	21°38'S. 69°14'W.	2312–13514	30 Nov 75	51	●	0	
1–72	17°19'S. 69°34'W.	1065–14091	26 Sep 72	52	●	0	
1–73	18°45'S. 69°56'W.	1065–14093	26 Sep 72	51	●	0	
			Landsat 5 images				
1–73	18°47'S. 68°48'W.	51281–14022	03 Sep 87	44	●	0	
231–94	48°52'S. 72°45'W.	50684–13530	14 Jan 86	43	◑	20	Northern part of Southern Patagonian Ice Field; image used for fig. 32
231–95	50°17'S. 73°20'W.	50684–13533	14 Jan 86	43	◑	20	Middle part of Southern Patagonian Ice Field; image used for fig. 32
231–96	51°42'S. 73°57'W.	50684–13535	14 Jan 86	42	◕	10	Southern tip of Southern Patagonian Ice Field; image used for fig. 32
232–92	46°01'S. 73°18'W.	51075–13514	09 Feb 87	39	◑	35	Northern part of Northern Patagonian Ice Field; image used for fig. 26
232–93	47°26'S. 73°50'W.	51075–13520	09 Feb 87	38	◕	10	Southern part of Northern Patagonian Ice Field; image used for fig. 26

[1] Six supplemental Landsat 5 images are included, three of which provide excellent coverage of the Southern Patagonian Ice Field (fig. 32).

[2] USGS GSP is the U.S. Geological Survey Glacier Studies Project.

Glaciers of the *Dry Andes*

By Louis Lliboutry[3]

Abstract

From a glaciological perspective, the *Dry Andes* can be divided into the *Desert Andes* north of latitude 31° South and the *Central Andes* between latitude 31° and 35° South. Because of lower precipitation and elevations, only permanent snow patches and glacierets are present in the *Desert Andes.* Large glaciers are situated in the *Central Andes* because of higher mountains and greater amounts of precipitation. In the *Desert Andes,* the glaciation level is variable and depends on the amount and source direction of the precipitation. At latitude 27° South, it lowers eastward from 6,200 meters to 5,500 meters or less. At latitude 29° South, it rises eastward from below 5,600 meters to about 6,000 meters. Glaciers of the *Central Andes* cover about 2,200 square kilometers and can be as much as 14 kilometers in length. Their lower ends are partly or completely covered with morainic debris and are indistinguishable from rock glaciers. Some surging glaciers are present. The Río del Plomo has been dammed at least three times historically by a surge of Glaciar Grande del Nevado. An ephemeral lake was created that eventually drained rapidly and caused a destructive flood downstream of the failed ice dam. During the "Ice Age," a significant expansion of the glaciers in the *Central Andes* took place. The lowering of the Equilibrium Line Altitude (ELA) should have been about 1,000 meters from today's ELA. The lowering of the mean annual temperature should have been small. The main factor was an increase of the annual precipitation, caused by a 200- to 250-kilometer shift northward of the wetter climate to the south.

Geographic Setting

The very high, semiarid plateau, known in southern Perú and western Bolivia as the Altiplano, extends southward into Chile and Argentina to lat 28°S. The plateau has an elevation of about 4,000 m above sea level and becomes narrower as it extends to the south. In Chile and Argentina, it is called *la Puna* (puna also means mountain sickness). At its west border, near the Chilean desert, are a series of Quaternary volcanoes, often reaching elevations of more than 6,000 m, an extension of the Cordillera Occidental in Bolivia. Mountain ranges, running in a north-south direction, exist on the east side of the *Puna.* The Cordillera de los Andes (the Andes Mountains) is a set of more or less parallel mountain ranges, not a single one. In Spain, a range is called sierra; in South America, it is called cordón or cordillera.

South of lat 28°S., isolated volcanoes do not exist. The main range is both the drainage divide between the rivers that flow into the Pacific and Atlantic Oceans and the international border between Chile and Argentina. The Tratado de Límites (Boundary Treaty) officially delimited the border between both countries as "the water divide," which, they thought, was a line connecting the highest mountain peaks. The existence of mountain ranges between drainage basins was, at the time, a very popular theory among military geographers to the extent that, in France, an imaginary mountain range was drawn between the Seine and the Loire (rivers), a region that is, in fact, completely flat. The nonsensical theory of such "natural frontiers" led to many border controversies in Patagonia up to recent times, but at the same time, it has been the motivation behind many useful expeditions to explore the region.

Mapping and Aerial Photography

Glaciologists and geographers should not trust any elevation that is indicated on maps of the Andes Mountains. The sources of their elevation data are never indicated, and these sources may differ from one another by several hundred meters. The critical work of a historian is often necessary to judge accuracy.

[3] 3, Avenue de la Foy, 38700 Corenc, France.

Considerable ground geodesy was done at the beginning of the 20th century by an Argentine-Chilean Comisión de Límites, which was charged to delimit the international border. The first edition in 1915 of the Carta Nacional de Chile (CNC), a set of maps at a scale of 1:500,000, used these data. Its last edition, with little modification, was published in 1945. Up to recent times, it was the best source for geographic place-names and for elevations north of lat 41°30'S. on the Chilean side and near the border. Near Santiago, Chile, the CNC was improved (more details and place-names, without modifying the elevations) in 1929 by W. Klatt and F. Fickenscher (KF). Their map at a scale of 1:250,000 was used by Chilean *andinistas* (mountaineers) up to 1956. On the Argentine side, very accurate maps at a scale of 1:25,000 of the Aconcagua group (lat 32°30'–32°50'S.) and of the glaciers in the Río del Plomo drainage basin (lat 32°55'–33°20'S.) were made by terrestrial photogrammetry (Helbling, 1919). Elsewhere, cartography of the Argentine Andes remained very poor up to recent times.

From April 1944 to April 1945, at the request of the Chilean Government, a Trimetrogon aerial survey of all of Chile was done by the U.S. Army Air Force and was compiled in Panama by the Army Map Service. Very few place-names were indicated, and glaciers of the *Central Andes* were not represented. (This region had been surveyed in winter, and the plotter's cartographic technicians did not recognize or discriminate glaciers in snow-covered areas.) The Instituto Geográfico Militar de Chile (IGMC) sold this preliminary chart (Carta Prelimínar, CP), at a scale of 1:250,000, in the 1950's without making changes other than metric conversions. At the same time, I drew a more detailed map at a scale of 1:150,000, extending from lat 32°30' to 34°30'S., long 69°40' to 70°30'W. (Lliboutry, 1956). For the first time, glaciers of this area were represented. The contour lines came from the CP (with some corrections near the border); the elevations came from CNC, KF, and Argentine maps.

Vertical aerial photographs that are suitable for accurate cartography were taken in 1955 and 1956 in Chile and in 1963, 1974, and 1980–81 in Argentina. They have been used, together with modern geodetic-control networks, for compilation of maps at scales of 1:50,000 in Chile (denoted IGMC) and at 1:100,000 in Argentina. Today all of these photographs and maps are on sale without restrictions in both countries. Nevertheless, many geographers still use the U.S. Operational Navigation Charts (ONC) at a scale of 1:1,000,000 (the same scale as the standard Landsat images), which were printed before the modern accurate maps became available (fig. 5). For Chile, the ONC is a reduction of the CP. For Argentina, the ONC reproduces the navigation chart Carta Aeronáutica Mundial (OAIC) made by the Instituto Geográfico Militar de Argentina (IGMA). In both cases, elevations were drawn from all the maps available at that time. Where the elevation of a given summit was not the same in the different maps, the highest elevation was kept, a logical choice for an aeronautical navigation chart. Many elevations, especially in the Argentine Andes, came from climbers who had reached a summit and merely read their pocket altimeters. They were calibrated in the early morning before the ascent, and the summit was reached in the afternoon, when atmospheric pressures are much lower. Therefore, their reported elevations are too high. For instance, Volcán San José (lat 33°45'S.) (5,830 m CNC, 5,856 m IGMC) is credited with 6,100 m on the ONC, and Cerro (*Volcán*) Tupungato (6,550 m CNC) is credited with 6,800 m on the ONC. The elevation of Cerro/Nevado Ojos del Salado (lat 27°07'S.) is 6,880 m on the CNC, 6,863 m according to a Polish triangulation in 1937, 6,937 m according to an Argentine one, 6,885 ±3 m according to a U.S. Commission led by Adams Carter in 1956, and 6,900 ±5 m according to Spedizione Condor (1989), whereas it is credited with 7,084 m on the ONC. This last elevation, which appears to make this summit shared by Chile and Argentina higher than the summit of Argentine Aconcagua, was obtained with a pocket altimeter by the official Chilean expedition of Captain Gajardo in 1956.

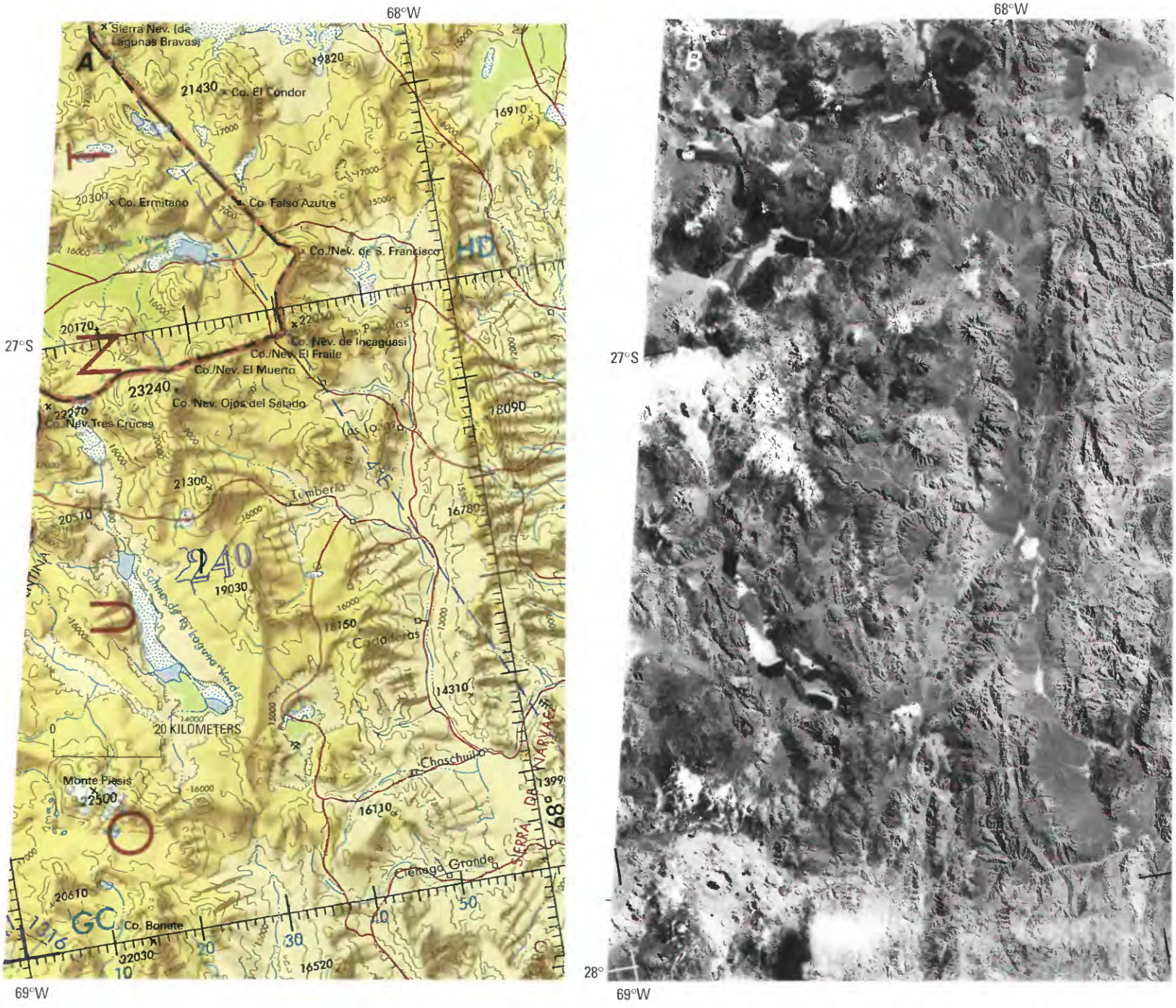

Figure 5.—*Comparison between an older U.S. Operational Navigation Chart (ONC) and a Landsat 2 image.* **A**, *Reproduction of part of 1:1,000,000-scale ONC Q–27, Edition 3, compiled in 1973, published in April 1974.* **B**, *The same area seen on Landsat 2 MSS image 2418–13400, band 7 (15 March 1976; Path 249, Row 79) from the EROS Data Center, Sioux Falls, S. Dak. Although valuable for basic reference, note that the ONC contains many geographic errors. For example, (1) the elevations are incorrect by about 180 m; (2) the boundary between Chile and Argentina is incorrect (The international border lies on the water divide between the two closed drainage basins of Laguna Verde (Chile) and Salina de la Laguna Verde (Argentina)); (3) a white tongue of sand just south of Cerro Solo (between Cerro/Nevado Tres Cruces and Cerro/Nevado Ojos del Salado) has been mismapped as a salar (blue dots); and (4) a caldera about 5 km in diameter northwest of Cerro Bonete is not shown.*

The elevation of Aconcagua has been often determined because it is the highest summit of the Americas and of the Southern Hemisphere. The first results were:

6,970 m (Güssfeldt in 1887)
6,960 m (Comisión de Límites in 1897)
7,035 m (Fitz-Gerald Expedition of 1897, which reached the summit)
6,960 and 6,946 m (two distinct triangulations by Schrader in 1904)
6,954 m (IGMA, unpublished; verbal commun. in 1951)

In spite of this last result, an elevation of 7,021 m was chosen by the Director of the IGMA for the maps published in the 1950's. In 1956, a very precise determination was made by the University of Buenos Aires, Argentina, which used 2,100 km of geodetic leveling from the Atlantic coast and direct triangulation for only the last 18 km (Baglietto, 1957). It yielded 6,959.75 ±1.18 m, exactly the old value of Comisión de Límites, which made its leveling from the Pacific coast, a distance of only 120 km. Therefore, on the OAIC and ONC, a correct value, 6,959 m, has been reestablished. An elevation determined by satellite geodesy, 6,962 ±1 m (Spedizione Condor, 1989) is less trustworthy because the geoid model OSU 89, which is used in the Global Positioning System (GPS), may well be inaccurate by 2 m in this region. For the same reason, the elevation of Cerro/Nevado Ojos del Salado should be about 6,885 m rather than about 6,900 m.

The following information on geographic place-names will assist in interpreting place-names found on Andean maps. In Spanish, the double ell (ll) is pronounced as the English y. In Chile, the popular pronunciation of hua/hue is gua/gue. As a result, Oyahue and Ollague are identical (both are given in table 6). Monte in Spanish denotes a hilly and forested terrain rather than a mountain. The Spanish word pico (beak) has a second meaning, peak; in Chile (but not in Argentina), it has a sexual meaning and is almost taboo. Therefore, Chilean mountains are called cerros (in Spain, a cerro is only a hill). If it holds permanent snow or glaciers, it is called nevado, a word usually abbreviated to nvdo. on maps. The abbreviation of nvdo. on maps explains the incorrect name of nudo (knot) given to some nevados by foreign geographers.

Precipitation Variability and Glaciation Level

The high elevations in the *Dry Andes* cause all precipitation to fall as snow. Cold powder snow is blown from the mountain summits. Glacierets in the *Desert Andes* may be found only on the leeward side of summits, in more or less well-pronounced cirques (glaciers eroded some of the cirques during the "Ice Age"). In the *Desert Andes*, precipitation is accompanied during local storms by a great deal of lightning. By comparison, lightning is almost unknown in the Chilean *Central Valley* and in Patagonia. The transient snowline may, therefore, differ from one mountain to another. Large glaciers of the *Central Andes* are found at the heads of high valleys. Glaciers are most commonly oriented to the southeast and their elevation increases from west to east (fig. 6). Thus, the concept of a snowline as a function of elevation, or the lower limit of glacierization, cannot be applied in the *Dry Andes*. Only a *glaciation level* may be defined (elevation of the lowest summits that have permanent snow patches), and even this concept must be handled with care, given the greater importance of local topography (fig. 2). For instance, the young Volcán Maipo (5,290 m) (lat 34°10'S.) has only a few permanent snow patches in gullies, although the glaciation level is about 4,500 m in this area.

As in all semiarid and arid regions, the range of annual precipitation is very large. For example, in Santiago (lat 33°30'S.) between 1846 and 1948, the minimum precipitation was 66 mm in 1924, and the maximum was 820 mm in 1901. The distribution of annual precipitation is distinctly bimodal.

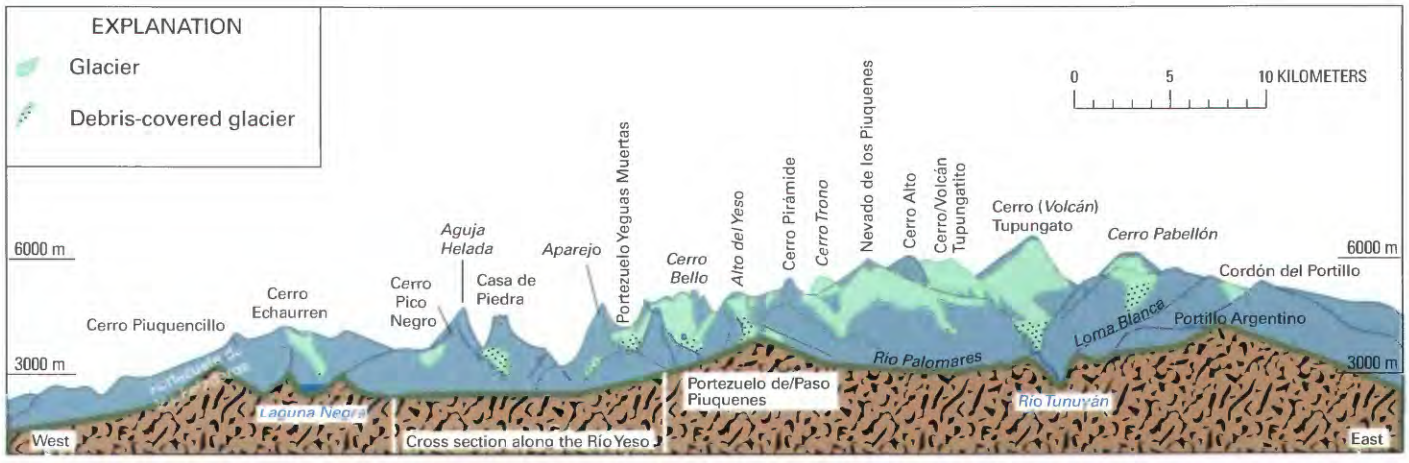

***Figure 6.**—West-east cross section through the* Central Andes *at Portezuelo de/Paso Piuquenes (lat 33°38'S.), the lowest pass east of Santiago, showing mountains and glaciers just to the north. The most common orientation of glaciers is to the southeast; their elevation rises to the east. The westernmost glacier is Glaciar Echaurren, which is monitored by Dirección General de Aguas (Santiago) (modified from Lliboutry, 1956).*

Instead of saying that the mean annual precipitation in Santiago is 370 mm, it is better to say that, 4 years out of 5, it fluctuates around 300 mm, and 1 year out of 5, around 660 mm. (These years of high precipitation will be called thereafter as "wet years.") At the town of Los Andes (about lat 33°S.), 70 km north of Santiago, the annual precipitation is about 300 mm. In Rancagua (about lat 34°S.), 80 km to the south, it is always about 660 mm a^{-1}. Clearly, Santiago is on the boundary between two climatic subregions.

Temperatures and Ice Formation

Air temperatures at high elevations have been published only for Paso de la Cumbre/de Uspallata (3,837 m) (lat 32°50'S.). In table 2, unpublished data from the Observatorio del Infiernillo (4,320 m) (lat 33°10'S.) are presented (Professor Gabriel Alvial, written commun., 1966). An interesting fact is that air temperature depends mainly on weather conditions. The range of mean daily temperatures within a given month is slightly larger than the range of monthly temperatures for the entire year (11°C). However, both are generally considerably larger than the daily range. The preceding refers only to air temperatures. Because of elevation and low humidity, diurnal oscillations of temperatures at the ground surface may be quite large.

Mean air temperatures and the vertical gradient given in table 3 show that at 4,400 m, which is the elevation of the ELA on the glaciers of this area, the mean air temperature during the dry season should be about –1.8°C, and for the entire year about –5.1°C. Thus, the glaciers are cold and all the more so throughout the *Dry Andes*, where glaciers are found at higher elevations.

Since 1968, the Dirección General de Aguas (Santiago, Chile) has maintained a meteorological station and has carried out mass-balance measurements of Glaciar Echaurren Norte (lat 33°33'S., long 70°08'W., 3,650 to 3,880 m above sea level (asl), drainage basin of Río Maipo (Peña, Vidal, and Escobar, 1984)) (see location in fig. 6 (Cerro Echaurren)). Summer is cloudless most of the time. Ice melt is about 2.4 cm per day in January and about 1.7 cm in May (water equivalent). During the night, the surface temperature of the glacier drops to –5.0°C to –7.0°C, and the cold wave penetrates to 40 cm. Consequently, a large amount of meltwater refreezes. In late spring, until all the firn reaches melting point, ice lenses form. Later, superimposed ice is accreted to cold glacier ice. Owing to this melting-refreezing process, any layer of newly fallen summer snow has a density of 0.4–0.6 after 3 weeks, independent of its thickness, and must be called firn. In January, the snow from the previous winter has a density of 0.63.

Because the nourishment of glaciers is by superimposed ice, the usual concept that the highest position of the transient snowline is the equilibrium line is wrong in the *Dry Andes*. This highest position is well above the

TABLE 2.—*Summary of air temperatures (°C) recorded every 2 hours at the Observatorio del Infiernillo, 1962–65*

[Lat 33°10'S., long 70°17'W., 4,320 m; —, no data. Source: Professor Gabriel Alvial (written commun., 1966)]

	Year	Monthly	Cold and snowy season						Cool and dry season					
			May	Jun	Jul	Aug	Sep	Oct	Nov	Dec	Jan	Feb	Mar	Apr
D	1962	Maximum	1.2	–0.9	1.1	–3.9	–0.8	–	3.7	5.3	–	–	2.3	4.0
A	to	Mean	–7.03	–7.53	–9.79	–10.81	–9.00	–	–2.10	.26	–	–	–1.57	–.46
I	1963	Minimum	–13.9	–15.2	–16.3	–17.8	–17.3	–	–6.4	–8.7	–	–	–7.0	–6.5
L														
Y	1963	Maximum	2.6	–6.7	–	–2.5	1.8	0.7	1.3	3.1	8.2	3.6	5.0	–.5
	to	Mean	–2.71	11.50	–	–9.67	–5.56	5.87	–3.84	–2.78	1.30	1.29	.05	–3.81
M	1964	Minimum	–7.9	–19.6	–	–17.4	15.1	–12.7	–9.5	–9.1	–4.7	–3.9	–3.9	11.4
E														
A	1964	Maximum	–1.5	1.9	–	–	–	–	–	–	4.1	4.4	6.0	2.1
N	to	Mean	–8.65	7.16	–	–	–	–	–	–	.19	–.18	1.40	5.79
S	1965	Minimum	–20.1	12.4	–	–	–	–	–	–	4.9	–5.2	–4.6	–10.4
	All 3 Years	Maximum	2.6	1.9	1.1	–2.5	1.8	.7	3.7	5.3	8.2	4.4	6.0	4.0
		Mean	–6.13	8.73	–9.79	–10.24	7.28	–5.87	2.97	–1.26	.74	.56	–.04	3.35
		Minimum	–20.1	–19.6	–16.3	–17.8	–17.3	–12.7	–9.5	–9.1	–4.9	5.2	–7.0	–11.4
	Absolute Bi-hourly	Maximum	6.0	4.2	4.6	1.5	7.0	5.9	8.2	9.8	12.1	9.1	8.5	7.8
		Minimum	–22.2	–22.7	–17.8	–19.4	–19.0	–14.4	–13.2	15.0	8.0	–10.1	11.4	-14.7

TABLE 3.—*Mean air temperatures at the Observatorio del Infiernillo (4,320 m) and at Paso de la Cumbre/de Uspallata (3,827 m)*

[Lat 32°50'S., long 70°05'W.]

	Mean temperature		
	Snowy season	Dry season	Entire year
Infiernillo (4,320 m)	–8.01°C	–1.05°C	–4.53°C
La Cumbre/de Uspallata (3,827 m)	–5.23°C	3.33°C	–.95°C
Vertical gradient (adiabatic lapse rate per 100 m)	.56°C	.89°C	.73°C

ELA. In fact, because the annual variability of precipitation is quite large, at the end of the melt season in normal years, only patches of firn (where local factors have provided an abnormally thick winter snow) are found on the glaciers. In wet years, the whole glacier may be an accumulation area.

Although the monitoring of the ELA is recommended by the Permanent Service for the Fluctuation of Glaciers (a permanent service, now merged with the World Glacier Monitoring Service in Zürich, Switzerland, and sponsored by the International Council of Scientific Unions), this monitoring is impossible in the *Dry Andes* and would be a useless exercise. Only cores and snow-pit studies allow monitoring of mass balance in successive years (and with a poor accuracy because of penitents). Past mass balance in an actual accumulation area cannot be determined because of large gaps in the stratigraphy (Cabrera, 1984; Escobar and Vidal, 1992; Escobar and others, 1995).

Penitents and Snow Hydrology

Penitents (the name derives from a resemblance to religious brothers wearing cowls and walking during Holy Week) are irregular blades of firn or ice, oriented east-west and pointing toward the Sun; thus, they tilt toward the north in the Southern Hemisphere. They are created as the result of differential snow-ice evaporation-sublimation rates when the air and dew-point temperatures are below 0°C, and solar radiation is intense over a period of many weeks (Lliboutry, 1954b, 1964). The temperature of the blades of the penitents remains below the melting point, whereas in the depressions between the blades, trapped solar radiation and humid air combine to melt the firn or underlying glacier ice.

The formation of penitents is the rule in the *Dry Andes*, except in the wet years of central Chile. We may even define the southern limit of the *Dry Andes* by the disappearance of penitents. (In this case, on the Argentine side, the *Dry Andes* should extend to Volcán Domingo at lat 37°S.)

In the Andes Mountains near Santiago in normal years, small penitents about 10 cm high (micropenitents) can be observed as soon as late winter (Lliboutry, 1961). At 3,500 m, they reach about 50 cm tall in spring and 1 m in January (summer). The north-south dimension always remains 2 to 3.5 times smaller than the height of the blades as the blades melt. But at moderate elevations with the rise of the mean air temperature, the blades melt and penitents become mere "sun spikes." It is only at elevations higher than 4,500 m that penitents keep their shape indefinitely.

When the furrows of penitents reach bare soil, the penitents may be blown down; when the furrows reach glacier ice, the carving by local melting goes on into this ice (figs. 7, 8). Penitents on glaciers are, in general, 2–3 m high. Therefore, mountaineers (in Latin America, *andinistas*) avoid crossing any glacier, unless traveling in the east-west direction of the furrows. Nevertheless, the tallest penitents ever observed (5–8 m high) were not found on a glacier but on a snowdrift that had become firn. It was at 6,000 m on the north slope of Cerro/Nevado Ojos del Salado (lat 27°S.) in November 1949 (Belastín, verbal commun., 1952).

Heat-balance measurements in a field of penitents may be done at two scales: (1) "microscopic" balances in the furrow on the south wall of a blade (which is in the shadow in summer because of the decreasing elevation of the Sun at midday) and on the north, sunny wall; and (2) "macroscopic" balances, which consider a heat-transfer layer several meters thick. For the latter, albedo measurements have been published by Peña, Vidal, and

Figure 7.—*Snow penitents (bottom) and ice penitents (left) on Glaciar Olivares Beta at 4,700 m. The highest mountain summit in the background is Nevado del/el Plomo (6,050 m) seen from the southwest. Man dressed in black in the foreground gives the scale. See figure 9 (number 11) for general location. Photograph by Louis Lliboutry taken on 28 January 1953.*

Figure 8.—*Ice penitents on the lower part of Glaciar Marmolejo. Cerro Marmolejo, source of the glacier, is near the south edge of figure 9. It is not possible to monitor fluctuations of the glacier terminus on an annual basis. Photograph by Louis Lliboutry taken on 13 January 1953.*

Salazar (1984). Whereas the albedo of fresh summer snow is 0.75–0.82 the first day and 0.70–0.74 after 3 days, and the albedo of firn from the previous winter is 0.45–0.55, the albedo of a field of penitents carved in this firn is only 0.30–0.40.

The water that flows out from a field of penitents, even with negative air temperatures, cannot be predicted by the mathematical models in common use in snow hydrology. The large drainage basin discharges given in table 4 cannot be attributed to dew or melting of rime ice. The probable smallness of the deficit in outflow of cordilleran drainage basins (in the *Dry Andes*) comes from the lack of plant and tree cover and associated transpiration.

Desert Andes (North of Lat 31°S.)

Mercer (1967) compiled all the published observations about snow patches and glacierets in the *Desert Andes*. In general, observers were unable to say whether a snow patch was permanent or not. A much better compilation could be made by the comparison of satellite images on successive years.

North of about lat 25°30'S., September is the month that has the least snow cover on the crests and summits of the mountains. In March, the snow cover differs widely from year to year. From an examination of Landsat images of the area, the following months were determined to have had minimum snow cover: September 1972, October 1972, March 1973, and March 1975; February 1976 had the most snow. The most useful Landsat 1, 2, and 3 images of the *Dry Andes* region for glaciological purposes are listed in table 5.

South of lat 25°30'S., the situation is different because moisture comes from the southeast during Sudestada, not from the northeast. In this region, the March Landsat images show the least snow cover. The snow cover also varies from year to year; much more snow was present in March 1975 than in March 1976. Landsat images of the region do not have sufficient resolution to determine if small white areas on mountain summits are firn or glaciers. However, the important thing is that, whether snow or ice, it provides the only source of ground water in these hyperarid regions.

TABLE 4.—*Area of drainage basin and discharge of mountain rivers in the Chilean Andes*

Drainage basin and river (measurement point)	Area of drainage basin (km^2)		Discharge[1] ($m^3 s^{-1}$)				Total annual discharge[1] ($10^6 m^3 a^{-1}$)	Specific discharge[1] (mm)
	Total[1]	Glacierized area[2]	Maximum		Minimum			
Río Aconcagua drainage basin:		151.5=10.4 %						
Río Colorado Provincia de Aconcagua (confluence)	830		31.45	(Dec)	4.3	(Jun)	399	480
Río Juncal (confluence)	247.2		14.86	(Jan)	1.9	(Aug)	206	840
Río Blanco (*Saladillo*)	384.6		27.62	(Jan)	1.5	(Jul)	308	800
Río Maipo drainage basin:		422.1=11.5 %						
Río Colorado Provincia de Santiago (confluence)	1,020		82	(Jan)	11	(Jul)	1,730	1,590
Río Yeso (confluence)	573		25	(Dec/Jan)	4.5	(May)	379	660
Río El Volcán (Los Queltehues)	546		37	(Jan)	6	(Aug)	505	920
Río Maipo superior	1,540		–		–		950	620
Río Cachapoal:		221.9=9.6 %						
(Coya)	2,320		171.5	(Jan)	41.9	(Jul)	2,610	1,120
Río Tinguiririca:		106.4=7.0 %						
(*Los Briones*)	1,525		114.1	(Jan)	24.8	(Apr)	1,730	1,130

[1] Data from Empresa Nacional de Electricidad, Sociedad Anónima (ENDESA) [National Electric Power Enterprise, Incorporated, Chile].

[2] Data from Valdivia (1984).

TABLE 5.— *Most useful Landsat 1, 2, and 3 images of the glaciers of the* Dry Andes

[Table 1 lists all the optimum Landsat 1, 2, and 3 images of the glaciers of Chile and Argentina]

Path-Row	Nominal scene center (lat-long)	Landsat identification number	Date
248–77	24°31'S., 65°40'W.	1223–13493	03 Mar 73
248–79	27°23'S., 66°27'W.	2417–13342	14 Mar 76
249–77	24°31'S., 67°06'W.	1008–13540	31 Jul 72
249–78	25°56'S., 67°29'W.	2418–13393	15 Mar 76
249–79	27°23'S., 67°53'W.	2418–13400	15 Mar 76
249–80	28°49'S., 68°17'W.	2418–13402	15 Mar 76
249–82	31°41'S., 69°06'W.	2040–13452	03 Mar 57
249–83	33°07'S., 69°32'W.	2022–13455	13 Feb 75
249–83	33°07'S., 69°32'W.	30675–13415 A,C,D	09 Jan 80
249–83	33°07'S., 69°32'W.	2418–13414	15 Mar 76
249–84	34°32'S., 69°58'W.	2022–13461	13 Feb 75
249–84	34°32'S., 69°58'W.	2418–13420	15 Mar 76
250–75	21°38'S., 67°48'W.	1243–14001	23 Mar 73
250–76	23°04'S., 68°10'W.	1243–14004	23 Mar 73
250–77	24°31'S., 68°33'W.	1243–14010	23 Mar 73
250–78	25°56'S., 68°55'W.	2401–13455	27 Feb 76
250–80	28°49'S., 69°43'W.	1243–14022	23 Mar 73
250–81	30°15'S., 70°07'W.	1243–14024	23 Mar 73
250–82	31°41'S., 70°33'W.	1243–14031	23 Mar 73
250–83	33°07'S., 70°58'W.	2419–13472	16 Mar 76
251–73	18°45'S., 68°30'W.	1010–14035	02 Aug 72
251–74	20°11'S., 68°51'W.	1244–14053	24 Mar 73
1–72	17°19'S., 69°34'W.	1065–14091	26 Sep 72

Table 6 lists all the mountain summits north of lat 31°S. where snow or ice was present in all the analyzed Landsat images. A total of 83 summits are listed, as compared to 38 reviewed by Mercer (1967). For sake of comparison, the southernmost cordillera in Perú (Cordillera del Barroso) has been included. From this list, the glaciation level may be estimated.

At about lat 24°42'S. and long 68°30'W., an ice field existed in December 1952 between 5,600 m and 6,500 m on Llullaillaco (Lliboutry, 1956, p. 305; 1958), whereas the highest lower summit, Volcán Socompa (6,050 m), has no ice. Thus, the glaciation level is at about 6,100 m. At the same latitude but at about long 66°W., it has lowered to less than 5,800 m (Nevado de Acay, Nevado de Chañí).

At about lat 27°S., long 68°42'W., ice is found at Nevado Tres Cruces (6,330 m) but not at Cerro Solo (6,190 m), which indicates a glaciation level at about 6,200 m. At the same latitude and long 66°W., it is at 5,500 m or less in Nevado de Aconquija (5,550 m), the easternmost mountain range.

At lat 29°S., where the source of precipitation is from the southwest, the situation is reversed. The glaciation level is below 5,600 m at Nevados de Tambillos on the border, and it is at about 6,000 m at Nevado de Famatina, 175 km to the east.

At about lat 30°S., Paskoff (1967) described young rock glaciers above 4,000 m at the head of Río La Laguna, near a road from La Serena, Chile, to San Juan, Argentina, that crosses the border at Paso de Agua Negra (4,775 m). The thick morainic dam of Lago La Laguna at 3,100 m indicates the terminus of a Pleistocene glacier about 30 km long.

TABLE 6.—*Mountains and volcanoes that have permanent snow patches and glaciers north of lat 31°S., Perú, Bolivia, Chile, and Argentina*

[Slash (/) indicates a place-name variation between Argentina and Chile (for example, Cerro/Nevado El Fraile: Argentina, Cerro El Fraile; Chile, Nevado El Fraile). Elevations from Carta Nacional de Chile (CNC), 1945 edition, unless otherwise indicated; ONC, U.S. Air Force Operational Navigation Chart; OAIC, Carta Aeronáutica Mundial; CP, Carta Preliminar; IGMC, Instituto Geográfico Militar de Chile. Information on eruptive history from "Volcanoes of the World" (Simkin and Siebert, 1994) and "Global Volcanism 1975–1985" (McClelland and others, 1989); n.a., not applicable, not considered a Holocene volcano]

Mountain or volcano name (alternate name) Argentina/Chile	Country	Elevation (meters)	Latitude south	Longitude west	Landsat Path-Row	Number of and last eruption(s)	Remarks
Cordillera del Barroso:							
Nevado Chontacollo	Perú	5,484	17°26'	69°52'	1–72	n.a.	
Nevado Casiri	Perú	5,699	17°28'	69°49'	1–72	n.a.	
Nevado Coruña	Perú	5,692	17°29'	69°52	1–72	n.a.	
Nevado Barroso	Perú	5,741	17°33'	69°52'	1–72	n.a.	
Cerro Churivicho	Perú	5,463	17°36'	69°53'	1–72	n.a.	
Cerro Ancochaullane	Perú	5,540	17°35'	69°48'	1–72	n.a.	
Nevado El Fraile	Perú, Chile	5,595	17°39'	69°48'	1–72	n.a.	
Nevado Chupiquiña	Perú, Chile	5,787	17°41'	69°49'	1–72	n.a.	
Volcán Tacora	Chile	5,988	17°43'	69°47'	1–72	Solfatari	ONC: 19,521 ft=5,950 m
Nevado de Chuquiananta	Chile	5,488	17°47'	69°31'	1–72	n.a.	
Cerro Cosapilla	Chile	5,330	17°51'	69°30'	1–72	n.a.	ONC: 17,671 ft=5,386 m
Nevado de Putre	Chile	5,815	18°07'	69°32'	1–72	n.a.	ONC: 19,357 ft=5,900 m
Cerro Anallacsi	Bolivia	5,583	17°56'	68°55'	1–72, 251–73	Holocene age	ONC: 18,316 ft=5,583 m
Nevado de Sajama	Bolivia	6,520	18°07'	68°53'	1–72, 251–73	Holocene age	ONC: 21,463 ft=6,542 m
Cerro Larancagua	Bolivia, Chile	5,530	18°02'	69°04'	1–72, 251–73	n.a.	
Nevados de Payachata:							
Cerro Pomerape	Bolivia, Chile	6,240	18°08'	69°07'	1–72, 251–73	n.a.	ONC: 20,413 ft=6,222 m
Cerro Parinacota	Bolivia, Chile	6,330	18°10'	69°08'	1–72, 251–73	Fumarolic	

TABLE 6.—*Mountains and volcanoes that have permanent snow patches and glaciers north of lat 31°S., Perú, Bolivia, Chile, and Argentina*—Continued

Mountain or volcano name (alternate name) Argentina/Chile	Country	Elevation (meters)	Latitude south	Longitude west	Landsat Path-Row	Number of and last eruption(s)	Remarks
Cerro Quisiquisini	Bolivia, Chile	5,480	18°14'	69°03'	251–73	n.a.	
Nevados de Quimsachata:							
Cerro Acotango	Bolivia, Chile	6,050	18°23'	69°03'	251–73	Holocene age	ONC: 19,918 ft=6,071 m
Cerro Capurata	Bolivia, Chile	5,990	18°25'	69°03'	251–73	n.a.	
Volcán Guallatiri	Chile	6,060	18°25'	69°06'	251–73	4 in 1960	
Cerro Puquintica	Bolivia, Chile	5,760	18°44'	68°58'	251–73	Solfatari	ONC: 18,852 ft=5,746 m
Volcán Isluga	Chile	5,530	19°09'	68°50'	251–73	8 in 1960	
Cerro Cabaray	Bolivia	5,860(?)	19°08'	68°37'	251–73	n.a.	ONC: 21,230 ft=6,471 m
Cerro Sillajguay	Bolivia, Chile	5,995	19°44'	68°42'	251–74	n.a.	ONC: 19,670 ft=5,995 m
Cerro Aucanquilcha	Chile	6,180	21°13'	68°28'	250–75	Solfatari	ONC: 20,300 ft=6,187 m
Volcán Oyahue (Ollague)	Bolivia, Chile	5,870	21°18'	68°11'	250–75	Solfatari	ONC: 19,248 ft=5,867 m
Cerros de Cañapa:							
Cerro Coyumiche	Bolivia	5,838	21°17'	67°58'	250–75	n.a.	ONC: 19,324 ft=5,890 m
Cerro de Callejón	Bolivia	5,880	21°29'	68°06'	250–75	n.a.	
Cerro Tapaquilcha	Bolivia	5,765	21°29'	67°56'	250–75	n.a.	
Cerro Aguas Calientes	Bolivia	5,765	21°36'	67°57'	250–75	n.a.	
Cerro Palpana	Chile	6,045	21°33'	68°32'	250–75	n.a.	
Cerro Polapi	Chile	5,957	21°39'	68°24'	250–75	n.a.	
Volcán San Pedro	Chile	6,063	21°54'	68°24'	250–75	5 in 1960(?)	ONC: 20,210 ft=6,160 m
Volcán San Pablo	Chile	6,118	21°53'	68°21'	250–75	n.a.	Twin volcano of Volcán San Pedro
Cerro Paniri	Chile	5,940	22°04'	68°14'	250–75	n.a.	ONC: 19,550 ft=5,959 m
Cerro del León	Chile	5,771	22°09'	68°07'	250–75	n.a.	
Cerros de Tocorpuri	Bolivia, Chile	5,833	22°26'	67°54'	250–76	Solfatari	ONC: 6,765 m (a misprint?)
Volcán Púlar	Chile	6,225	24°12'	68°03'	250–77	n.a.	ONC: 20,420 ft=6,244 m
Cerro Pajonales	Chile	5,958	24°15'	68°07'	250–77	n.a.	
Cerro/Volcán Llullaillaco	Argentina, Chile	6,723	24°43'	68°33'	250–77	3 in 1577	ONC: 22,060 ft=6,724 m
Cerro Miñique	Chile	5,916	23°49'	67°45'	249–77, 250–77	n.a.	ONC: 19,450 ft=5,928 m
Cerro Aracar	Argentina	6,080	24°17'	67°47'	249–77	n.a.	ONC: 19,950 ft=6,081 m
Nevado de Chañí	Argentina	5,803 (ONC)	24°04'	65°45'	248–77	n.a.	OAIC: 6,200 m
Cerro Quironcollo	Argentina	6,130 (ONC)	24°18'	66°44'	249–77	n.a.	
Nevado de Acay	Argentina	5,886 (ONC)	24°25'	66°10'	248–77	n.a.	OAIC: 5,950 m
Unnamed	Argentina	6,047 (ONC)	24°08'	66°37'	249–77	n.a.	
Nevados de Cachí	Argentina	6,380 (ONC)	24°56'	66°23'	249–77	n.a.	
Volcán Antofalla	Argentina	6,440 (ONC)	25°33'	67°53'	249–78	Fumarolic	
Cerro Galán	Argentina	6,114 (ONC)	25°53'	67°05'	249–78	n.a.	OAIC: 6,600 m
Unnamed	Argentina	~6,000 (ONC)	25°58'	66°55'	249–78	n.a.	
Cerro Laguna Blanca	Argentina	6,194 (ONC)	26°32'	67°04'	249–78	n.a.	
Sierra Nevada de Lagunas Bravas: Cumbre del Laudo	Argentina	6,400	26°29'	68°34'	249–78, 250–78	n.a.	ONC: 20,750 ft=6,325 m
Cerro El Cóndor	Argentina	6,300	26°38'	68°21'	249–78, 250–78, 249–79	n.a.	ONC: 21,430 ft=6,532 m
Cerro Ermitaño	Chile	6,140	26°47'	68°36'	249–79	n.a.	ONC: 20,300 ft=6,187 m

TABLE 6.—*Mountains and volcanoes that have permanent snow patches and glaciers north of lat 31°S., Perú, Bolivia, Chile, and Argentina*—Continued

Mountain or volcano name (alternate name) Argentina/Chile	Country	Elevation (meters)	Latitude south	Longitude west	Landsat Path-Row	Number of and last eruption(s)	Remarks
Cerro/Nevado de San Francisco	Argentina, Chile	6,005	26°55'	68°16'	249–79	n.a.	
Cerro/Nevado de Incaguasi	Argentina, Chile	6,610	27°02'	68°18'	249–79	n.a.	ONC: 22,010 ft=6,708 m
Cerro/Nevado El Fraile	Argentina, Chile	6,044	27°03'	68°23'	249–79	n.a.	CP: 6,060 m
Cerro/Nevado El Muerto	Argentina, Chile	6,478	27°03'	68°29'	249–79	n.a.	CP: 6,470 m
Cerro/Nevado Ojos del Salado Norte	Argentina, Chile	6,863	27°07'	68°32'	249–79	n.a.	CP: 6,880 m; ONC: 23,240 ft=7,083 m; OAIC: 6,900 m
Cerro/Nevado Ojos del Salado Sur	Argentina, Chile	6,660 (CP)	27°12'	68°34'	249–79	n.a.	
Cerro del Nacimiento	Argentina	6,493	27°17'	68°31'	249–79	n.a.	ONC: 21,300 ft=6,492 m
Cerro/Nevado Tres Cruces	Argentina, Chile	6,330	27°06'	68°47'	249–79	n.a.	ONC: 22,270 ft=6,788 m; OAIC: 6,356 m
Cerro de los Patos	Argentina, Chile	6,250	27°18'	68°49'	249–79	n.a.	
Nevado Pissis	Argentina	6,858 (ONC)	27°47'	68°47'	249–79	n.a.	
Cerro Bonete	Argentina	6,714 (ONC)	28°01'	68°46'	249–79	n.a.	Mercer (1967): 6,410 m; OAIC: 6,872 m
Nevado de Aconquija	Argentina	5,550 (ONC)	27°13'	66°05'	248–79	n.a.	
Nevado de Famatina	Argentina	6,251 (ONC)	29°01'	67°50'	249–80	n.a.	OAIC: 6,421 m
Cerro El/del Potro	Argentina, Chile	5,830	28°23'	69°37'	250–80	n.a.	ONC: 19,080 ft=5,816 m
Cerro Cantaritos	Chile	5,590	28°32'	69°43'	250–80	n.a.	ONC: 18,360 ft=5,596 m
Nevados de Tambillos	Argentina, Chile	5,630	28°58'	69°45'	250–80	n.a.	ONC: 18,460 ft=5,627 m; OAIC: 5,547 m
Cerro del Toro	Argentina, Chile	6,380	29°08'	69°47'	250–80	n.a.	ONC: 19,490 ft=5,940 m
Unnamed	Argentina, Chile	5,440	29°17'	70°00'	250–80	n.a.	ONC: 18,180 ft=5,541 m
Cordillera de la Ortiga, Norte	Argentina	5,780	29°16'	69°48'	250–80	n.a.	ONC: 18,530 ft=5,648 m; OAIC: 6,050 m
Cordillera de Colangüil	Argentina	6,020 (OAIC)	29°36'	69°27'	250–81	n.a.	ONC: 19,780 ft=6,029 m
Cerro Doña Ana	Chile	5,690	29°46'	70°06'	250–81	n.a.	ONC: 18,580 ft=5,663 m
Cerro Las/de las Tórtolas	Argentina, Chile	6,323	29°56'	69°53'	250–81	n.a.	ONC: 20,030 ft=6,105 m
Cerro de Tapado(?)	Argentina, Chile	5,915	30°07'	69°57'	250–81	n.a	IGMC: 5,820 m
Cerro Agua Negra	Argentina	5,602 (ONC)	30°13'	69°46'	250–81	n.a.	
Cerro de Olivares	Argentina, Chile	6,252	30°17'	69°54'	250–81	n.a.	ONC: 20,330 ft=6,197 m
Cordillera de Olivares	Argentina	6,215 (OAIC)	30°25'	69°47'	250–81	n.a.	ONC: 20,270 ft=6,178 m
Cerro San Lorenzo	Argentina	5,570	30°25'	69°57'	250–81	n.a.	ONC: 18,150 ft=5,532 m
Cerro del Volcán	Chile	5,510	30°30'	70°16'	250–81	n.a.	OAIC: 5,540 m

Central Andes (Between Lat 31° and 35°S.)

As mentioned earlier, the *Central Andes* have large glaciers covering about 2,200 km^2, but very few people have ever come close to them. In spite of the proximity of the city of Santiago, the *Central Andes* have virtually no inhabitants (the large Maipo valley being an exception) and very few roads. Hiring mules has become very expensive. Unless a helicopter is chartered, a visit to the Cerro/Volcán Tupungatito, perhaps the most picturesque journey in the *Central Andes*, requires 8 days, with 6 of those days on muleback following a sometimes giddy and dangerous track along the Río Colorado. On the Argentine side, the glaciers are even farther from any road.

The two best Landsat MSS images that cover the Cordillera Central are reproduced in figures 9 and 10. From the images, a sketch map of the Cerro (*Volcán*) Tupungato-Nevado de los Piuquenes area has been drawn (fig. 11); the sketch map improves upon the information included in the 1:150,000-scale map published by Lliboutry (1956). A cross section of the same area is given in figure 6. Some of the major advances to the glaciological and geographical knowledge of the region gained from the Landsat images are provided in the following paragraph.

Glaciar de los Polacos on the east slope of Cerro Aconcagua, at the head of Arroyo Relincho, is much broader and longer than previously suspected, with a length of 5.6 km (fig. 9, no. 3). Cordillera del Tigre has much more complex topography than is depicted on Argentine charts. Glaciers of the Cordón del Plata are much more important than realized by Mercer (1967, p. 100); the main glacier is 8 km long. East of Cerro Marmolejo (fig. 9), a debris-covered glacier exists at the head of *Arroyo Piedras Negras*. *Arroyo los Plomos* does not come from Cerro Marmolejo. Meltwater from the large debris-covered glacier east-northeast of Cerro Marmolejo drains through *Arroyo Barroso* instead. Lastly, the east glacier of Cerro Marmolejo, at the head of *Arroyo Barroso*, is much longer than previously thought; it is about 10 km long. On the east slope of Volcán San José the two bare glacier tongues are in fact linked and continue as a debris-covered glacier until 9 km from the crater (fig. 10). Just south of Volcán Maipo, *Cerro Listado* (4,850 m) contains several glaciers; the main one is in the drainage basin of *Río Bayo*. Its ice cover is similar to the one of Nevado de Arhüelles (4,840 m), just north of Volcán Maipo.

Glaciers of the *Central Andes* can be quite large for such moderate latitudes, sometimes as much as 14 km long. Some of them, such as the ones on the plateau that gently descends from 4,700 m to 3,800 m at the head of Río Olivares (see southwestern part of fig. 9 for general location), have no cover of morainic debris along nearly their entire length. But many other glaciers have morainic cover in their lower part or sometimes over almost their entire length, such as Glaciar Horcones Inferior (no. 4 south of Cerro Aconcagua in fig. 9), *Glaciar del Tunuyán* (see fig. 12), or Glaciar Cachapoal (south of *Picos del Barroso*) (central part of fig. 10 and fig. 13). In the standard false-color satellite images, the debris-covered glaciers appear as dark green (not to be confused with the lighter green of large thalwegs without vegetation). Where the morainic debris-cover consists only of rocky blocks, as at the terminus on the right side of Glaciar Universidad (lat 34°40'S., fig. 10), the false color appears as dark blue.

Mercer (1967), in his "Southern Hemisphere Glacier Atlas," gathered all the available information on the glaciers in South America. However, the information derived from individuals who have little knowledge of glaciers must be used with caution because, in general, they do not recognize debris-covered glaciers as glaciers. For instance, they did not realize that the huge field of rubble at the head of Río Cachapoal is actually a debris-covered glacier, 12 km long, the longest one on the Chilean side of the *Central Andes* (fig. 13) (see west edge of fig. 10 for general location).

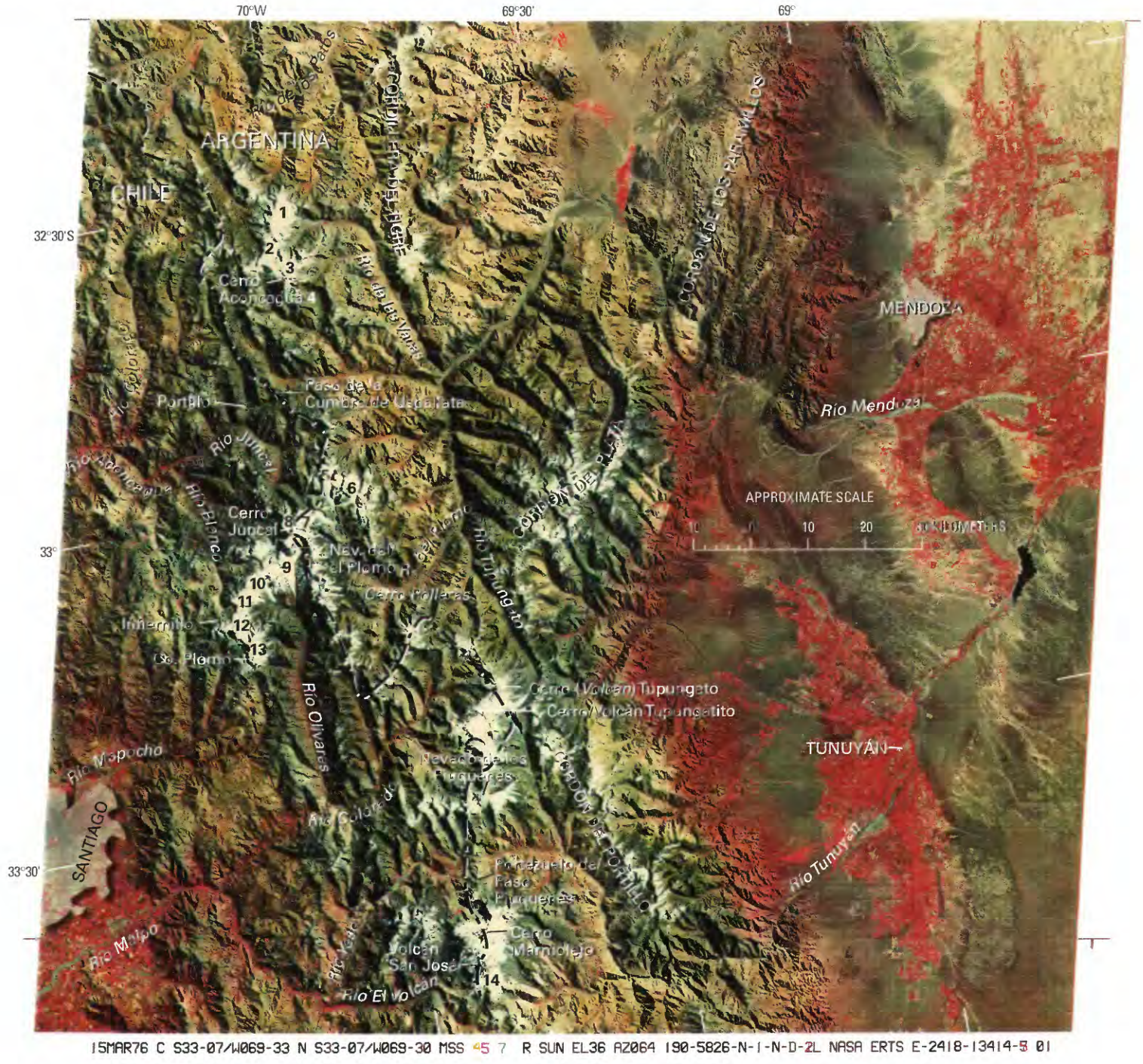

Figure 9.—*Annotated Landsat MSS false-color composite image (2418–13414, bands 4, 5, and 7; 15 March 1976; Path 249, Row 83) of the* Central Andes *between Santiago and Mendoza from Cerro Aconcagua to Volcán San José. Landsat image is from the EROS Data Center, Sioux Falls, S. Dak.The following glaciers are indicated by numbers:*

1, Glaciar de las Vacas
2, Glaciar Güssfeldt
3, Glaciar de los Polacos
4, Glaciar Horcones Inferior
5, Glaciar Alto del Río Plomo
6, Glaciar Bajo del Río Plomo
7, Glaciar Juncal E–2
8, Glaciar Juncal Norte
9, Glaciar Juncal Sud
10, Glaciar Olivares Gamma
11, Glaciar Olivares Beta
12, Glaciar Olivares Alfa
13, Glaciar Esmeralda
14, Glaciar Nieves Negras Chileno

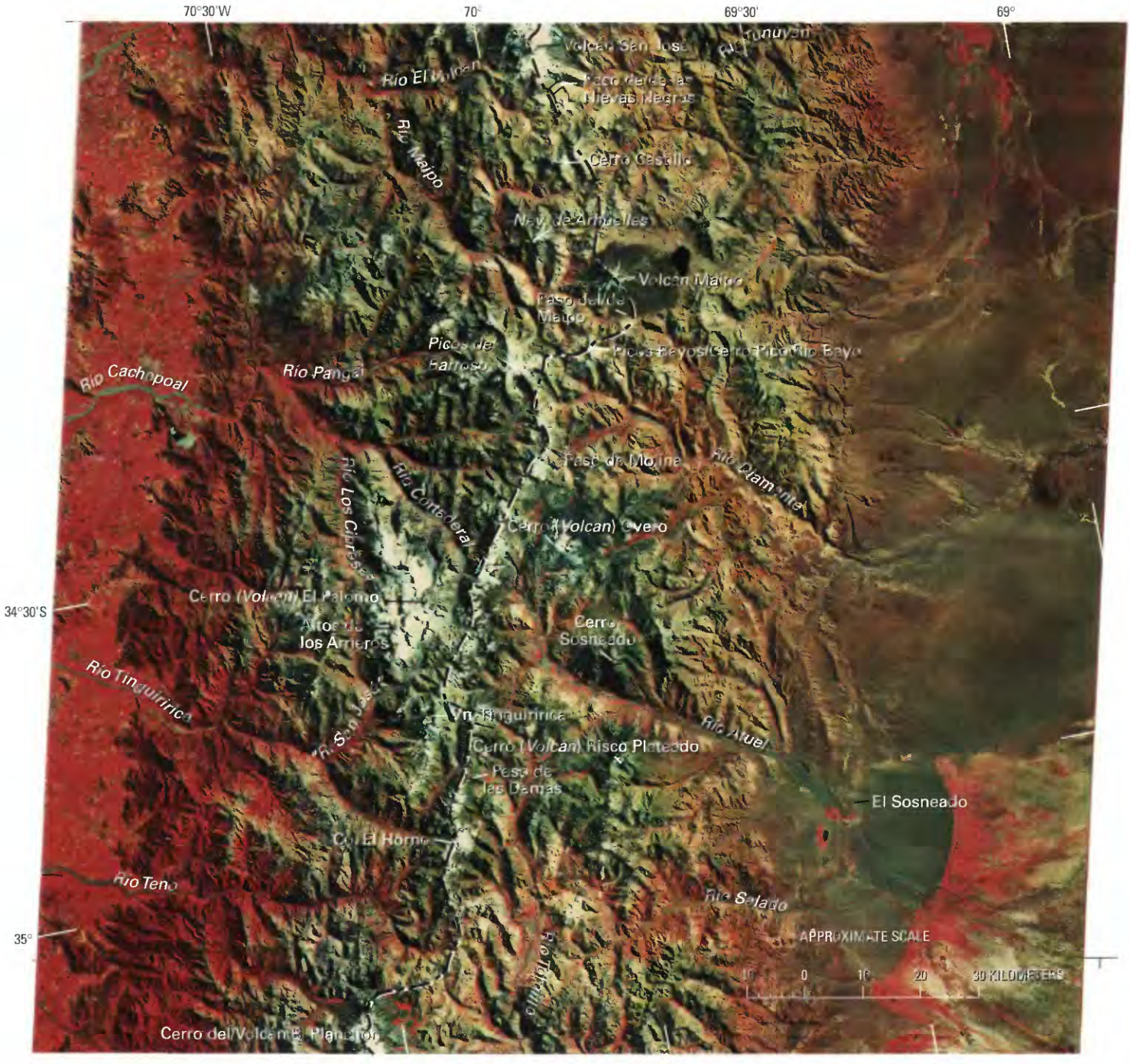

Figure 10.—*Annotated Landsat MSS false-color composite image (2418–13420, bands 4, 5, and 7; 15 March 1976; Path 249, Row 84) of the* Central Andes. *The area covered is just to the south of figure 9. Abbreviations: Co., Cerro, mountain; Nev., Nevado, snow and (or) ice-capped mountain; R., Río; Vn., Volcán. Landsat image is from the EROS Data Center, Sioux Falls, S. Dak.*

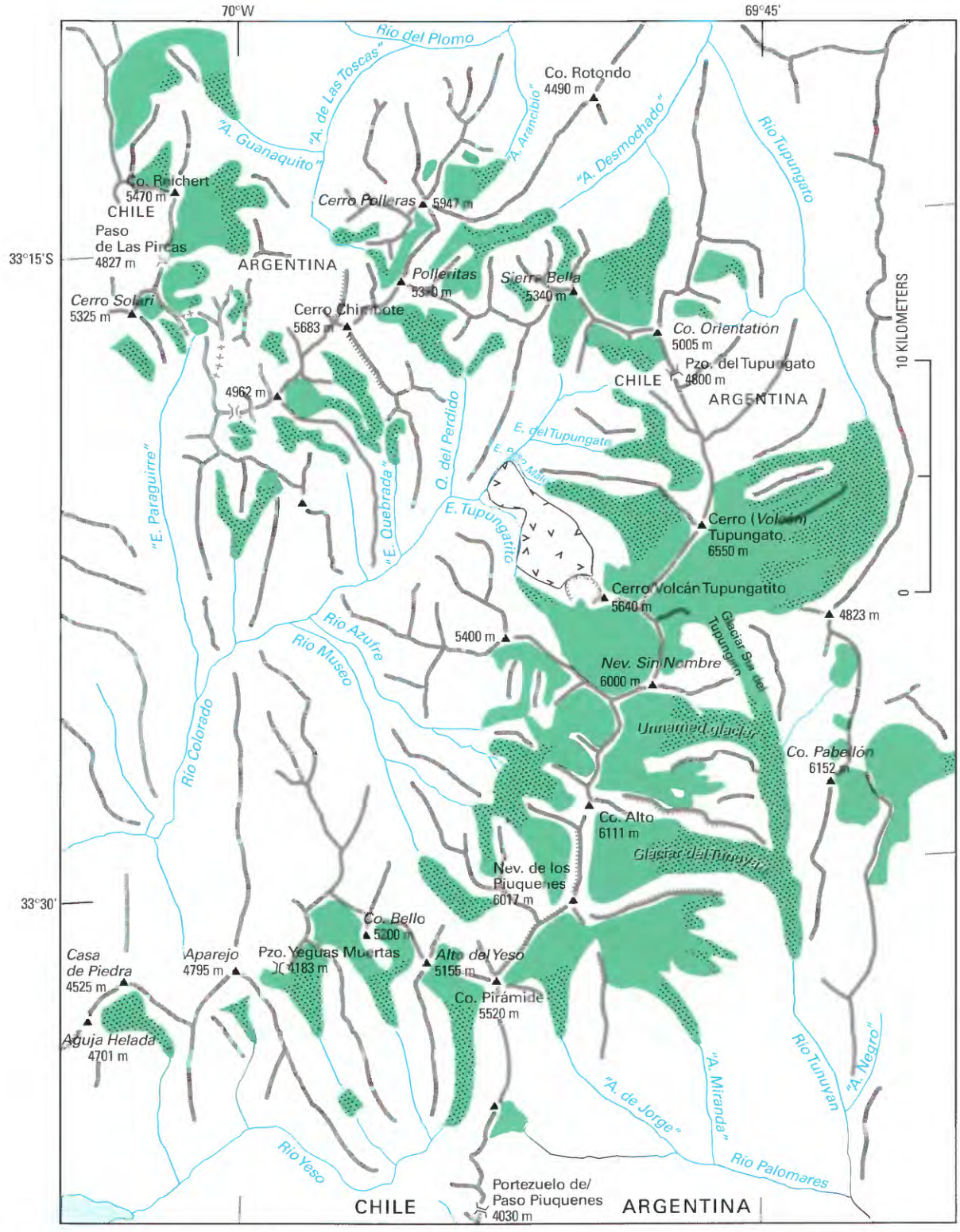

Figure 11.—*Cerro (*Volcán*) Tupungato-Nevado de los Piuquenes area in the* Central Andes, *50–85 km east of Santiago. Features have been delineated on the basis of published maps and analysis of Landsat images. The area shown by the small "v" pattern is a lava field erupted from Cerro/Volcán Tupungatito. Glaciers are shown in green, and the dotted areas are debris-covered glaciers or rock glaciers. The thick gray lines show ridgelines, the hachured gray lines show cliffs or depressions. The map projection is the same as the one for Landsat image 2022–13455 (13 February 1975; Path 249, Row 83). The coordinates are inferred from Paso de Las Pircas, Portezuelo del Tupungato, and Portezuelo de/Paso Piuquenes as given in Carta Nacional (scale 1:500,000, Instituto Geográfico Militar de Chile), although with such a map projection, the scale can only be approximate. Elevations are from several different sources and are derived from Lliboutry's 1:150,000-scale map (Lliboutry, 1956). The border between Chile and Argentina follows the main ridgeline (+++ where ridgeline is not continuous). Names in italics and names enclosed in quotation marks are names that are not listed in the gazetteers for Argentina (U.S. Board on Geographic Names, 1992a) and Chile (U.S. Board on Geographic Names, 1967, 1992c). Abbreviations: Co., Cerro, mountain; Nev., Nevado, snow- and (or) ice-capped mountain; E., Estero, creek (in Chile); and A., Arroyo, creek (in Argentina); and Q., Quebrada, creek. Paso is a cross-border pass and mule track; Pzo., Portezuelo, is any other pass.*

Figure 12.—*Vertical aerial photograph of glaciers at the head of Río Tunuyán (from IFTA, 1973). The very long (20.2 km) glacier shown south of Cerro (*Volcán*) Tupungato on Lliboutry's 1:150,000-scale map (Lliboutry, 1956) is, in fact, formed by three successive glaciers: (1) Glaciar Sur del Tupungato, which enters at the upper right-hand corner of the photograph; (2) an unnamed glacier located between Nevado sin Nombre (6,000 m) (just off the top of the photograph) and Cerro Alto (6,111 m) (off bottom left of photograph), which contains a large névé; and (3) a glacier located in a deep cirque between Cerro Alto and Nevado de los Piuquenes (6,017 m) (see fig. 11) that may be named* Glaciar del Tunuyán. *The two latter glaciers are heavily debris-covered and contain small supraglacier lakes and a distinct thermokarst facies (note especially the course of the creeks flowing from the west). In the unnamed glacier, festooned areas of bare glacier ice show the diagnostic evidence of surge behavior.*

Figure 13.—*Glaciar Cachapoal, the largest debris-covered glacier in Chile, is 12 km long. The glacier is entirely covered with debris that is indistinguishable from its left margin. The rocky wall in the background of the photograph marks the border between Chile and Argentina. The foreground is at an elevation of about 2,400 m. The mountain around which Glaciar Cachapoal flows is 4,500 m high.*

At the foot of rock walls, "ice-debris glacierets" commonly are found, where a new layer of ice forms most winters, and a layer of rubble falls down (or appears at the surface) each summer. In many glacier tongues, clean ice is superimposed on a very thick layer of dragged and sheared debris-layered ice. The latter may have been either a frozen soft bed (permafrost) or an "ice-debris glacieret," but in both cases, it has been dragged and sheared during a glacier advance or a glacier surge (Lliboutry, 1954a, 1956, 1965, 1986). Near the terminus, where melting reaches the lower debris-laden layer, a thick ablation moraine forms.

Where ice has melted (see the section on "Rock Glaciers" below), a continuum (all intermediate cases are possible) exists between a debris-covered glacier, an ice-debris glacier, and a rock glacier. It is possible to make separate inventories of glaciers (covered or not) on the one hand and of rock glaciers (with or without some ice included) on the other hand. For this reason, all young rock glaciers are listed in the glacier inventories. Consequently, in table 7, the area of covered glaciers is overestimated.

The first glacier inventory, based on sketches drawn by Chilean *andinistas* (mountaineers), personal exploration, and Trimetrogon aerial photographs, is found in Lliboutry (1956). Glacier inventories based on the Chilean aerial photographic coverage of 1955–56 have been made by C. Marangunic (basins of Río del Plomo and Río Cachapoal) and by G. Casassa (Chile). Glacier inventories based on the Argentine aerial photographic coverage of 1980–81 have been made by C. Aguado (Río de los Patos basin), by L. Espizúa (most of Río Mendoza and Río Tunuyán basins), and by D. Cobos (Río Atuel basin). Except for the inventory available in Corte and Espizúa (1981), all these inventories remain unpublished.

Rock Glaciers

By Arturo E. Corte[4]

A rock glacier is defined by Jackson (1997, p. 554) as "a mass of poorly sorted angular boulders and fine material, with interstitial ice a meter or so below the surface (ice-cemented) or containing a buried ice glacier (ice-cored). It occurs in high mountains in a permafrost area, and is derived from a cirque wall or other steep cliff." [Lliboutry (written commun., 1997) does

[4] Instituto Argentino de Nivología y Glaciología, CONICET, Casilla de Correo 330, Mendoza, Argentina.

TABLE 7.—*Total glacier area in the* Central Andes

[Given in square kilometers. Data for Chile from Valdivia (1984); data for Argentina from Espizúa and Aguado (1984)]

Location	Uncovered	Covered	Total
Chile			
Basin of Río Aconcagua	~76	~76	~152
Río Maipo	257.5	164.6	422.1
Río Cachapoal	175.3	46.6	221.9
Río Tinguiririca	103.2	3.2	106.4
Subtotal	~612	~290	~902
Argentina			
Basin of Río San Juan	140	206	346
Río Mendoza	304	363	667
Río Tunuyán	57	87	144
Río Atuel	148	38	186
Subtotal	649	694	1,343
Total	~1,261	~984	~2,245

not agree with this definition. He notes that old rock glaciers have no ice at depth; young ones may reach an elevation where permafrost is absent. The main characteristic is to appear like a mountain glacier and to show signs of flow.] A survey of the literature suggests that rock glaciers can be classified by genetic groups. Seven rock-glacier types are suggested that are created from four genetic groups (fig. 14*A*) (Giardino and others, 1987). A taxonomic classification of active rock glaciers is shown in figure 14*B*. In Argentina and Chile, the term rock glacier is used to describe a series of ice bodies covered with debris that are produced by different processes. At one end of the series are the primary type of rock glaciers, those that are formed below snow- and debris-avalanche chutes (fig. 15). At the other end of the series are glaciers that have varying amounts of surface debris (fig. 12). Between these two extremes is a range of various morphological types of ice-and-debris bodies. However, both Louis Lliboutry and the author, following the concept of French morphologists concerning "pattern convergence," conclude that no matter what the origin of rock glaciers, they will tend to produce the same pattern if the climate, rock type, exposure, and cryogenic processes involved are similar (Lliboutry, 1956, 1961, 1965, 1986, 1990a, b). The main pattern consists of arched rolls (fig. 16). In the furrows, meltwater has washed down the silt, and squeezed clasts lie on the edge. In certain areas of the *Dry Andes*, where glaciers do not surge, glaciers covered by debris can contain up to four facies: (1) nondebris-covered ice, (2) thermokarst, (3) structural debris, and (4) inactive debris-covered ice. Some glaciers of the last type have been found to contain fossil ice that is a relict feature of a past colder climate during the Holocene (Corte, 1980). The different facies are present in different proportions on different glaciers. The Glaciar Sur del Tupungato is noted for a very large area of thermokarst features that is 9.3 km long and 900 m wide. Figure 12 illustrates the thermokarst facies of Glaciar Sur del Tupungato as seen from the air.

In other areas of the *Dry Andes* where surging glaciers are observed, it is possible to recognize some, like the Glaciar Grande del Nevado in the Río del Plomo basin, that reach old rock glaciers (Corte, 1976). Other glaciers that could be surging glaciers intercept (Glaciar del Tigre) or overtop (Glaciar del Plata) older rock glaciers. This is also visible in the Cerro Mercedario area (fig. 17). Under such conditions, the four glacier facies above are absent, isolated, or superimposed.

A, Rock Glacier Systems

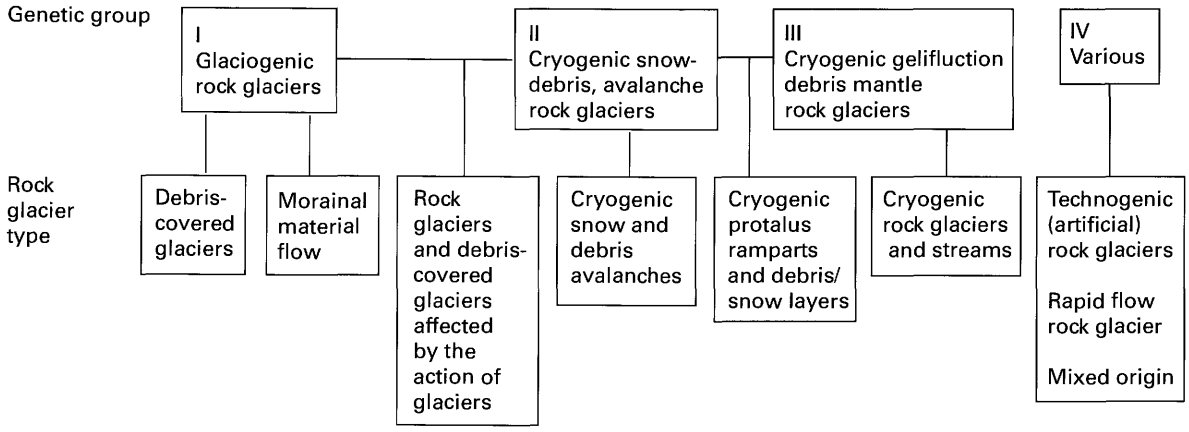

B, Taxonomic Classification of Active Rock Glaciers

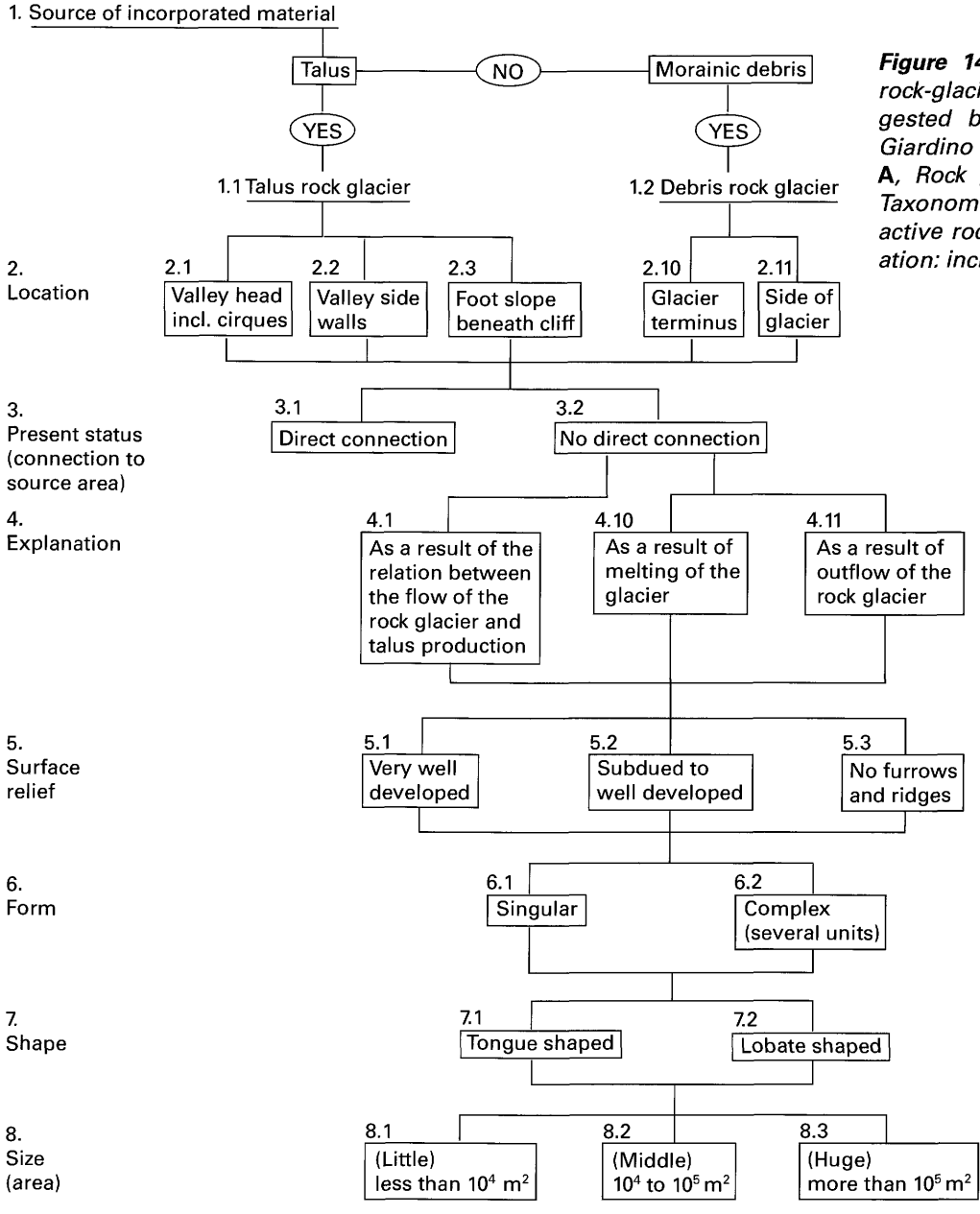

Figure 14.—*Classification of rock-glacier systems as suggested by A.E. Corte from Giardino and others (1987).* **A**, *Rock glacier systems,* **B**, *Taxonomic classification of active rock glaciers. Abbreviation: incl., including.*

Figure 15.—*Tres Dedos rock glacier in the Cerro Aconcagua group seen from the south. Photograph by A.E. Corte taken in 1977.*

Figure 16.—*Rock glaciers at the head of Río Blanco (Provincia de Aconcagua, Chile) between about 4,600 m and 4,000 m. The upper part of Glaciar Olivares Alfa can be seen in the upper left-hand corner. Remnants of winter snow in the hollows enhance the arched rolls and pattern of flow. The general location of the Río Blanco area can be seen in figure 9 (north of number 12). Photograph by Louis Lliboutry taken on 28 January 1953.*

The continental climate, intense frost shattering, and steep topography of the *Central Andes* combined with low precipitation (about 600 mm a^{-1}) produce ideal conditions for the development of numerous rock glaciers of different types. In the central high Andes, the area around Cerro (*Volcán*)Tupungato and Cerro Aconcagua (6,550 m and 6,959 m, respectively; see fig. 2) is the region of the greatest development of both debris-covered and nondebris-covered glaciers in the *Dry Andes*. This region, within a 200-km radius centering on Cerro Aconcagua, includes the Cerro Mercedario (fig. 17), del Plata, and del Plomo regions. The inventory of glaciers in the Mendoza basin of the *Central Andes* shows that uncovered and debris-covered glaciers and rock glaciers have a similar areal extent (303 and 340 km^2, respectively) (Corte and Espizúa, 1981) (fig. 18).

In the more northerly part of the dry *Desert Andes*, around Nevado de Acay (lat 24°25'S.), small rock glaciers exist that are related to avalanche activity. Such rock glaciers are produced by the accumulation of avalanche and debris material generated by summer storms (Igarzábal, 1981) and are located in cirques formed during glaciation in the Pleistocene Epoch. These rock glaciers are important sources of irrigation waters for the aboriginal Inca communities. Nevado de Famatina (lat 29°01'S.) farther to the south has similar conditions and might contain similar types of glaciers, but field data are unavailable for this region.

In the most southerly part of the *Dry Andes*, a region that receives about 800 mm of precipitation annually, debris-covered glaciers exist but in a much smaller proportion than in the Cerro Aconcagua area. The inventory of the Río Atuel glaciers (Cobos, 1981) (see central part of fig. 10), representative of this area, listed 80 percent of the glaciers as nondebris-covered and 20 percent as debris-covered glaciers. Although not as common, debris-covered glaciers exist farther south in the *Wet Andes*. Glaciar Casa Pangue, on the west slope of Monte/Cerro Tronador (fig. 2), was found to have 50-cm-deep debris at elevations of 800–850 m (Sigfrido Rubulis, personal commun.).

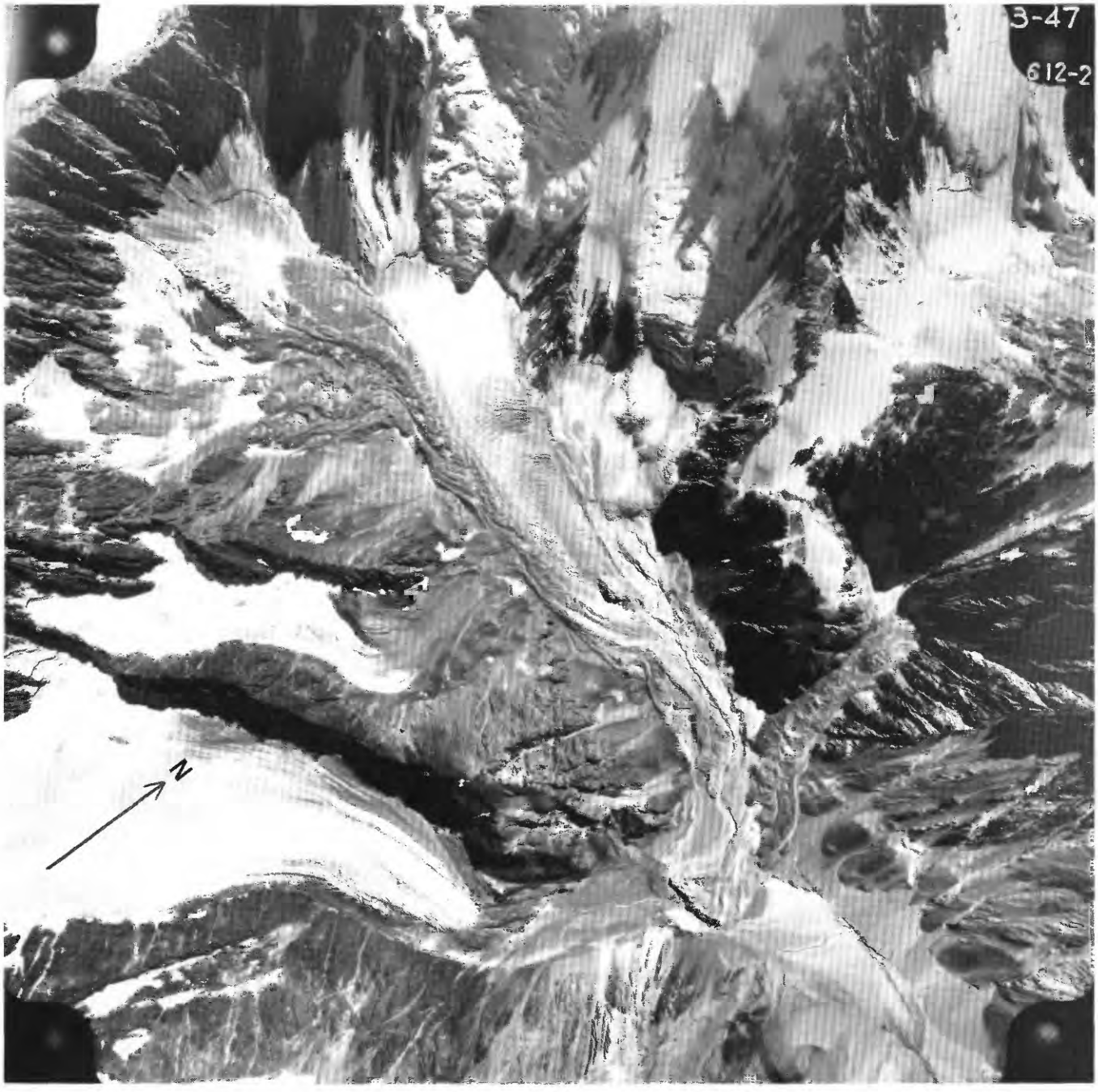

Figure 17.—*Vertical aerial photograph of glaciers on the southeast side of Cerro Mercedario (6,700 m). Note the north arrow. In the upper middle, a hanging glacier flowing from* Pico Polaco *becomes a valley glacier and merges with a shorter glacier flowing from Cerro Mercedario (lat 32° S.). At their termini, Arroyo Colorado has its source, after which the creek forces its way across, along, or through rock glaciers and remnants of old surges. Toward the bottom right-hand corner of the photograph, a small, steep, debris-covered glacier ends in several small tongues that can be considered to be rock glaciers. They are superimposed on a broad lobe of drift that crosses the valley; it is probably an older rock glacier. At the bottom right-hand corner, shoulders of scree above the valley probably contain buried glacier ice. They may be called "buried avalanche glacierets," which will eventually evolve into true rock glaciers.*

► ***Figure 18.***— *Mendoza basin in Argentina west of Cerro Aconcagua (fig. 9) showing the location of glaciers, ice-cored moraines, rock glaciers, and thermokarst features. Numbers refer to a map prepared by L.E. Espizúa. Stream IJA11854 flows into Quebrada de los Horcones at the west foot of Aconcagua. Stream IJA1184 flows into Quebrada Matienzo along the border.*

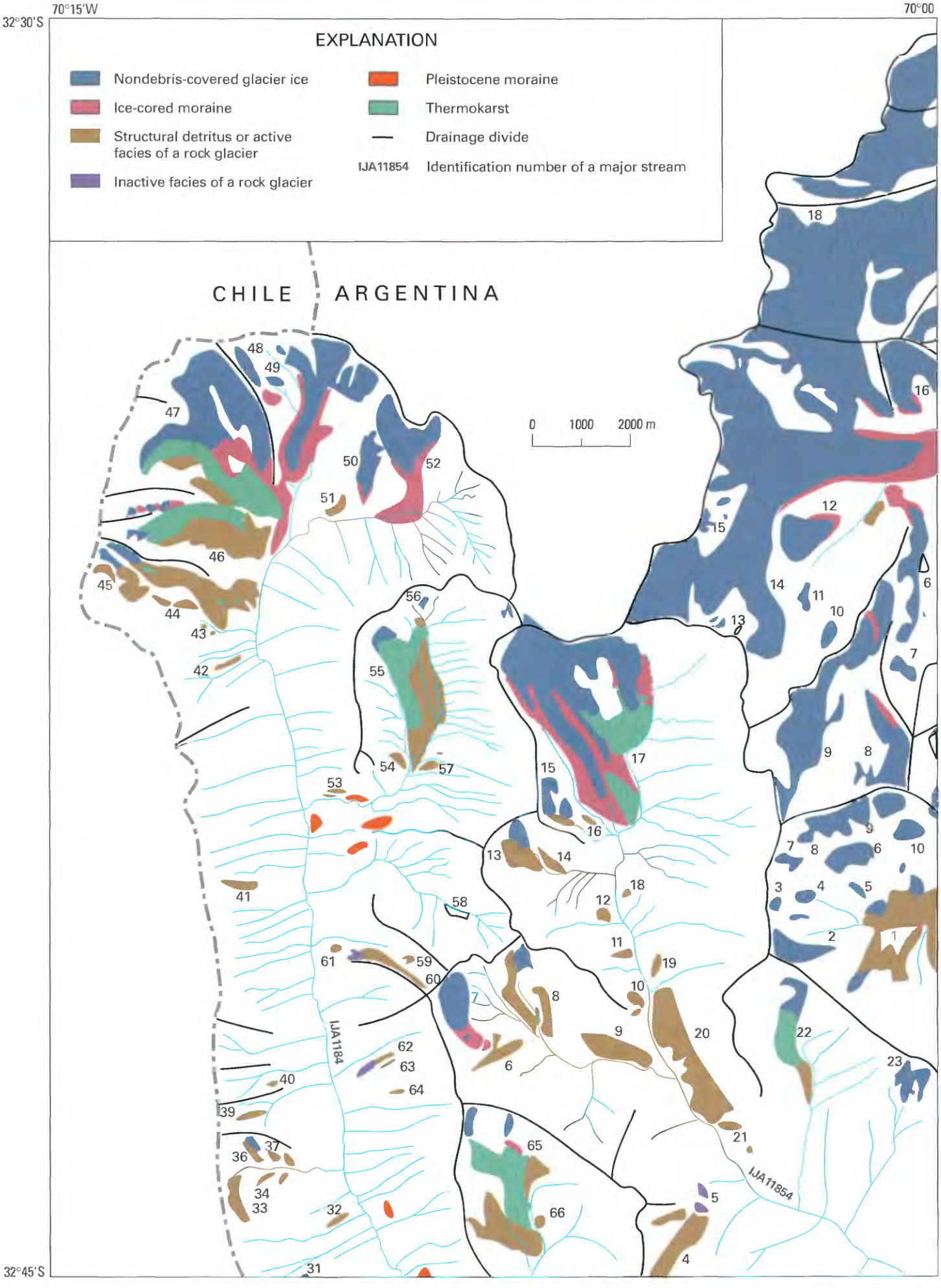
70°15'W
70°00
32°30'S
32°45'S
EXPLANATION
Nondebris-covered glacier ice
Ice-cored moraine
Structural detritus or active facies of a rock glacier
Inactive facies of a rock glacier
Pleistocene moraine
Thermokarst
Drainage divide
IJA11854 Identification number of a major stream
CHILE
ARGENTINA
0 1000 2000 m
IJA1184
IJA11854

Surging Glaciers in the *Central Andes*

Because almost all the glaciers of the *Central Andes* end in rock glaciers or ice-cored moraines, the precise determination of glacier termini and their monitoring on an annual basis, as asked for by the World Glacier Monitoring Service, is an impossible task. Notwithstanding, from time to time, some glaciers of the *Central Andes* advance by several kilometers in less than 1 year. This phenomenon is well documented in Alaska, Tadjikistan, and Svalbard and is called a surge (Raymond, 1987). Surges can be detected and followed by using satellite imagery.

Surging glaciers have been reported in Lliboutry (1956) for Glaciar Nieves Negras Chileno (southwest of Volcán San José; see no. 14 in fig. 9) in 1927, Glaciar del Río in 1935, and Glaciar Juncal Sud (no. 9 in fig. 9) in 1947. The volume of ice that was discharged by this last surge is of the same order of magnitude as the excess of accumulation during the period 1898 to 1905, when 6 out of 8 years were wet in Santiago. We may add the west tributary of Glaciar Universidad as surging in 1944–45 (Lliboutry, 1958), although this glacier is temperate in its lower part because, at lat 34°40'S., the climate is wetter. It is located in the transitional area between the *Dry Andes* and the *Wet Andes*, where snow and (or) ice penitents are not found.

Satellite imagery makes it possible to infer the existence of surging glaciers because medial moraines of surging glaciers are contorted into sinuous patterns, a telltale sign of a surging glacier. This is the case for a glacier east of *Cerro Polleras* (at the head of *Arroyo Desmochado*) (see center of fig. 9), for the east glacier of Cerro Marmolejo (that gives rise to *Arroyo Barroso*) (see bottom of fig. 9), and for the unnamed glacier east-northeast of Cerro Alto. In the last case, a photograph taken by Luis Krahl from Cerro Alto in 1946 (fig. 19; compare also with fig. 12) seems to indicate that the main glacier was surging at that time. Nearby, the east glacier of Nevado de los Piuquenes was found to be surging in January 1997 (A. Aristarain, oral commun.). This very interesting area is in Argentina, but its access is much easier from Chile, where a road ends 25 km away.

A surging glacier may dam a river and create an ephemeral lake. This has been the case for Río del Plomo, a river that drains the most heavily glaciated area of the Argentine *Central Andes* (central part of fig. 9). (This river is a tributary of the Río Tupungato, but it discharges more water than the latter at their confluence. In the same way, Río Tupungato is a tributary of Río Mendoza, although it discharges more water at their confluence. In former times, the name of a river was maintained upstream along the most frequented track, without consideration of the discharge. In case of doubt, confluent rivers were each named differently from the one downstream.)

Río del Plomo has been dammed at least three times by Glaciar Grande del Nevado (fig. 20). This glacier originates in a large cirque on the southeast side of Nevado del/el Plomo (6,050 m). It then flows from 4,500 m to 3,500 m over a distance of more than 5 km and is covered by an ablation moraine. Along its course, it receives a tributary from Cerro Risopatrón, improperly called Glaciar Pequeño (small) del Nevado. To dam Río del Plomo, Glaciar Grande del Nevado must advance down to 3,200 m and make contact with an outcrop of polished rock (*Roca Pulida*) on the east bank of Río del Plomo.

The first known flood due to the rupture of such a dam happened on 2 January 1788. The lake had existed in February 1786 according to the historian Prieto (1986). This conscientious historian did not find a record of any similar event during the 19th century. Therefore, the flood of 10 January 1934, which destroyed bridges and 12.6 km of railroad along Río Mendoza, was quite a surprise (Helbling, 1935). Inspection of the site showed that Glaciar del Nevado had advanced 900 m since its last inspection, 22 years before. It had produced a lake 3 km long, with a

Figure 19.—*View from the summit of Cerro Alto (6,111 m) looking to the east-northeast. Photographed by Luis Krahl on 20 January 1946 during the first ascent of the mountain. Compare with the vertical aerial photograph (fig. 12). Much more bare glacier ice can be noted in 1946 between the looped moraines of the unnamed glacier than in 1973, which denotes the recentness of a surge.*

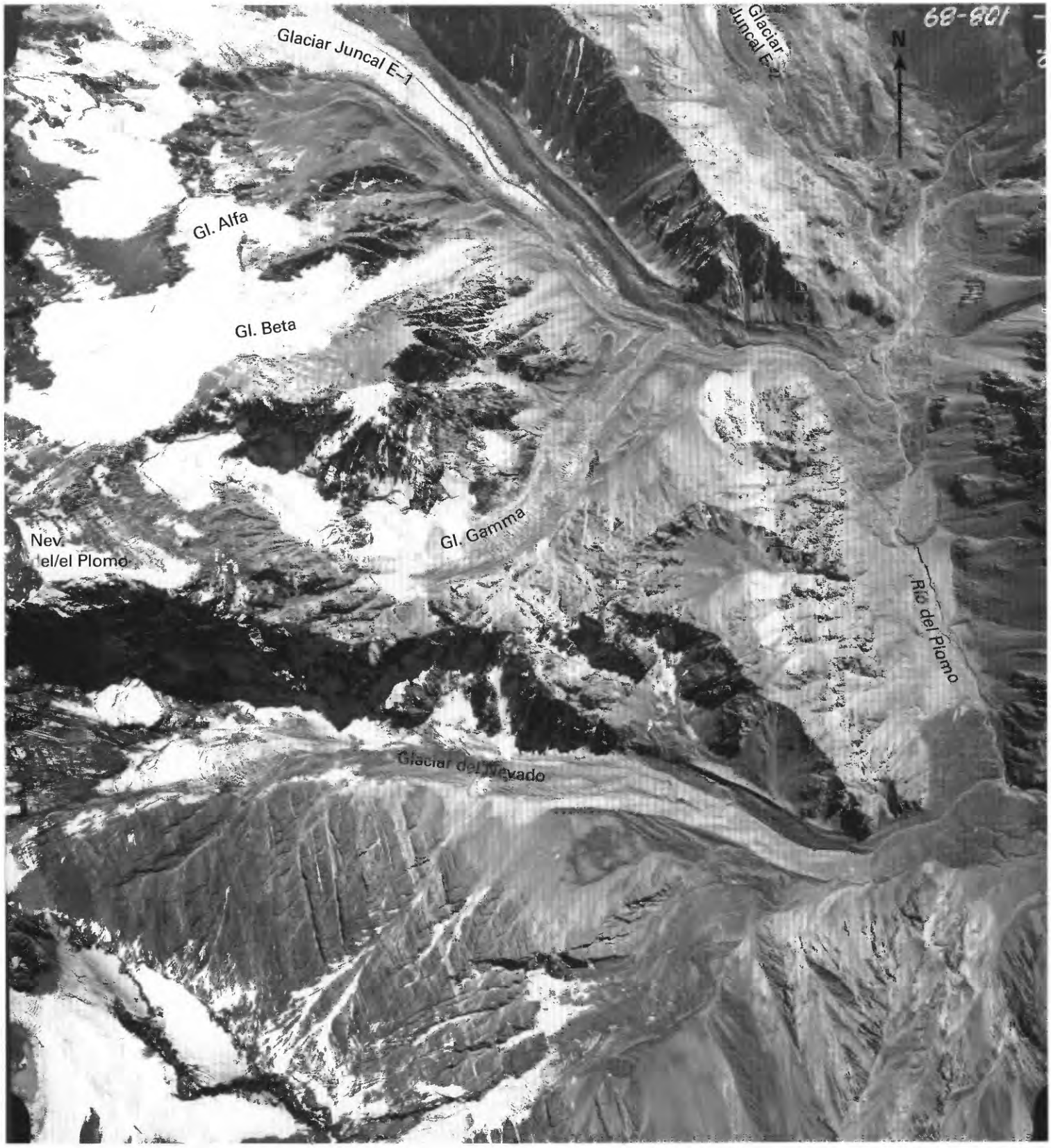

Figure 20.—*Origin of the disastrous flood of 1934 (see text). The vertical aerial photograph (from IFTA, 1973) shows the Río del Plomo valley on the right (about 3,100 m asl). At the upper right-hand corner of the photograph is the lower end of Glaciar Oriental del Juncal No. 2, as named by R. Helbling. (The name is abbreviated to Glaciar Juncal E–2. Numbers 1 and 2 are reversed in the map by Lliboutry, 1956). At the upper left of the photograph is Glaciar Juncal E–1; below it, a white glacier has two tongues (Alfa and Beta), and another has a debris-covered gray tongue (Gamma). Nevado del/el Plomo (6,050 m) appears on the left in the central part of the photograph. From the cirque flows Glaciar Grande del Nevado, its heavily debris-covered terminus ending about 2 km from Río del Plomo. Helbling surveyed the region in 1919. At that time, Glaciar Beta and Glaciar Gamma joined Glaciar Juncal E–1, which, in turn, joined Glaciar Juncal E–2, the latter being 3 km longer than at present. Glaciar Grande del Nevado reached Río del Plomo, and tongues of drift attest to this older position of the glacier.*

maximum depth of 75 m. Clean white ice overthrusted the old moraine. The duration of the advance was unknown and controversial (Espizúa, 1986).

Pertinent Landsat MSS and Thematic Mapper (TM) imagery has been studied by Espizúa and Bengochea (1990) in order to monitor recent movement. It shows that from March 1976 to 16 February 1984, Glaciar del Nevado was covered with debris and ended 2.7 km west of *Roca Pulida*. On an image of 4 April 1984, the glacier terminus was free of supraglacier drift and had advanced 500 m. Thus, in less than 48 days, the upper part of Glaciar del Nevado had overthrust the lower part. It shows that the friction coefficient of ice over debris-covered ice is only about 0.2.

On a 26 August 1984 image, Glaciar del Nevado had advanced 2 km farther and was only 150 m from *Roca Pulida*. No further advance is seen on a 13 October 1984 image. Contact with *Roca Pulida* happened between 22 October and 14 November 1984, and the lake began to form some days later. On 9 January 1985, the lake had reached 2.8 km in length and 1.1 km in width. The potential hazard raised concern by the authorities, but this time, the lake emptied progressively by having peak discharges on 13–15 and 22 February 1985 and on 13 March 1985.

Also in 1984, Glaciar Horcones Inferior (no. 4 in fig. 9), on the south face of Cerro Aconcagua, surged. Given the frequent transit of this valley by groups climbing Cerro Aconcagua, we can be certain that this glacier had not surged during the 20th century.

With the exception of these surges, which are not a common rule, the glaciers of the *Central Andes* have been strongly receding in recent times. Glaciar Olivares Beta (no. 11 in fig. 9) receded by almost 1 km between 1956 and 1976. In the upper Río del Plomo valley, a comparison of the survey by Helbling in 1919 with the aerial view taken in 1973 (fig. 20) and a Landsat image acquired in 1976 (fig. 9) shows that, in 1919, Glaciar Alto del Río Plomo and Glaciar Bajo del Río Plomo (nos. 5 and 6 in fig. 9) joined Glaciar Juncal E–2 (no. 7 in fig. 9) to form a single valley glacier 16.7 km long. Today, a large gap exists between them. However, because Río del Plomo is flowing freely along the west side of Glaciar Juncal E–2 (Glaciar Oriental del Juncal No. 2), no dangerous lake should form there (fig. 20).

Old Glaciations in the *Central Andes*

"U-shaped" valleys and moderate subaerial erosion prove that the inner parts of the *Dry Andes* south of Cerro Aconcagua have been covered with ice several times in the past. The limits of this heavily glaciated area can be observed on Landsat imagery. However, remote sensing from space (or from the air) does not provide evidence for the extension of past glaciers, in particular those that, in more ancient times, should have reached the *Central Valley* of Chile. The three reasons for this are

(1) As observed in very high semiarid regions of *Central Andes*, these glaciers were heavily covered and did not leave clear terminal moraines.
(2) The glaciers flowed in the middle of the valleys without modifying their transversal profiles, so the valleys kept their "V-shape."
(3) The glaciers transported older deposits, which commonly makes it difficult to infer their age by dating interbedded tephra layers. Moreover, tephra deposits have been remobilized and transported by lahars more often than by glaciers (Lliboutry, 1956, p. 419–421). A large arcuate string of springs and ponds where the Río Atuel opens into the pampa, very noticeable on Landsat MSS images (see fig. 10), is the limit of the permeable material deposited by some unknown lahar and is not a morainic arc (Lliboutry, 1992).

In the field along the Argentine Río Mendoza and the Chilean Río Juncal-Aconcagua, which flow in opposite directions, the following morainic systems have been recognized (Caviedes and Paskoff, 1975; Espizúa, 1993):

Chilean side	Argentine side
Portillo (2,650 m)	Horcones (2,750 m)
Ojos de Agua (2,100 m)	Penitentes (2,500 m)
Guardia Vieja (1,600 m)	Punta de Vacas (2,350 m)
Salto del Soldado (1,300 m)	Uspallata (1,870 m)

Today, large glaciers in the region flow down to 3,000–3,600 m on the Chilean side and down to 3,200–3,800 m on the Argentine side. The lowest, oldest moraines should correspond in the Río Maipo drainage basin (southwestern part of fig. 9) to moraines at 1,400–1,800 m, in particular the huge moraine in the Río Yeso valley studied by Marangunic and Thiele (1971) (south-central part of fig. 9).

According to Espizúa (1993), the glacial drift of the Uspallata morainic system is older than 360 ka (10^3 years). Therefore, a moraine that has abundant pumice and was deposited by a piedmont glacier at Pudahuel (Santiago airport, 600 m) should be even older. It might have been deposited at 1.2 Ma (10^6 years), the time of the largest glaciation in Patagonia. At the Santiago site, the moraine has been covered by fluvial sediments. Corings reveal other fluvial sediments below the pumice moraine and, below that, very old and altered glacial drift. We speculate that this altered drift may be of the same age (3.5 Ma) as the glacial drift discovered by Mercer and Sutter (1982) in Patagonia.

Kuhle (1985) found erratic boulders 7.5 km upstream from Punta de Vacas at 3,620 m, 1,020 m above the bottom of the valley. If they were deposited by the glacier ending at Uspallata, 51 km downstream, the mean surface slope of this "Ice Age" glacier would have been 3.43 percent. It was surrounded by summits 800 m higher. These figures are very similar to the ones for the Batura Glacier (Karakoram, Pakistan), which has been thoroughly studied by a Chinese group (Batura Glacier Investigation Group, 1976, 1980). The ablation zone of the Batura Glacier is a valley glacier 43.5 km long that has a mean slope of 3.55 percent. Therefore, we may assume similar balances and temperatures. The Uspallata Glacier probably had an ELA at about 4,000 m (instead of the present 5,000-m ELA in this area). In fact, it was less than 4,000 m because of the subsequent uplift of the Andes Mountains by several hundred meters. At that elevation, the mean air temperature was about –5°C, and the mean precipitation over the glacier was the equivalent of about 1.35 m of water per year, a value that is now reached 200–250 km farther to the south. Thus, contrary to Kuhle's assertion, the lowering of the air temperatures was small and might only have compensated for the somewhat lower elevation of the Andes. As already suggested by Viers (1965) and by Caviedes and Paskoff (1975), the main factor of the "Ice Age" was a northward shift of the rainy province. Lower mean temperatures on a global scale might have caused this shift of the general atmospheric circulation.

References Cited

Baglietto, E.E., 1957, Contributions to applied geodesy presented to the XIth General Assembly of the IUGG at Toronto: Buenos Aires, Universidad de Buenos Aires, Engineering Faculty, 24 p.

Batura Glacier Investigation Group, 1976, 1974–1975 investigation report on the Batura Glacier in the Karakoram Mountains, The Islamic Republic of Pakistan: Beijing, People's Republic of China, Batura Glacier Investigation Group of Karakoram Highway Engineering Headquarters, 123 p. [In Chinese, summaries and captions in English.]

———1980, Professional papers on the Batura Glacier, Karakoram Mountains: Lanchow, People's Republic of China, Academia Sinica, compiled in 1978 by the Institute of Glaciology, Cryopedology and Desert Research, 271 p., 16 plates, color map at a scale of 1:60,000.

Cabrera, G.A., 1984, Balances de masa de los glaciares del Cajón del Rubio, nacientes del Río de Las Cuevas, Andes Argentinos, 1982/84 [Mass balances of glaciers in Cajón del Rubio, sources of Río de Las Cuevas, 1982–84], *in* Jornadas de hidrología de nieves y hielos en América del Sur, Santiago de Chile, 3–8 de Diciembre 1984: United Nations Educational, Scientific, and Cultural Organization, International Hydrology Programme, v. 1, p. 17.1–17.27.

Caviedes, C.N., and Paskoff, R., 1975, Quaternary glaciations in the Andes of north-central Chile: Journal of Glaciology, v. 14, no. 70, p. 155–170.

Cobos, D., 1981, Evaluación de los recursos hídricos sólidos de la Cordillera de los Andes: Cuenca del Río Atuel [Evaluation of the snow and ice resources of the Andes: the Río Atuel basin]: Mendoza, Informe del Instituto Argentino de Nivología y Glaciología-Consejo Nacional de Investigaciones Cientificos y Técnicos (IANIGLA–CONICET), 50 p.

Corte, A.E., 1976, Rock glaciers: Biuletyn Peryglacjalny, no. 26, p. 174–197.

———1980, Glaciers and glaciolithic systems of the central Andes, *in* World glacier inventory, proceedings of the Riederalp (Switzerland) workshop: International Association of Hydrological Sciences-Association Internationale des Sciences Hydrologiques, Publication 126, p. 11–24.

Corte, A.E., and Espizúa, L.E., 1981, Inventario de glaciares de la cuenca del Río Mendoza [Glacier inventory of the Río Mendoza Basin]: Mendoza, IANIGLA–CONICET, 62 p., 19 maps.

Escobar, Fernando, Casassa, Gino, and Pozo, V., 1995, Variaciones de un glaciar de montaña en los Andes de Chile central en las últimas 2 decadas [Variations of a mountain glacier in the Andes of central Chile during the last two decades]: Institut Français d'Études Andines Bulletin (Lima), v. 24, no. 3, p. 683–695.

Escobar, Fernando, and Vidal, F., 1992, Experiencia sobre la determinación de la linea de nieve en cuencas de Chile central [Experience on the determination of the snowline in drainage basins of central Chile]: Sociedad de Ingeniería Hidráulica Revista (Santiago), v. 7, no. 2, p. 5–18.

Espizúa, L.E., 1986, Fluctuations of the Río del Plomo glaciers: Geografiska Annaler, v. 68A, no. 4, p. 317–327.

Espizúa, L.E., 1993, Quaternary glaciations in the Río Mendoza valley, Argentine Andes: Quaternary Research, v. 40, p. 150–162.

Espizúa, L.E., and Aguado, C., 1984, Inventario de glaciares y morenas entre los 29° y 35° de lat. Sur, Argentina [Inventory of glaciers and moraines between lat 29° and 35°S., Argentina], *in* Jornadas de hidrología de nieves y hielos en América del Sur, Santiago de Chile, 3–8 de Diciembre 1984: United Nations Educational, Scientific, and Cultural Organization, International Hydrology Programme, v. 1, p. 7.1–7.17.

Espizúa, L.E., and Bengochea, J.D., 1990, Surge of Grande del Nevado glacier (Mendoza, Argentina) in 1984: Its evolution through satellite images: Geografiska Annaler, v. 72A, no. 3–4, p. 255–259.

Giardino, J.R., Shroder, J.F., Jr., and Vitek, J.D., eds., 1987, Rock glaciers: Boston, Allen and Unwin, 355 p.

González-Ferrán, Oscar, 1995, Volcanes de Chile: Santiago, Instituto Geográfico Militar, 641 p.

Helbling, R., 1919, Beiträge zur topographischen Erschliessung der Cordillera de los Andes zwischen Aconcagua und Tupungato [Contribution on the topographic exploration of the Andes Mountains between Aconcagua and Tupungato]: Ak. Alpenclub Zürich, 23d Jahresbericht, 1918, 77 p., maps.

———1935, The origin of the Río Plomo ice-dam: Geographical Journal, no. 85, p. 41–49.

Igarzábal, A.P., 1981, El sistema glaciolítico de la cuenca superior del Río Juramento, Provincia de Salta [The rock glacier system of the upper drainage basin of the Río Juramento basin, Salta Province]: Congreso Geológico Argentino, VIII, San Luis, 20–26 September 1981, Actas 4, p. 167–183.

Jackson, J.A., ed., 1997, Glossary of geology (4th ed.): Alexandria, Va., American Geological Institute, 769p.

Kuhle, M., 1985, Spuren der hocheiszeitlichen Gletscherbedeckung in der Aconcagua-Gruppe (32–33°S.) [Traces of the greatest extent of an Ice Age glacier in the Aconcagua Group (lat 32°–33°S.)]: Zentralblatt der Geologie und Paläeontologie, Teil I, Verhandlungen der Südamerika-Symposiums 1984 in Bamberg, v. 11–12, p. 1635–1646.

Lliboutry, Louis, 1954a, Le massif du Nevado Juncal, ses pénitents et ses glaciers [The Nevado Juncal Massif, its penitents and its glaciers]: Revue de Géographie Alpine, v. 42, no. 3, p. 465–495.

———1954b, The origin of penitents: Journal of Glaciology, v. 2, no. 15, p. 331–338.

———1956, Nieves y glaciares de Chile, fundamentos de glaciológia [Snow and glaciers of Chile, fundamentals of glaciology]: Santiago, Universidad de Chile Ediciones, 472 p., maps.

———1958, Studies of the shrinkage after a sudden advance, blue bands, and wave ogives on Glaciar Universidad (central Chilean Andes): Journal of Glaciology, v. 3, no. 24, p. 261–272.

———1961, Phénomènes cryonivaux dans les Andes Santiago (Chili) [Cryological phenomena in the Andes of Santiago (Chile)]: Biuletyn Peryglacjalny, no. 10, p. 209–224.

———1964, Traité de glaciologie, tome 1: Glace, neige, hydrologie nivale [Treatise of glaciology, v. 1: Ice, snow, snow hydrology]: Paris, Masson et Cie, 427 p.

———1965, Traité de glaciologie, tome 2: Glaciers, variations du climat, sols gelés [Treatise of glaciology, v. 2: Glaciers, climatic variations, frozen ground]: Paris, Masson et Cie, 612 p.

Lliboutry, Louis, 1986, Rock glaciers in the dry Andes, in International symposium on glacier mass-balance, fluctuations and runoff, Alma-Ata, U.S.S.R., 30 September–5 October 1985, Proceedings: Materialy Glyatsiologicheskikh Issledovaniy [Data on glaciological studies], no. 58, p. 18–25 and p. 139–144.

———1990a, About the origin of rock glaciers (letter to the editor): Journal of Glaciology, v. 36, no. 122, p. 125.

———1990b, The origin of waves on rock glaciers (letter to the editor): Journal of Glaciology, v. 36, no. 122, p. 130.

———1992, Sciences géométriques et télédétection [Geometric and remote-sensing sciences]: Paris, Masson et Cie, 289 p.

Lliboutry, Louis, Gonzalez, O., and Simken, J., 1958, Les glaciers du désert chilien [The glaciers of the Chilean desert], *in* General Assembly of Toronto, v. 4, 3–14 September, 1957: Association Internationale d'Hydrologie Scientifique, Publication 46, p. 291–300.

Marangunic, C., and Thiele, R., 1971, Procedencia y determinaciones gravimétricas de espesor de la morena de la Laguna Negra, Provincia de Santiago [Origin and gravimetric surveys of the thickness of the moraine of the Laguna Negra, Santiago Province]: Santiago, Universidad de Chile, Departamento de Geología Publication 38, 25 p.

McClelland, Lindsay, Simkin, Tom, Summers, Marjorie, Nielsen, Elizabeth, and Stein, T.C., eds., 1989, Global volcanism 1975–1985, the first decade of reports from the Smithsonian Institution's Scientific Event Alert Network (SEAN): Englewood Cliffs, N.J., Prentice Hall, and Washington, D.C., American Geophysical Union, 655 p.

Mercer, J.H., ed., 1967, Southern Hemisphere glacier atlas: U.S. Army Natick Laboratories, Earth Sciences Laboratory, Series ES–33, Technical Report 67–76–ES, 325 p., maps.

Mercer, J.H., and Sutter, J.F., 1982, Late Miocene-earliest Pliocene glaciation in southern Argentina: Palaeogeography, Palaeoclimatology, Palaeoecology, v. 38, p. 185–206.

Paskoff, R., 1967, Notes de morphologie glaciaire dans la haute vallée du Río Elquí (Province de Coquimbo, Chili) [Notes on glacial morphology in the upper valley of Río Elquí (Coquimbo Province, Chile)]: Association des Géographes Français Bulletin, Jan–Feb, 1967, p. 44–55.

Peña, H., Vidal, F., and Escobar, Fernando, 1984, Caracterización del manto nival y mediciones de ablación y balance de masa en Glaciar Echaurren Norte [Characterization of the snow cover and measurements of ablation and mass balance on Glaciar Echaurren Norte], *in* Jornadas de hidrología de nieves y hielos en América del Sur, Santiago de Chile, 3–8 de Diciembre 1984: United Nations Educational, Scientific, and Cultural Organization, International Hydrology Programme, v. 1, p. 12.1–12.16.

Peña, H., Vidal, F., and Salazar, C., 1984, Balance radiativo del manto de nieve en la alta cordillera de Santiago [Radiation balance of the snow cover in the high cordillera of Santiago], *in* Jornadas de hidrología de nieves y hielos en América del Sur, Santiago de Chile, 3–8 de Diciembre 1984: United Nations Educational, Scientific, and Cultural Organization, International Hydrology Programme, v. 1, p. 14.1–14.28.

Prieto, M. del R., 1986, The glacier dam on the Río Plomo: A cyclic phenomenon: Zeitschrift für Gletscherkunde und Glazialgeologie, v. 22, no. 1, p. 73–78.

Raymond, C.F., 1987, How do glaciers surge? A review: Journal of Geophysical Research, v. 92B, no. 9, p. 9121–9134.

Simkin, Tom, and Siebert, Lee, eds., 1994, Volcanoes of the world (2d ed.): Tucson, Ariz., Geoscience Press, Inc., in association with the Smithsonian Institution, 349 p.

Spedizione Condor, 1989, Relazioni Geodetiche [Geodetic relationships]: Padova, Italy, Istituto di Scienza e Tecnica delle Costruzioni, Internal report, 67 p.

U.S. Board on Geographic Names, 1967, Chile (2d ed.): Washington, D.C., Department of the Interior, Office of Geography, 591 p.

———1989, Gazetteer of Peru (2d ed.): Washington, D.C., Defense Mapping Agency, 869 p.

———1992a, Gazetteer of Argentina: Washington, D.C., Defense Mapping Agency, 2 v., 1,202 p.

———1992b, Gazetteer of Bolivia (2d ed.): Washington, D.C., Defense Mapping Agency, 719 p.

———1992c, Supplement to Chile gazetteer: Washington, D.C., Defense Mapping Agency, 171 p.

Valdivia, P., 1984, Inventario de glaciares Andes de Chile central (32°–35° lat. S), Hoyas de los ríos Aconcagua, Maipo, Cachapoal y Tinguiririca [Inventory of glaciers in the central Andes of Chile (lat 32°–35°S.) in the basins of the Aconcagua, Maipo, Cachapoal, and Tinguiririca Rivers], *in* Jornadas de hidrología de nieves y hielos en América del Sur, Santiago de Chile, 3–8 de Diciembre 1984: United Nations Educational, Scientific, and Cultural Organization, International Hydrology Programme, v. 1, p. 6.1–6.24.

Viers, G., 1965, Observations sur la glaciation quaternaire dans les Andes de Mendoza [Observations on the Quaternary glaciation in the Mendoza Andes]: Revue Géographique des Pyrénées et du Sud-Ouest, v. 36, p. 89–116, color sketch map of the glaciers and old moraines in the Río Atuel drainage basin.

Glaciers of the *Wet Andes*

By Louis Lliboutry[1]

Abstract

In the southern part of South America in the *Wet Andes*, the mean air temperature at sea level decreases progressively from 13.7 degrees Celsius at latitude 37°23' South to 6.5 degrees Celsius at latitude 53°10' South, where west winds become almost permanent and very strong. Precipitation reaches 4.0 to 4.7 meters per year on the west, windward side of the mountains, and 6 to 7.5 meters per year on the Patagonian ice fields, but it remains very low on the east, leeward side. In Patagonia, precipitation is evenly distributed throughout the year, but in summer, it is frequently rainy even on the ice fields.

Between latitude 35° and 45°30' South (extended *Lakes Region*), 37 volcanoes have about 300 square kilometers of glaciers, most of them on the west side of the ice divide. South of latitude 41° South, cirque glaciers are found as well. South of latitude 45°30' South in the *Patagonian Andes*, a very large number of glaciers are present in addition to three large ice fields: the Northern Patagonian Ice Field (4,200 square kilometers, with 30 outlet glaciers [Editor's note: Masamu Aniya inventoried 28 outlet glaciers in 1988 from this field]), the Southern Patagonian Ice Field (13,000 square kilometers, with 48 outlet glaciers of more than 20 square kilometers in area), and the ice field of Cordillera Darwin in the southwest part of Tierra del Fuego (2,300 square kilometers).

In the 1990's in Patagonia, the time of geographical exploration and of the conquest of virgin summits is almost over, but glaciological investigations have replaced them. Some glacier-velocity, mass-balance, and even energy-balance measurements have been made on 4 outlet glaciers of the Northern Patagonian Ice Field and 11 outlet glaciers of the Southern Patagonian Ice Field. Subglacier topography has been determined along a single east-west profile across the Northern Patagonian Ice Field; the elevation of the glacier bed ranges there between +596 meters and −223 meters. Two glaciers flowing westward, Glaciar San Rafael (Northern Patagonian Ice Field) and Glaciar Brüggen (or *Pío XI*) (Southern Patagonian Ice Field) have flow velocities near their calving fronts of more than 17 meters per day and 15.2–36.8 meters per day, respectively. Three bands of tephra ejected by *Cerro (Volcán) Lautaro* are visible on a large part of the Southern Patagonian Ice Field. They are the outcrops of three layers of tephra within the ice.

Patagonian ice fields are temperate. The mean mass balance at 1,296 meters on Glaciar San Rafael, about 250 meters above the equilibrium line altitude, was found to be 3.45 meters per year (water equivalent). The main climatic factor providing glacier fluctuation is the elevation of the limit between rain and snowfall during every precipitation event.

Glacier fluctuations in the *Wet Andes* have been monitored since 1945 by aerial photographic surveys and satellite imagery. A general recession has taken place, but different patterns emerge from one glacier to another. The largest recessions are those of Glaciar O'Higgins (12.4 kilometers), which calves into Lago San Martín/O'Higgins, and of Glaciar Upsala, which calves into Lago Argentino. An abnormal behavior is the large advance of Glaciar Brüggen (*Pío XI*) into Fiordo Eyre. It is suggested that its former recession was due to the volcanic activity of *Cerro (Volcán) Lautaro*.

Many glaciations (maybe 40) have taken place in Patagonia during the last 7 million years, but only one at 1.2–1.0 Ma was more extensive than the last glaciation (by 80 kilometers at the latitude of Lago Argentino). The last glaciation left two morainic systems, the inner one resulting from at least five glacier advances between 70 ka and 11 ka. The elevation of the ice divide on the northern Southern Patagonian Ice Field was probably 2,100±200 meters at that time, 300 to 700 meters higher than today. Thus, all the relief was not covered by a convex ice cap, as assumed by others. To explain the scouring and overdeepening of north-trending Patagonian channels, it is suggested that local ice fields often formed on the Pacific islands. Four "Little Ice Ages," dated at 3.6 ka, 2.3 ka, 1.4 ka, and 250 years before present, have been recognized in Patagonia. The last one followed a time that had a milder climate than the one today, and had winds from the northeast, as documented by old logbooks.

Mapping, Aerial Photography, and Satellite Imagery

In 1954, the orography of the Andes Mountains south of lat 35°S. was more or less well known as far south as lat 42°S. on the Chilean side and as far south as lat 43°S. on the Argentine side. This was because mountaineers from Club Andino Bariloche (C.A.B.) had explored the area around Lago

[1] 3, Avenue de la Foy, 38700 Corenc, France.

Puelo (lat 42°10'S., long 71°38'W.). In the same year, the U.S. Army Air Force Preliminary Charts (Carta Prelíminar, CP) became available. At a scale of 1:250,000, these were compiled from 1945 Trimetrogon aerial surveys. After reduction, they became the 1:1,000,000-scale U.S. Air Force (USAF) Operational Navigation Charts (ONC) R–23, S–21, and T–18 that cover the *Wet Andes* area. On the CP's, contour lines were drawn at 500 feet, 1,000 feet, and then at 1,000-foot contour intervals. On a large part of the ONC's, no contour lines are shown at all.

North of Puerto Aisén (lat 45°25'S., long 72°42'W.), the Trimetrogon aerial photographic survey was done too early in the season, when extensive snowpack covered the terrain. Therefore, these charts, CP's at a scale of 1:250,000 and ONC's at a scale of 1:1,000,000, cannot be used as a basis for a glacier inventory. In particular, the extensive glaciers shown on the northern part of ONC S–21 on the Argentine side of the popular Lakes Region simply do not exist.

South of Puerto Aisén, most of the Andes lie in Chile. The west side is almost always hidden in the rain and fog. At Grupo Evangelistas (lat 52°20'S., long 75°05'W.), there are 360 rainy days a year! Rain forest, swamps, fjords, and ice fields that have tidal outlet glaciers make ground exploration exceptionally difficult and commonly nearly impossible. In spite of considerable effort by mariners since the 16th century, the fantastic labyrinth of channels and fjords along the west coast of Chile south of Puerto Aisén was very poorly known before publication of the CP. The Trimetrogon aerial surveys were carried out in this area from December 1944 to March 1945 on the very rare cloudless days. Publication of the chart in 1953–54 allowed the biggest map revision in the Earth's geography to be made in modern times. Only mysterious Isla Santa Inés at lat 53°46'S., long 72°40'W., remained incompletely surveyed. This highly dissected island has several fjords, one of which hid the German battleship *Dresden* in 1914 after the battle of the Falkland Islands (Islas Malvinas).

In spite of the fact that the aerial surveys of the southern *Wet Andes* were carried out under optimum conditions, the ice fields, outlet glaciers, and other glaciers are very poorly defined on the CP and on the three ONC's (R–23, S–21, and T–18). In addition, geographic place-names are few and far between, and many are incorrect. For this reason, my sketch maps, published in Lliboutry (1956), are reproduced here and have some new geographic names added (see figs. 27, 29, 30, and 37).

Because the Trimetrogon aerial survey of January and February 1945 remains an essential source of data for the Northern and Southern Patagonian Ice Fields, the following information is provided on Sorties (flights) and photographic frame numbers in order to complete the ones given by Mercer (1967, p. 133–145). The survey mission designation for all the U.S. Army Air Force aerial survey flights over southern Patagonia is 91–PC–5M–4028, except for Sortie 406, which is 91–PC–4M–4028 (Masumu Aniya, written commun., 1997).

Northern Patagonian Ice Field:

Sortie 406, Frames 85–124: East side from Glaciar Circo (Glaciar Grosse) to Glaciar Pared Sur
Sortie 558, Frames 10–41: West side from Glaciar Steffen to Golfo Elefantes

Southern Patagonian Ice Field (northern part):

Sortie 556 (2 January 1945),
Frames 1 6–49: East side from Río Pascua to Glaciar Viedma
Frames 53–85: West side from *Meseta del Comandante (Caupolicán)* to the north limit of the ice field
Frames 100–110: West side, 30 km farther west overflying

Glaciar Occidental
Frames 115–149: Center of ice field from Glaciar Brüggen to the vicinity of Fiordo Calén (*Cerro (Volcán) Lautaro* on 556–V–124)

Southern Patagonian Ice Field (southern part):

Sortie 410 (23 January 1945),
Frames 115–223: From the south end (Cordillera Sarmiento) to Glaciar O'Higgins (valley from Fiordo Peel to *Fiordo Mayo*) on 410–V–168 (*Nunatak del Viedma* on 410–V–207)
Sortie 411, Frames 1–25: From Lago Argentino to the Paine group (terminus of Glaciar Moreno on 411–V–9)

[In Lliboutry (1956), I wrote 1946 instead of 1945 for the date of the photography, as was told to me at the Instituto Geográfico Militar of Chile (IGMC). However, Prof. Aniya has brought to my attention that the months and years are printed on all of the CP maps, and they are always from December 1944 to March 1945.]

The era without accurate maps is now over. Aerial surveys by the Chilean Air Force and by the USAF started in May 1966 and used Doppler positioning to measure and locate surveyed peaks accurately. The surveys allowed the progressive publication from north to south in the 1970's and 1980's by the IGMC of maps at a scale of 1:50,000. The map of the Northern Patagonian Ice Field, based on aerial photographs of 1974, was published in 1982. However, the elevations and contour lines that are essential for glaciological work remain questionable on the large ice fields of southern Patagonia, where the ground is uniformly white and stereoscopic observation of photographs is impossible. As for the highest summit, Monte San Valentín, an elevation of 3,876 m was based on terrestrial triangulation by Nordenskjöld in 1921. Later the elevation was thought to be 4,058 m. The 1:50,000-scale map shows 3,910 m. A French group that climbed the peak in 1993 included two surveyors, who calculated an elevation of 4,080±20 m by using a Global Positioning System (GPS).

On the Argentine side, the IGMA compiled maps at a scale of 1:100,000 that cover the east side of the ice field from Monte FitzRoy/Cerro Chaltél to *Lago Frias*. Geodetic ground control was provided through triangulation, traversing, and some Doppler (Transit system) satellite determinations. Although these maps have been available for sale to the public since their publication in the late 1980's, my sketch maps of 1956 are still used by mountaineers visiting this region. Argentina also made aerial surveys of the area between Monte FitzRoy/Cerro Chaltél and Lago San Martin/O'Higgins in 1966 and 1981. The IGMA compiled maps at a scale of 1:50,000 from the coverage of 1966, as required by the Argentine-Chilean Commission in charge of establishing the international boundary in this region. From this map and the 1981 aerial photographs, González and Veiga (1992) drew a map of the FitzRoy group.

A comparison of the 1945 aerial surveys and more recent data (Landsat images, aerial photographs, and maps, for example) allows a comparative time-lapse study of glacier variation in Patagonia. Unfortunately, good satellite images without cloud cover are scarce. The most useful Landsat 1, 2, and 3 multispectral scanner (MSS) images of glaciers of the *Wet Andes* are listed in table 8. Naruse and Aniya (1992) published a Landsat 5 Thematic Mapper (TM) false-color mosaic of the Southern Patagonian Ice Field [see fig. 32*B*] using three images (table 1) acquired on 14 January 1986 under very rare, almost cloudless conditions.

In spite of extremely adverse weather conditions, the mountains and ice

TABLE 8.—*Most useful Landsat 1, 2, and 3 images of the glaciers of the* Wet Andes
[Table 1 lists all the optimum Landsat 1, 2, and 3 images of the glaciers of Chile and Argentina]

Path-Row	Nominal scene center (lat-long)	Landsat identification number	Date
242–98	54°22'S. 67°54'W.	30380–13120	20 Mar 79
246–95	50°09'S. 71°30'W.	21441–13200	02 Jan 79
246–96	51°34'S. 72°11'W.	21441–13202	02 Jan 79
247–96	51°34'S. 73°37'W.	30385–13400	25 Mar 79
248–91	44°30'S. 71°58'W.	21515–13324	17 Mar 79
248–92	45°55'S. 72°32'W.	2399–13401	25 Feb 76
248–93	47°20'S. 73°07'W.	2399–13404	25 Feb 76
248–93	47°20'S. 73°07'W.	30368–13444	08 Mar 79
248–94	48°44'S. 73°44'W.	2399–13410	25 Feb 76
248–94	48°44'S. 73°44'W.	30368–13450–D	08 Mar 79
248–94	48°44'S. 73°44'W.	30368–13450	08 Mar 79
248–94	48°44'S. 73°44'W.	30368–13450–B	08 Mar 79
248–95	50°09'S. 74°22'W.	30368–13453	08 Mar 79
249–84	34°32'S. 69°58'W.	2418–13420	15 Mar 76
249–85	35°58'S. 70°24'W.	2022–13464	13 Feb 75
249–86	37°24'S. 70°52'W.	2382–13440	08 Feb 76
249–87	38°49'S. 71°20'W.	2382–13442	08 Feb 76
249–88	40°14'S. 71°50'W.	2436–13431	02 Apr 76
249–89	41°40'S. 72°20'W.	2436–13433	02 Apr 76
249–90	43°05'S. 72°51'W.	21516–13380	18 Mar 79
249–91	44°30'S. 73°24'W.	2130–13485	01 Jun 75

fields of southern Patagonia have been the goal of many expeditions (Naruse and Aniya, 1992, 1995). The results of these expeditions allow confirmation of interpretations made from aerial photographs and satellite images.

This section of the "Satellite Image Atlas of Glaciers of the World" ("Glaciers of South America" volume) is an assessment of existing knowledge in 1997. An extremely important development of Patagonian glaciology is foreseeable in the near future with the use of spaceborne imaging radar, which can survey the Earth's surface through cloud cover. Moreover, interferometric observations from sequential radar images will allow daily measurements of the velocities of fast outlet glaciers (Rignot and others, 1996b).

Climatic Setting

As one travels to the south, the mean annual temperatures decrease progressively. Near sea level, the mean annual temperatures at the following meteorological stations are as follows:

Los Ángeles (*Central Valley*, lat 37°23'S.)	13.7°C
Melinca (Islas Guaitecas, lat 43°54'S.)	10.0°C
Punta Arenas (Strait of Magellan, lat 53°10'S.)	6.5°C

At the same time, the wind (always from the west or northwest) becomes stronger and stronger, and the climatological differences between the west and the east sides of the Andes Mountains become more pronounced.

Very few meteorological stations exist in the Andes and in Chilean Patagonia. Therefore, the type of vegetation present is a very useful indicator of the climate and for preparing climatic maps (Quintanilla, 1974).

At lat 35°S., the annual precipitation in the Andes is about 1,500 mm a^{-1}. It is 2,471 mm a^{-1} at the Albanico hydroelectric plant (lat 37°20'S., elevation 850 m) and 3,083 mm a^{-1} at the Las Raíces tunnel on the Lonquimay railroad (lat 38°30'S., elevation 1,200 m). In this region at moderate elevations, the characteristic flora (which includes *Peumus boldus* and *Quillaja saponaria*) of the Tinguiririca and Cachapoal valleys is replaced by a roble forest (*Nothofagus obliqua*). At higher elevations, the forest is mainly the spectacular pehuén (*Araucaria araucana*).

At lat 39°30'S., the already high annual precipitation shows a major increase, and precipitation becomes distributed throughout the year. Whereas the annual precipitation is 2,489 mm a^{-1} at Valdivia on the Pacific coast (lat 39°50'S.), in the Andes at the same latitude, 4,970 mm a^{-1} has been measured at Puerto Fuy on Lago Pirehueico (lat 39°52'S., elevation 750 m). At Petrohué on Lago Todos Los Santos (lat 41°08'S., elevation 700 m), the figure is 4,000 mm a^{-1}, although this site is in the lee of Volcán Osorno. Under this extremely wet climate at moderate elevations, the roble forest is replaced by the *Bosque valdiviano* along with *Aextoxicum punctatum* (olivillo), *Eucryphia cordifolia* (ulmo), and *Drimys winteri* (canelo). At higher elevations, the *Araucaria* forest is replaced by an impenetrable rain forest that has evergreen leaves of *Nothofagus dombeyi* (coigüe) and other species.

South of lat 42°S., the *Bosque valdiviano* disappears, and *Nothofagus dombeyi* is progressively replaced by *Nothofagus betuloides* (guindo). On the drier Argentine side, forests of *Fitzroya cupressoides* appear (alerce, which has given its name to an Argentine national park), including individuals as old and as large as those in the sequoia forests of North America.

Near sea level, no further increase in precipitation exists. On most west coasts, it has only been measured at lighthouses, the only inhabited places. At Valdivia (lat 39°50'S.), the precipitation was measured at 2,489 mm a^{-1}. At Melinca (lat 43°54'S.), the measurement was 3,174 mm a^{-1}; at Cabo Raper (lat 46°50'S.), it was 2,000 mm a^{-1}; and at Islas Evangelistas (lat 52°20'S.), it was 2,900 mm a^{-1}. In the interior of fjords and channels, precipitation is higher, similar to that in the Lakes District (Región de los Lagos) of Chile. At the meteorological station of Laguna San Rafael (lat 46°37'S.), the mean annual precipitation during the years 1981–85 was 4,440 mm a^{-1}; at the entrance from the Pacific Ocean to the Strait of Magellan (lighthouse of Bahía Félix, lat 52°58'S.), it was 4,700 mm a^{-1}. Precipitation increases with elevation and exceeds 6,000 mm a^{-1} of water equivalent on the Patagonian ice fields (Inoue and others, 1987; Peña and Gutiérrez, 1992). From the discharge of rivers, Escobar and others (1992) infer 7,000 mm a^{-1} of water equivalent on the western part of the Northern Patagonian Ice Field, 6,000 mm a^{-1} on its eastern part, and 6,000 to 7,500 mm a^{-1} on the Southern Patagonian Ice Field.

In the lee of the Andes, precipitation decreases sharply. At *Estancia Madsen* (12 km east-southeast of FitzRoy, at lat 49°10'S.), 850 mm a^{-1} was measured in the 1940's. Farther east, the Patagonian pampa is a steppe that has 200–300 mm a^{-1} of annual precipitation. This steppe extends south to the east side of Torres del Paine, where a small endorheic salty lake, Laguna Amarga, is found.

To the south, changes in vegetation are the result of colder temperatures. Evergreen species are replaced by deciduous species, such as *Nothofagus pumilio* (lenga) and *Nothofagus antarctica* (ñirre), and the forest becomes penetrable wherever no bogs are found. The highland forest extends upward in elevation to bare rock, perennial snow, or glaciers. No intervening highland zone of grasses exists, as in the European Alps.

Wet Andes between Tinguiririca Pass and Puerto Aisén (Lat 35° to 45°30'S.)

As shown in figure 2 of the "Glaciers of the *Dry Andes*," the elevation of the main mountain range that forms the water divide is much lower south of lat 35°S. than in the *Central Andes* (lat 31°S. to lat 35°S.). Thus, in spite of the existence of cirque basins, no cirque glaciers are present until one reaches the vicinity of Lago Nahuel Huapí (lat 41°S.).

On the west side of the main range dominating the Chilean *Central Valley* and the sea of Chiloé, an extensive string of 37 volcanoes has sufficient elevation to rise above the equilibrium line for glaciers. These volcanoes are listed in table 9. The total area of glaciers, according to an unpublished inventory by Gino Casassa, is 267 km^2. Almost no glaciological observations have been made on these ice-capped volcanoes because scientific interest in them is minimal. The main utility of satellite imagery in this area is to analyze any changes that follow effusive or explosive volcanic eruptions (González-Ferrán, 1995). A preliminary inventory of the glaciers and snowfields in the Argentine Andes between lat 39° and 42°20'S. was published by Rabassa (1981). A review of the inventories of the glaciers of Chile was done by Casassa (1995).

TABLE 9.—*Ice-capped volcanoes south of lat 35°S., Chile and Argentina*

[Slash (/) indicates a place-name variation between Argentina and Chile (for example, Monte/Cerro Tronador: Argentina, Monte Tronador; Chile, Cerro Tronador). Elevations from Carta Nacional de Chile (CNC), 1945 edition, unless otherwise indicated; CP, Carta Preliminar, which became a U.S. Air Force Operational Navigation Chart (ONC) after reduction; C.A.B., Club Andino Bariloche. Information on eruptive history from "Volcanoes of the World" (Simkin and Siebert, 1994) and "Global Volcanism 1975–1985" (McClelland and others, 1989); additional information from Andrés Rivera; n.d., no data are available. ** indicates that the volcano is not listed in either volume]

Volcano (alternate name) Argentina/Chile	Country	Elevation (meters)	Latitude south	Longitude west	Landsat Path-Row	Number of and last eruption(s)	Remarks
Cerro del Planchón/Volcán El Planchon	Argentina, Chile	3,891	35°15'	70°34'	249–84, 248–85	n.d.	
Volcán Peteroa	Argentina, Chile	3,951	35°17'	70°34'	249–84, 249–85	13 in 1991	
Volcán Descabezado Chico	Chile	3,250	35°31'	70°37'	249–85	n.d.	
Volcán Descabezado Grande	Chile	3,880	35°33'	70°45'	249–85	1 in 1932 (fumarolic)	CP: 3,830 m
Volcán Quizapu	Chile	3,810 (before explosion)	35°35'	70°45'	249–85	13 in 1967	CP: 3,050 m (after explosion that covered entire region with white tephra)
Cerro Campanario	Argentina, Chile	4,002	35°55'	70°22'	249–85	**	
Volcán San Pedro=Las Yeguas	Chile	3,500	35°59'	70°51'	249–85	**	CP: 3,499 m
Cerro Lástimas	Chile	3,050	35°59'	71°08'	249–85	**	
Nevado Longaví	Chile	3,230	36°12'	71°10'	249–85	**	CP: Nevado de Lonquen
Volcán Domuyo	Argentina	4,709	36°38'	70°26'	249–85	**	CP: 4,785 m
Nevados de Chillán	Chile	3,180	36°50'	71°25'	249–86	17 in 1987	CP: 3,169 m

TABLE 9.—*Ice-capped volcanoes south of lat 35°S., Chile and Argentina*—Continued

Volcano (alternate name) Argentina/Chile	Country	Elevation (meters)	Latitude south	Longitude west	Landsat Path-Row	Number of and last eruption(s)	Remarks
Volcán Antuco	Chile	2,985	37°24'	71°22'	249–86	12 in 1972	
Sierra Velluda	Chile	3,585	37°28'	71°26'	249–86	**	CP: 3,385 m
Volcán Copahue	Argentina, Chile	3,010	37°51'	71°10'	249–86	2 in 1992	CP: 2,969 m
Volcán Callaquén (Callaqui)	Chile	3,164	37°55'	71°25'	249–86	2 in 1980 (fumarolic)	
Volcán Tolhuaca	Chile	2,780	38°18'	71°39'	249–87	**	CP: 3,780 m (misprint)
Volcán Lonquimay	Chile	2,822	38°22'	71°35'	249–87	4 in 1989	Place-name misplaced on ONC R–23
Cordillera Blanca	Chile	2,554 (CP)	38°34'	71°34'	249–87	** Late Pleistocene-Holocene age	CP: Sierra Nevada
Volcán Llaima	Chile	3,124	38°42'	71°42'	249–87	36 in 1994	
Nevados de Sollipulli	Chile	2,326	39°00'	71°34'	249–87	**	CP: Picos de Llollicupi
Volcán Villarrica	Chile	2,840	39°25'	71°57'	249–87, 249–88	51 in 1985	
Volcán Quetrupillán	Chile	2,360	39°29'	71°42'	249–87, 248–88	Holocene age	
Volcán Lanín	Argentina, Chile	3,774	39°39'	71°31'	249–87, 249–88	Holocene age	
Volcán Shoshuenco (Chos Huenco)	Chile	2,430	39°56'	72°02'	249–88	n.d.	
Cerro (*Volcán*) Puntiagudo	Chile	2,490	40°57'	72°16'	249–88, 249–89	1 in 1930(?)	
Monte/Cerro Tronador	Argentina, Chile	3,470	41°09'	71°55'	249–89	**	CP: 3,460 m
Volcán Osorno	Chile	2,660	41°06'	72°30'	249–89	11 in 1869	
Volcán Calbuco	Chile	2,015	41°19'	72°36'	249–89	10 in 1972	Small glacier on south flank
Monte Yate	Chile	2,185	41°47'	72°24'	249–89	**	
Volcán Minchinmávida (Minchinmahuida)	Chile	2,470	42°47'	72°26'	249–90	1 in 1835	CP: 2,481 m; name and elevation given to a much lower caldera to the west-southwest
Volcán Yelcho	Chile	2,020	43°09'	72°34'	249–90	**	
Volcán Corcovado	Chile	2,300 (CP)	43°11'	72°47'	249–90	2 in 1835	ONC S–21
Cerros *(Volcán)* Yanteles	Chile	2,042 (CP)	43°30'	72°49'	249–90	Fumarolic (3 volcanoes)	
Monte Melimoyu	Chile	2,400	44°05'	72°52'	248–91, 249–91	Holocene age	
Monte Mentolat (on Isla Magdalena)	Chile	1,660	44°41'	73°05'	248–91, 249–91	n.d.	
Monte Cay	Chile	2,200 (CP)	45°03'	72°59'	248–91, 249–91, 248–92	**	ONC S–21
Monte (*Volcán*) Macá	Chile	2,960	45°06'	73°12'	249–91, 248–92	Holocene age	Elevation is much less according to Neumeyer (C.A.B., 1954, p. 20)
Volcanoes of the *Patagonian Andes*							
Cerro (*Volcán*) Hudson	Chile	~2,500	45°55'	72°57'	248–92	1991	Tephra over a wide area in 1971
Cerro (*Volcán*) Arenales	Chile	3,437	47°12'	73°29'	248–93	1979	Landsat image 30368–13444 shows tephra
Cerro Mimosa	Chile	~2,000	48°57'	73°32'	248–94	Fumarolic in 1973	
Cerro (Volcán) Lautaro	Chile	3,380	49°02'	73°33'	248–94	5 in 1979	
Cerro Aguilera	Chile	2,438	50°25'	73°47'	248–95	Holocene age	Recognized as a volcano in 1985
Monte (*Volcán*) Burney	Chile	1,758	52°21'	73°23'	246–97	1910	

Glaciers of Volcán Lanín (lat 39°40'S.) and Monte/Cerro Tronador (an old, dissected volcano) (lat 41°10'S.) (fig. 21) have been studied by Argentine scientists (Rabassa and others, 1978). In particular, Monte/Cerro Tronador has been mapped several times (fig. 22). The terminus of Glaciar Alerce, the easternmost of its 11 outlet glaciers, has been surveyed repeatedly since 1953; it shows a continuous retreat except for the period 1976–77 (fig. 23). Two of its other outlet glaciers, Glaciar Negro and Glaciar Castaña Overo, have been surveyed since 1970.

South of Lago Nahuel Huapí (fig. 22), small cirque glaciers appear, and south of Paso Cochamó (lat 41°30'S.), they become ubiquitous (see sketch maps of the area west of Lago Puelo in Lliboutry (1956, p. 346) and of the area west of Lago Menéndez in Juárez and Puente Blanco (1963)). By using Chilean vertical aerial photographs and Landsat images that cover the area (Paths, Rows 249–89, 248–90, 248–91, and 249–91; table 1), a preliminary glacier inventory can be achieved. The first glaciers that are large enough (about 12 km long) to be monitored by satellite imagery are two outlet glaciers that flow from two small ice fields. One, the Queulat ice cap (about 80 km^2), is centered at lat 44°25'S., long 72°25'W., and is at an elevation of 1,889 m according to ONC S–21. The other (about 40 km^2) is centered at an unnamed summit at lat 44°30'S., long 72°19'W., at an elevation of 2,255 m according to ONC S–21 (fig. 24). This area borders a fjord called Seno Ventisquero (ventisquero is the old Spanish name for glacier).

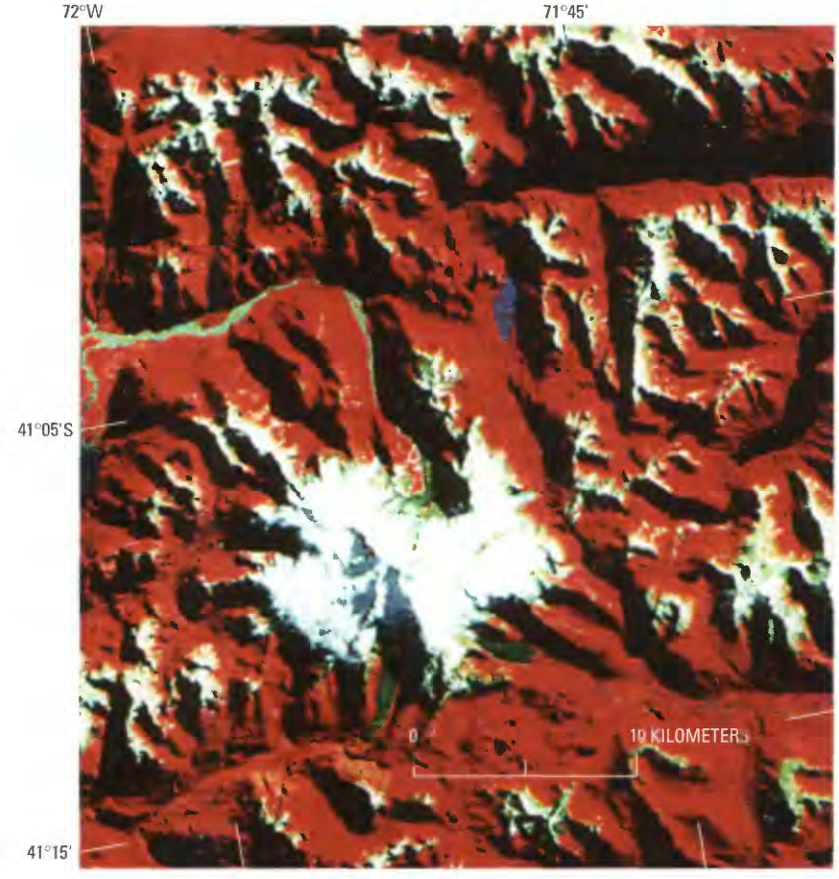

Figure 21.—*Section of a Landsat 2 MSS false-color composite image (2436–13433; 2 April 1976; Path 249, Row 89) of Monte/Cerro Tronador, an old, dissected volcano that has an ice cap and 11 outlet glaciers. Landsat image is from the EROS Data Center, Sioux Falls, S. Dak.*

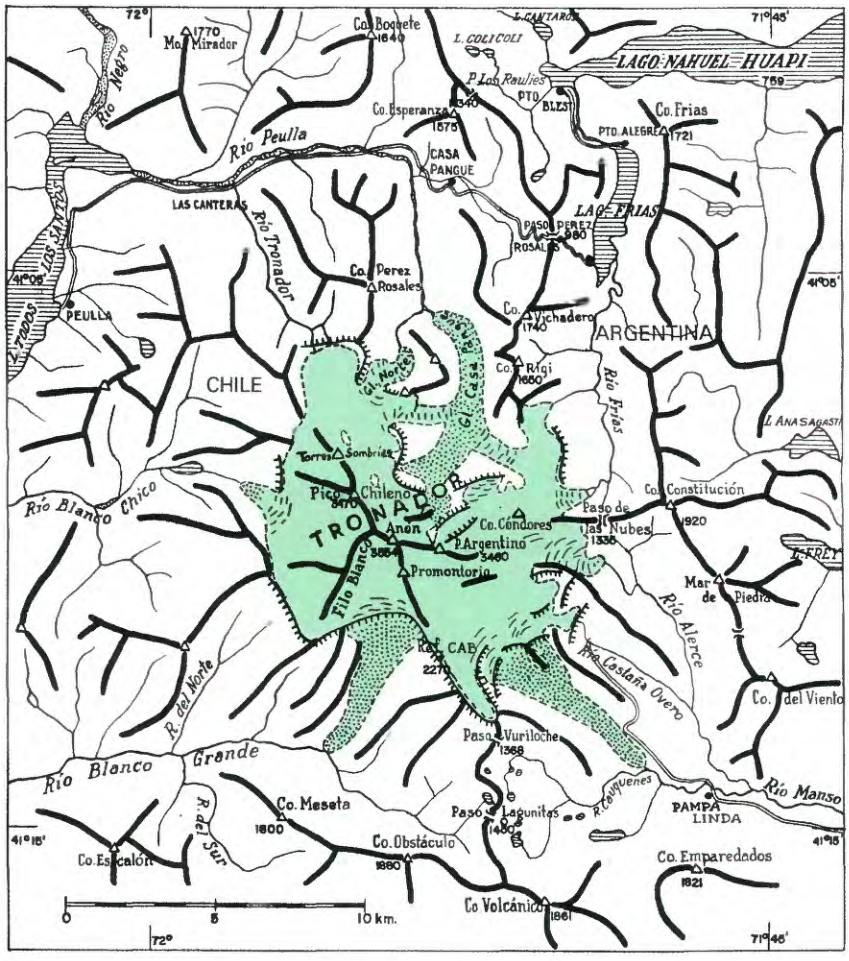

Figure 22.—*Monte/Cerro Tronador and environs, Chile and Argentina, by Lliboutry (1956). Drawn from the Carta Preliminar (CP) at a scale of 1:250,000 and from sketch maps published by Club Andino Bariloche. Since the Trimetrogon survey of 1945 (from which the CP was compiled), the east glacier at the head of Río Alerce has receded, and Laguna Alerce has formed (fig. 23). The thick lines are ridge-lines, the hachured lines are cliffs, the short lines on the glacier indicate steepness, and the dotted areas are debris-covered glaciers or rock glaciers. The border between Chile and Argentina follows the ridgelines north from south of Cerro Volcánico to Pico Argentino to west of Laguna Frias. Abbreviations: Co., Cerro; Mo., Montana; P., Pico; Pto., Puerto; L., Lago; R., Río; and Lag., Laguna.*

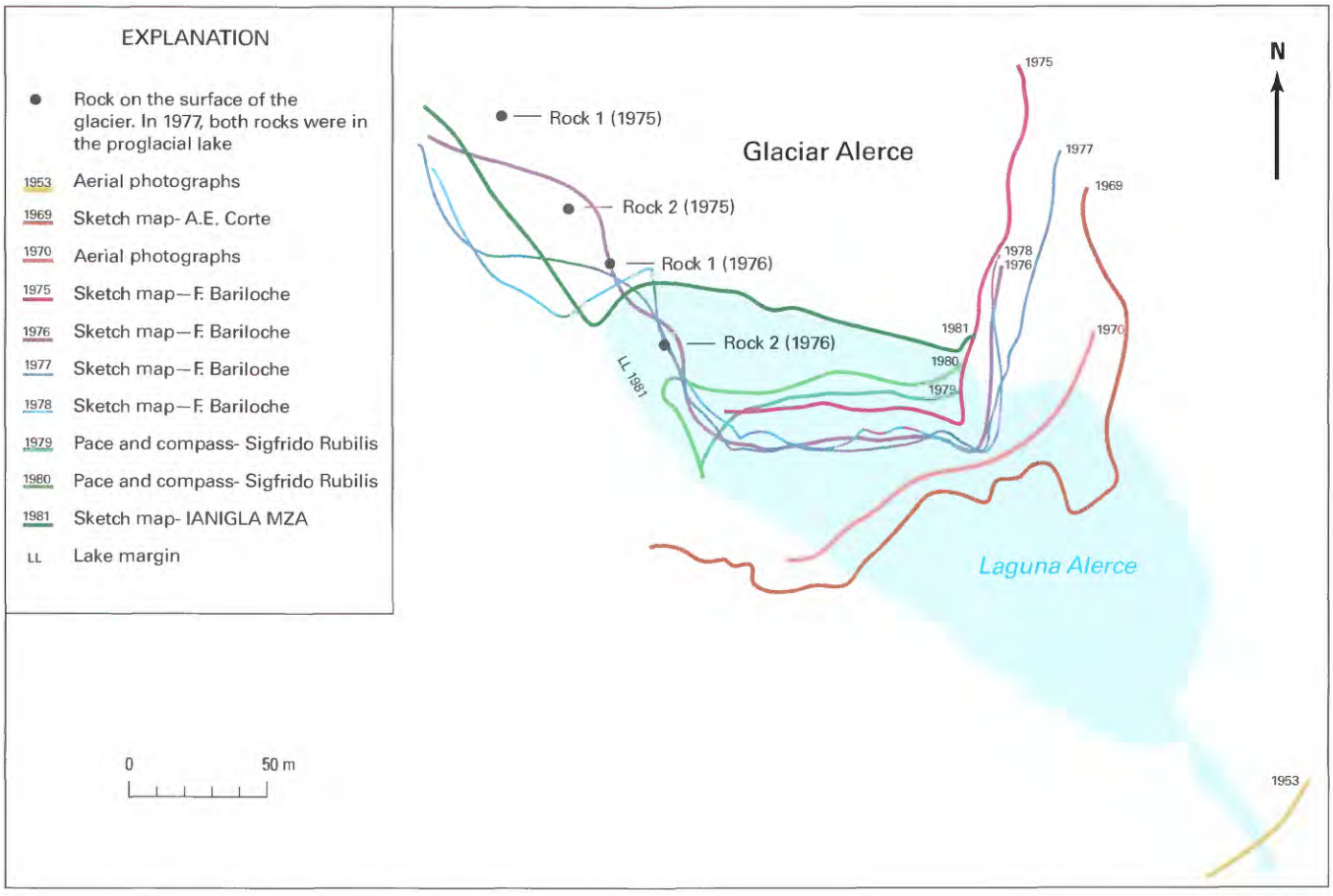

Figure 23.—*Fluctuations of the terminus of Glaciar Alerce (east flank of Monte/Cerro Tronador) between 1953 and 1981. Modified from a sketch map compiled by A.E. Corte (Instituto Argentino de Nivología y Glaciología, Mendoza (IANIGLA, MZA)).*

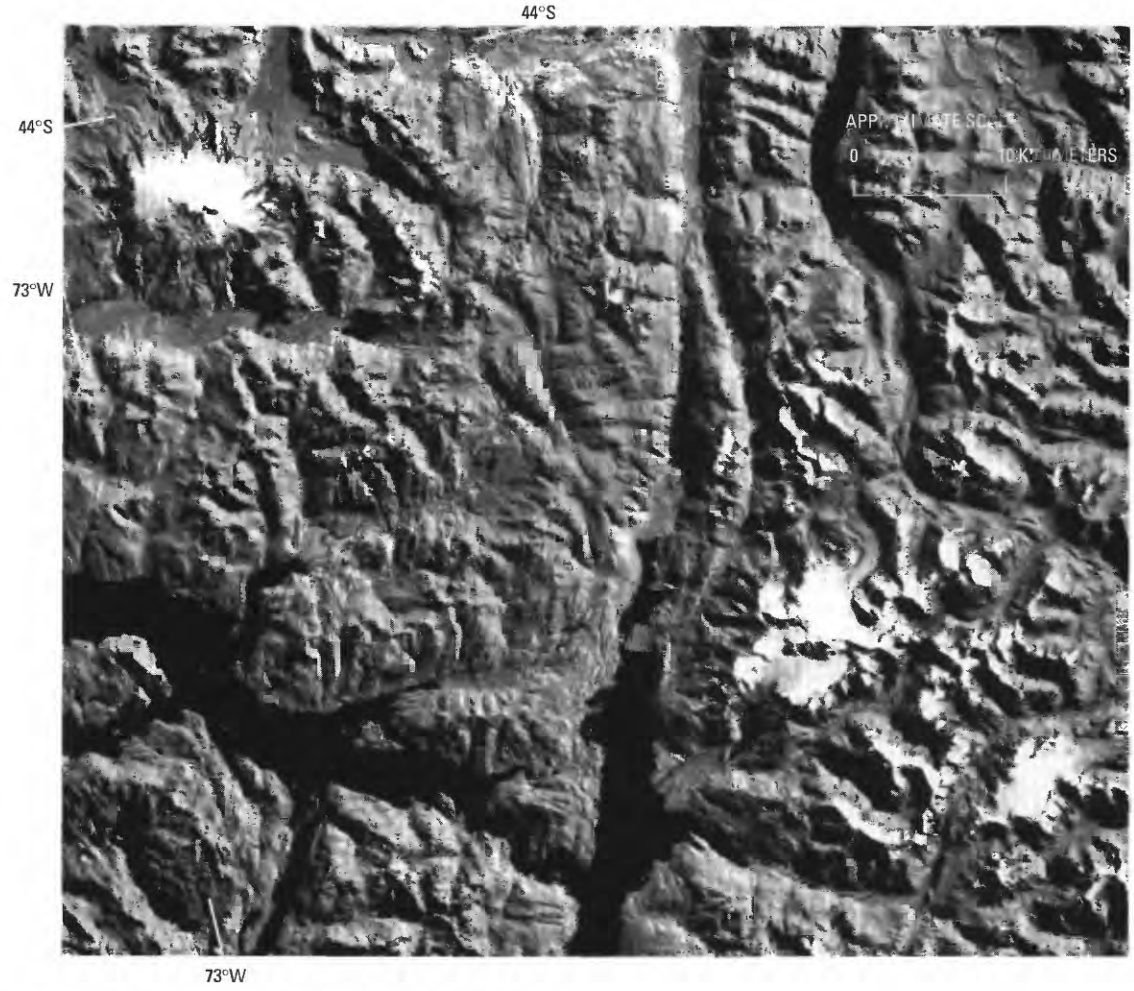

Figure 24.—*Part of a Landsat 2 MSS image (21515–13324, band 7; 17 March 1979; Path 248, Row 91) of the northern* Wet Andes *showing the volcano Monte Melimoyu in the upper left and two small ice fields that have outlet glaciers in the lower right. Landsat image is from the EROS Data Center, Sioux Falls, S. Dak.*

Patagonian Andes

Patagonian Andes Between Puerto Aisén and Río Pascua (Including the Northern Patagonian Ice Field) (Lat 45°30' to 48°S.)

Only on Landsat images (Paths, Rows 248–92, 248–93, and 248–94; table 8) can one appreciate the large number of glaciers that are present in the region. On the images, it is possible to distinguish the following:

(1) A relatively straight line of ice-capped mountain groups extending approximately along the 73°W. meridian, including mainly:
   (a) Nevado Cóndor, 1,960 m (lat 45°37'S.) (fig. 25)
   (b) An apparent, large, circular caldera (centered on lat 45°55'S.), 10 km in diameter, filled with ice, Cerro (*Volcán*) Hudson. From the caldera's ice field, a heavily debris-covered outlet glacier flows to the northwest more than 12 km to Río Huemules (fig. 25). Note that in 1971, 5 years before this image was made, Cerro (*Volcán*) Hudson had a very big explosive eruption
   (c) Another ice field of the same size that has 20 outlet glaciers at lat 46°08'S. The main outlet glacier, 2 km wide, flows to the northwest (fig. 25)
   (d) Seven other unnamed mountain groups extending to the mouth of Río Baker (the outlet of Lago Buenos Aires/General Carrera) at lat 47°50'S. (see figs. 26, 27).

(2) East of Río Baker, between Lago Buenos Aires/General Carrera and Lago San Martín/O'Higgins to the south, lies a wide belt of glacierized mountains that is dissected into many groups (southeast quadrant of figs. 26, 27, and 28). The mountains extend into Argentina, where

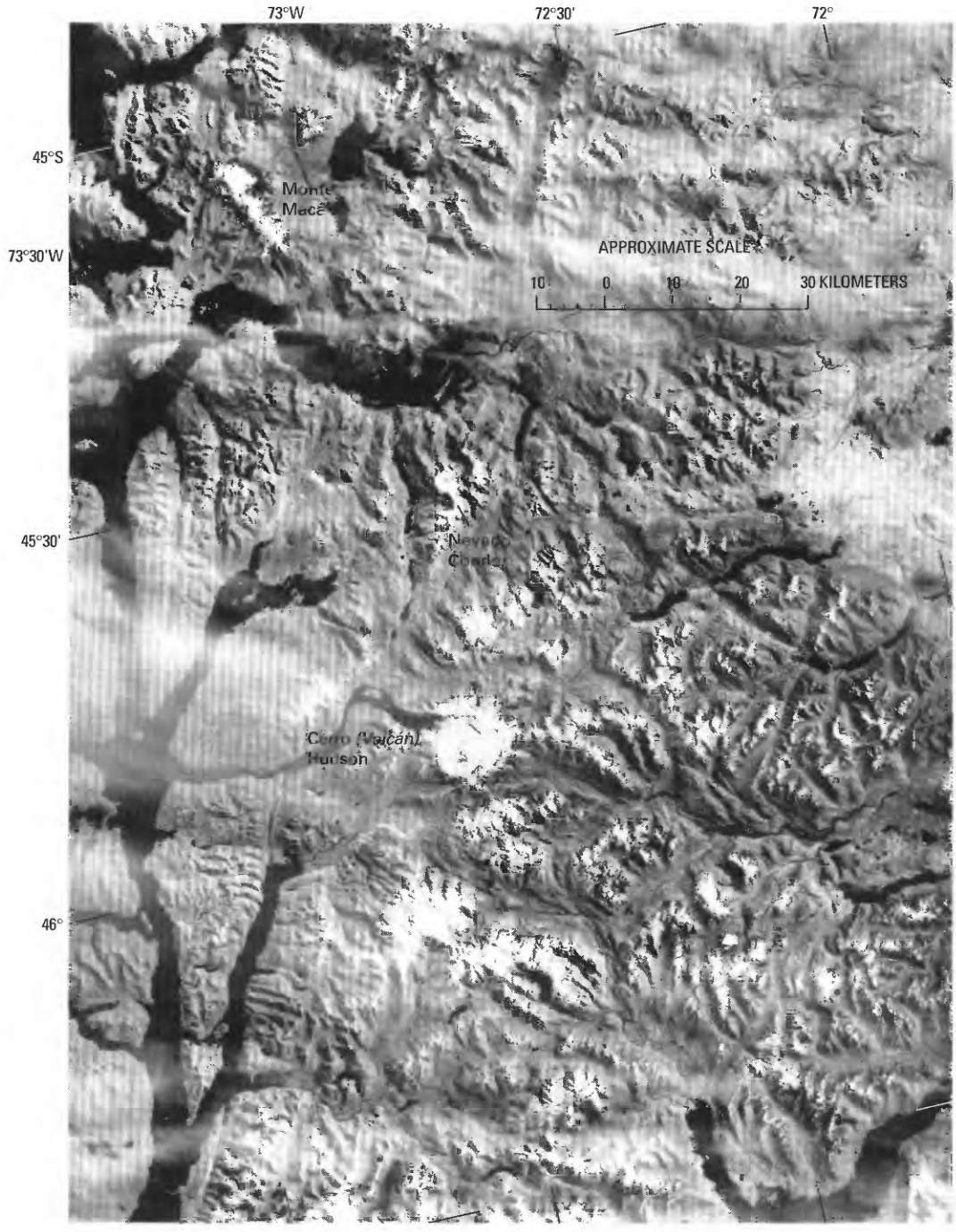

Figure 25.—*Part of a Landsat 2 MSS image (2399–13401, band 7; 25 February 1976; Path 248, Row 92) of the* Wet Andes *north of Lago Buenos Aires/General Carrera showing Monte Macá, Nevado Cóndor, and two ice fields that have outlet glaciers, one of which is located on Cerro* (Volcán) *Hudson. Landsat image is from the EROS Data Center, Sioux Falls, S. Dak.*

Bertone (1960) completed a preliminary glacier inventory. The main glacierized mountain is Cerro San Lorenzo (3,700 m, lat 47°36'S., long 72°19'W.) on the international border (east of fig. 26). (See maps in Buscaini and Metzeltin, 1989, p. 190 and p. 192). It has three large glaciers, all debris covered on their lower parts. The west, 12-km-long glacier (in Chile) shows little evidence of retreat, whereas the south (12-km-long) and east (8-km-long) glaciers (both in Argentina) are situated well below their lateral moraines.

(3) West of the central line of mountains, the Northern Patagonian Ice Field (NPIF, called in Spanish, Hielo Patagónico Norte) covers about 4,200 km^2 (figs. 26, 27, 28). Most of the NPIF is a plateau 1,100 to 1,500 m in elevation. The plateau extends 90 km from north to south and 30 km from east to west, and it is crossed by a northwest-trending range (*Cordón Aisén*). Thirty outlet glaciers discharge from this ice field

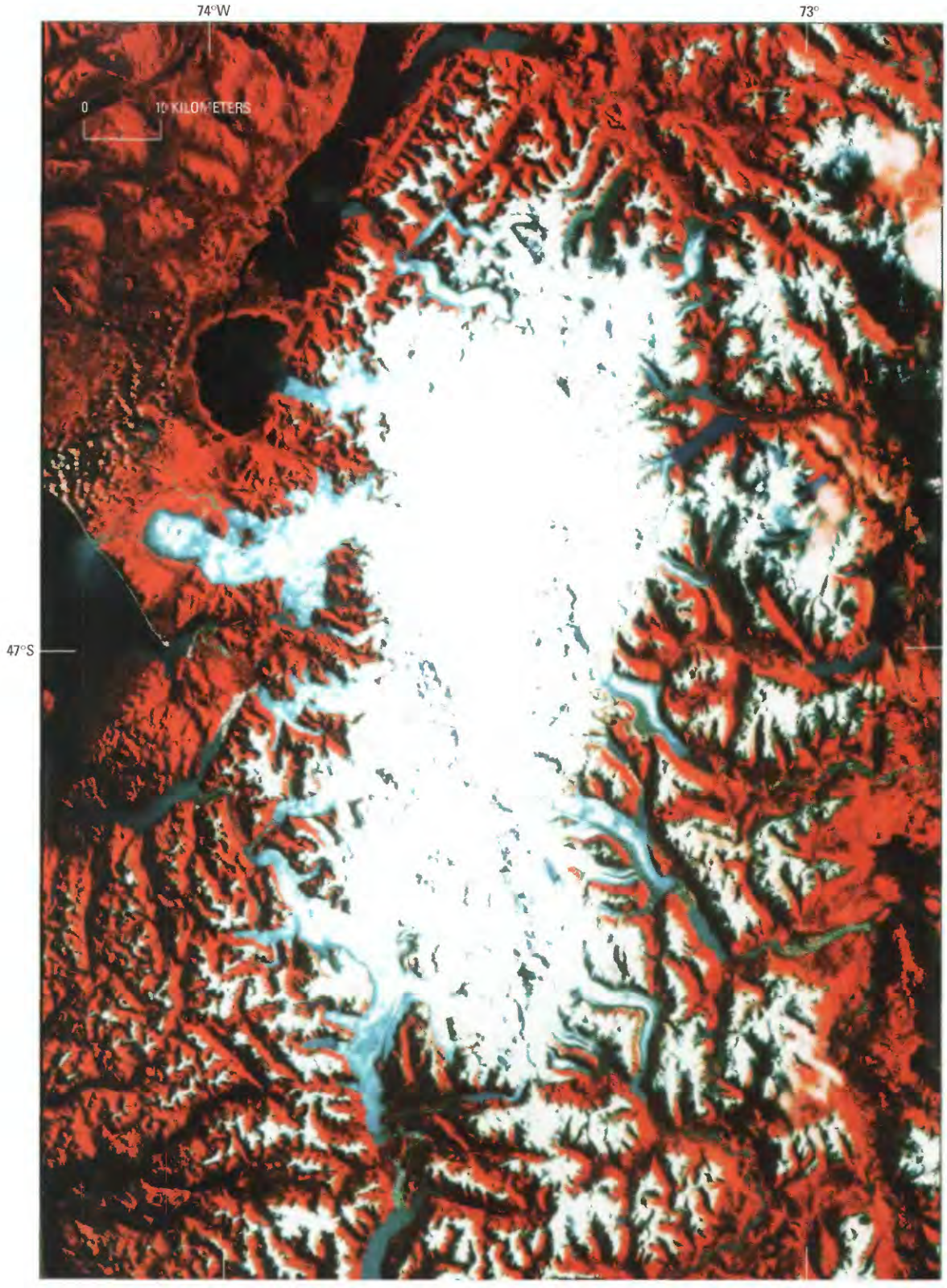

Figure 26.—*Landsat 5 MSS false-color composite image mosaic (51075–13514, bands 4, 5, and 7; 9 February 1987; Path 232, Row 92; and 51075–13520, bands 4, 5, and 7; 9 February 1987; Path 232, Row 93) of the Northern Patagonian Ice Field. See geographic place-names in figure 27. Landsat image mosaic courtesy of Masamu Aniya, Institute of Geoscience, University of Tsukuba, Ibaraki, Japan. Geometrically corrected from 1:50,000-scale topographic maps.*

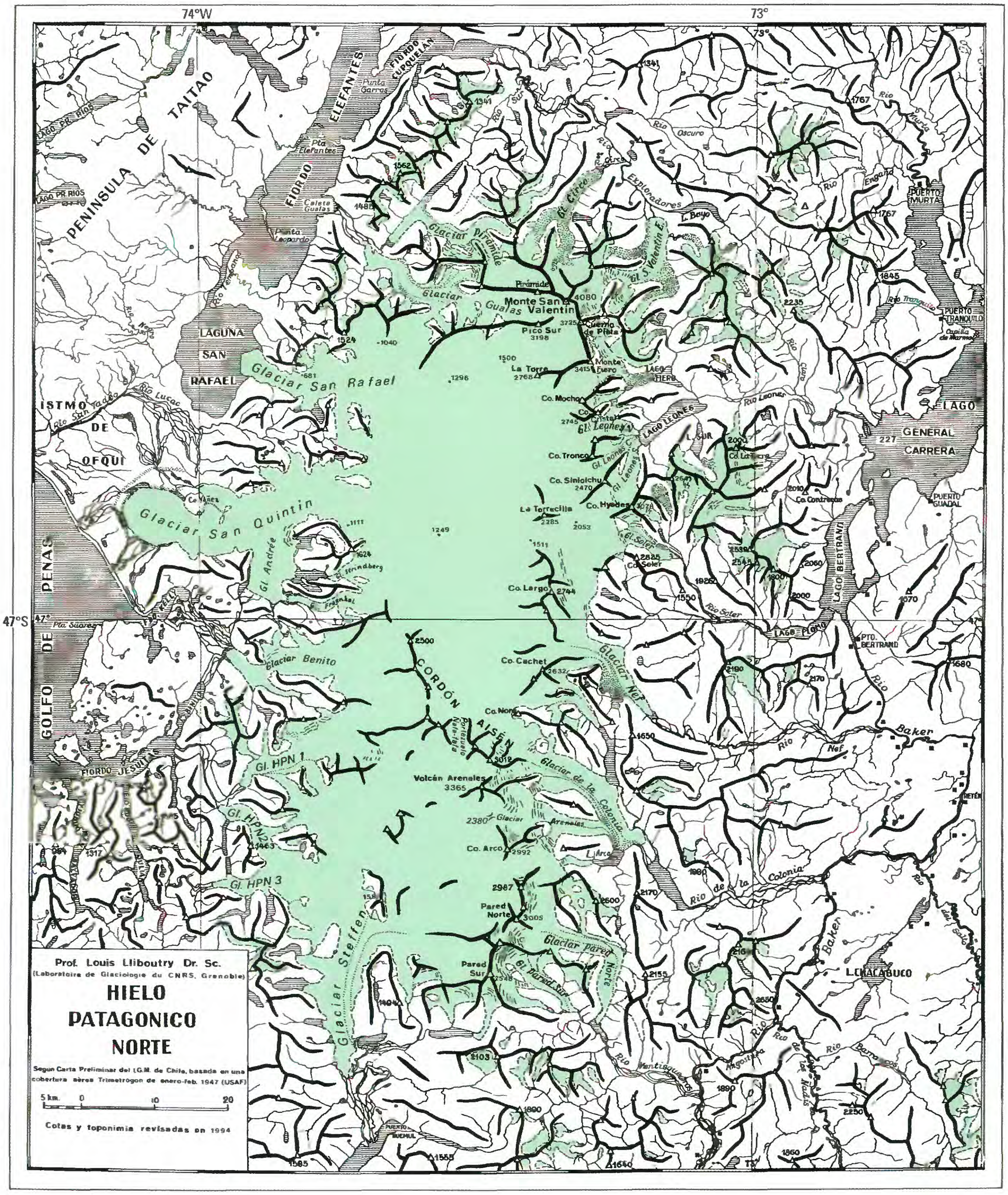

Figure 27.—Northern Patagonian Ice Field (green). Taken from Lliboutry (1956); additional geographic place-names supplied by Cedomir Marangunic. The thick lines are ridgelines. Some geographic place-names are inconsistent with those used in the text, and those in the text conform to the usage recommended by the U.S. Board on Geographic Names in the gazetteers of Argentina (1992a) and Chile (1967, 1992b).

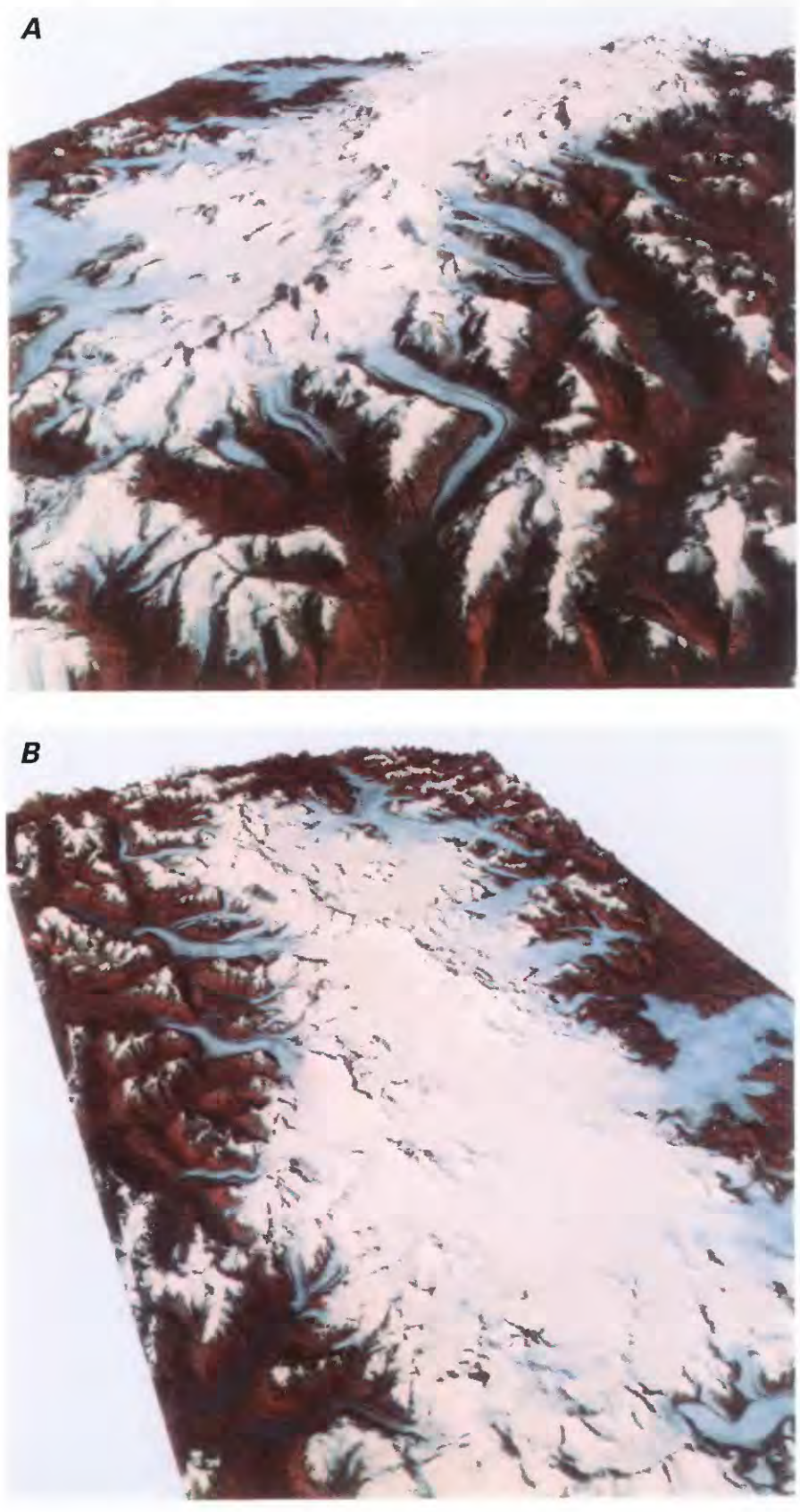

Figure 28.—*Perspective views of the Northern Patagonian Ice Field.* **A**, *Perspective view from the southeast showing the trace of* Cordón Aisén *across the ice field.* **B**, *Perspective view from the northeast. In the foreground is Monte San Valentín (compare with fig. 41A). The views were created by draping Landsat 5 MSS images of 9 February 1987 (51075–13514; Path 232, Row 92; 51075–13520; Path 232, Row 93) over a digital-elevation model. Courtesy of Masamu Aniya, Institute of Geoscience, University of Tsukuba, Ibaraki, Japan.*

[Editor's note: Aniya (1988) inventoried 28 outlet glaciers from the NPIF]. The main glaciers from the northern part of the ice field are two that flow to the west: Glaciar San Rafael (the lowest latitude tidewater glacier in the world) and Glaciar San Quintín (the largest outlet from NPIF that ends in a piedmont lobe), and two glaciers that flow to the southeast: Glaciar Nef and Glaciar de la Colonia. The main outlet glaciers of the southern part of the ice field are Glaciar Benito and three unnamed glaciers that flow to the west (HPN 1 to 3), Glaciar Steffen and Glaciares Pared (Norte and Sur) that flow to the south, and Glaciar Arenales that flows to the east, where it merges with Glaciar de la Colonia.

The equilibrium line altitude (ELA) on Glaciar San Rafael was at 1,050 m in December 1952 (Club Andino Bariloche, 1954) and at 1,200 m in October 1994 (Rignot and others, 1996b). On Glaciar Soler on the east side of the NPIF, Aniya and Naruse (1987) found the ELA at 1,350 m.

Ice thickness has been determined by using gravimetry along an east-west traverse at about lat 46°52'S. (Casassa, 1987). The surface lowers westward progressively from 1,511 m to 1,111 m over 21.85 km, whereas the bed elevation ranges irregularly between +596 m and –223 m, and the thickness ranges between 620 m and 1,458 m.

Southern Patagonian Ice Field (Lat 48°15' to 51°30'S.)

Río Pascua, the 50-km-long outlet of Lago San Martín/O'Higgins (see northeast corner of fig. 29), has no name on ONC T–18, in spite of its important discharge (510 $m^3 s^{-1}$). South of Lago San Martín/O'Higgins and Fiordo Calén (top center of fig. 29), the Southern Patagonian Ice Field (SPIF or, in Spanish, Hielo Patagónico Sur) extends more than 330 km between the watersheds of Lagos San Martín/O'Higgins, Viedma, and Argentino (fig. 30) on the east and the fjords of the Pacific Ocean on the west. Its total area (including 1,500 km^2 of contiguous glaciers) was 13,500 km^2 in 1945, reduced to about 13,000 km^2 in 1986. The ice divides between its outlet glaciers, and the equilibrium lines in 1986 have been determined from Landsat TM images by Aniya and others (1996). The number of outlet glaciers in successive ranges of areas is given below.

Total area (km^2)	>1,280	1,280–640	640–320	320–160	160–80	80–40	40–20	<20
Number of glaciers	0	4	7	9	12	13	3	?

A description of the Southern Patagonian Ice Field and its outlet glaciers from north to south is as follows (see figs. 29–39).

North of lat 49°S., most of the ice field is a uniform plateau that has only a few nunataks. The main outlet glaciers are Glaciar Jorge Montt (464 km^2), flowing northward to Fiordo Calén; Glaciar Bernardo (536 km^2), flowing westward to Fiordo Bernardo; Glaciar Greve (438 km^2), flowing westward and then southward; and Glaciar O'Higgins (820 km^2), flowing eastward to Lago San Martín/O'Higgins (fig. 29). In 1986, the ELA's on these four glaciers were at 950 m, 1,300 m, 1,000 m, and 1,300 m, respectively.

Between lat 49° and 50°S., three parallel north-south ranges about 20 km apart may be recognized (figs. 29, 34). They are not continuous, and the ice fields that fill the north-south valleys between them can escape eastward or westward through some gaps. The central range consists of *Cordón Pío XI*, which culminates at *Cerro (Volcán) Lautaro* (3,380 m), and Cordón Mariano Moreno, which culminates at Cerro Francisco Moreno (3,536 m). (One must not confuse the writer and journalist Mariano Moreno (1711–1811) with the expert (perito) of the Comisión de Límites Francisco Moreno (1852–1919). The title of Perito is, therefore, commonly kept in placenames.) Except for the active *Cerro (Volcán) Lautaro*, this range is made up of metamorphic schists of Paleozoic age that were thrust eastward over

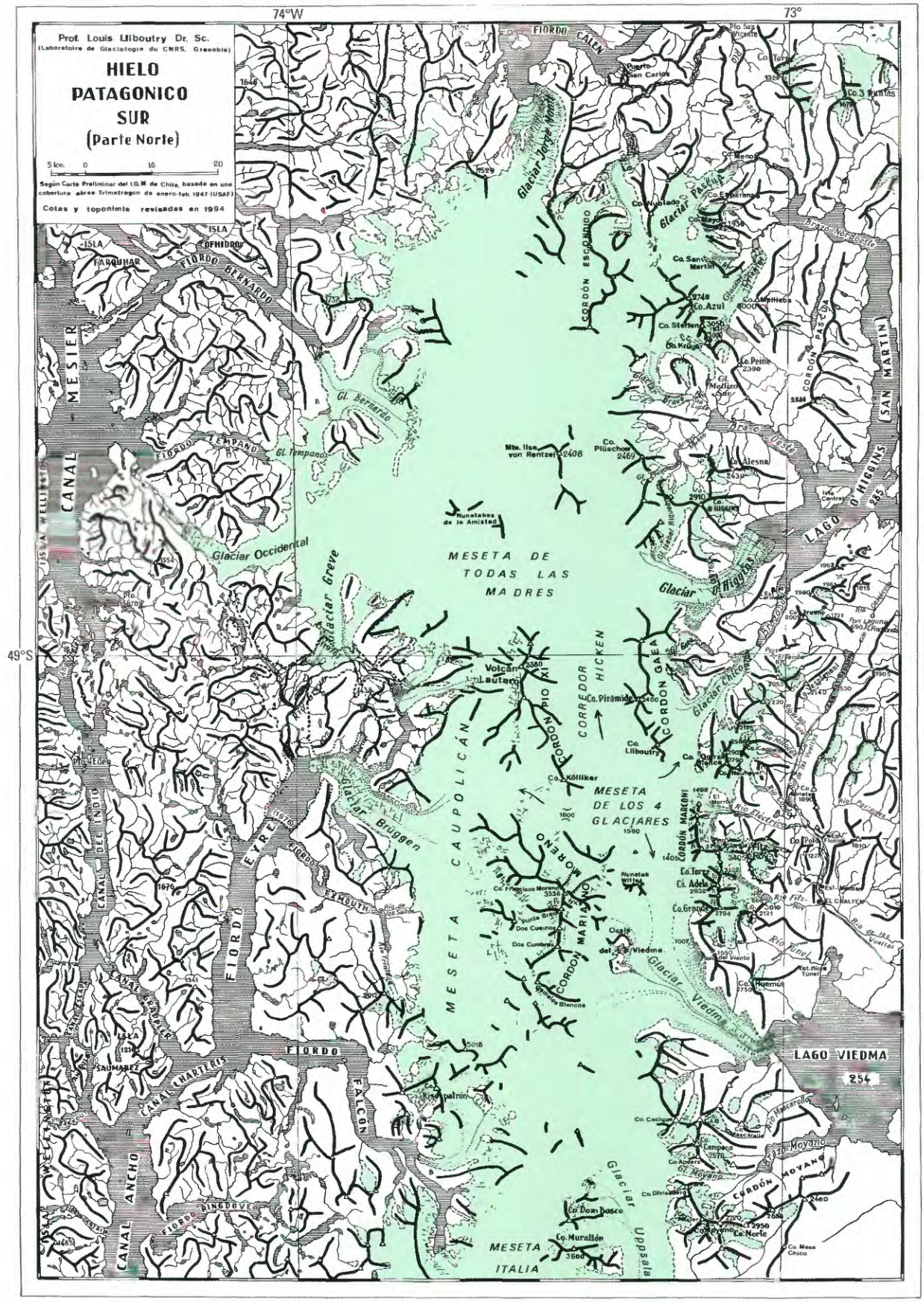

Figure 29.—*Northern part of the Southern Patagonian Ice Field (green). Taken from Lliboutry (1956); additional names supplied by Cedomir Marangunic, J. Hardt, and M. Puente (in the Anuario Club Andino Bariloche, 1963). The thick lines are ridgelines. Some geographic place-names are inconsistent with those used in the text, and those in the text conform to the usage recommended by the U.S. Board on Geographic Names in the gazetteers of Argentina (1992a) and Chile (1967, 1992b).*

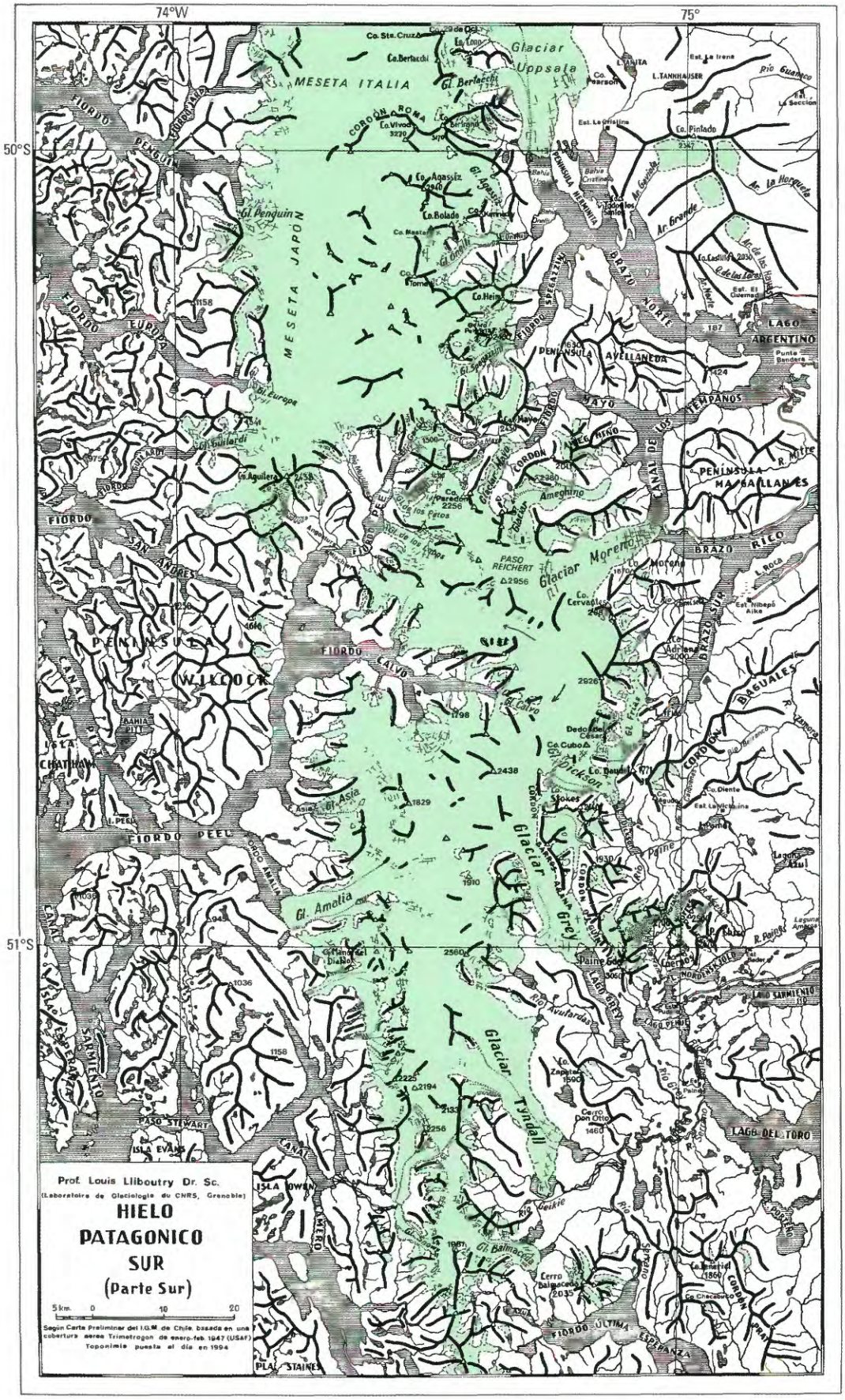

Figure 30.—*Southern part of the Southern Patagonian Ice Field (green), just south of the map in figure 29. Taken from Lliboutry (1956). The thick lines are ridgelines. Some geographic place-names are inconsistent with those used in the text, and those in the text conform to the usage recommended by the U.S. Board on Geographic Names in the gazetteers of Argentina (1992a) and Chile (1967, 1992b).*

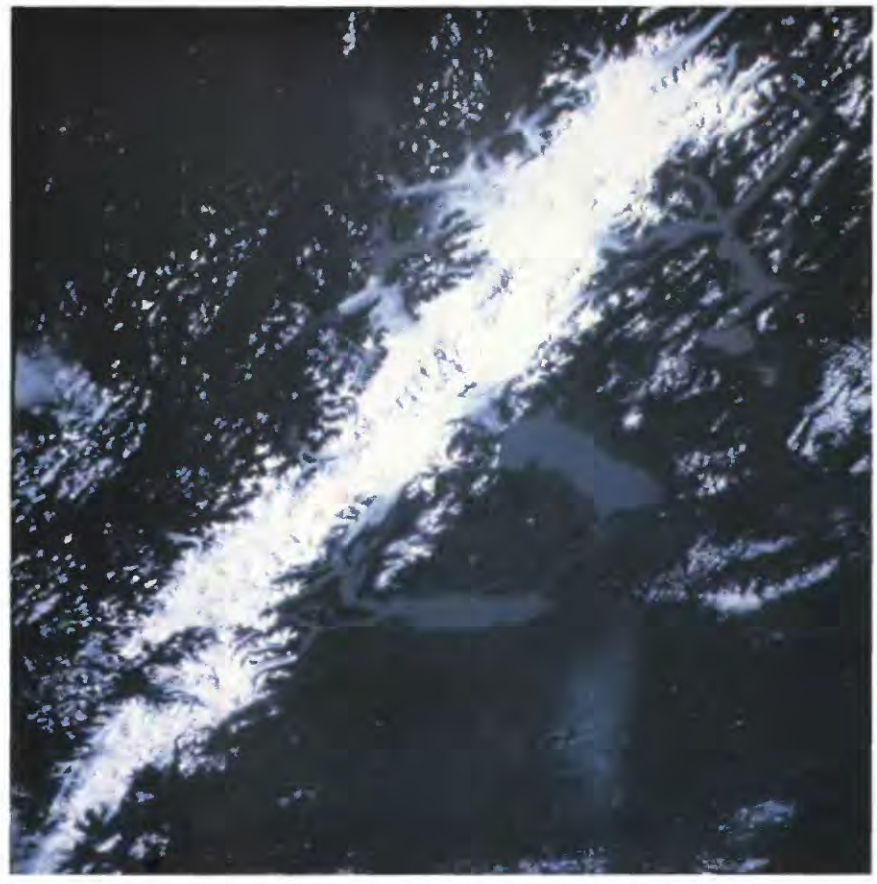

Figure 31.—*Oblique color satellite photograph of the Southern Patagonian Ice Field, Chile and Argentina. Photograph acquired on 10 March 1978 by Russian cosmonauts G.M. Grechko and Yu.V. Romanenko, courtesy of Vladimir M. Kotlyakov. This is 1 of 40 photographs taken from the Salyut-6 orbital space station of the ice fields, outlet glaciers, and other glaciers in South America that were analyzed in a paper by Desinov and others (1980); see also Williams (1986, p. 544–555; 1987).*

sedimentary rocks of Jurassic and Early Cretaceous age (Kraemer, 1992). Therefore, the north-south valleys should be primarily of tectonic, not glacial, origin.

The entire northern part of the ice-filled west valley is part of the accumulation zone of Glaciar Brüggen (1,265 km^2), discussed in a special subsection below. It was christened by its discover, Father de Agostini, as *Glaciar Pío XI* (Agostini, 1945). The official name of Glaciar Brüggen was applied 20 years later. Out of respect for the intention of Father de Agostini, I christened the range nearby as *Pío XI* (*Cordón Lautaro*) instead, but the name of *Cordón Lautaro* has prevailed. The plateau of the accumulation zone was christened *Meseta del Comandante* by an official Chilean expedition that found an access route to it from Fiordo Exmouth, and it was rechristened *Meseta Caupolicán* (named after an Araucan hero) by the Instituto de la Patagonia. Farther to the south are Glaciar Penguín (507 km^2) and Glaciar Europa (403 km^2) (fig. 30).

The east valley is filled by the ice of *Corredor Hicken*, which flows northward to join Glaciar O'Higgins; by Glaciar Viedma (903 km^2), which flows eastward and has a calving front in Lago Viedma (254 m) (fig. 35); and by Glaciar Upsala, flowing southward to a north arm of Lago Argentino (187 m) (figs. 29, 30). The ice divides that separate *Corredor Hicken* of Glaciar O'Higgins, Glaciar Chico (also calving in Lago San Martín/O'Higgins), and Glaciar Viedma, cannot be determined because the area, known as *Meseta de los Cuatro Glaciares* (plateau of the four glaciers), is very flat and almost horizontal. The fourth glacier, separated by a very slight sill, is Glaciar Brüggen to the west. Another slight sill separates *Meseta de los Cuatro Glaciares* from the Glaciar Marconi on the east, at the head of the *Río Eléctrico* valley (fig. 36). The name *Río Eléctrico* does not come from electrical storms, which are almost unknown in Patagonia. It is a name given by the local farmers, who compared the noise made by the gusts of the fierce west wind with thunder. The elevation of *Meseta de los Cuatro Glaciares* is 1,500–1,590 m (Puente Blanco, 1963b), and the ELA on Glaciar Upsala was at 1,150 m in 1986.

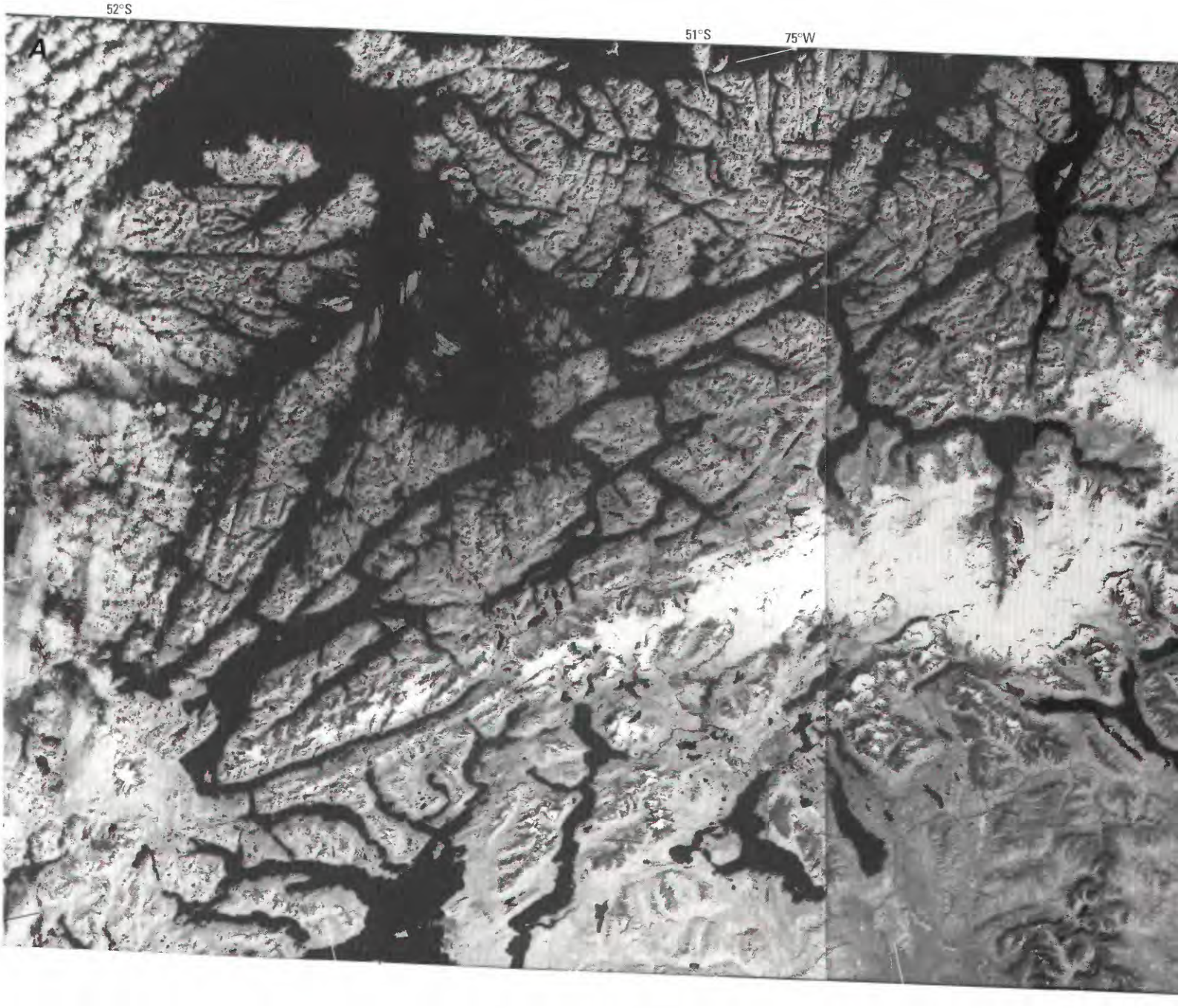

***Figure 32.**—Mosaics of the Southern Patagonian Ice Field.* **A,** *Landsat 5, band 4, Thematic Mapper (TM) mosaicked images acquired on 14 January 1986 (50684–13530; Path 231, Row 94; 50684–13533; Path 231, Row 95; and 50684–13535; Path 231, Row 96). Landsat images are from the EROS Data Center, Sioux Falls, S. Dak.* **B,** *see page I168.*

The east series of short ranges includes, from north to south, *Cordón GAEA, Cordón Marconi, Cordón Torre*, and several mountains on the northwest and southwest of Lago Viedma. *Cordón Torre* is a series of needles culminating at Cerro Torre (3,102 m) (fig. 37). Five kilometers to the northeast, another series of needles culminates at Monte FitzRoy/Cerro Chaltél (3,405 m). Both series of peaks are young intrusive stocks of granite and granodiorite intruded at 10 Ma. Thus, the floor of the very deep valley between the ranges, whose depth ranges from 1,870 m to about 600 m, has been entirely carved by glacial erosion. In February 1952, the ELA on the east glaciers of this group was at 1,250–1,300 m (Lliboutry, 1952). The needles and huge vertical walls of the FitzRoy group (fig. 38) are famous among climbers worldwide (Buscaini and Metzeltin, 1989). They are extremely difficult to climb because of the typically bad weather and very strong winds, as well as the paucity of cracks or zones of fractured rock.

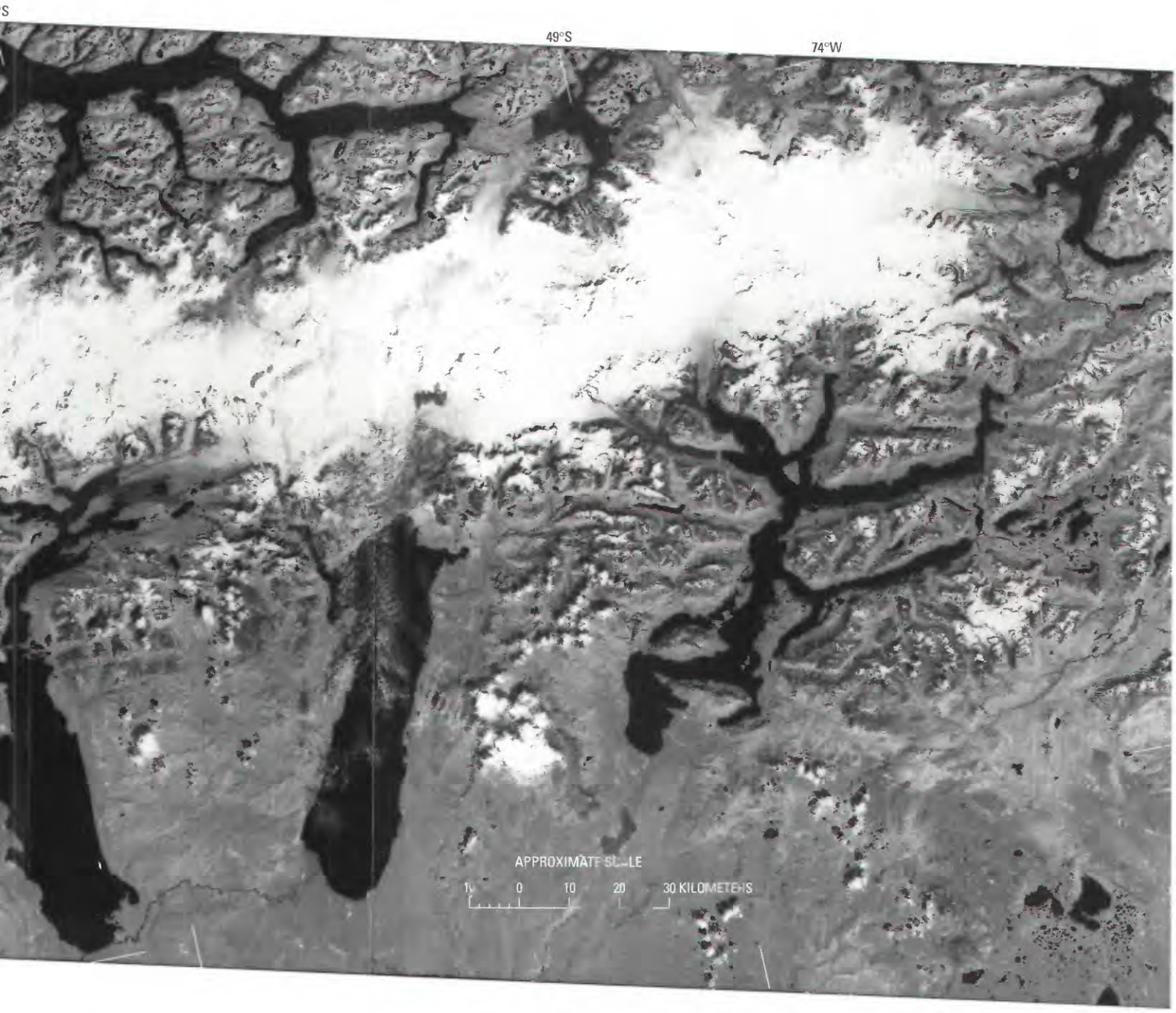

The massif has not undergone tectonic stresses, and the maritime climate allows little frost cracking.

At lat 50°24'S., the SPIF is interrupted by two transverse fjords, *Fiordo Mayo* from Lago Argentino and the northeast arm of Fiordo Peel from the Pacific Ocean (fig. 30). This arm was confused with Fiordo Andrés by F. Reichert when he saw it in the distance from the ice divide, which explains the erroneous name of Seno Andrew found on many maps. The distance between *Fiordo Mayo* and Fiordo Peel is about 18 km. In the valley between them is a small lake, *Laguna Escondida*, into which Glaciar Mayo is calving. Sometime between 1970 and 1975, this lake lost about 44 percent of its area by draining off into *Fiordo Mayo* (Pedro Skvarca, written commun.).

South of this constriction, the SPIF is narrower, without large ice plateaus. The largest glaciers are Glaciar (*Perito*) Moreno (255 km^2), which has a calving front in Lago Argentino (fig. 39), and Glaciares

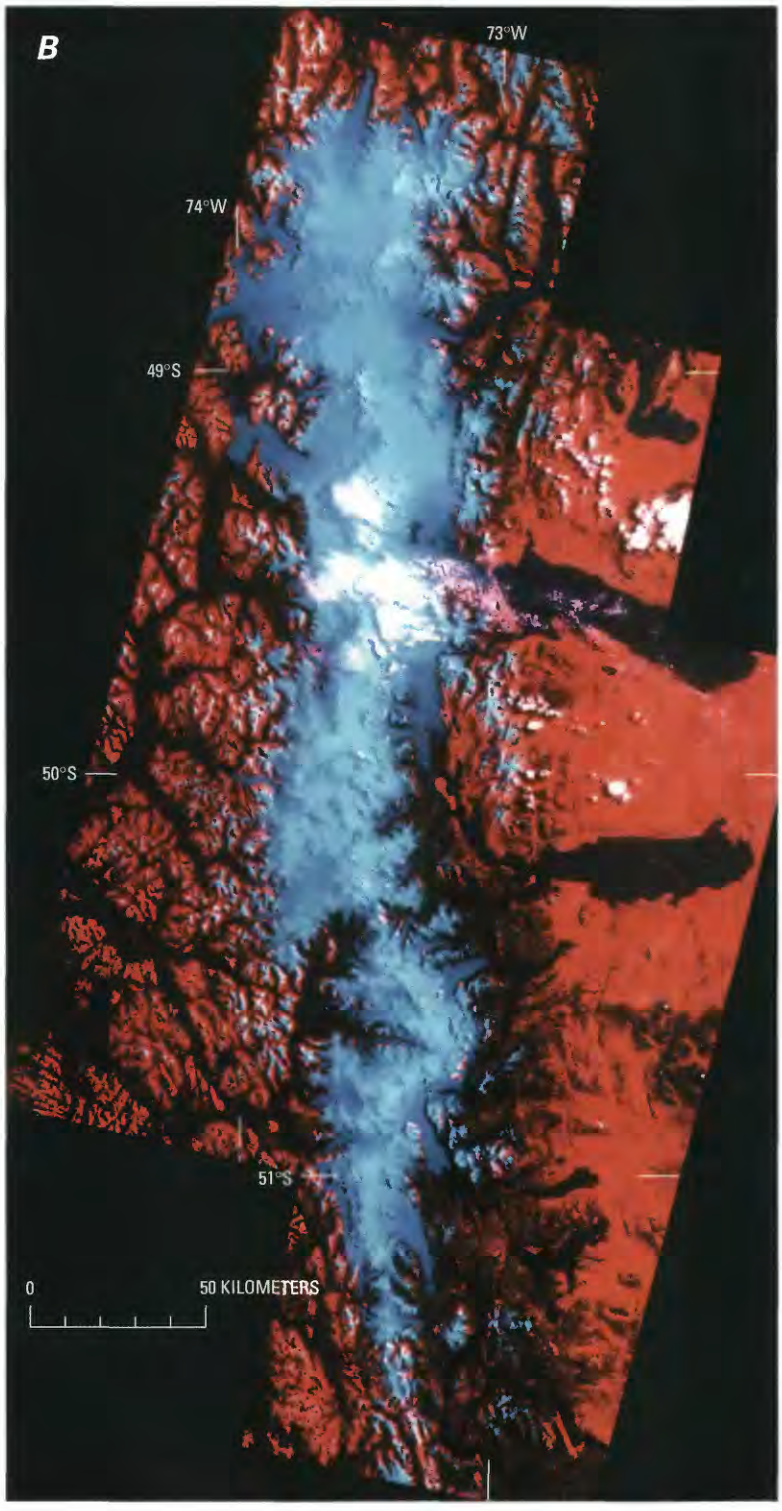

Figure 32B.—*False-color composite mosaic (TM bands 1, 2, and 5) of the same images used for* A. *Landsat mosaic courtesy of Masamu Aniya, Institute of Geoscience, University of Tsukuba, Ibaraki, Japan. Previously published in Photogrammetric Engineering and Remote Sensing by Aniya and others (1996, plate 1, p. 1364).*

Grey (269 km^2) and Tyndall (331 km^2), both flowing southward (fig. 30). The ELA on Glaciar Tyndall is at 900 m. Casassa (1992) measured its thickness across a transverse profile using a radio-echosounder. Echoes were no longer obtained beyond 3 km from the glacier's east margin where the ice thickness exceeded 600 m, the maximum range of radio-echosounding in temperate glaciers.

The spectacular Paine group, a young granodioritic intrusion similar to the FitzRoy group, and perhaps even more beautiful, stands between Glaciar Grey and the dry pampa. On a small glacier on the west side of the ice field, Glaciar Olguín, the ELA was at 1,400–1,500 m in 1955 (Luis Krahl, oral commun.). On the southernmost glacier of the SPIF, Glaciar Balmaceda (lat 51°23'S.), the ELA was at 650 m in 1986 (Aniya and others, 1996).

Figure 33.—*Landsat 2 false-color composite image of the northern part of the Southern Patagonian Ice Field on 25 February 1976. (In the lower left-hand corner, obscured by clouds, is Isla Wellington.) See geographic place-names in map, figure 29, which shows the glacier termini as they were in 1946. Note that between 1946 and 1976, Glaciar O'Higgins receded about 11 km, whereas Glaciar Brüggen advanced 9 km. A 25-km-long lake formed between Glaciar Brüggen and Glaciar Occidental. Glacier rock flour makes this lake and Lago O'Higgins appear light blue, as do the sediment plumes entering the fjords from glacial rivers or tidal glaciers. Note also that on most glaciers, the moraines and bands of tephra appear deep blue. Landsat image (2399–13410, bands 4, 5, and 7; 25 February 1976; Path 248, Row 94) is from the EROS Data Center, Sioux Falls, S. Dak.*

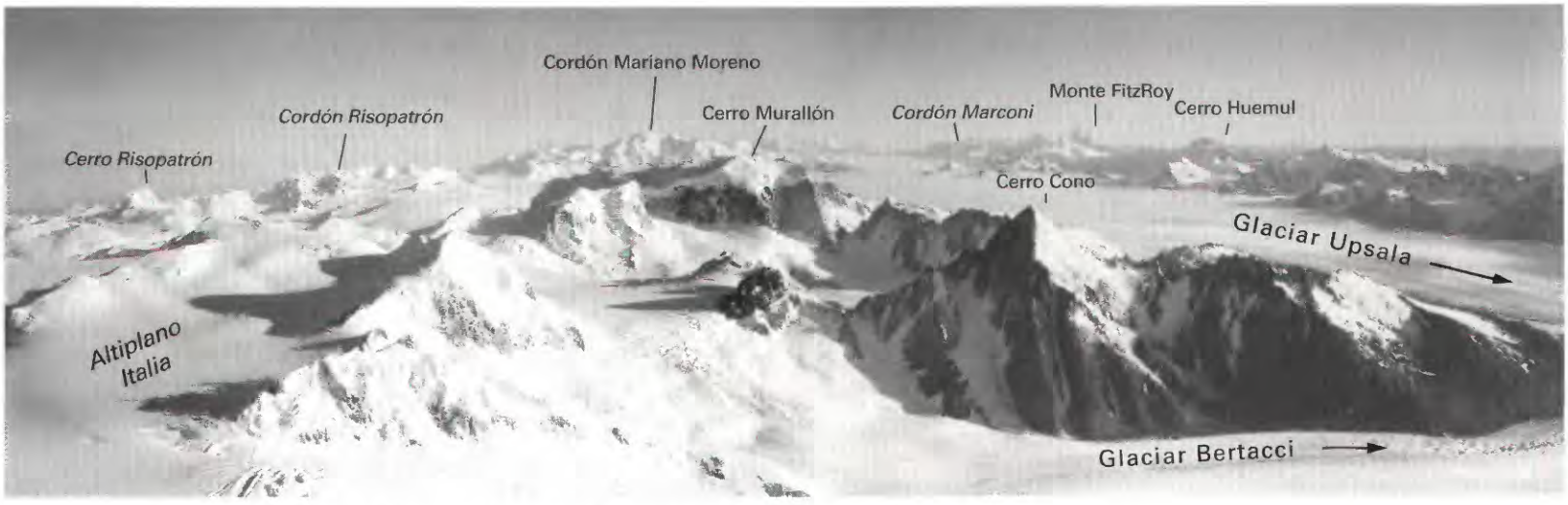

Figure 34.—*View on 11 February 1966 from the summit of Cerro Bertrand looking toward the north and showing the three mountain ranges in the middle part of the Southern Patagonian Ice Field. The west range includes* Cordón Risopatrón*; the central range includes Cordón Mariano Moreno; the east range includes* Cordón Marconi, *Monte FitzRoy, and Cerro Huemul. Photograph courtesy of Pedro Skvarca, Instituto Antártico Argentino, División Glaciología, Buenos Aires, Argentina.*

Figure 35.—*Oblique aerial photograph taken in March 1989 looking northwest at Glaciar Viedma in the Southern Patagonian Ice Field as it calves into Lago Viedma. In the background on the right is* Nunatak del Viedma *at the foot of an extensive mountain range, Cordón Mariano Moreno. Photograph courtesy of Daniel Rivademar, Buenos Aires, Argentina (furnished by Pedro Skvarca, Instituto Antártico Argentino, División Glaciología, Buenos Aires, Argentina).*

Figure 36.—*Head of the valley of the* Río Eléctrico, *just north of the FitzRoy group. Photograph taken from a helicopter looking toward the west-northwest on 29 November 1993 by Louis Lliboutry. Left:* Cordón Marconi. *Bottom right: very slightly marked* Paso Marconi *(1,498 m) on the international border, a route to the Southern Patagonian Ice Field, and behind, in the distance,* Cordón GAEA. *Middle: Glaciar Marconi; it does not reach* Laguna Eléctrico *(bottom), as was the case in 1952. On the bottom-left corner, a shoulder of moraine and scree indicates the level of the glacier that entered* Valle Eléctrico *through* Paso Marconi *during the last glacial maximum.*

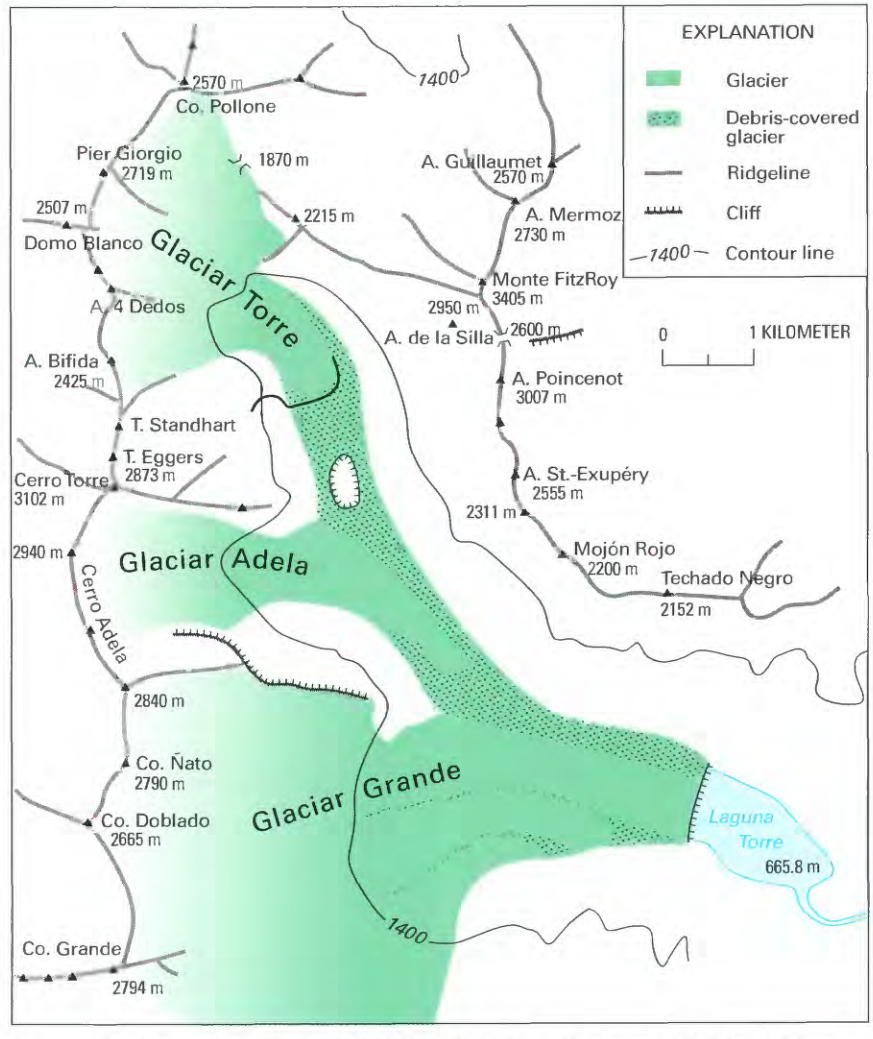

Figure 37.—*Glaciar Torre in 1967. Modified from Lliboutry (1993). Abbreviations: A., Aguja; Co., Cerro; T., Torre.*

Figure 38.—*FitzRoy-Torre massif.* **A**, *View from the surface of the Southern Patagonian Ice Field looking east toward the west side of the FitzRoy-Torre massif. Monte FitzRoy/Cerro Chaltél (3,405 m) is on the left and the spire of Cerro Torre (3,102 m) is on the right.* **B**, *Looking west toward the FitzRoy-Torre massif with Monte FitzRoy/Cerro Chaltél on the right and Cerro Torre on the left. Both photographs courtesy of Pedro Skvarca, Instituto Antártico Argentino, División Glaciología, Buenos Aires, Argentina.*

Southernmost *Patagonian Andes* (South of Lat 51°30'S.)

In spite of the lower elevations, mountain glaciers and small ice fields are found along the north-south axis of the *Patagonian Andes* south of the SPIF. The main ones are listed below. (The source of information is the Carta Preliminar at a scale of 1:250,000.)

(1) **Cordillera Sarmiento** (not to be confused with Monte Sarmiento) is a north-south range that culminates at 2,012 m (lat 51°48'S., long 73°24'W.). It has many small mountain glaciers.

(2) On **Peninsula Muñoz Gamero** are found the following:
   (a) In the northwest, an ice-capped volcano, Monte Burney, at 1,750 m (lat 52°20'S., long 73°25'W.).
   (b) In the south, an ice field that has an area of about 200 km^2 and culminates at 1,585 m (lat 52°50'S., long 73°10'W.); the largest of its 19 outlet glaciers is 15 km long.

(3) On **Isla Riesco** are found the following:
   (a) In the north, 7 outlet glaciers flow from an ice field more than 1,200 m in elevation (lat 52°52'S., long 72°50'W.), and 12 other outlet glaciers flow around Cerro Ladrillero (1,665 m; lat 52°55'S., long 72°35'W.).

Figure 39.—*Looking west at Glacier* (Perito) *Moreno from Cerro Buenos Aires. The water to the left is Brazo Rico, and to the right is Canal de los Témpanos of Lago Argentino. In between, where the ice dam forms, the access road to the tourist sightseeing area called "El Mirador" is visible. The mountains in the background, including* Cerro Pietrobelli *(2,950 m), the highest in this region, divide the ice draining eastward into Lago Argentino and westward (not visible) into fjords of the Pacific Ocean. Photograph taken on 5 December 1996 courtesy of Pedro Skvarca, Instituto Antártico Argentino, División Glaciología, Buenos Aires, Argentina.*

(b) In the south, Península Córdova, which borders the western part of the Strait of Magellan, culminates at 1,220 m (lat 53°15'S., long 73°W.) and has many mountain glaciers.

(4) On **Isla Santa Inés**, on the south border of the Strait of Magellan, is an ice field of about 300 km^2, culminating at 1,370 m.

(5) On **Tierra del Fuego**: The western part of the Strait of Magellan runs from northwest to southeast. South of it, the Andes Mountains have the same trend from Isla Santa Inés to Cape Horn. In the southwestern part of Tierra del Fuego, the mountains are higher and culminate at *Monte Shipton* (2,469 m). This set of short ranges and mountains is called Cordillera Darwin (fig. 40). Most of its mountain glaciers merge in a large ice field of about 2,300 km^2. At the western extremity of Tierra del Fuego near Canal Magdalena (lat 54°27'S.), the ELA was at 600 m in 1956 on Monte Sarmiento (2,300 m) (Morandini, oral commun.).

Because of persistent cloudiness, Landsat images of all of this uninhabited region do not exist, as yet, and all of our knowledge comes from aerial photography.

Early Expeditions and Recent Field Work on the Patagonian Ice Fields

Early Expeditions to the Northern Patagonian Ice Field

The highest summit of Patagonia, Monte San Valentín (4,080 m), is at the north border of the NPIF (figs. 27, 41). In 1921, F. Reichert endeavored to reach its summit by way of Glaciar San Rafael, and Nordenskjöld attempted a route by way of Glaciar San Quintín, which he christened unofficially Glaciar San Tadeo. Reichert and Hermann Hess made five other attempts during the period 1939–42, but Monte San Valentín was first climbed in December 1952 by members from the Club Andino Bariloche (1954). In December 1963, Eric Shipton, J. Ewer, E. García-Soto, and C. Marangunic crossed the NPIF heading southeast from Laguna San Rafael to Río de la Colonia and accomplished on the way the second ascent of Cerro (*Volcán*) Arenales (3,365 m), a mountain that they recognized to be a volcano. They assumed it to be extinct, but a small eruption of tephra can be seen on Landsat image 30368–13444 (Path 248, Row 93) taken on 8 March 1979 (fig. 42). The second ascent of Monte San Valentín was not achieved until December 1986 by Philippe Modéré and others. In 1993, another

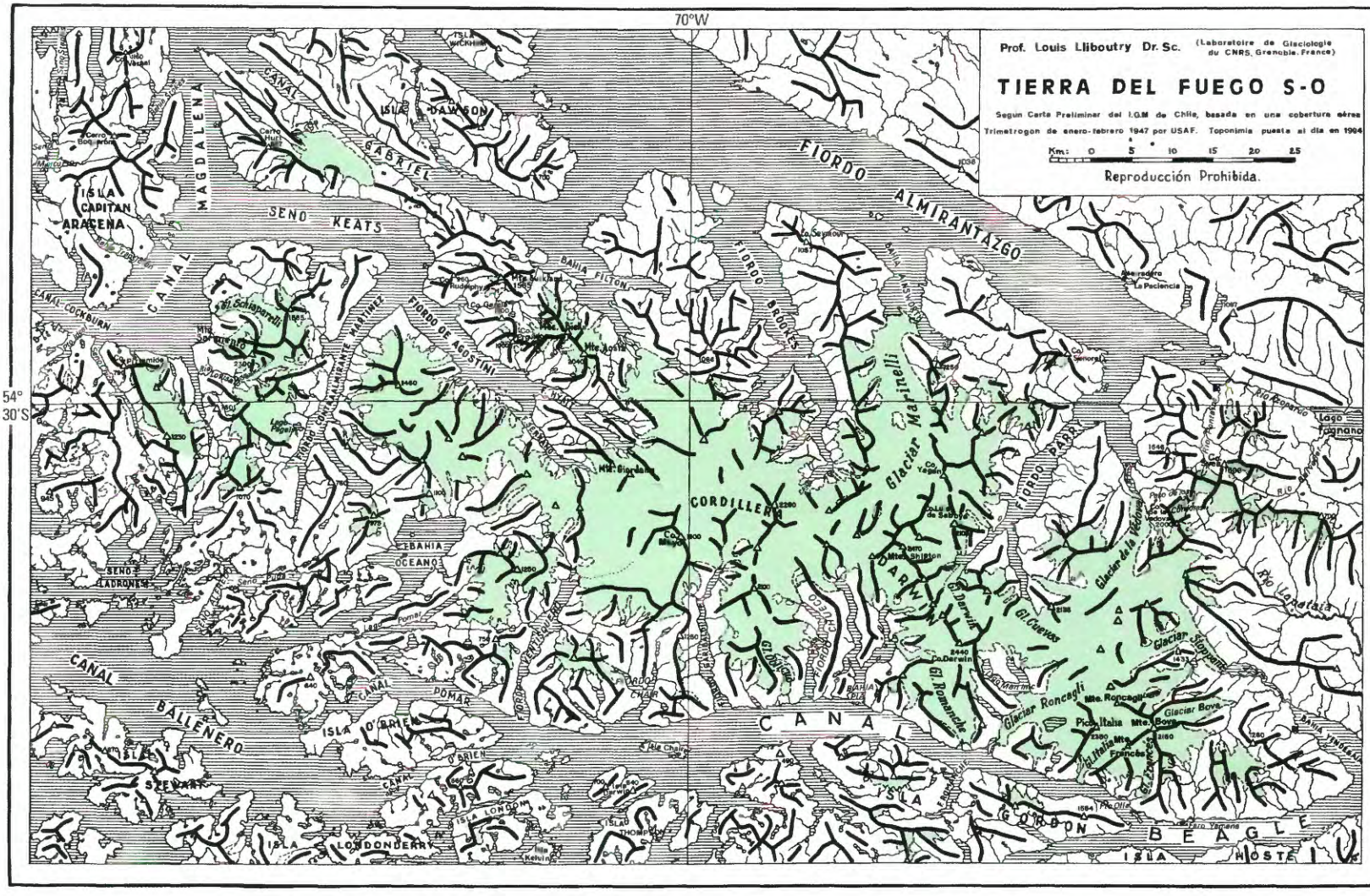

French group led by Philippe Modéré completed the sixth ascent before making the second crossing of the NPIF from north to south. The exploration history of the NPIF has been published by Casassa and Marangunic (1987) and by Buscaini and Metzeltin (1989).

***Figure 40.**—Southwestern Tierra del Fuego. Taken from Lliboutry (1956). In this area are the southernmost Andes, which are heavily glacierized (shown in green) between Seno Almirantazgo [Fiordo Almirantazgo] and the Beagle Channel [Canal Beagle]. Very little glaciological work has been done there because of logistical difficulties. The access is by ship from Punta Arenas (fig. 1), and the area is not inhabited. The Andes continue eastward but have only local glaciers in Argentine territory. The access in the east is from the town of Ushuaia on the Beagle Channel (fig. 1). The thick lines are ridgelines. Some geographic place-names are inconsistent with those used in the text, and those in the text conform to the usage recommended by the U.S. Board on Geographic Names in the gazetteers of Argentina (1992a) and Chile (1967, 1992b).*

Early Expeditions to the Southern Patagonian Ice Field

Of the many expeditions that have been made to the SPIF, the 11 treks made by the Salesian Father Alberto de Agostini between 1928 and 1944 are highlighted in his handsome book (Agostini, 1945), which includes many photographs of glaciers. Unfortunately, the precise camera position and orientation are never provided by Father de Agostini, so it is impossible to draw a sketch map of the FitzRoy or Paine groups from his photographs.

The primary interest of most explorers focused on the east-to-west crossing of the SPIF. F. Reichert made the attempt in 1914 by way of Glaciar (*Perito*) Moreno (fig. 30), Kölliker, in 1933 by Glaciar O'Higgins and in 1916 by the *Río Túnel* valley (Sociedad Científica Alemana, 1917) (fig. 29), and Father de Agostini, in 1931 by Glaciar Upsala (figs. 29, 30). Hector Gianolini and John Mercer tried the crossing in 1949, Bruno Guth and others, in 1951, and Major Huerta and other Argentines, in 1952, the last three groups by way of the *Río Eléctrico* valley (fig. 29). All the expeditions reached or even crossed the interoceanic ice divide, but to cross the ice field entirely and come back was beyond their capability. Saint-Loup (1951) suggested starting from the west, where the main difficulties are found. This was done by Harold Tilman and Jorge Quinteros between 18 December 1955 and 28 January 1956. They crossed the ice field from Fiordo Calvo

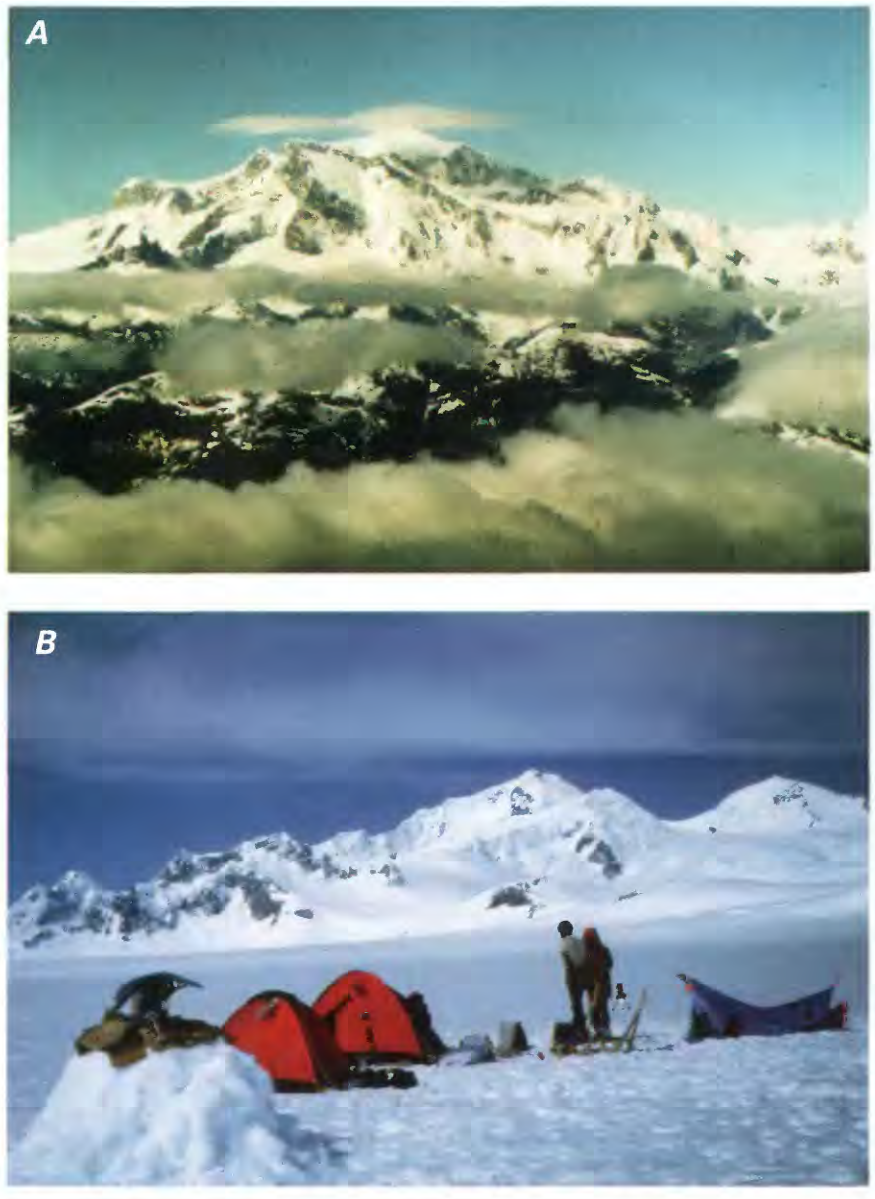

Figure 41.—*Monte San Valentín in the Northern Patagonian Ice Field.* **A**, *Monte San Valentín, the highest mountain in Patagonia, taken from the precipitous north flank on 27 November 1995.* **B**, *Camp for the drilling operations on the Northern Patagonian Ice Field (the accumulation area of Glaciar San Rafael) with Monte San Valentín in the background in December 1985. Photograph by Tomomi Yamada. Both photographs courtesy of Masamu Aniya, Institute of Geoscience, University of Tsukuba, Ibaraki, Japan.*

to the south arm of Lago Argentino and came back (fig. 30). (The CP had shown that Fiordo Calvo is less than 15 km from the ice divide. On the old maps available to Reichert in 1914, the nearest fjord was Fiordo Andrés at 35 km.) The many east-west crossings and the north-south crossing from Glaciar Jorge Montt to Glaciar Upsala by Eric Shipton, J. Ewer, C. Marangunic, and E. García-Soto from 10 December 1960 to 31 January 1961 (Shipton, 1963) (fig. 29) were arduous athletic undertakings but had little scientific value. More useful from a cartographic viewpoint was the official Chilean expedition of 1962–63 led by Lieutenant Colonel Florián Silva-Arce. With the patrol ship *Lientur*, they explored the Eyre and Exmouth fjords (fig. 29). At the *Río de Los Saltos*, they found the best way to reach the ice field at a snowy plateau christened *Meseta del Comandante* (*Caupolicán*), a way that avoided Glaciar Brüggen, which is heavily crevassed and impassable. They crossed the ice field to *Río Eléctrico* and came back the same way (oral commun., from E. García-Soto and C. Marangunic, who were members of the expedition). Since that time, Japanese expeditions have crossed the ice field from Fiordo Exmouth to Glaciar Upsala (December 1968 to March 1969) (fig. 29) and from Fiordo Falcón to Fiordo Europa (1971–72) (figs. 29, 30). In the following years, two British expeditions used sledges that had parachutes as spinnakers.

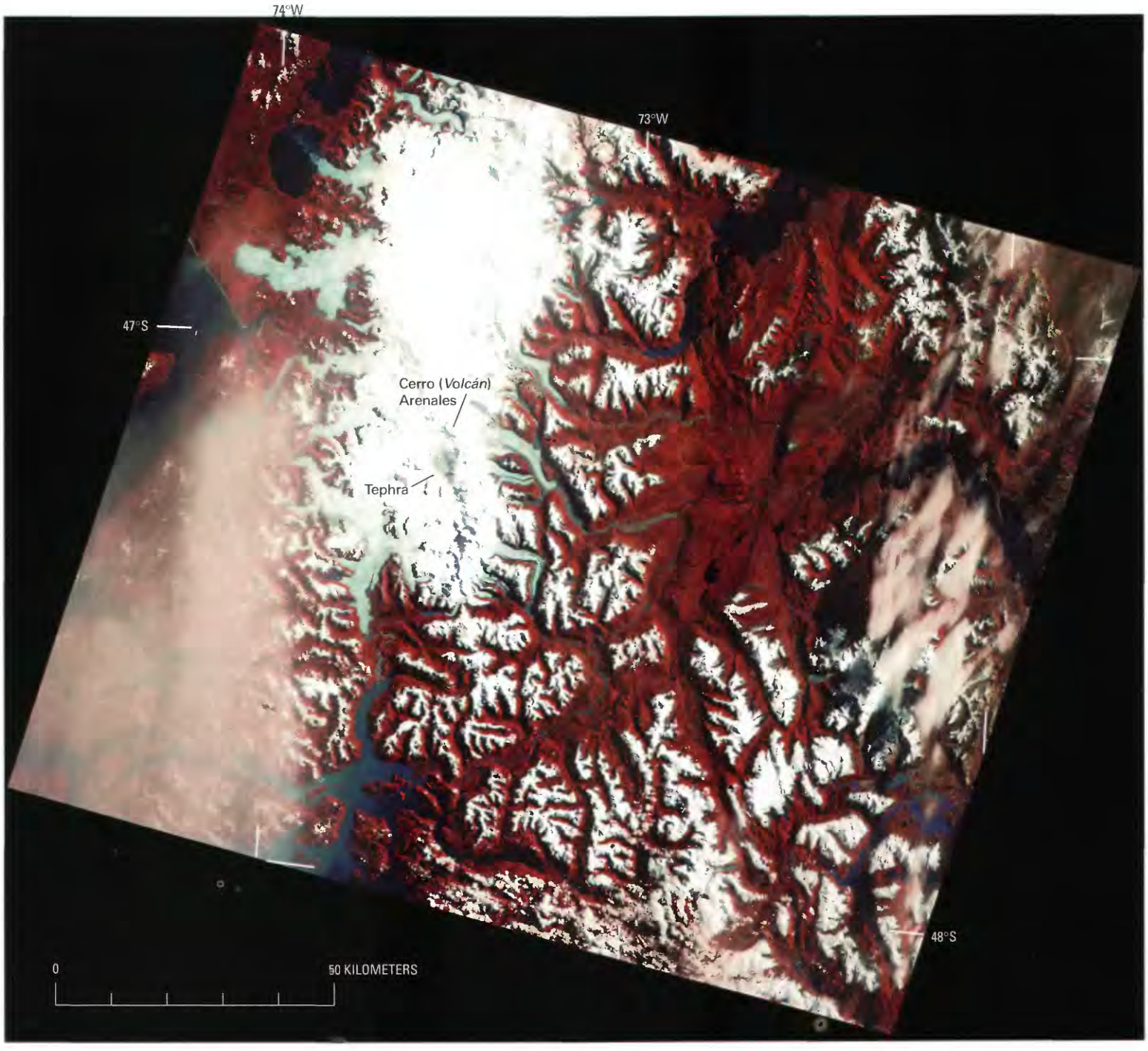

Eric Shipton's expeditions in 1958–59 and 1959–60 (Shipton, 1963) had a goal, a unique one, that was to determine the geographic position of an active volcano known to exist in the middle of the ice field. Actually, Reichert had seen the volcano in 1933, but he published his discovery in his memoirs that were not widely read (Reichert, 1947). The Argentine expedition that had christened it *Cerro Lautaro* in 1952 did not recognize it as a volcano. When I analyzed the Trimetrogon survey aerial photographs of this area, I wrote that "*Cerro Lautaro* looks like a dissected volcano" (Lliboutry, 1956, p. 408), with an unknown crater northwest of it. (I also stated that the strange unglaciated area at the lee of Cordón Mariano Moreno could be a maar; this conclusion proved to be incorrect when the feature was visited by Shipton during his first expedition.) In my analysis, I had used aerial photographs from Sortie 410 of 23 January 1945 rather than from Sortie 556 of 2 January 1945. On 2 January,

Figure 42.—*Landsat 3 MSS false-color composite image of the Northern Patagonian Ice Field on 8 March 1979. The tephra airfall pattern is visible through the clouds on the southwest flank of Cerro (*Volcán*) Arenales (see fig. 27). Landsat image (30368–13444; 8 March 1979; Path 248, Row 93) is from the EROS Data Center, Sioux Falls, S. Dak.*

tephra could be seen at the summit of *Cerro (Volcán) Lautaro* on its east side. Three weeks later, the freshly fallen tephra was again covered by snow. J. Ewer became aware of this fact and directed Shipton to the right site on his second expedition. The volcano was then emitting vapor and tephra from "a black fissure on the northern slope, about 300 feet below the summit." When Pedro Skvarca made his first ascent, from the southeast, on 29 January 1964, he found an 80-m-wide depression about 100 m below the summit, and some 50 m below it, he saw an opening within the ice of 2–3 m in diameter that had intense vapor and gas emissions (Skvarca, 1967). On March 1973, Leo Dickinson, Mike Coffey, and Eric Jones made the second ascent. Next they climbed a secondary summit about 10 km northward, which they christened *Cerro Mimosa*. They found it to be a fumarolic volcano (Buscaini and Metzeltin, 1989, p. 207).

I will not review here the many mountaineers who have gone to the FitzRoy area and climbed its impressive vertical walls of granodiorite (see fig. 38). Those readers interested in technical climbing should refer to the excellent, comprehensive book by Buscaini and Metzeltin (1989). The only scientific work carried out in this area was during the French expedition that made the first ascent of FitzRoy in January 1952 (Lliboutry, 1952) and during an expedition by Club Andino Bariloche in 1963 (Puente Blanco, 1963a). Cerro O'Higgins, farther to the north, was climbed on 1 March 1960 by the Chileans Espinoza, E. García-Soto, C. Marangunic, and R. Vivanco, and *Cerro Steffen* was climbed on 28 January 1965 by the Argentines Pedro and Jorge Skvarca. The same climbers and others have ascended most of the summits around Glaciar Upsala (Arko, 1979), in particular Cerro Bertrand, from which the view of fig. 34 was taken. Before becoming a glaciologist, Pedro Skvarca had climbed no fewer than 27 virgin summits of Patagonia!

Farther to the south, some glaciological work can be reported. During the Italian expedition to Monte Sarmiento in Tierra del Fuego, some glaciological observations were made by Prof. A. Morandini. Nevertheless, the ground data that were compiled by Mercer (1967) in the "Southern Hemisphere Glacier Atlas" are very meager indeed.

Improved Accessibility and Modern Scientific Investigations

With the development of tourism, trekking, and technical climbing in the Argentine Parque Nacional de Los Glaciares, the access to the east side of the SPIF is now easy. The tourist center, El Calafate, on the south shore of Lago Argentino, has an airport. Classic tours are available by boat to the calving front of Glaciar Upsala and to the lodge at *Bahía Onelli*, as well as by road to the front of Glaciar (*Perito*) Moreno (figs. 30, 39, 43). During the summer, lodges are open at *El Chaltél*, 13 km southeast of Monte FitzRoy, and excellent guides are found there (fig. 29). Two journeys on the ice field have become classic: behind the Cerro Torre and *Cordón Marconi*, as well as to the *Nunatak del Viedma* (fig. 29) (the area that I erroneously called *Volcán Viedma* on my first map). This site to the east and in the lee of Cordón Mariano Moreno is a local ablation zone because of lower precipitation (fig. 44). In February 1945, the ice-free area was about 10 km^2, including a 1-km-wide lake and seven much smaller ponds. A guide recently reported that he found a depression 200 m deep in place of the lake. The lake may form and empty periodically, as many ice-margin lakes do.

On the Chilean side, the departure points for access to the periphery of the northern ice field are Coihaique (about lat 45°30'S. and long 72°W.) and Chile Chico on the south shore of Lago Buenos Aires/General Carrera. Punta Arenas (about lat 53°10'S., long 70°55'W.) and Puerto Natales (about lat 51°40'S., long 72°30'W.) are departure points for visiting the Chilean Torres del Paine National Park and the south tip of the SPIF. The Pacific Ocean side of this ice field remains difficult to access, and the time of exploration is not over (for example, see Hickman and Newton, 1987).

Figure 43.—*South part of the calving front of Glaciar (*Perito*) Moreno on 27 November 1993. The glacier touches the opposite bank for a short distance. The level of Brazo Rico (left) has only risen slightly. It drains into Lago Argentino (right) by a small subglacial conduit at the very edge, a route favored by the orientation of rock strata. Photograph by Louis Lliboutry from an overlook built by the Parque Nacional de Los Glaciares.*

Figure 44.—Nunatak del Viedma *from* Paso del Viento *(in fig. 29) in February 1994. In the foreground is the huge lateral moraine of Glaciar Viedma; three conspicuous tephra bands can be seen on the glacier surface. Behind is the* Nunatak del Viedma *with Cordón Mariano Moreno within the clouds. Photograph courtesy of Pedro Skvarca, Instituto Antártico Argentino, División Glaciología, Buenos Aires, Argentina.*

It must be emphasized that today trekking, technical climbing, and serious glaciological work separately demand quite different people and logistics. Glaciological and related meteorological or limnological investigations have been done mainly by Japanese scientists: Renji Naruse (Institute of Low Temperature Science, University of Hokkaido, Sapporo), Chotaro Nakajima (Disaster Prevention Institute, Kyoto University), Hiroyuki Enomoto and Masamu Aniya (University of Tsukuba, Ibaraki), Tetsuo Ohata (Water Research Institute, Nagoya), and many others. After preliminary work in 1967, 1969, and 1981–82, the [Japanese] Glaciological Research Project in Patagonia studied the NPIF during the summers 1983–84 and 1985–86. The Chilean glaciologist Gino Casassa joined them and determined ice thicknesses by use of gravimetry. In addition, Glaciar Tyndall, in the SPIF, was studied (Naruse and others, 1987; Kadota and others, 1992). Since 1990, with the collaboration of the Argentine glaciologist Pedro Skvarca, two other large glaciers of the SPIF have also been studied, Glaciares (*Perito*) Moreno and Upsala. All the results have been published by the Data Center for Glacier Research of the Japanese Society of Snow and Ice, first as ad hoc publications (Naruse, 1983; Nakajima, 1985) and then in its Bulletin of Glacier

Research, nos. 4 (Naruse, 1987), 10 (Naruse and Aniya, 1992), and 13 (Naruse and Aniya, 1995). A comprehensive review of glaciological studies in Patagonia was published by Warren and Sugden (1993).

Glaciological Observations on the Northern Patagonian Ice Field

The 600-m-wide Río de la Colonia valley is flooded each summer by the outburst of an ice-dammed lake, a fact that has destroyed any hope of a permanent settlement (colonia) there (southeast side of NPIF, fig. 27). The Trimetrogon aerial survey first documented the location of the lake 2 km from the glacier terminus, on the right bank of the glacier. It is crossed by an arcuate terminal moraine, hence its name of *Lago Arco*. Landsat MSS images of 25 February 1976 and 8 March 1979 (table 8 and fig. 42, respectively) show a situation just after a flood, when dry land is downstream of the arcuate moraine. They also show that a second lake, 9 km from the glacier terminus on the left bank of Río de la Colonia, was partially drained on those dates; thus, this lake also contributes to the flooding. A Japanese-Chilean expedition headed by Professor Tanaka, which made the first ascent of Cerro (*Volcán*) Arenales in 1958, studied the flood problem (weekly "Ercilla" of 2 April and 21 May 1958: Tanaka, 1980).

Supraglacier debris produced by rockfalls and avalanches on two glaciers south of Cerro (*Volcán*) Arenales has been used to calculate the glacier surface velocity between two dates of Landsat MSS images (25 February 1976 and 8 March 1979). The surface velocity was about 200 m a^{-1} on Glaciar Pared Norte, at its elbow near the right bank, and about 260 m a^{-1} on Glaciar Pared Sur (fig. 27). Velocities can also be inferred from wave ogives forming at the foot of ice falls (Lliboutry, 1957). These data are of little interest as long as glacier thicknesses remain unknown.

Glaciar Soler is the only east outlet of the NPIF that has been thoroughly studied (Aniya and Naruse, 1987; Casassa, 1987; Naruse, 1987). At the foot of its ice fall, wave ogives show that the surface velocity in the middle of the glacier is 300 m a^{-1}. It decreases progressively downstream on the tongue. At 1.5 km from the ice fall, the surface velocity is 200 m a^{-1}. At that point, the glacier is 1,590 m wide and has a maximum thickness of 575 m. Bottom sliding probably accounts for one-third of the surface velocity, whereas near the terminus, where the ice is thinner, it accounts for 90 percent. At the equilibrium line, found at 1,350 m in the ice-fall area, the Glaciar Soler discharges about 1×10^8 m^3 a^{-1} of ice from an accumulation area of 36.4 km^2.

The drift in the proglacial area and in ice-cored moraines consists mostly of well-rounded gravel and boulders, which the glacier has picked up from an outwash plain (Aniya, 1987). Similar forms have been observed, sometimes akin to eskers, in the *Central Andes* (Lliboutry, 1958).

On the west side of the NPIF, interest has focused on Glaciar San Rafael, which is one of the fastest flowing ice streams in the world. It has a calving ice cliff 3 km long and 30–70 m high above the tidal Laguna San Rafael (a circular lagoon about 15 km in diameter that is limited by a Holocene moraine (Heusser, 1960), which was reached again during the "Little Ice Age"). Velocities at the terminus were measured in the summer of 1984 by Kondo and Yamada (1988). More detailed investigations, including bathymetry and monitoring of calving rates, were done by Warren and others (1995) in February 1991 and February 1992. Lastly, velocities more than 17 m d^{-1} were determined in October 1994 by Rignot and others (1996a, b). They used a National Aeronautics and Space Administration imaging radar (SIR–C) on board the space shuttle at an altitude of 175 km that employed a radar-interferometry technique.

Over its last 18 km, Glaciar San Rafael has a very regular slope of 5.7 percent. A rule of thumb estimation of its mean thickness is 11.3 m/0.057≈200 m. Nevertheless, it probably exceeds 300 m in thickness along its axis,

where a fast ice stream is found. However, the transversal profile of the bottom of Laguna San Rafael near the calving front is concave, and has a maximum depth of 272 m at the middle. In this ice stream, surface velocities are about 3.0 m d^{-1} all along a 12-km distance. Only about 1.0 m d^{-1} can be explained by ice deformation, and about 2.0 m d^{-1} comes from sliding. Such a large sliding velocity has never been observed over such a long distance in temperate mountain glaciers, even at the climax of the melting season. On the last 6 km, the ice stream speeds up, progressively but dramatically, reaching 17.0±0.2 m d^{-1} at the calving front. Such a large velocity has only been observed during some glacier surges, but in this case, it is not a surge; the velocities were about the same in 1984, 1991, 1992, and 1994. The flux of ice that is calved amounts to 2,170,000 m^3 d^{-1} (Warren and others, 1995). Glaciar San Rafael can well provide this amount of flux continuously on an annual basis because it corresponds to an ice layer about 1.35 m thick over the entire accumulation area (585 km^2), several times less than the mean mass balance in this area. The acceleration area 6 km from the front is probably where the bed becomes lower than the surface of Laguna San Rafael, and the water pressure in the subglacier cavities begins to increase.

Glaciological Observations on the Southern Patagonian Ice Field

Among the west-calving glaciers of the SPIF, Glaciar Brüggen (*Pío XI*) is the only one where velocities have been measured (Rivera and others, 1997). At four points (S3 to S6) in its central part, at 1.4 to 2.7 km from its calving front in Fiordo Eyre, the mean velocity ranged from 15.2 to 36.8 m d^{-1} on 14–17 November 1995. These velocities are faster than at Glaciar San Rafael, but they oscillate much more. No precipitation fell during these 4 days, and air temperatures were higher on 15–16 November 1995. Therefore, the doubling of the sliding velocity seems to have been caused by surface melting. Meltwater reaching the bottom probably does not drain off easily.

Glaciers calving into east lakes do not flow as fast (Naruse and others, 1992). In November 1990, the velocity of Glaciar Upsala at about 4 km from the front was 3.5–3.7 m d^{-1}, and the velocity of Glaciar (*Perito*) Moreno at 4.5 km from the calving front was about 2.0 m d^{-1}.

A puzzling feature on the SPIF is the presence of looping bands of volcanic tephra that were discovered from the Trimetrogon aerial photographic surveys (figs. 45–48). We now know that the tephra originates from *Cerro (Volcán) Lautaro* (lat 49°01'S., long 73°33'W.; 3,380 m). The explorers of Patagonia during the years 1867 to 1878 were told by natives on the Argentine side that an active volcano was present within the ice field. On the Chilean side, Lord Thomas Brassey, on board his yacht *Sunbeam* along Canal Messier, observed a fall of tephra in 1876, and the officers of the American corvette *Omaha* reported in 1878 that they had seen an active volcano within the ice field, which they called *Humboldt* (Martinic, 1982). In recent times, *Cerro (Volcán) Lautaro* has had five documented eruptions:

(1) 1933 (seen by Reichert (1947); compare Shipton (1963, p. 38–39) and Agostini (1945, p. 24))
(2) January 1945 (documented by Trimetrogon survey flight, aerial photograph 556–L–124)
(3) January 1960 (reference in Shipton (1963, p. 73))
(4) 1972 (evidence reported by farmers to C. Marangunic, oral commun.)
(5) June 1978 (evidence reported by farmers to C. Marangunic, oral commun.)

Landsat 3 RBV (30368–13450–D, Path 248, Row 94; 30368–13453–B, Path 248, Row 94) and MSS (30368–13450, band 5; Path 248, Row 94) images taken on 8 March 1979 show the tephra airfall pattern extending

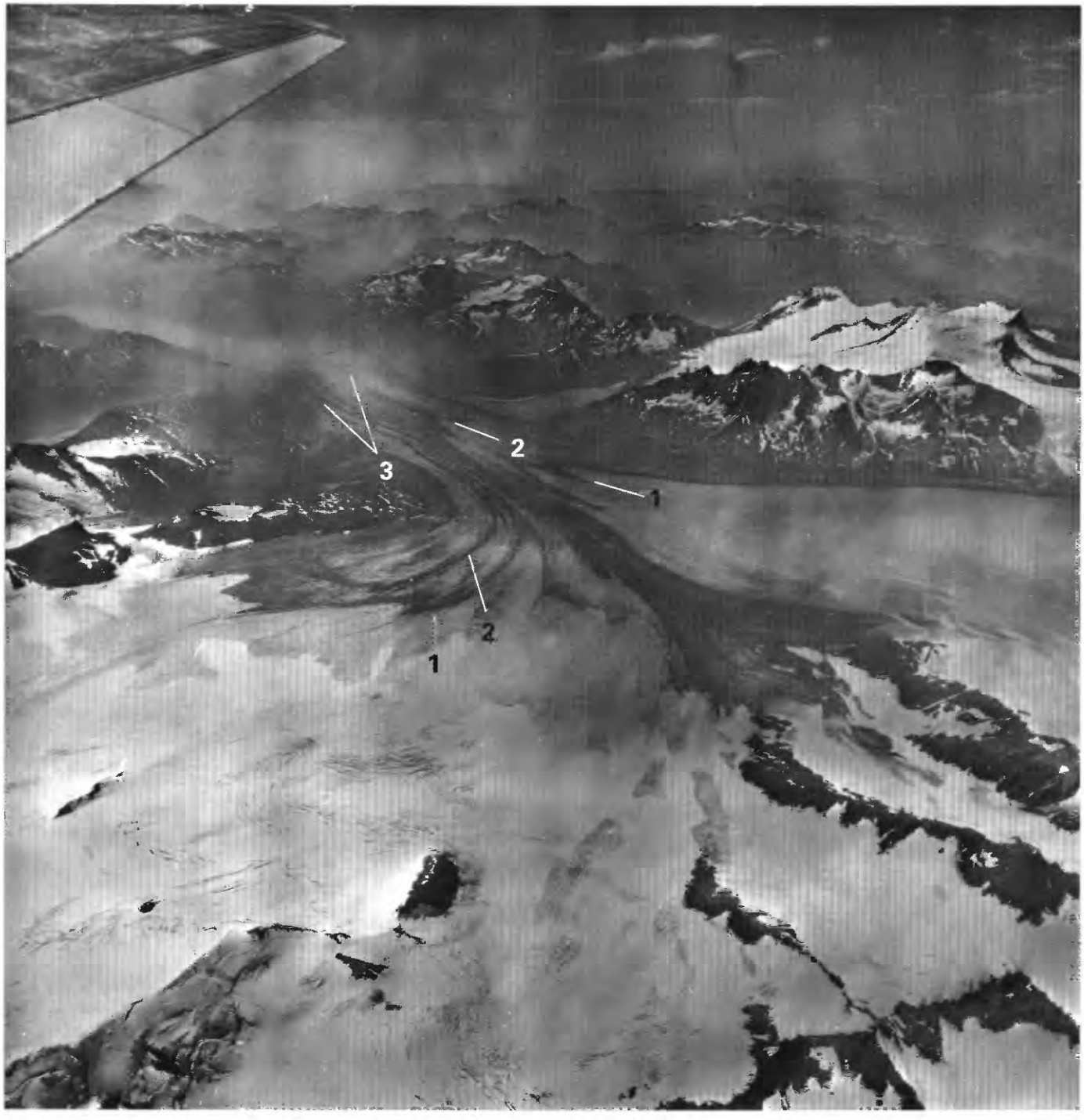

Figure 45.—*Trimetrogon (oblique) aerial photograph 410–R–219 taken on 23 January 1945 showing three bands of tephra on Glaciar Chico; the uppermost one (1) is definitely below the firn line. The ice-capped mountain on the right is Cerro Gorra Blanca.*

110 km south of the volcano (figs. 49–51). The pattern covers a wider area when seen in MSS band 5 (visible) than when seen in MSS band 7 (near-infrared). The location of the tephra poses intriguing questions. The first is how, with the exception of a small spot east-southeast of *Cerro (Volcán) Lautaro*, tephra covers the southwest slope of the volcano and extends to the south in a region where the prevailing wind direction is almost always from the southwest or northwest. Considering the fact that Cerro (*Volcán*) Arenales to the north had tephra on its southwest flank on the same day (fig. 42), two possible explanations are that (1) both eruptions, at two volcanoes 205 km apart, took place at about the same period during a northerly to northeasterly wind direction, or (2) westerly winds have blown off any posteruption deposit of snow on windward slopes and only uncovered the tephra layer on that side of the volcanoes.

The second question is how tephra, at first disseminated over a wide area, becomes concentrated into narrow bands. Figure 52 shows that a tephra layer is formed, becomes embedded within the ice, and appears in the ablation zone as a dark layer in the ice. Next, rain and running meltwater wash the tephra from the ice surface, and only a narrow belt contiguous to the emergence line is left. I called this kind of banding "sedimentary bands" (Lliboutry, 1957). According to Williams (1976), this sequence probably takes place on the outlets of Vatnajökull (Iceland), where similar layers of tephra are observed.

All the outlet glaciers around *Cerro (Volcán) Lautaro* exhibited three tephra bands in 1945 (figs. 45–47) (Lliboutry, 1957, figs. 32 and 41). The bands may be recognized on satellite images and might be used in the future to calculate (1) ice velocity and (2) the interval of time between the

Figure 46.—*Trimetrogon (oblique) aerial photograph 410–R–206 taken on 23 January 1945 showing three transverse bands of tephra on Glaciar Viedma. Although the photograph was taken at the same time as that of figure 45, the uppermost tephra layer (1) is located at the firn limit. Glaciers in the left background are in the drainage basin of* Río Túnel. *The pass through which F. Reichert gained access to the ice field in 1916, called* Paso del Viento, *is clearly visible. In the foreground is* Nunatak del Viedma, *which I originally mistook for a crater.*

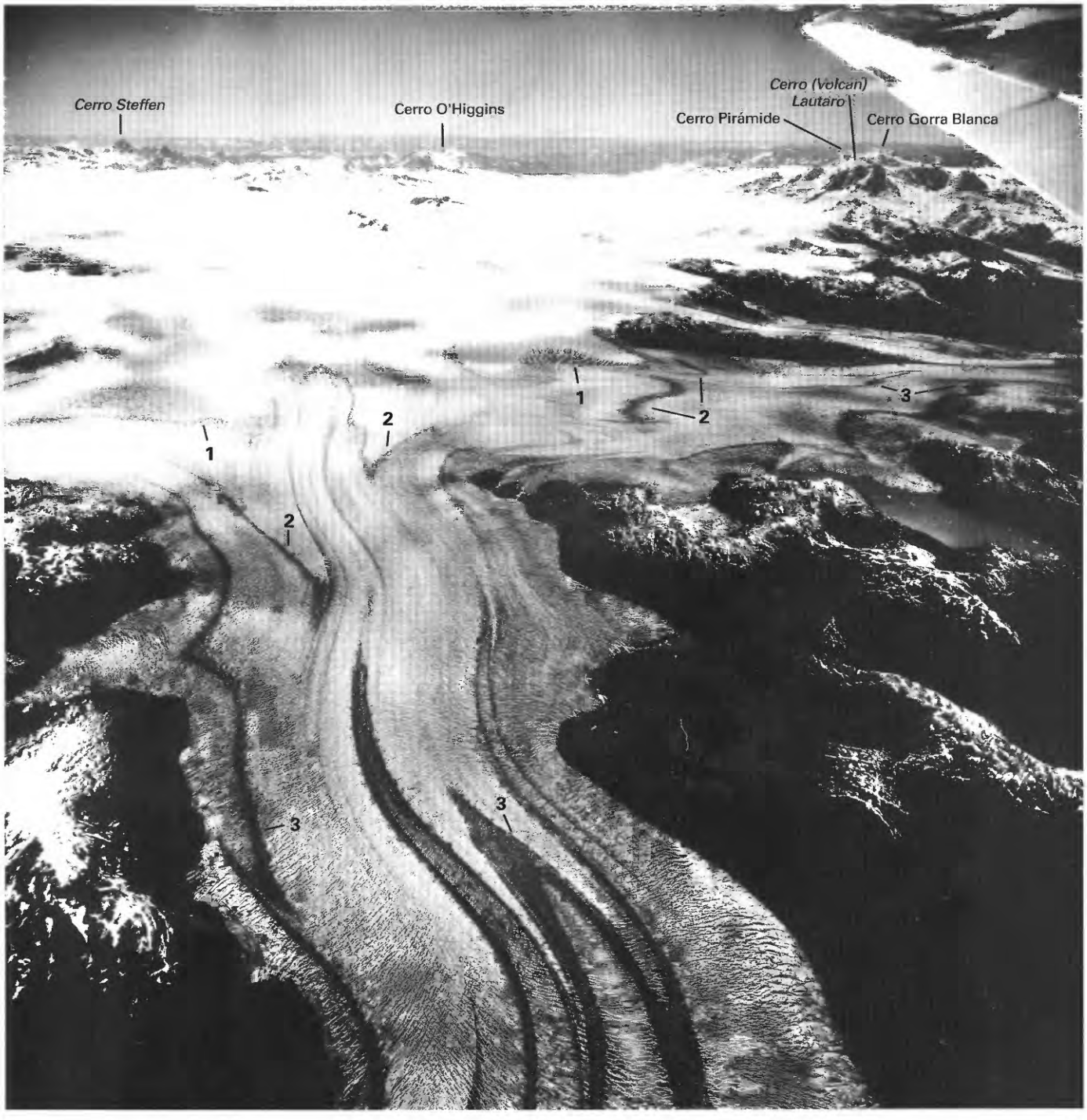

Figure 47.—*Trimetrogon (oblique) aerial photograph 556–L–105 taken on 23 January 1945 showing three bands of tephra on Glaciar Occidental and, flowing to the right, Glaciar Greve. In the right background is* Cerro (Volcán) Lautaro, *which obscures the white cone of Cerro Pirámide (just to the left) and the foot of Cerro Gorra Blanca. In the center background is Glaciar O'Higgins and Cerro O'Higgins on its left. The black peak in the left background is* Cerro Steffen *(3,056 m), mistaken by de Agostini as Cerro Mellizos.*

big eruptions that produced the tephra layers. Because southerly winds are almost unknown in the area, the presence of the three characteristic tephra layers north of *Cerro (Volcán) Lautaro* indicates that ice flows toward the north. Conversely, the finer bands found on Glaciar Pascua (figs. 29, 48) cannot have formed from the same eruptions because they have a quite different pattern. Perhaps they represent tephra whose origin is from Cerro (*Volcán*) Arenales?

In piston cores recovered from the bottom of Lago Argentino, near Glaciar (*Perito*) Moreno (fig. 30), three layers of tephra have been discovered (del Valle and others, 1995). They probably do not correspond to the three bands of tephra just discussed. First, the two upper bands are much thicker (12 cm and 9 cm, respectively) than the third one (1 cm). Second, if we assume a constant rate of sedimentation, the same as the one that has been

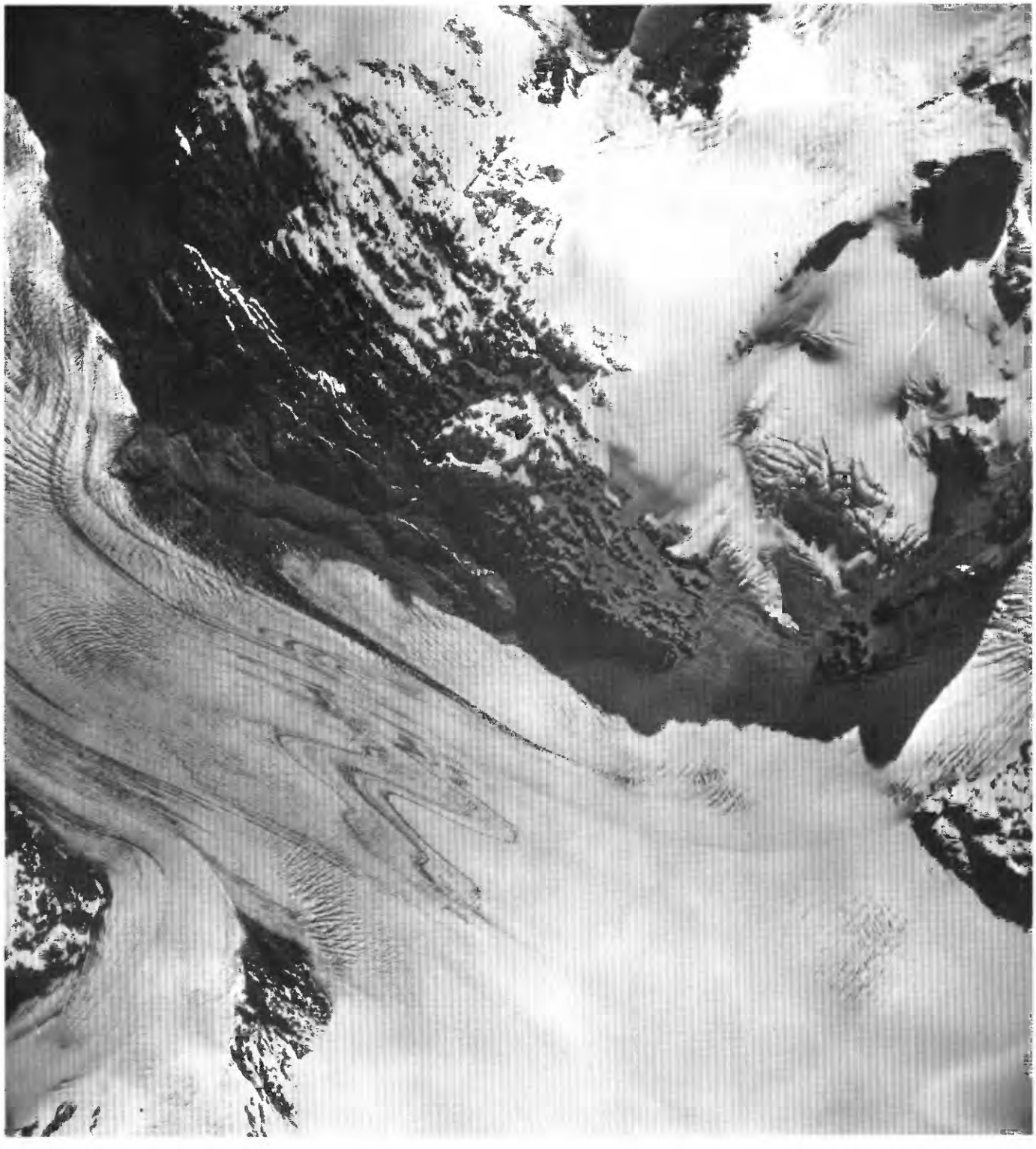

Figure 48.—*Trimetrogon (vertical) aerial photograph 556–V–14 showing several thin tephra layers on Glaciar Pascua. I suggest that the source of the tephra is not from eruptions of* Cerro (Volcán) Lautaro *but rather from Cerro (Volcán) Arenales, 150 km to the north-northwest.*

accurately determined during the last 71 years, the three big explosive eruptions should have taken place in A.D. 1200, 1520, and 1620. The tephra layers that are observed today at the surface of the SPIF are obviously younger. In my opinion, they were ejected during the 19th century.

Mass and Energy Balances of Glaciers

In southern Patagonia, precipitation is equally distributed throughout the year, without the maximum in winter that is observed farther to the north. Whether the precipitation falls as rain or snow depends on the air temperature, which ranges in general between 2°C and 13°C at sea level.

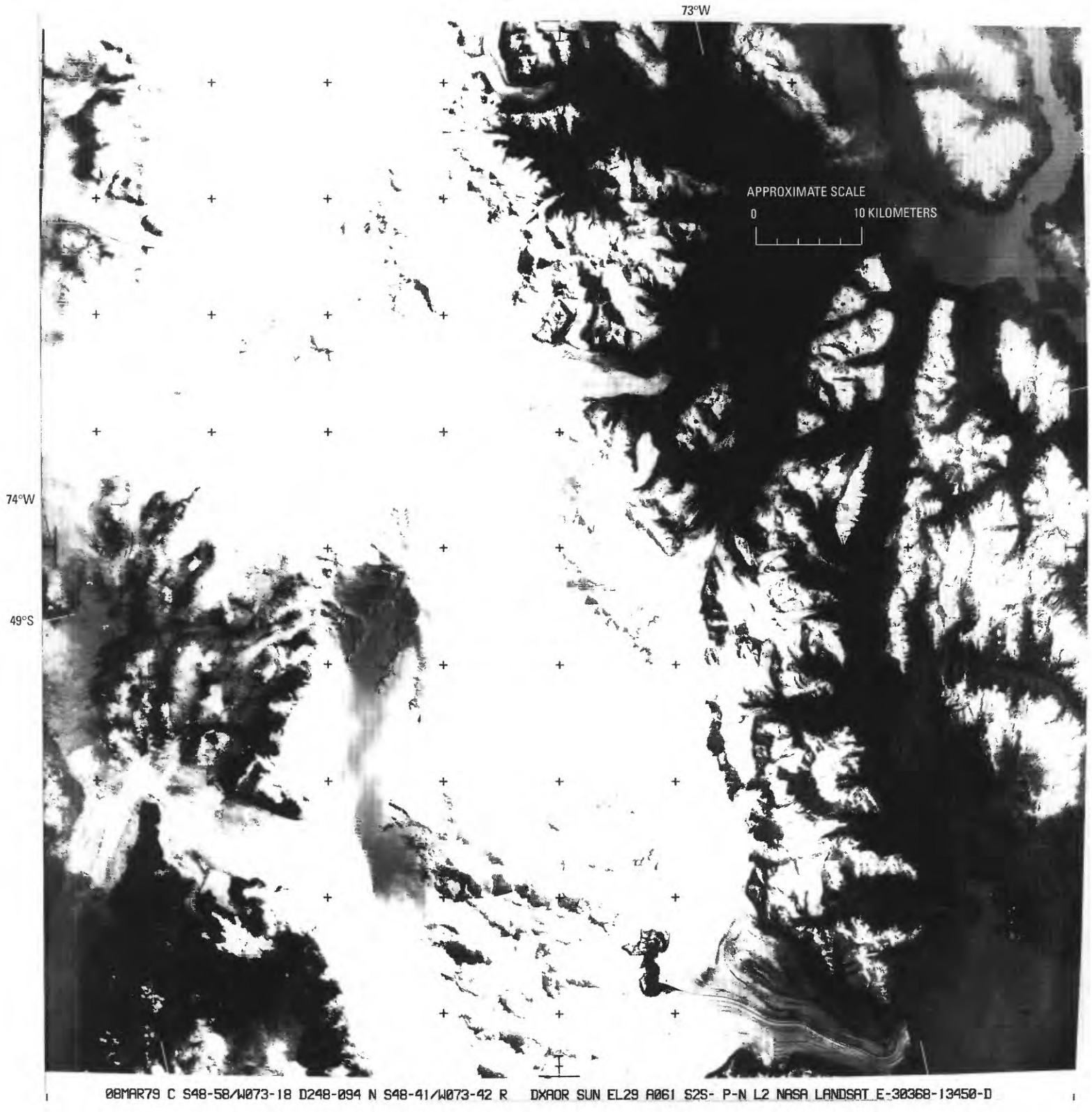

Figure 49.—*Landsat 3 RBV image of the Southern Patagonian Ice Field on 8 March 1979. Tephra airfall is visible from the west slope of* Cerro (Volcán) Lautaro *south to* Meseta Caupolicán (*first named* Comandante), *a distance of more than 32 km. On the left border, in the middle, is* Lago Greve. *Landsat image (30368–13450–D; 8 March 1979, Path 248, Row 94) is from the EROS Data Center, Sioux Falls, S. Dak.*

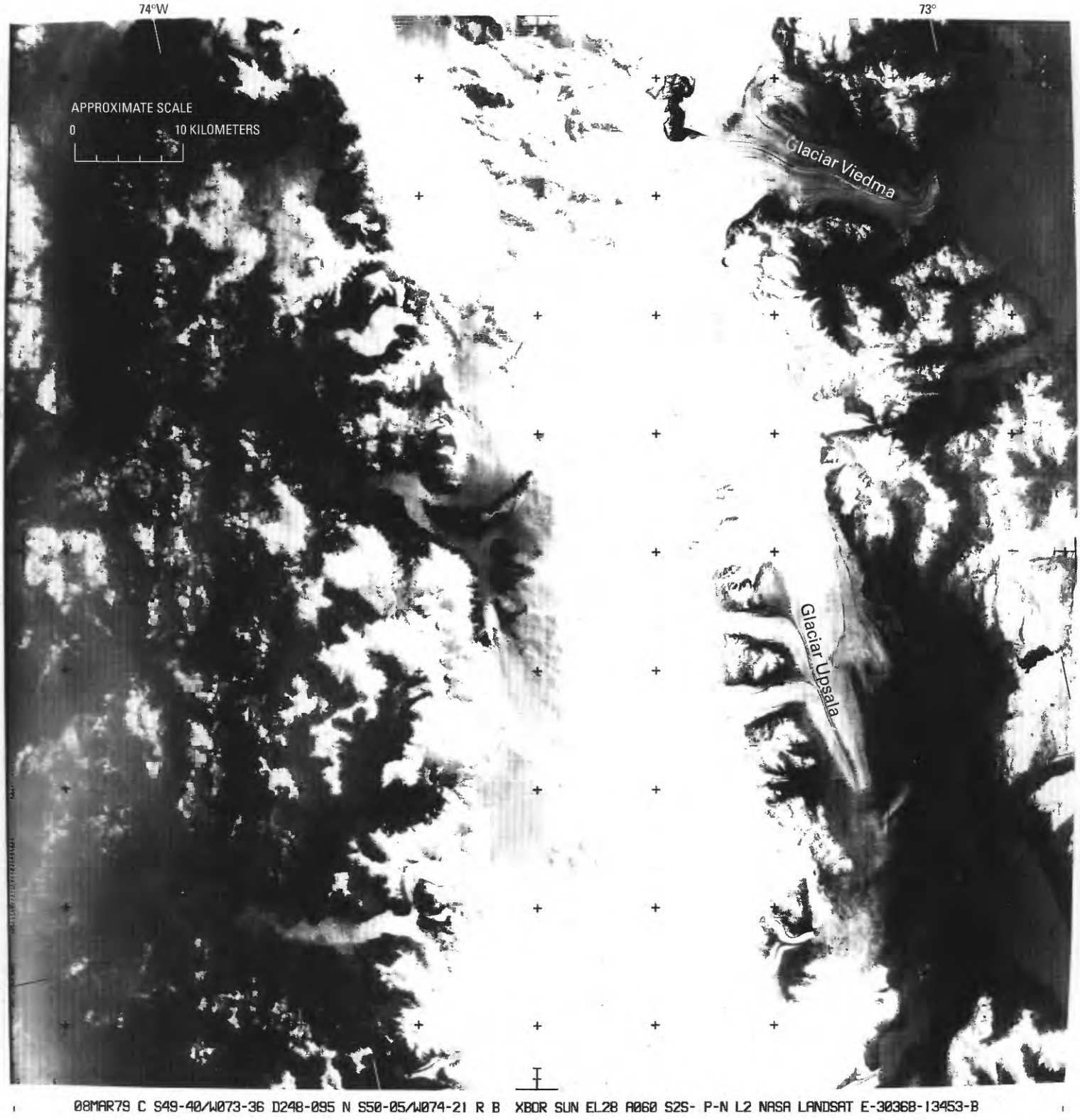

Figure 50.—*Landsat 3 RBV image (30368–13453–B; Path 248, Row 94) of the central part of the Southern Patagonian Ice Field taken on 8 March 1979. Tephra from* Cerro (Volcán) Lautaro *can be seen on the west side of the ice field in the vicinity of Fiordo Falcón and Fiordo Penguín, 110 km south of the volcano. On the east side, medial moraines and looped bands of tephra on Glaciar Viedma and Glaciar Upsala are visible. Landsat image is from the EROS Data Center, Sioux Falls, S. Dak.*

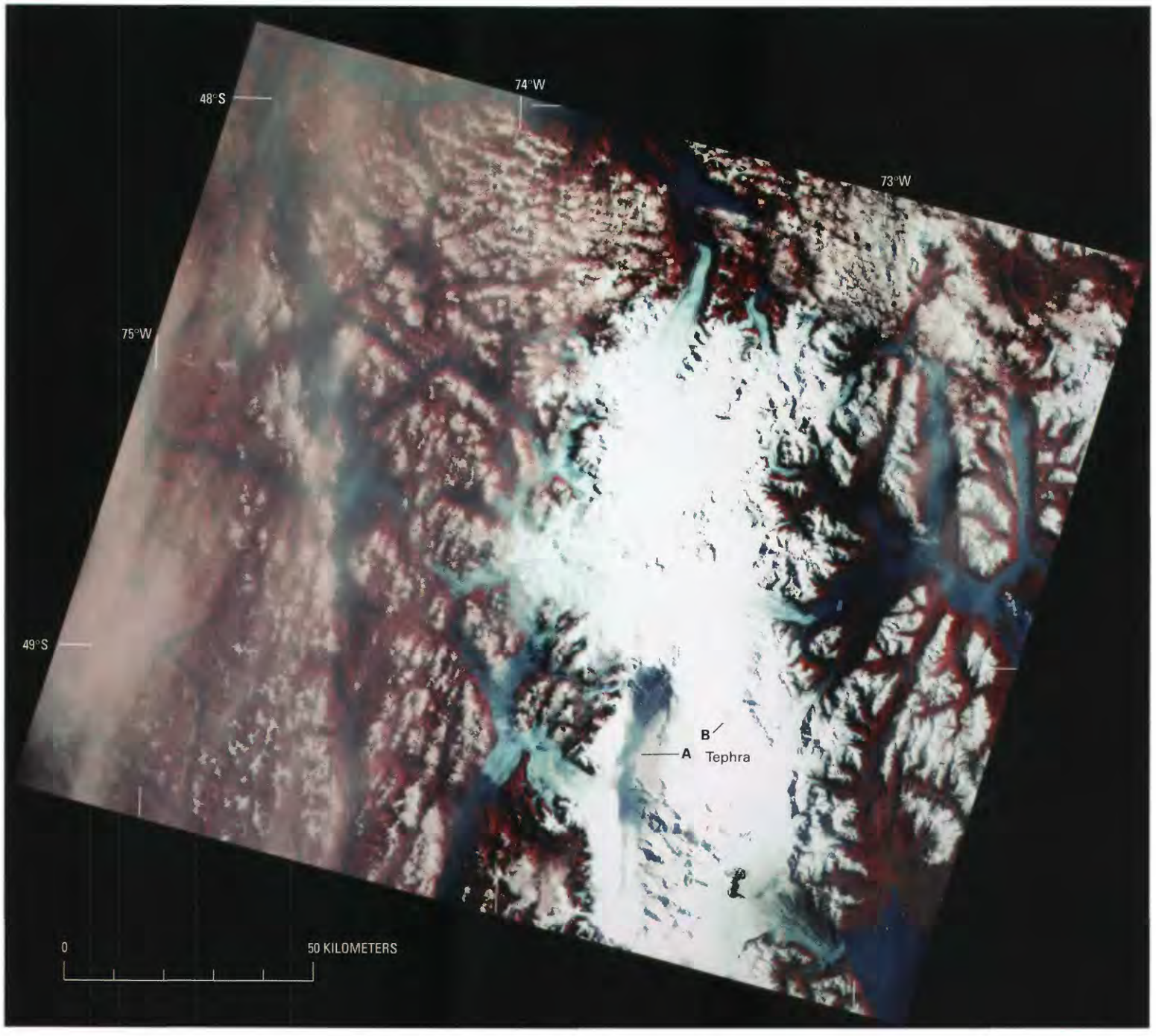

Figure 51.—*Landsat MSS false-color composite image of the Southern Patagonian Ice Field (see fig. 29). In this image, tephra is visible more than 50 km to the south (A) and also as an isolated spot on* Corredor Hicken *(B), 15 km to the east-southeast of* Cerro (Volcán) Lautaro. *A thin fog covers the ice field. Landsat image (30368–13450, band 5; 8 March 1979; Path 248, Row 94) is from the EROS Data Center, Sioux Falls, S. Dak.*

The 0°C isotherm varies accordingly between 700 m and 2,500 m. During summer, rain is more frequent on the ice fields than snowfall, and when snow does fall, it is very wet and heavy.

For the preceding reason, and not only because of melting, annual mass balances in the accumulation area, although almost unknown, are certainly much lower than the 6 to 7.5 m of precipitation. At 1,296 m above sea level on Glaciar San Rafael in the NPIF, coring down to 37.6 m revealed the mean mass balance to be 3.45 m of water equivalent per year (Yamada, 1987; Yamada and others, 1987), whereas the equilibrium line has been established to be about 250 m lower—at least at 1,050 m (Club Andino Bariloche, 1954). Thus, the activity coefficient should be at least 1.5 m per 100 m of difference in elevation. Many ice crusts and ice layers were found in the cores. At the end of November 1985, the firn had a density of 0.50 near

Figure 52.—*The second tephra band of the three observed within layers in depression crevasses on Glaciar Viedma during the reconnaissance made in late February 1994. The person on the left provides scale. Photograph courtesy of Pedro Skvarca, Instituto Antártico Argentino, División Glaciología, Buenos Aires, Argentina.*

the surface and turned into impermeable ice at a depth of 26.7 m. Over this ice was an aquifer 2.8 m thick, as well as a "water-soaked layer" (owing to capillarity) 5 m thick.

The preceding observations confirm that the ice fields of Patagonia are entirely at the melting point (temperate), except at the highest summits. They are quite similar in their size, ELA, and velocities to the temperate ice fields of southern Alaska (Bagley, St. Elias Mountains, and Juneau Ice Fields). They have less dissymmetry between their sides, however, because the summits are about 1,000 m lower.

On the SPIF at 2,680 m above sea level, Aristarain and Delmas (1993) found a mean mass balance of only 1.2 m water equivalent per year by coring to a depth of 13.7 m, whereas the equilibrium line on Glaciar Moreno nearby is at 1,150 m. At this elevation, many ice crusts and some ice layers continue to be found, which testifies to frequent episodes of melting. Such large differences in accumulation come from the persistent and very strong easterly wind, which causes dry winter snow to drift. Consequently, accumulation is not a constantly increasing function of elevation. On the other hand, the highest peaks and needles that remain most of the year within the clouds are capped by fantastic mushrooms of ice, rime, and snow and have overhangs that can exceed 10 m. They have caused the rock climbing attempts of many first-class alpinists to end in failure.

Measured negative balances in the ablation zone are more consistent. On Glaciares (*Perito*) Moreno and Upsala, the balance is –12.5 m of ice a^{-1} at 350 m, whereas it is zero at 1,150 m (Naruse and others, 1995; Skvarca, Satow, and others, 1995). Thus, the mean balance gradient in the ablation zone is 1.56 m a^{-1} of ice per 100 m of elevation, a very high value. The very negative balances of the ablation zone and calving at the front together explain the high values of the accumulation area ratio (AAR).

Values of the AAR on the SPIF have been determined from Landsat TM satellite imagery by Aniya and others (1996). The values span a wide range because of local factors (even deleting one very low value, 0.25, which might be an error). For tidewater glaciers (13 values in total), the AAR ranges between 0.65 and 0.97 and has 0.854 as a mean. The values close to one, denoting that almost all the discharge of ice disappears by calving, explain why some fjords of the Pacific coast, such as Fiordo Falcón (fig. 29), are crowded with icebergs and growlers and are closed even to small boats. For the other glaciers (14 in total, including Glaciares Ofhidro, Bernardo, and Occidental (fig. 29), which do not reach the sea as indicated in the table in Aniya and others (1996)), the AAR ranges between 0.58 and 0.87 and has 0.736 as a mean. On the NPIF, the

TABLE 10.— *Energy balances on ablation zones of the* Patagonian Andes

[Given in megajoules per square meter per day (MJ m^{-2} d^{-1}). Based on data from Ohata and others (1985), Fukami and Naruse (1987), and Takeuchi and others (1995). Asterisk (*) indicates a kind of föhn blows on some days]

Glacier, elevation, latitude, aspect	Period	Radiation balance (solar + thermal infrared)	Sensible heat	Latent heat	Melting cm d^{-1} of ice
San Rafael, 104 m, lat 46°41'S., west	29–31 Dec 1983	11.7	8.9	3.5	7.1
	19–23 Jan and 30 Jan–1 Feb 1985	2.3	4.5	2.5	7.7
Soler, 370 m, lat 46°54'S., east	1–5 Nov 1985	5.30	5.54	–.76	3.0
	25–29 Nov 1985	14.34	7.62	–.32	5.9
	15–29 Dec 1983*	7.0	11.9	7.1	8.6
Moreno, 330 m, lat 50°28'S., east	14–15 and 18–26 Nov 1993	12.0	10.9	–.8	7.4
	16–17 Nov 1993*	16.3	23.6	1.6	13.8
Tyndall, 700 m, lat 51°15'S., south	11–16 Dec 1993	11.8	9.6	1.6	7.7

mean value of the AAR is only 0.63 (Aniya, 1988). In the European Alps at the beginning of the century, the AAR was 0.75 according to Penck and Brückner (Lliboutry, 1965, p. 444), but it is much less today, often less than 0.60.

Energy balances have been determined by Ohata and others (1985) and by Fukami and Naruse (1987) on two ablation zones of the NPIF; later, by Takeuchi and others (1995) on two ablation zones of the SPIF. Measurements were done at low elevations, during periods of 2 to 14 days, in summer. Given the very large variability of the different terms of the balance (excepting the energy emitted in the thermal infrared by melting ice), this sampling cannot be extrapolated to the whole ablation season nor to the whole ablation zone. The results are very interesting, however, and are given in table 10.

On leeward Glaciares Soler and (*Perito*) Moreno, a kind of föhn blows on some days (indicated by asterisk in table 10). This is a wind that has warmed by losing a large percentage of its moisture on the windward side of the mountain. Its dew point remains more than 0°C, however, and thus, it conveys latent heat to the melting ice surface. On Glaciar San Rafael, a katabatic wind at the surface blows westward, in the opposite direction of the wind at higher altitude (Inoue, 1987). This air has been cooled by contact with the glacier, but when it reaches the site of the measurements, it has been warmed by adiabatic compression.

Historic Fluctuations of Outlet Glaciers from the Patagonian Ice Fields

Northern Patagonian Ice Field

Laguna San Rafael was discovered in 1675. The glacier that bears its name did not reach the lagoon at that time. It probably reached it at some time between 1741 and 1766 (Casassa and Marangunic, 1987), and it has maintained a calving front since then. It has been inferred from actual glacier velocities that the lagoon extends 6 km eastward of the 1994 calving front.

The first documents on Glaciar San Quintín followed a visit by Nordenskjöld in 1921 and another by Brüggen in 1935. Its front had receded by 2 km between those dates (Lliboutry, 1956). Between 1939 and 1959, it advanced by 2.3 km. Between 1959 and 1992, it receded by 3.7 km (Warren, 1993). Comparison of the oscillations of Glaciars San Quintín and San Rafael were made by Winchester and Harrison (1996) using dendrochronology.

Variations of all the outlet glaciers of the NPIF have been determined from Trimetrogon aerial photography acquired in January and February 1945, as well as from Landsat MSS imagery of 1974–75 and 1985–86 (Aniya, 1988, 1992). Hirano and Aniya (1996) compared MSS Landsat imagery of 1987 and Russian satellite photography (KFA–1000) of 1988. Wada and

TABLE 11.— *Mean variation of the glaciers of the Northern Patagonian Ice Field*

[Given in ha a^{-1}=10^{-2} km^2 a^{-1}. Based on data from Aniya and Wakao (1997). Those marked with an asterisk (*) are not outlet glaciers of the ice field]

Glacier name	1945 to 1975	1975 to 1996
North side (from east to west)		
Exploradores* (San Valentín east)	–0.53	–3.10
Grosse* (Circo)	–1.30	–3.00
Reichert* northeast arm	–2.03	–8.43
southwest arm	–1.20	–17.19
West side (from north to south)		
Gualas north	–.43	–3.00
south	–.57	–2.86
San Rafael	–11.87	–40.19
San Quintín	–25.00	–23.57
Benito	–2.20	–4.43
HPN–1	–5.83	–6.76
HPN–2	–4.70	–8.22
HPN–3	–.73	–7.81
South side (from west to east)		
Steffen	–8.07	–14.67
Piscis*	–1.63	–.10
Pared Sur*	–4.73	–1.29
Pared Norte	–3.23	–1.52
East side (from south to north)		
de la Colonia	–3.23	–4.95
Cachet*	–8.93	–6.48
Nef	–4.87	–13.24
Soler	–1.27	–3.57
León	–.07	–2.44
Fiero	–.50	–1.33
Total of the NPIF	–92.9	–174.2

Aniya (1995) and Aniya and Wakao (1997) used oblique aerial photographs taken by hand-held 35 mm cameras in 1990–91, 1993–94, and 1995–96. The variation in areas between 1945, 1975, 1986, 1991, 1994, and 1996 are given in a paper by Aniya and Wakao (1997). To smooth out the short-term irregularities and to obtain smoothed data pertinent to climatological studies, the mean recession rates between 1945 and 1975 (30 years) are compared in table 11 with the ones between 1975 and 1996 (21 years). It appears that all outlet glaciers are receding and that the recession rates increased after 1975, except for four glaciers on the southeast, which are not outlet glaciers of the ice field.

The area of the NPIF in 1945 was 4,400 km^2, according to Lliboutry (1956). In 1975, it was 4,200 km^2, according to Aniya (1992). Because the area of the NPIF was measured on different maps by different authors, it is difficult to judge the accuracy of the change. According to Aniya and Wakao (1997), the change between 1945 and 1975 has been only –28 km^2 (and –37 km^2 between 1975 and 1996). The general recession of the Patagonian ice fields is probably related to a general warming by 0.4°C to 1.4°C since the beginning of the century south of lat 46°S. and to a decrease of the precipitation on the Pacific Ocean side of the ice field by as much as 1.4 m a^{-1} (Rosenblüth and others, 1995).

TABLE 12.—*Glacier variation in the Southern Patagonian Ice Field*
[Based on data from Aniya and others (1997)]

Glacier name	Area in 1945	Variation from 1944–45 to 1985–86	
	(square kilometers)	Square kilometers	Percent
Brüggen	1,205	+59.9	+4.97
Moreno	254	+4.1	+1.61
Penguín	525	+2.5	+.48
Viedma	903	–.3	–.03
Upsala	869	–11.9	–1.37
Ameghino	80	–4.3	–5.38
O'Higgins	870	–49.6	–5.70
Jorge Montt	494	–29.6	–5.99
Greve	471	–33.3	–7.07
Lucía	218	–18.4	–8.43
Amalia	190	–33.4	–17.54
Total of the SPIF	13,500	–500	–3.70

Southern Patagonian Ice Field

In 1952, glaciers of the FitzRoy group had not varied significantly since Father de Agostini had taken pictures of them 20 years before (Lliboutry, 1953). In contrast, during this same period of time, the recession of many alpine glaciers had been impressive. Nevertheless, such ground observations cannot yield a global picture of the behavior of Patagonian ice fields. This can be attained only by the use of aerial photography and satellite imagery.

Aniya and others (1997) published the variation in area of most glaciers of the SPIF between the summer 1944–45 (Trimetrogon aerial photography) and the summer 1985–86 (Landsat imagery). During these 41 years, the areal variation of the SPIF was –3.7 percent. In contrast, the areal variation of the NPIF during these same years was only –1.0 percent (Aniya and Wakao, 1997). The variations of the largest glaciers and of those that deviate the most from this mean are given in table 12.

The nonstandard cases of Glaciar Brüggen and Glaciar (*Perito*) Moreno are presented below. The advance of Glaciar Brüggen created a lake in the 1960's, and the large recession of Glaciar Greve is probably because its tongue became afloat in this lake. The most dramatic recessions are those of Glaciar O'Higgins in Lago San Martín/O'Higgins and of Glaciar Amalia, a tidewater glacier at lat 50°57'S. Between 1945 and 1986, their calving fronts receded by 11.2 km and 7 km, respectively.

In 1914, explorers found the upstream, uncrevassed part of Glaciar O'Higgins on the same level as its lateral moraine (Shipton, 1963). In 1933, the ice was lower than the moraine by 60 m, and in 1959, when the recession was at its climax, it was lower by 240–300 m. The fast recession between 1945 and 1978 (about 400 m a^{-1}) probably resulted from the ice tongue's becoming afloat. Between 1978 and 1986, the recession stopped (Casassa and others, 1997), probably because the terminus again became completely grounded. The grounding line cannot remain where the subglacier terrain has a reverse slope, and thus, the glacier terminus commonly recedes by fits and starts. Mercer (1961) suggested the width of the fjord as another reason for its history of irregular fluctuation.

The large differences in variation among the glaciers of the SPIF contrast with the more uniform behavior of the glaciers of the NPIF. The main reason is that the SPIF has many more calving fronts of outlet glaciers than the NPIF. Wherever glaciers that have calving fronts are used to monitor climatic changes, only the mean variation during 20 years or more should be considered.

Some outlet glaciers consist of two ice streams side by side that have distinct, individual flow regimes. The east, main ice stream of Glaciar Jorge Montt, which reaches Fiordo Calén, lost 4.2 km^2 between 1945 and 1986, whereas the west one, which does not reach the fjord, lost 25.4 km^2 between these dates. The west ice stream of Glaciar Upsala receded continuously between 1945 and 1986, whereas the east one advanced between 1968 and 1978 and later receded rapidly (Aniya and Skvarca, 1992). The accumulation zone of this east stream has lowered by about 80 m between the sixties and 1993 at a training site for landing on snow (guide Claudio Schurer-Stolle, oral commun.).

After 1986, data are less complete. On the east side of the SPIF, Glaciar Ameghino has continued to recede by 0.1 $km^2\ a^{-1}$, as it had previously (Aniya and Sato, 1995c), whereas the recession rate of Glaciar Upsala has increased by four times. After a maximum rate in 1993–94 (700 m a^{-1}), the recession almost stopped in 1994–95 (Naruse and others, 1997) (fig. 53). It lost 10.3 km^2 between 1986 and 1995 (Aniya and others, 1997). Its large icebergs, dispersed by the wind, can be seen throughout Lago Argentino. On occasion, they impede the entrance of tourist boats into the west arm.

The recession of Glaciar Viedma has become significant but remains very low: 500 m between 1986 and 1994. It caused the outburst of an ice-dammed lake in 1994, as documented by X-Band Synthetic Aperture Radar (X–SAR) images (Skvarca, Rott, and Stuefer, 1995). Nearby in the FitzRoy group, Glaciar Grande has receded, which has allowed the bedrock to appear in the middle of the calving front since 1990. On FitzRoy itself, facing west, was a very steep couloir of ice, the "supercanaleta," by which Argentine climbers made the second ascension, digging grottos into the ice to bivouac. By 1993, all this ice had disappeared (guide Alberto del Castillo, oral commun., and visual inspection by the author from a helicopter, courtesy of the Argentine authorities).

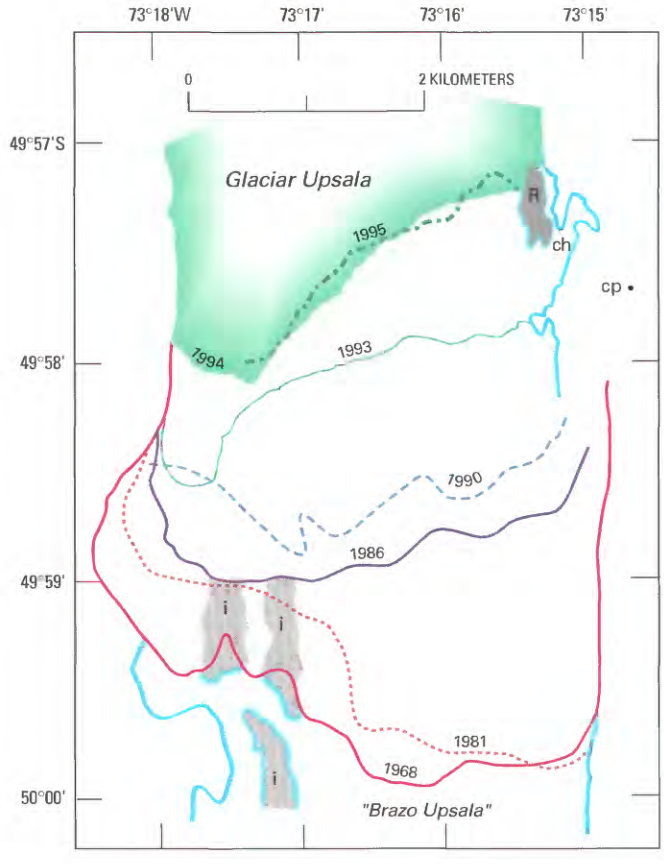

Figure 53.—*"Front margins of Glaciar Upsala. The front positions of 1968 (November) and 1981 (February) were determined by vertical aerial photographs and that of 1986 (January) by Landsat Thematic Mapper (Aniya and Skvarca, 1992). The 1990 (November) position is based on observation from the east bank and the proglacial lake [Brazo Upsala], which has been modified from the front position shown by Aniya and Skvarca (1992). The 1993 (November), 1994 (December), and 1995 (December) positions of the front and the east margin were measured by conventional angle surveys from the control point (cp) on the east bank to prominent points at the terminus, as well as by Global Positioning System (Trimble Pathfinder Basic receivers) surveys at some points on the ice-rock boundary. R indicates a bare-rock ridge [extent shown by dark grey] seen along the east glacier margin in 1993, which was almost covered with ice in 1990; ch indicates a lateral water channel; and i indicates an island [extent shown by light grey] as seen in 1986 at the glacier front." Taken from Naruse and others, 1997, fig. 2, p. 39.*

Cordillera Darwin

Holmlund and Fuenzalida (1995) compared aerial photography of Cordillera Darwin taken in 1943–44, 1960, and 1984–85. They also visited the area in 1993–94. During all this time, in general, glaciers have receded slowly on the order of -1.0 m a^{-1}. Nevertheless, the front of the largest glacier, Glaciar Marinelli (142 km^2), receded by –0.2 km between 1943 and 1960 and by –5.0 km between 1960 and 1993. Probably the front of this tidewater glacier became afloat. On the other hand, during the second period of time, three out of the six glaciers flowing to the southwest into Bahía Pía (an embayment of the Beagle Channel) advanced by +0.2 to +0.4 km in 33 years.

In the Cordillera Darwin area, cyclonic fronts are less active than in the SPIF, and thus, annual precipitation is lower. The cyclones, which cross the Drake Passage to the south from northwest to southeast, are generally occluded systems and provide precipitation in their lee. Therefore, snowfalls are accompanied by southwest winds. In the SPIF, which runs north to south, a strong dissymmetry is found in the precipitation from west to east. In Cordillera Darwin, which runs northwest to southeast, the same dissymmetry is recorded from southwest to northeast.

The meteorological station at Punta Arenas (figs. 1 and 3) has monitored temperature and precipitation on the leeward side of the region (the semiarid pampa) since the beginning of the century. Mean annual temperature has increased by only 0.3°C, and precipitation (about 400 mm a^{-1}) shows no significant trend. The data from the lighthouse of Islas Evangelistas, at the west entrance of the Strait of Magellan, show an increase in mean temperature by about 1°C and a decrease in mean precipitation from about 3,000 mm a^{-1} to about 2,000 mm a^{-1}. Holmlund and Fuenzalida (1995) suggest that the same trends hold for the southwest, windward side of Cordillera Darwin. Given that its glaciers have been more or less in equilibrium, such is probably not the case.

Contrasting Behaviors Due to Glacier Geometry

Aniya and others (1997) did not find any correlation between the variations of the SPIF glaciers and latitude, accumulation area ratio (AAR), total glacier area, or surface gradient at the equilibrium line. The first absence of correlation is not a surprise: around lat 50°S., the variation in climate with latitude is insignificant compared to the climate variation between the windward and leeward sides of the Andes. The three other factors that cannot be correlated are discussed as follows:

AAR. Glaciers that have smaller AAR's would be expected to recede, and the opposite would be true for glaciers that have larger AAR's. However, the history of variation in AAR for SPIF glaciers does not meet this expected norm. Two classes of outlet glaciers have been distinguished: tidewater glaciers and glaciers that terminate on land. In 1945 among tidewater glaciers, the lowest AAR's were for Glaciar Asia (0.65) and Glaciar Amalia (0.66). The very large recession of Glaciar Amalia has raised its AAR to 0.80, its standard value. The surprising fact is that, up to 1986 at least, the recession of its neighbor, Glaciar Asia, has been insignificant. As for glaciers that calve into lakes or that lack a calving front, their mean AAR in 1986 was 0.736. The three glaciers of this kind that had the largest recession between 1945 and 1986 are Glaciar Lucía, whose AAR increased from 0.66 to 0.72, Glaciar Greve (0.62 to 0.67), and the west stream of Glaciar Jorge Montt (0.70 to 0.75 for the entire glacier). In contrast, with smaller AAR's of 0.62, Glaciar Tyndall had a normal recession, and Glaciar Grey, a small one. Glaciar Viedma, having an AAR of 0.58, did not recede at all.

Total glacier area. Table 12 shows that even the relative change in area is not correlated with the total glacier area. The most important variable is

the glacier length because of the well-known lag in time between any change of the mass balance and the response of the front. The response may be considered as the sum of kinematic waves starting from all the points of the glacier, and the velocity of these waves is independent from the glacier area. In the case of Glaciar Upsala, its east stream, which is about 60 km long, should lag in time behind its west stream, which is fed by tributaries 10–15 km long.

Surface gradient. As a first, rough approximation, kinematic waves may be ignored. The discharge of ice through a fixed cross section near the glacier terminus, which governs the position of this front, equals the sum of the mass balance over the entire glacier surface. With z denoting the surface elevation, $S(z)$ the area from the cross section, and $b(z)$ the mass balance, the discharge is $\int b\ (\partial S/\partial z)\ \partial z$. The variations of the discharge depend on the surface gradient ($\partial S/\partial z$), where the variations of b are the largest. In Patagonia, the main factor in the variations of b is a change in the mean altitude of the rain-snowfall limit (mean RSLA). Aniya and others (1997) consider implicitly that the mean RSLA is the ELA, but this assumption is questionable. In Patagonia, the RSLA ranges from nearly sea level in winter to 2,600–2,700 m in February, and precipitation falls all year and has comparable monthly totals. Therefore, the statistical distribution of the RSLA and the whole hypsography of the glacier are involved, not only $\partial S/\partial z$ at some elevation.

We have no statistics of the RSLA for a full year in the *Patagonian Andes*. An estimate of its mean value might be drawn from the contrasting behaviors of Glaciares (*Perito*) Moreno and Upsala, the only ones whose hypsographies have been published (Aniya and Skvarca, 1992). If the highest 10 percent and the lowest 10 percent of their areas are ignored, the elevation of the surface of Glaciar (*Perito*) Moreno ranges between 530 m and 2,130 m, and the median elevation (50 percent of the area above and 50 percent below) is 1,560 m, whereas its ELA (in 1986) was at 1,150 m. Glaciar Upsala, over 80 percent of its area, ranges between 800 m and 1,800 m, and its median elevation is 1,290 m, whereas the ELA is at 1,200±50 m. Because Glaciar (*Perito*) Moreno is more or less in equilibrium and Glaciar Upsala has receded at an accelerating rate, we suggest that the difference between the median elevation and the ELA is critical.

The Unusual Case of Glaciar Brüggen (*Pío XI*)

The first records about glacier termini in both Americas came from Spanish seamen who, starting from Valparaíso, Chile, tried to pass through the Strait of Magellan in a direction opposite to that traveled by Magellan in 1520. (Remember that no other way into the Atlantic Ocean was known until 1578.) Francisco de Ulloa in 1553 and Cortés Ojeda and Ladrillero in 1557 (both captains of ships sent by Governor García Hurtado de Mendoza) all made the same error. They entered Estrecho de Concepción (Canal Concepción) thinking that it was the Strait of Magellan (Estrecho de Magallanes), whose entrance is 200 km farther south (see fig. 54). The fact that a series of channels and a fjord (Fiordo Eyre) ran northeast or north-northeast instead of southeast did not induce them to turn around until they were stopped by the calving front of Glaciar Brüggen, which was as advanced as it is today. In 1993, Rivera, Aravena, and Casassa (1997) found trees up to 524 years old (Ciprés de las Guaitecas, *Pilgerodendron uviferum*) close to the glacier margin, north of the mouth of Fiordo Exmouth. Thus, since at least 1469, Glaciar Brüggen has never advanced as far southward as in recent times (fig. 55).

No other visit to Fiordo Eyre is known until the one by Captain Parker King on board H.M.S. *Beagle* in 1830. He described *Río Greve* as flowing at the head of the fjord over flat land from Glaciar Greve, but no calving front

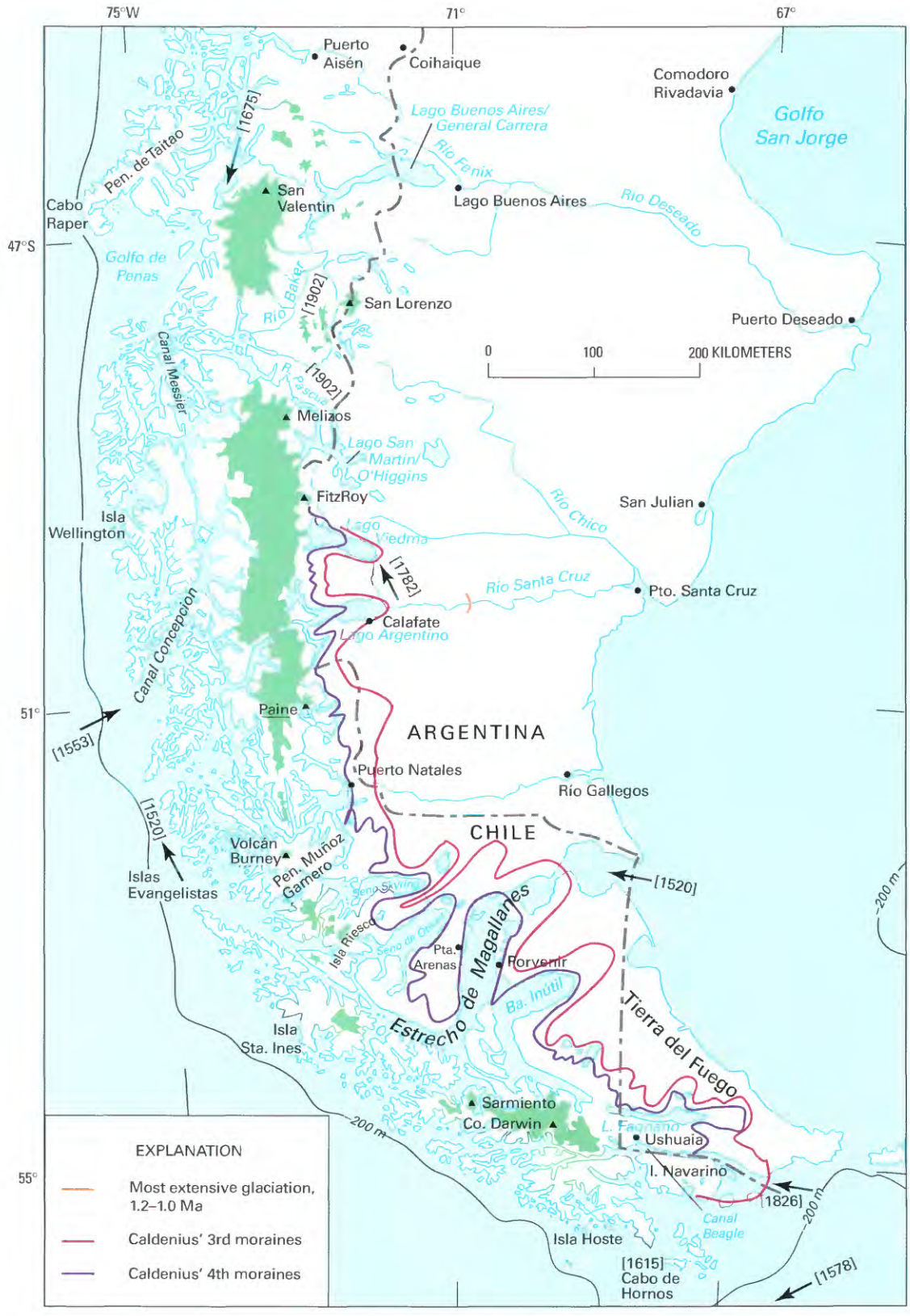

Figure 54.—*Southern Patagonia showing towns and some meteorological stations that are referred to in the text. Numbers between brackets are the dates of discovery. Dashed line is the border between Argentina and Chile, as fixed in 1902 by British arbitration. Red and purple lines are Caldenius' "third" and "fourth" systems of end moraines, which are dated at 18 ka and 10 ka (from varves) or at 19 ka and 13 ka (from ^{14}C), respectively. The –200 m bathymetric contour line corresponds more or less with the limit of the continental shelf. The three largest green areas are the Northern and Southern Patagonian Ice Fields and the ice field of Cordillera Darwin (modified from Lliboutry, 1956, 1965). Abbreviations: Ba., Bahía; Co., Cordillera; I., Isla; L., Lago; Pen., Peninsula; Pta., Punta; R., Río; Sta., Santa.*

was observed (Mercer, 1964). The calving front of Glaciar Brüggen was probably hidden in a lateral bay 12 km from the west coast of Fiordo Eyre, as is depicted in the Carta Nacional de Chile.

In 1925, a Norwegian farmer named Samsing attempted to establish a homestead in the grasslands of *Río Greve*. (The fact that this area was unforested supports the idea that it was a lake bottom not many years before.) The front of Glaciar Brüggen was then about 1 km from the opposite coast. In September 1926, it advanced and closed off the end of the fjord. Samsing was able to escape, but he lost all his cattle and his farmstead (Agostini, 1945, p. 62–63).

The end of the fjord began to open again in 1930. In 1945, inspection of Trimetrogon aerial photographs showed that the front of Glaciar Brüggen was 2.2 km from the opposite coast. The Chilean expedition of 1962 found that it had advanced and reached the opposite bank and that a lake began to form behind this ice dam (fig. 55). In 1976, an early satellite image showed an extensive lake, 24 km long and 15 km wide in the center, where it reached Glaciar Greve. The glacier had advanced 4 km between 1962 and 1976, probably caused by its becoming afloat. The lake was still present in 1978, when it was photographed from the Salyut-6 orbital space station (Desinov and others, 1980) (fig. 31).

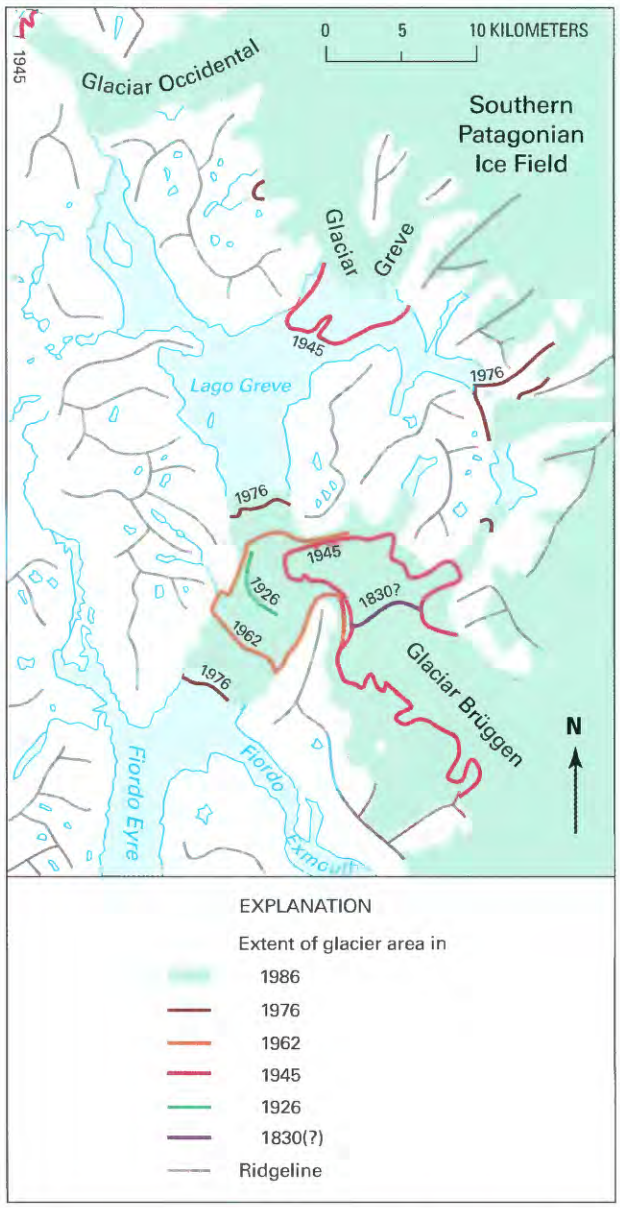

Figure 55.—*Documented changes in the position of the terminus of Glaciar Brüggen (see text for discussion of fluctuations).*

Inspection of Landsat imagery shows that Glaciar Brüggen has undergone little change since 1976 (Aniya and others, 1992).

In my opinion, the situation as it was in 1553–57, and as it has been again since 1947, is the normal one. The considerably large recession observed in 1830 was probably caused primarily by the nearby volcanic activity of *Cerro (Volcán) Lautaro* (see Rivera and others, 1997).

Periodic Dammings by Glaciar (*Perito*) Moreno

Glaciar (*Perito*) Moreno has repeatedly blocked Canal de los Témpanos (the "channel of theSoler icebergs") and separated Lago Argentino from its southernmost arms, Brazo Rico and Brazo Sur. According to Raffo and others (1953), the water level in the dammed part (called *Lago Rico*) rose 14.9 m in March 1942 and 14.4 m in March 1953 and flooded as much as 66.7 km^2 of grassland. However, height measurements to the vegetation line, which is clearly marked by water erosion, indicate that the maximum rise of *Lago Rico* during this century was around 23 m, and it was about 19 m in 1988 (Pedro Skvarca, written commun.). The outburst of the stored water (on the order of 1×10^9 m^3) floods the shores of Lago Argentino and its outlet, Río Santa Cruz (fig. 54).

The width of the dam formed by Glaciar (*Perito*) Moreno is only a few hundred meters, although the calving fronts in Canal de los Témpanos and in Brazo Rico are 3.0 km and 2.1 km wide, respectively (figs. 39 and 43). The depth of these arms and the temperature and circulation of their water have never been studied. In Brazo Rico, which trends west to east, the wind propels the icebergs into warmer water. A return current at about 4°C (the temperature for which the density of pure water is a maximum) probably exists at depth. This water would melt the ice cliff at its bottom, and thus, the calving process would be different from the one in tidewater glaciers, where most melting is near the ocean surface. In Canal de los Témpanos, which runs north to south, the circulation should be much slower. Advances and retreats of the calving front result from the balance of glacier velocities and calving rates, the former being more variable than the latter. Therefore, the monitoring of closures is useful. Over the long term, Glaciar (*Perito*) Moreno is more or less in equilibrium (Naruse and others, 1995).

Raffo and others (1953) gathered all information previously known about ice dammings. The first reported one was in January 1917, after a 1-km advance of the front. (Other dammings might have taken place prior to this, but no local inhabitants were around to report their occurrence.) After January 1917, the following ice dams formed:

From January to December 1935
From July 1939 to 17 February 1940
From the beginning of January 1941 to 21 March 1942
In December 1946
In November 1947
From April to December 1948
From the end of September 1951 to the beginning of March 1952
From October 1952 to the end of March 1953

Ice dammings also took place in 1966, 1970, 1972, 1975, 1977, 1980 (together with an outburst flood on 17 February 1980), 1984, 1988, and 1990 (del Valle and others, 1995). The successive lapses of time during which the channel has been open have lasted 216, 43, 11, 69, 11, 5, 33, 7, 36, and 156 months. The duration of the ice dammings (excepting the very short ones in 1946 and 1947) has been more regular: 8±3 months. About 8 months is probably the time needed for subglacial waterways to become enlarged by melting of the conduit walls, which precedes the final collapse of their roofs. The fact that the failure of the ice dam always happens in summer, especially in late summer, indicates that the water flowing into the

waterway probably consists of surface water warmed by the Sun and that the melting of the ice walls by this warmth is the main factor for the opening of the dam.

A rough modeling of the opening is possible assuming that, at a given instant t, the water in the conduit is at a uniform temperature (θ) in spite of the melting at the walls, an assumption that implies that the increase of the discharge (Q) along the conduit is negligible. Then, the cross-sectional area of the conduit (S) remains uniform over its entire length (L), and H denotes the level of Brazo Rico above Canal de los Témpanos, so the piezometric gradient is H/L. The Manning empirical formula for turbulent steady flows reads

$$Q=k_1 S^{4/3} H^{1/2}$$

where k_1 is a constant. With ϕ denoting the water input into Brazo Rico, we have

$$\partial H/\partial t=k_2 (\phi-Q).$$

Last, the melting of the walls of the waterway yields

$$\partial S/\partial t=k_3 \theta Q$$

where ϕ and θ are given functions of time. At the start, $H=Q=0$, and $S=S_0$. The cross section S is an ever-growing function of time. H is a maximum when $Q=\phi$, and then Q is still increasing. Later, assuming ϕ and θ are constant, Q decreases and tends toward ϕ, S goes on increasing more or less linearly with time, and H decreases as $t^{-8/3}$. The model is no longer valid when open flow takes place in the subglacial channel. The tunnel is then about 30 m in diameter, and it collapses the following day. Photographs of this spectacular event have been taken by DeRoy Moore (1981), and a videotape of it is for sale.

Past Glaciations and "Little Ice Ages"

Past Glaciations

Satellite images show the amazing labyrinth of channels, fjords, and elongated lakes along the Pacific coast of Patagonia, which had been mapped in the Carta Preliminar of the 1950's. It is strikingly noticeable that the features trend in only three directions: the direction of the Andean ranges and two others at about a 60° angle to the ranges (fig. 56). The two latter directions correspond to the directions of maximum shear stress caused by plate convergence. The orientation of these features probably represents shear zones that have been preferentially scoured by glaciers in the past. It cannot be denied that the entire Pacific continental shelf of Patagonia has been covered by ice in the past: the emerged islands are almost devoid of sedimentary terrane, and the granodiorite batholith is exposed at the surface everywhere.

The bottom of channels and fjords is normally about 200 m below the sea bottom, whereas their shores commonly rise above 1,000 m. The largest measured overdeepening is 1,344 m in Fiordo Baker (approximately 48°S.), which trends east, but a depth of 1,288 m has been measured in the north part of Canal Messier, which trends north between Isla Wellington and other Pacific islands and the continent (fig. 54). This strong glacial erosion seems to indicate that local glaciers and ice fields have existed repeatedly on the Pacific islands and that the ice streams ran in directions other than from east to west. The Northern and Southern Patagonian Ice Fields were often larger than today, but their western outlet glaciers flowed generally in the south to north channels. Today, a negative isostatic anomaly exists on the SPIF and on the Pacific islands but not between them (Kraemer, 1992). This indicates that in the late Pleistocene another ice field was present on the Pacific islands, together with a thicker SPIF. The idea of a single, elongated ice cap, with a convex east-west profile, covering the *Patagonian Andes* from the limit of the continental shelf to the Argentine pampa must be dismissed.

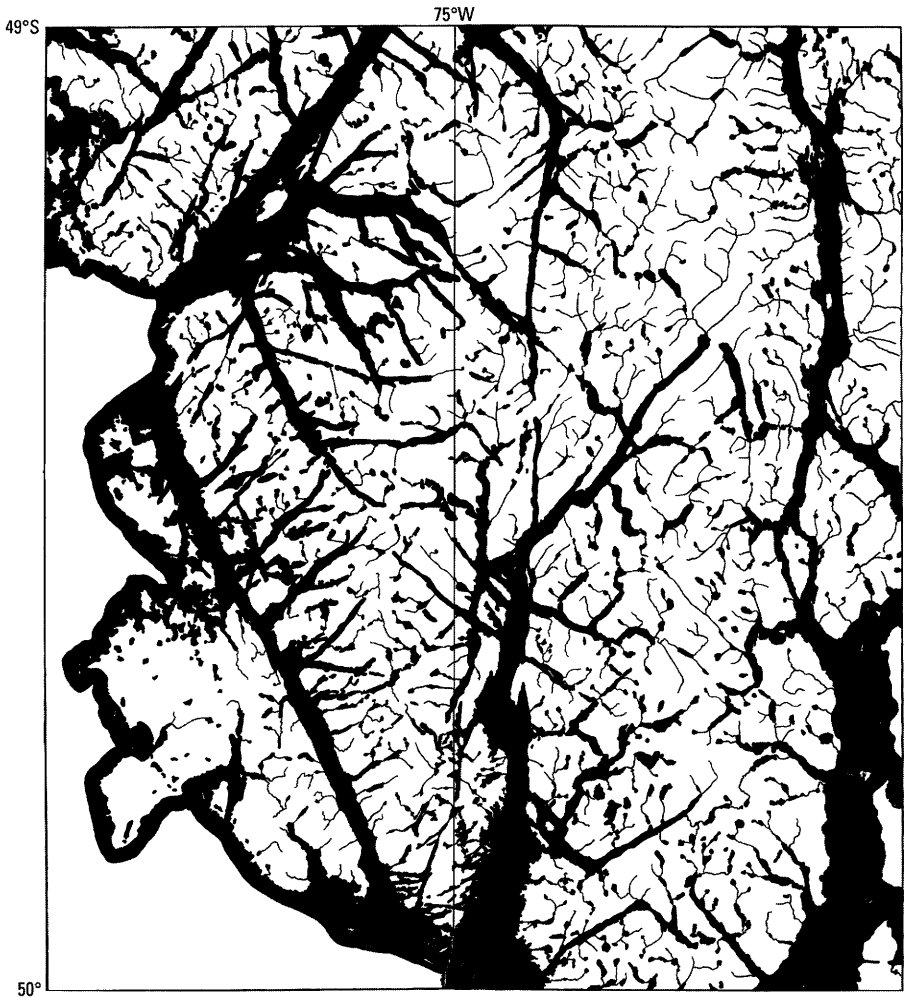

Figure 56.—*Isla Wellington between lat 49° and 50°S. showing that channels and fjords have three preferred orientations. They cannot have been scoured by glacier flow from east to west during glacial epochs. The topography is very rough; steep slopes and rain forest make the island impenetrable. Nevertheless, the elevation does not exceed 1,463 m anywhere.*

The glacial history of Patagonia has begun to be deciphered, in particular thanks to the work of the late John Mercer (Mercer, 1968, 1970, 1976; Mercer and Sutter, 1982). More detailed studies, leading to a major revision in the dating of the last morainic system, have been done by Clapperton and others (1995).

Caldenius, in his pioneering work of 1932, recognized an "old glaciation" and a young one (Lliboutry, 1956, p. 421–424). In fact, at least three old glaciations are evident.

(1) The oldest glacial drift is found between lava flows at 7.0 and 4.6 Ma from ^{40}Ar dating. This glaciation might have been synchronous with the formation of the ice sheet in West Antarctica (6–5 Ma) and with a glaciation in southern Alaska.

(2) A second glaciation happened at around 3.6 Ma.

(3) The third glaciation at 1.2–1.0 Ma was the most extensive. Caldenius and other authors thought that it reached long 69°W., the location of the current Atlantic coast. (During the glaciation, the continental shelf, which extends to the east of the Strait of Magellan as far as the Falkland Islands (Islas Malvinas), had emerged, and the coast was farther east.) According to Mercer's studies and K-Ar dating, however, this greatest glaciation only went 80 km farther than the existing Lago Argentino in the Río Santa Cruz valley, a position 140 km inland from the current coast (fig. 54).

Between these main glaciations, smaller ones probably took place. At Cerro del Fraile (just east of Brazo Rico of Lago Argentino), glacial drift alternates with lava flows that are well dated by magnetic reversals. This

exposure reveals five glaciations between 2.43 Ma and 1.67 Ma. At that rate, one could speculate at least 40 glaciations in Patagonia.

The youngest glaciation, more or less simultaneous with the Wisconsinan stage in North America and the Weichselian stage in northern Europe, left terminal moraines at or near the east shores of the large piedmont lakes of central Patagonia and the piedmont embayments of southern Patagonia. From north to south, they are Lago Buenos Aires/General Carrera, Lago San Martín/O'Higgins, Lago Viedma, Lago Argentino, Seno Skyring, Seno de Otway, the Strait of Magellan, and Bahía Inútil in Tierra del Fuego (fig. 54). Two distinct systems can be recognized, Caldenius' "third" and "fourth" systems of end moraines, which are better identified by the names of the narrows created by their moraines in the Strait of Magellan: the Primera Angostura (the outer "third" system) and the Segunda Angostura (the inner "fourth" system). The outer system limits the four mentioned lakes, and the inner one limits the Senos Skyring and de Otway and Bahía Inútil. Caldenius' second system, farther to the east, was not confirmed by his successors.

Caldenius thought that the moraines corresponded to the Gotiglacial and Finiglacial stages in Scandinavia (dated at about 18 ka and 10 ka, respectively), but they are older. According to Clapperton and others (1995), the moraines of Segunda Angostura were deposited not at 10 ka but during at least five advances ranging in age from about 70 ka to about 11 ka. The last advance is also documented in the Beagle Channel, near Ushuaia (Heusser and Rabassa, 1987) (figs. 40 and 54). It corresponds to the Younger Dryas in Europe. Nevertheless, around Laguna San Rafael at 11 ka, glaciers were probably smaller than today (Mercer, 1970), a fact that would confirm that the cooling of the Younger Dryas had its origin in the Atlantic Ocean.

During the last glacial maximum at 20–18 ka, the Patagonian ice fields would have been relatively extensive and thick. In fact, only 1 glaciation among maybe 40 earlier glaciations was more extensive, and at the time of the most extensive glaciation at 1.2–1.0 Ma, the "piedmont glacier Argentino" extended only 80 km farther to the east from this last glacial maximum. The extension and thickening of the Patagonian ice fields was probably only slightly less during previous glaciations.

When looking at the FitzRoy group from the northeast, a striking difference is revealed between the lower half of *Cerro Eléctrico*, smoothed by glacial erosion below about 1,300 m, and its upper part, without any sign of erosion. On its north side in *Valle Eléctrico*, a glacial terrace exists at 1,300–1,400 m (fig. 36). It confirms that this was the elevation of the surface of an outlet glacier, probably about 80 km long, that discharged ice from the SPIF through *Paso Marconi*. At *Paso Marconi*, 10 km upstream, the surface elevation was probably 1,800±100 m (200–400 m higher than today). The ice stream thinned and locally had a large surface slope as it flowed through *Paso Marconi*. Consequently, the central part of the ice sheet should have been at 2,100±200 m (300–700 m higher than today) during the last glacial maximum.

According to a numerical simulation by Hulton and others (1994), the ice-sheet surface would have exceeded 2,700 m. With a maximum width of about 400 km, the bottom drag would have been about 3.6 bar (0.36 megapascal), much too large a value. In fact, the calculation by Hulton and others cannot be trusted at all because it is based on an arbitrary model for the ELA, an isothermal, albeit cold, ice sheet, always at –6°C, and a fanciful topography. In their model, all the relief of the unglaciated land has been smoothed out; all the elevated islands and deep channels have been replaced by a flat, emerged land below 300 m, and all north to south ranges exceeding 1,200 m in height have been erased. With this model, only a large thickness of the ice sheet allows its surface to rise above the ELA. With elevations more than 2,700 m, the ice sheet would

have been cold, and the accumulation would have been a weak function of the mean temperature. With elevations of about 2,000 m, the ice sheet would have been temperate as the ice fields are today, and the accumulation would have been a strong function of the mean air temperature because of the changes in the rain-snow limit. Because of the temperate nature of the glacier and this strong function, the lowering of the temperature required to start a glaciation would have been much smaller in Patagonia than in the polar regions.

We may also be skeptical about the changes in the ELA that have been inferred from various "models." Although Hulton and others (1994) claim that their model is grounded on mass and energy balances, it is, in fact, a mere correlation with some meteorological averages. Owing to the rain-snowfall discontinuity, relations are not linear, and averages cannot be used. For instance, Kerr and Sugden (1994) predict activity coefficients of about 0.9 m of ice per 100 m of elevation, whereas in Patagonia, the measured ones are about 1.5 m/100 m.

"Little Ice Ages"

The story of the late Pleistocene has not been as well studied in continental Patagonia as it has been in the Strait of Magellan by Clapperton and others (1995). On the shores of Lagos Buenos Aires/General Carrera, Viedma, and Argentino, several benches of outwash (kame terraces) can be seen clearly on Landsat imagery. According to Lliboutry (1952) and Mercer (1965), they were formed after the last glacial maximum at 20 ka. If the oscillations of the Pleistocene ice sheet were about the same as those in the Strait of Magellan, the highest terraces might be older than 20 ka.

Climatic changes and terminal moraines of the Holocene are better known. A review of knowledge of that time, and a comparison between Patagonia and western North America, is found in Heusser (1961).

The chronology of Holocene moraines in front of Glaciares Upsala and Tyndall has been established by Aniya and Sato (1995a, b). The moraines were deposited around 3.6 ka, 2.3 ka, 1.4 ka, and 250 years before present. (In the Lakes District, Mercer's (1976) dating of the oldest moraine is different, 4.6–4.2 ka, and the third one is not found.) It is preferable to call the first three epochs of temporary glacier advance "Little Ice Ages" rather than neoglaciations. The last "Little Ice Age" began in Patagonia between A.D. 1614 and A.D. 1600. In Europe and Iceland, it had already started by A.D. 1570, but to the contrary, the climate in Patagonia at the end of the 16th century was much milder. These facts were established in 1993 by María del Rosario Prieto and Herrera in an important work, which unfortunately has not yet been published. These two historians located at the Archives of the Merchant Marine in Seville, Spain, 20 logbooks of ships crossing the Strait of Magellan to or from Valparaíso (fig. 1), 5 from each of the following intervals of time: 1520–26, 1535–58, 1578–99, and 1615–24. Only during the second and third time periods was any mention made of numerous icebergs in the channels and of winds from the northeast. During the period 1578–99, mild northeast winds, quite unusual today, were the most common, and the weather was warm, whereas in the interval 1615–24, the wind blew from the southwest quarter one-half of the time and from the northwest quarter one-third of the time, and the weather was very cold.

The icebergs found in the channels in 1535–58 and 1578–99 were blown there by the northeast winds. In 1615–24, as today, the westerly winds kept the icebergs calved by the SPIF at the far ends of the fjords. To have had winds from the northeast, a high-pressure system must have existed to the south of the ships over the Strait of Magellan. The synoptic situation would have been still more extreme than the one depicted in figure 3*C*, which is rather unusual today (note in this figure a northeast wind at Comodoro

Rivadavia).

Compared with the big climatic change around A.D. 1600, the climatic changes in Patagonia during the two last centuries have been extremely modest. Around the NPIF, dendrochronological studies of *Podocarpus nubigemus* have been used to infer paleoclimate (Sweda, 1987; Sweda and Inoue, 1987). The only significant change in tree-ring widths during the last 200 years is a very strong increase between 1963 and 1978, uncorrelated with any change in the temperature or precipitation at Puerto Aisén (fig. 54).

Conclusions

This critical review of Patagonian glaciology has a broader scope than that of a mere glacier inventory because now, in 1997, a copious literature has appeared, most of which remains poorly known. Because this review overturns several preconceived ideas, such as the utility of monitoring glacier advances on an annual basis, the synchronism of glaciations and "Little Ice Ages" in the Northern and Southern Hemispheres, and the existence in the past of a single ice sheet covering all Patagonia, investigators in glaciology and in paleoclimates should pay attention to the actual hard facts. Patagonian glaciology poses fascinating problems. This paper stresses the utility of satellite imagery for studies of these problems, not only for periodic mapping of the glaciers.

Acknowledgments

This review would not have been possible without the aid of many investigators who sent me documents or reviewed the manuscript. Information came from Eduardo García, Cedomir Marangunic, Humberto Peña, and Andrés Rivera (Santiago de Chile); from Mateo Martinic and Gino Casassa (Punta Arenas); from Pedro Skvarca (Buenos Aires); from Arturo Corte, Lydia Espizúa, and María del Rosario Prieto (Mendoza); from several mountain guides in Mendoza and Chaltél; and last but not least, from the two main leaders of glaciological expeditions to Patagonia, Renji Naruse (Sapporo) and Masamu Aniya (Ibaraki). In addition, the Argentine Department of Foreign Affairs kindly offered me a trip to Patagonia and Mendoza in December 1993.

The main documents, of course, were all the Landsat images supplied by the editors. The composite satellite images and perspective views offered by Masamu Aniya and the spectacular photographs given by Pedro Skvarca were very valuable for illustrating the Patagonian ice fields. I thank heartily all these unselfish collaborators.

References Cited

Agostini, A.M., de, 1945, Andes Patagónicos [Patagonian Andes] (2d ed., corrected and amplified): Buenos Aires, Guillermo Kraft Ltda., 437 p.

Aniya, Masamu, 1987, Moraine formation at Soler Glacier, Patagonia: Bulletin of Glacier Research, no. 4, p. 107–117.

———1988, Glacier inventory for the Northern Patagonia Icefield, Chile, and variations 1944–45 to 1985–86: Arctic and Alpine Research, v. 20, no. 2, p. 179–187.

———1992, Glacier variation in the Northern Patagonia Icefield, Chile, between 1985–86 and 1990–91: Bulletin of Glacier Research, no. 10, p. 83–90.

Aniya, Masamu, and Naruse, Renji, 1987, Structural and morphological characteristics of Soler Glacier, Patagonia: Bulletin of Glacier Research, no. 4, p. 69–77.

Aniya, Masamu, Naruse, Renji, Shizukuishi, M., Skvarca, Pedro, and Casassa, Gino, 1992, Monitoring recent glacier variations in the Southern Patagonian Icefield, utilizing remote sensing data: International Archives of Photogrammetry and Remote Sensing, v. 29, no. B7, p. 87–94.

Aniya, Masamu, and Sato, Hiroaki, 1995a, Holocene glacial chronology of Upsala Glacier at Peninsula Herminita, southern Patagonia: Bulletin of Glacier Research, v. 13, p. 83–96.

———1995b, Holocene glacier variations at Tyndall Glacier area, southern Patagonia: Bulletin of Glacier Research, v. 13, p. 97–109.

———1995c, Morphology of Ameghino Glacier and landforms of Ameghino Valley, southern Patagonia: Bulletin of Glacier Research, v. 13, p. 69–82.

Aniya, Masamu, Sato, Hiroaki, Naruse, Renji, Skvarca, Pedro, and Casassa, Gino, 1996, The use of satellite and airborne imagery to inventory outlet glaciers of the Southern Patagonia Icefield, South America: Photogrammetric Engineering and Remote Sensing, v. 62, no. 12, p. 1361–1369.

———1997, Recent glacier variations in the Southern Patagonia Icefield, South America: Arctic and Alpine Research, v. 29, no. 1, p. 1–12.

Aniya, Masamu, and Skvarca, Pedro, 1992, Characteristics and variations of Upsala and Moreno Glaciers, southern Patagonia: Bulletin of Glacier Research, no. 10, p. 39–53.

Aniya, Masamu, and Wakao, Yoshitaka, 1997, Glacier variations of Hielo Patagónico Norte, Chile, between 1944–45 and 1995–1996: Bulletin of Glacier Research, v. 15, p. 11–18.

Aristarain, A.J., and Delmas, R.J., 1993, Firn-core study from the southern Patagonia ice cap, South America: Journal of Glaciology, v. 39, no. 132, p. 249–254.

Arko, V., 1979, Un decenio de la Cordillera Patagónica [A decade of the Patagonian Cordillera]: Bariloche, Argentina, Anuario Club Andino Bariloche 1968–1979, p. 12–81.

Bertone, M., 1960, Inventario de los glaciares existentes en la vertiente Argentina entre los paralelos 47°30' y 51°S. [Inventory of existing glaciers in the watersheds of Argentina between lat 47°30' and 51°S.]: Buenos Aires, Instituto Nacional del Hielo Continental Patagónico Publicación 3, 103 p.

Buscaini, Gino, and Metzeltin, Silvia, 1989, Les orgues de Patagonie [Organs of Patagonia]: Grenoble, Glénat, 272 p.

Casassa, Gino, 1987, Ice thickness deduced from gravity anomalies on Soler Glacier, Nef Glacier and the Northern Patagonia Icefield: Bulletin of Glacier Research, no. 4, p. 43–57.

———1992, Radio-echo sounding of Tyndall Glacier, southern Patagonia: Bulletin of Glacier Research, no. 10, p. 69–74.

———1995, Glacier inventory in Chile: Current status and recent glacier variations: Annals of Glaciology, v. 21, p. 317–322.

Casassa, Gino, Brecher, Henry, Rivera, Andrés, and Aniya, Masamu, 1997, A century-long recession record of Glaciar O'Higgins, Chilean Patagonia: Annals of Glaciology, v. 24, p. 106–110.

Casassa, Gino, and Marangunic, Cedomir, 1987, Exploration history of the Northern Patagonia Icefield: Bulletin of Glacier Research, no. 4, p. 163–175.

Clapperton, C.M., Sugden, D.E., Kaufman, D.S. and McCulloch, R.D., 1995, The last glaciation in central Magellan Strait, southernmost Chile: Quaternary Research, v. 44, p. 133–148.

Club Andino Bariloche, 1954, San Valentín, cumbrera del Hielo Continental [San Valentín, greatest height of the continental glacierization]: Bariloche, Argentina, Club Andino Bariloche, 48 p.

De Roy Moore, Tui, 1981, The day of the glacier: Adventure Travel, v. 3, no. 9, p. 60–67.

Desinov, L.V., Nosenko, G.S., Grechko, G.M., Ivanchenko, A.S., and Kotlyakov, V.M., 1980, Glaciological studies and experiments from the Salyut-6 orbital space station: Issledovaniye Zemli iz Kosmosa, no. 1, p. 25–3 [English translation edited by Williams, R.S., Jr., and Tamberg, Nora, *in* Polar Geography and Geology, v. 11, no. 1, p. 12–24, 1987].

Escobar, Fernando, Vidal, F., Garin, C., and Naruse, Renji, 1992, Water balance in the Patagonia Icefield, *in* Naruse, Renji, and Aniya, Masamu, eds., Glaciological researches in Patagonia, 1990: Nagoya, Japanese Society of Snow and Ice, Data Center for Glacier Research, p. 109–119.

Fukami, Hiroshi, and Naruse, Renji, 1987, Ablation of ice and heat balance on Soler Glacier, Patagonia: Bulletin of Glacier Research, no. 4, p. 37–42.

González, Marcelo, and Veiga, Javier, 1992, Monte FitzRoy-Cerro Torre, trekking-mountaineering map: Miami, Zagier and Urruty Publications, scale 1:50,000.

González-Ferrán, Oscar, 1995, Volcanes de Chile: Santiago, Instituto Geográfico Militar, 641 p.

Heusser, C.J., 1960, Late-Pleistocene environments of the Laguna de San Rafael area, Chile: Geographical Review, v. 50, no. 4, p. 555–577.

———1961, Some comparisons between climatic changes in northwestern North America and Patagonia: New York Academy of Science Annals, v. 95, p. 642–657.

Heusser, C.J., and Rabassa, J., 1987, Cold climatic episode of Younger Dryas age in Tierra del Fuego: Nature (London), v. 328, p. 609–611.

Hickman, M.J.K., and Newton, A.C., eds., 1987, Patagonia '85, expedition report: Cambridge, U.K., Anglo-Chilean Patagonian Expedition 1985, 88 p.

Hirano, Akira, and Aniya, Masamu, 1996, Glacier variations in the Northern Patagonia Icefield, *in* Bainum, P.M., May, G.L., Ohkami, Y., Uesugi, K., Faren, Q., and Furlong, L., eds., Strengthening cooperation in the 21st century (6th ISCOPS): Advances in the Astronautical Sciences v. 91, p. 713–725. (Reprinted by the American Astronautical Society.)

Holmlund, P., and Fuenzalida, H., 1995, Anomalous glacier responses to 20th century climatic changes in Darwin Cordillera, southern Chile: Journal of Glaciology, v. 41, no. 139, p. 465–473.

Hulton, Nick, Sugden, David, Payne, Antony, and Clapperton, Chalmers, 1994, Glacier modeling and the climate of Patagonia during the last glacial maximum: Quaternary Research, v. 42, p. 1–19.

Inoue, Jiro, 1987, Wind regime of San Rafael Glacier, Patagonia: Bulletin of Glacier Research, no. 4, p. 25–30.

Inoue, Jiro, Kondo, Hiroshi, Fujiyoshi, Yasushi, Yamada, Tomomi, Fukami, Hiroshi, and Nakajima, Chotaro, 1987, Summer climate of the Northern Patagonia Icefield: Bulletin of Glacier Research, no. 4, p. 7–14.

Juárez, Tito, and Puente Blanco, Manolo, 1963, Exploración de los ríos Vodudahue y Alerces [Exploration of the Vodudahue and Alerces Rivers]: Bariloche, Argentina, Anuario Club Andino Bariloche 30/31/32, p. 35–43, map.

Kadota, Tsutomu, Naruse, Renji, Skvarca, Pedro, and Aniya, Masamu, 1992, Ice flow and surface lowering of Tyndall Glacier, southern Patagonia: Bulletin of Glacier Research, no. 10, p. 63–68.

Kerr, Andrew, and Sugden, David, 1994, The sensitivity of the south Chilean snow line to climatic change: Climatic Change, v. 28, p. 255–272.

Kondo, Hiroshi, and Yamada, Tomomi, 1988, Some remarks on the mass balance and the terminal-lateral fluctuations of San Rafael Glacier, the Northern Patagonia Icefield: Bulletin of Glacier Research, no. 6, p. 55–63.

Kraemer, P.E., 1992, La ubicación de la línea de altas cumbres divisoria de aguas en el campo de hielo patagónico sur [The location of the line of high summits that is a water divide in the Southern Patagonian Ice Field]: Cordoba, Argentina, Academia Nacional de Ciencias, Miscelanea 88, 21 p.

Lliboutry, Louis, 1952, Estudio cartográfico, geológico y glaciológico de la zona del Fitz-Roy [Cartographic, geologic, and glaciologic studies of the Fitz-Roy region]: Buenos Aires, Universidad de Buenos Aires, Instituto de Geografía, series A, no. 17, 64 p., photographs, maps.

———1953, More about advancing and retreating glaciers in Patagonia: Journal of Glaciology, v. 2, no. 13, p. 168–172.

———1956, Nieves y glaciares de Chile, fundamentos de glaciológia [Snow and glaciers of Chile, fundamentals of glaciology]: Santiago, Universidad de Chile, 472 p., maps.

———1957, Banding and volcanic ash on Patagonian glaciers: Journal of Glaciology, v. 3, no. 21, p. 18–25.

———1958, Studies of the shrinkage after a sudden advance, blue bands, and wave ogives on Glaciar Universidad (central Chilean Andes): Journal of Glaciology, v. 3, no. 24, p. 261–272.

Lliboutry, Louis, 1965, Traité de glaciologie, tome 2: Glaciers, variations du climat, sols gelés [Treatise of glaciology, v. 2: Glaciers, climatic variations, and frozen ground]: Paris, Masson et Cie, 612 p.

———1993, Thrust of Glaciar Torre over itself: Journal of Glaciology, v. 39, no. 133, p. 707–708.

Martinic, Mateo, 1982, Hielo Patagónico Sur [Southern Patagonian Ice Field]: Punta Arenas, Chile, Instituto de la Patagonia, 119 p.

McClelland, Lindsay, Simkin, Tom, Summers, M., Nielsen, E., and Stein, T.C., eds., 1989, Global volcanism, 1975–1985, the first decade of reports from the Smithsonian Institution's Scientific Event Alert Network (SEAN): Englewood Cliffs, N.J., Prentice Hall, and Washington, D.C., American Geophysical Union, 655 p.

Mercer, J.H., 1961, The response of fjord glaciers to changes in the firn limit: Journal of Glaciology, v. 3, no. 29, p. 850–858.

———1964, Advance of a Patagonian glacier: Journal of Glaciology, v. 5, no. 38, p. 267–268.

———1965, Glacier variations in southern Patagonia: Geographical Review, v. 55, no. 3, p. 390–413.

———1967, ed., Southern Hemisphere glacier atlas: U.S. Army Natick Laboratories, Earth Sciences Laboratory, Series ES–33, Technical Report 67–76–ES, 325 p., maps.

———1968, Variations of some Patagonian glaciers since the late glacial: American Journal of Science, v. 266, no. 2, p. 91–109.

———1970, Variations of some Patagonian glaciers since the late glacial II: American Journal of Science, v. 269, no. 1, p. 1–25.

———1976, Glacial history of southernmost South America: Quaternary Research, v. 6, no. 2, p. 125–166.

Mercer, J.H., and Sutter, J.F., 1982, Late Miocene-earliest Pliocene glaciation in southern Argentina: Palaeogeography, Palaeoclimatology, Palaeoecology, v. 38, p. 185–206.

Nakajima, Chotaro, ed., 1985, Glaciological studies in Patagonia Northern Icefield 1983–1984: Nagoya, Japanese Society of Snow and Ice, Data Center for Glacier Research, 133 p.

Naruse, Renji, ed., 1983, Glaciological and meteorological studies in Patagonia, Chile, by Japanese research expeditions in 1967–1982: Nagoya, Japanese Society of Snow and Ice, Data Center for Glacier Research, 18 p.

———1987, Characteristics of ice flow of Soler Glacier, Patagonia: Bulletin of Glacier Research, no. 4, p. 79–85.

Naruse, Renji, and Aniya, Masamu, eds., 1992, Glaciological researches in Patagonia, 1990: Nagoya, Japanese Society of Snow and Ice, Data Center for Glacier Research, 130 p. (The first 60 pages are reprints of Bulletin of Glacier Research, no. 10, 1992.)

———1995, Glaciological researches in Patagonia, 1993: Nagoya, Japanese Society of Snow and Ice, Data Center for Glacier Research, p. 1–10. (Reprint of Bulletin of Glacier Research, no. 13, 1950.)

Naruse, Renji, Peña, Humberto, Aniya, Masamu, and Inoue, Jiro, 1987, Flow and surface structure of Tyndall Glacier, the Southern Patagonia Ice Field: Bulletin of Glacier Research, no. 4, p. 133–140.

Naruse, Renji, Skvarca, Pedro, Kadota, Tsutomu, and Koizumi, Ken, 1992, Flow of Upsala and Moreno Glaciers, southern Patagonia: Bulletin of Glacier Research, v. 10, p. 55–62.

Naruse, Renji, Skvarca, Pedro, Satow, Kazuhide, Takeuchi, Yukari, and Nishida, Kenro, 1995, Thickness change and short-term flow variation of Moreno Glacier, Patagonia: Bulletin of Glacier Research, v. 13, p. 21–28.

Naruse, Renji, Skvarca, Pedro, and Takeuchi, Yukari, 1997, Thinning and retreat of Glaciar Upsala, and an estimate of annual ablation change in southern Patagonia: Annals of Glaciology, v. 24, p. 38–42.

Ohata, Tetsuo, Kondo, Hiroshi, and Enomoto, Hiroyuki, 1985, Meteorological observations at San Rafael Glacier, *in* Nakajima, Chotaro, ed., Glaciological studies in Patagonia Northern Icefield 1983–1984: Nagoya, Japanese Society of Snow and Ice, Data Center for Glacier Research, p. 22–31.

Peña, Humberto, and Gutiérrez, R., 1992, Statistical analysis of precipitation and air temperature in the Southern Patagonia Icefield, *in* Naruse, Renji, and Aniya, Masamu, eds., Glaciological researches in Patagonia, 1990: Nagoya, Japanese Society of Snow and Ice, Data Center for Glacier Research, p. 95–107.

Puente Blanco, Manolo, 1963a, Aporte científico de la primera expedición invernal al Fitz-Roy [Scientific report of the first winter expedition to Fitz-Roy]: Bariloche, Argentina, Anuario Club Andino Bariloche, 30/31/32, p. 51–57, map at a scale of 1:100,000.

———1963b, Cuarta expedición patagónica del CAB, invierno de 1961, Resumen de los trabajos tecnicos llevados a cabo [Fourth Patagonian Expedition of the CAB, winter of 1961, summary of the completed technical work]: Bariloche, Argentina, Anuario Club Andino Bariloche 30/31/32, p. 22–31, map at a scale of 1:100,000.

Quintanilla, V.E.G., 1974, Les formations végétales du Chili tempéré [The plant species of temperate Chile]: Grenoble, Université de Grenoble, thesis, 120 p., map.

Rabassa, Jorge, 1981, Inventario de glaciares y cuerpos de nieve permanentes en los Andes Patagónicos septentrionales, Argentina [Inventory of the glaciers and permanent snow patches in the northern Patagonian Andes, Argentina]: Congreso Geológico Argentino, VIII, San Luis, 20–26 September 1981, Actas 4, p. 109–122.

Rabassa, Jorge, Rubulis, Sigfrido, and Suarez, Jorge, 1978, Los glaciares del Monte Tronador [The glaciers of Mount Tronador]: Buenos Aires, Anales de Parques Nacionales, v. 4, p. 259–318.

Raffo, J.M., Colqui, B.S., and Madejski, M.E., 1953, Glaciar Moreno: Meteoros, v. 3, no. 4, p. 293–341.

Reichert, Fritz, 1947, Auf Berges- und Lebenshohe [Heights of mountains and of life; Spanish translation, En la cima de las montañas y de la vida]: Buenos Aires, Kave, 2 v., 650 p., photographs, 1950.

Rignot, Eric, Forster, Richard, and Isacks, Bryan, 1996a, Interferometric radar observations of Glaciar San Rafael, Chile: Journal of Glaciology, v. 42, no. 141, p. 279–291.

———1996b, Mapping of glacial motion and surface topography of Hielo Patagónico Norte, Chile, using satellite SAR L-band interferometry data: Annals of Glaciology, v. 23, p. 209–216.

Rivera, Andrés, Aravena, J.C., and Casassa, Gino, 1997, Recent fluctuations of Glaciar Pío XI: Discussion of a glacial surge hypothesis: Mountain Research and Development, v. 17, no. 4, p. 309–322.

Rivera, Andrés, Lange, Heiner, Aravena, J.C., and Casassa, Gino, 1997, The 20th-century advance of Glaciar Pío XI, Chilean Patagonia: Annals of Glaciology, v. 24, p. 66–71.

Rosenblüth, Benjamín, Casassa, Gino, and Fuenzalida, Humberto, 1995, Recent climatic changes in western Patagonia: Bulletin of Glacier Research, v. 13, p. 127–132.

Saint-Loup, 1951, Monts Pacifique, de l'Aconcagua au Cap Horn [Pacific mountains, from Aconcagua to Cape Horn]: Grenoble, Arthaud, 277 p.

Shipton, Eric, 1963, Land of tempest, travels in Patagonia 1958–1962: London, Hodder and Stoughton, 224 p.

Simkin, Tom, and Siebert, Lee, eds., 1994, Volcanoes of the world: 2d ed.: Tucson, Ariz., Geoscience Press, Inc., in association with the Smithsonian Institution, 349 p.

Skvarca, Pedro, 1967, Hielo Patagónico sur 1964 [Southern Patagonian Ice Field 1964]: Bariloche, Argentina, Anuario Club Andino Bariloche 33/34/35, p. 7–18.

Skvarca, Pedro, Rott, Helmut, and Stuefer, Martin, 1995, Synergy of ERS–1 SAR, X–SAR, Landsat TM imagery and aerial photography for glaciological studies of Viedma Glacier, southern Patagonia: Simposio Latinoamericano de Percepción Remota (SELPER), VII, Puerto Vallarta, Mexico, November 1995, Proceedings, p. 674–682.

Skvarca, Pedro, Satow, Kazuhide, Naruse, Renji, and Leiva, J.C., 1995, Recent thinning, retreat and flow of Upsala Glacier, Patagonia: Bulletin of Glacier Research, v. 13, p. 11–20.

Sociedad Científica Alemana, 1917, Patagónia, resultados de las expediciones realizadas de 1910 a 1916 [Results of the expeditions to Patagonia between 1910 and 1916]: Buenos Aires, Co. Sudamericana Impresora de Billetes de Banco, XII, 431 p., maps, photographs.

Sweda, Tatsuo, 1987, Recent retreat of Soler Glacier, Patagonia, as seen from vegetation recovery: Bulletin of Glacier Research, no. 4, p. 119–124.

Sweda, Tatsuo, and Inoue, Jiro, 1987, Dendrochronologies of San Rafael and Soler areas, Patagonia: Bulletin of Glacier Research, no. 4, p. 125–132.

Takeuchi, Yukari, Naruse, Renji, and Satow, Kazuhide, 1995, Characteristics of heat balance and ablation on Moreno and Tyndall Glaciers, Patagonia, in the summer 1993–94: Bulletin of Glacier Research, v. 13, p. 45–56.

Tanaka, K., 1980, Geographical contribution to a periglacial study of the Hielo Patagónico Norte with special reference to the glacial outburst originated from glacier-dammed Lago Arco, Chilean Patagonia: Tokyo, Center Company, Ltd., 97 p.

Valle, R.A., del, Skvarca, Pedro, Mancini, M.V., and Lusky, Jorge, 1995, A preliminary study of sediment cores from Lago Argentino and fluctuations of Moreno Glacier, Patagonia: Bulletin of Glacier Research, v. 13, p. 121–126.

Wada, Yumiko, and Aniya, Masamu, 1995, Glacier variations in the Northern Patagonia Icefield between 1990–91 and 1993–94: Bulletin of Glacier Research, v. 13, p. 111–119.

Warren, C.R., 1993, Rapid recent fluctuations of the calving San Rafael Glacier, Chilean Patagonia: Climatic or non-climatic?: Geografiska Annaler, v. 75A, no. 3, p. 111–125.

Warren, C.R., Glasser, N.F., Harrison, Stephan, Winchester, Stephen, Kerr, A.R., and Rivera, Andrés, 1995, Characteristics of tide-water calving at Glaciar San Rafael, Chile: Journal of Glaciology, v. 41, no. 138, p. 273–289.

Warren, C.R., and Sugden, D.E., 1993, The Patagonian icefields, a glaciological review: Arctic and Alpine Research, v. 25, no. 4, p. 316–331.

Williams, R.S., Jr., 1976, Vatnajökull icecap, Iceland, *in* Williams, R.S., Jr., and Carter, W.D., eds., ERTS–1: A new window on our planet: U.S. Geological Survey Professional Paper 929, p. 188–193.

———1986, Glaciers and glacial landforms, chapter 9 of Short, N.M., and Blair, R.W., Jr., eds., Geomorphology from space, a global overview of regional landforms: National Aeronautics and Space Administration Special Publication SP–486, p. 521–596.

———1987, Background to the Soviet glaciological studies from the Salyut-6 orbital space station: Polar Geography and Geology, v. 11, no. 1, p. 1–11.

Winchester, Vanessa, and Harrison, Stephan, 1996, Recent oscillations of the San Quintín and San Rafael Glaciers, Patagonia, Chile: Geografiska Annaler, v. 78A, no. 1, p. 35–49.

Yamada, Tomoni, 1987, Glaciological characteristics revealed by 37.6–m deep core drilled at the accumulation area of San Rafael Glacier, the Northern Patagonia Icefield: Bulletin of Glacier Research, no. 4, p. 59–67.

Yamada, Tomoni, Kondo, Hiroshi, and Fukuzawa, Takuya, 1987, Ice core drilling operations in the Northern Patagonia Icefield: Bulletin of Glacier Research, no. 4, p. 151–155.

☆ U.S. GOVERNMENT PRINTING OFFICE: 1999 — 773-051 / 20127 Region No. 8